

# **Evaluating and Avoiding Risk Tradeoffs in Water Treatment**

Submitted in partial fulfillment of the requirements for

the degree of

Doctor of Philosophy

in

Engineering and Public Policy

Daniel B. Gingerich

B.S., Civil Engineering, Mississippi State University

B.A., Political Science, Mississippi State University

M.S., Civil Engineering, Auburn University

Carnegie Mellon University  
Pittsburgh, PA

August, 2017

© Daniel B. Gingrich, 2017

All Rights Reserved

## **ACKNOWLEDGEMENTS**

First, I would like to thank the many funders of my research. These include the National Science Foundation under awards SEES-1215845 and CBET-1554117; the Department of Energy under award DE-FE0024008; the Steinbrenner Graduate Fellowship; the Phillips & Huang Family Foundation Fellowship; the Pittsburgh Chapter of the ARCS (Achievement Rewards for Collegiate Scientists) Foundation; the CMU Provost's Office; and the CMU Graduate Student Assembly. None of these funders have reviewed this work. They, nor any of their employees, make any warranty, express or implied, or assume any legal liability or responsibility for the accuracy, completeness, or usefulness of any information. The views and opinions in this thesis do not necessarily state or reflect theirs. Any findings and recommendations are the sole responsibility of myself (and my co-authors).

The point of a Ph.D. is to develop the skills necessary to become an independent researcher and scholar. My committee, consisting of Dr. Meagan S. Mauter, Dr. Jared L. Cohon, Dr. David A. Dzombak, and Dr. M. Granger Morgan have been vital in pushing to refine my thinking, to develop novel approaches, and to chase interesting questions. I knew Meagan would push me to be the best scholar I could be after my interview on visit day, and I am deeply grateful for her guidance during this entire process. Jerry, Dave, and Granger also contributed to my growth by challenging me throughout my career in classes, my qualifiers, and research.

I would also like to thank the many individuals that have made my time at CMU as wonderful as it has been. Among my fellow EPP students, who've provided me with countless pieces of feedback and advice, conversations, and distractions, I would like to thank Tobi Adekanye, Kristen Allen, Matthew Babcock, Vanya Britto, Casey Canfield, Anabel Castillo Mora, Rebecca Ciez, Christophe Combemale, Michael Craig, Amy Dale, Jaison Desai, Barry

Dewitt, Ty Drayton, Alessandro Giordano, Brock Glasgo, Alan Jenn, Jeremy Keen, Long Lam, Aviva Loew, Sonia Mangones, Erin Mayfield, Octavio Mesner, Serban Mogos, Sinnot Murphy, I. Daniel Posen, Michael Roth, Manar Saria, Sara Schwetschenau, Stephanie Seki, Shayak Sengupta, Brian Sergi, Evan Sherwin, Daniel Sun, Shuchi Talati, Paul Tisa, Logan Warberg, Jacob Ward, and Arthur Yip. I've been lucky to work alongside many amazing and inspiring student leaders in GSA and student government including Travis Carless, Carolyn Commer, Erin Farenkhopf, Will Frankenstein, Chetali Gupta, Beth Halayko, Hassan Khan, Stephanie Laughton, Sneha Narra, Clive Newstead, Rony Patel, Nicole Rafidi, Vaasavi Unnava, Amanda Willard, and Jon Willcox. I also have many wonderful colleagues in the Water and Energy Efficiency for the Environment Lab to thank including Tim Bartholomew, Moiz Bohra, Alexander Dudchenko, Sneha Shanbhag, Paul Welle, and Xingshi Zhou. Finally, I owe much of my success to the unsung heroes of academia, the staff and administrators, including Elisabeth Bass-Udyawar, Vicki Finney, Debbie Kuntz, Dr. Suzie Laurich-McIntyre, Brittani McKenna, Adam Loucks, Kaycee Palko, Jamie Rossi, M. Shernell Smith, and Patti Steranchak.

I would not be doing my Ph.D. without the support of my loving family. I have been incredibly blessed to have two parents who have their own Ph.D.s, Dr. Samuel Gingerich and Dr. Erin Holmes. Without their guidance, advice, and love over the past 29 years (and weekly Sunday night calls), I would not be the scholar and person that I am today. I am also deeply appreciative of my non-academic family members for reminding me that there is life outside of graduate school. These members include my brother Matthew Gingerich and the Huttleston, Jones, Lehman, and Snyder aunts, uncles, and cousins. The love these family members have shown me started somewhere, and that is my grandparents. Grandma Jean and Grandpa Philip Holmes and Grandma Eunice and Grandpa Beryl Gingerich, thank you.



## ABSTRACT

Treating water in order to reduce human and environmental risks requires the use of electricity and chemicals, the generation of which creates emissions of air pollutants such as  $\text{NO}_x$ ,  $\text{SO}_2$ ,  $\text{PM}_{2.5}$ , and  $\text{CO}_2$ . Emissions of air pollutants establishes a health and environmental risk tradeoff between air and water pollution. Addressing air-water tradeoffs by adopting a one environment framework requires new methods for quantifying these tradeoffs, new technologies to minimize air-water tradeoffs, and new tools for decision makers to incorporate these tradeoffs into compliance decisions. In my thesis, I develop methods for quantifying damages from air emissions associated with water treatment; assess the feasibility of forward osmosis (FO), a technology which holds the promise to avoid air-water tradeoffs; and create a tool to holistically assess compliance with air and water emission standards for coal-fired power plants (CFPPs).

I start my thesis by creating a method to quantify the damages caused by the air emissions that resulting from the treatment of drinking water (Chapter 2), municipal wastewater (Chapter 3), and flue gas desulfurization (FGD) wastewater (Chapter 4). These studies use life-cycle models of energy and chemical consumption for individual water treatment unit processes in order to estimate embedded emissions of criteria air pollutants and greenhouse gasses per cubic meter of treated water. Damages from these additional air emissions are assessed and incorporated into benefit-cost analyses. I find that for drinking water rules, the net benefit of currently implemented rules remains positive but the promises of net benefits for some proposed rules are conditional on the compliance technology that is selected. For municipal wastewater, I find that while there are ~\$240 million (in 2012 USD) benefits in air emission reduction from installing biogas-fueled electricity generation nationwide, there are several states where biogas-fueled electricity creates more air emissions than it displaces. For FGD wastewater treatment, I

find that complying with the effluent limitation guidelines has an expected ratio of benefits to cost of 1.7-1.8, with damages concentrated in regions with large chemical manufacturing industries or electricity grids that are heavily reliant on coal.

In the next part of the thesis, I assess the techno-economic feasibility of power plant waste heat driven FO to reduce the air emissions associated with FGD wastewater treatment. In Chapter 5, I assess the quantity, quality and the spatial and temporal availability of waste heat from US coal, nuclear, and natural gas power plants. I find that while 18.9 billion GJ of potentially recoverable waste heat is discharged into the environment, only 900 million GJ of that heat is from the flue gas and is at a temperature high enough to drive water purification using forward osmosis (FO). In Chapter 6, I build a model of FO to assess its thermal energy consumption and find that the 900 million GJ of waste heat produced at coal and natural gas power plants is sufficient to meet their boiler feedwater and FGD wastewater treatment needs. In Chapter 7, I incorporate cost into the energy consumption model of FO, and conclude that treatment of FGD and gasification wastewater using waste heat driven FO is economically competitive with mechanical vapor recompression.

In Chapter 8, I create an energy-balance model of a CFPP and nine environmental control technologies for compliance with FGD wastewater and carbon capture regulations. I use this model to maximize plant revenue at the National Energy Technology Laboratory's 550 MW model CFPP without carbon capture. I find that revenue is maximized by using residual heat for water treatment or carbon capture. If both carbon capture and zero liquid discharge water treatment regulatory standards are in place, I conclude that the plant maximizes revenue by allocating residual heat and steam to amine-based carbon capture and electricity to mechanical vapor recompression for FGD wastewater treatment.

## TABLE OF CONTENTS

<b>Acknowledgements.....</b>	<b>ii</b>
<b>Abstract.....</b>	<b>iv</b>
<b>Table of Contents.....</b>	<b>vi</b>
<b>List of Tables.....</b>	<b>xi</b>
<b>List of Figures and Illustrations.....</b>	<b>xii</b>
<b>1.0 Introduction.....</b>	<b>1</b>
1.1 Context.....	1
1.2 Towards a One Environment Approach in Water Treatment.....	5
1.3 Overview.....	6
1.4 References.....	10
 <b>Part I – Quantifying Air-Water Tradeoffs Associated with Water Treatment</b>	
<b>2.0 Air Emission Damages from Municipal Drinking Water Treatment Under Current and Proposed Regulatory Standards.....</b>	<b>17</b>
2.1 Abstract.....	17
2.2 Introduction.....	17
2.3 Methods.....	20
2.3.1 Estimating Air Emission Damages from Drinking Water Treatment.....	20
2.3.2 Benefit-Cost Analysis of Drinking Water Regulations.....	24
2.3.3 Evaluating Regulatory Compliance Options.....	25
2.3.4 Forecasting Emissions from Electricity Generation.....	25
2.4 Results and Discussion.....	26
2.4.1 Air Emission Damages from Operating Baseline and Compliant Treatment Trains.....	26
2.4.2 Benefit-Cost Analysis of Drinking Water Regulations.....	29
2.4.3 Evaluating Regulatory Compliance Options.....	30
2.4.4 Future Air Emission Damages from Electricity Consumed in Drinking Water Treatment.....	31
2.5 Implications.....	32
2.6 Acknowledgements.....	34
2.7 Nomenclature.....	34
2.8 References.....	36
 <b>3.0 Air Emission Benefits of Biogas Electricity Generation at Municipal Wastewater Treatment Plants.....</b>	 <b>43</b>

3.1	Abstract.....	43
3.2	Introduction.....	43
3.3	Methods.....	45
3.3.1	Air Emission Damages from Municipal Wastewater Treatment.....	45
3.3.2	Evaluating the Energy Self-Sufficiency of Wastewater Treatment Plants.....	50
3.3.3	Air Emissions from Biogas Collection and Combustion.....	52
3.3.4	Uncertainty Analysis.....	55
3.4	Results.....	56
3.4.1	Damages from Municipal Wastewater Treatment.....	56
3.4.2	Energy Self-Sufficiency of POTWs.....	58
3.4.3	Air Emission Benefits from Biogas-Fueled Electricity Generation.....	61
3.4.4	Uncertainty Analyses.....	62
3.5	Discussion.....	65
3.6	Conclusions.....	67
3.7	Acknowledgements.....	68
3.8	Nomenclature.....	68
3.9	References.....	69

#### **4.0 Spatially Resolved Air-Water Emissions Tradeoffs Improve Regulatory Analyses for Electricity Generation.....79**

4.1	Abstract.....	79
4.2	Introduction.....	80
4.3	FGD Wastewater Treatment Process Inventories.....	83
4.4	Air Emissions from FGD Wastewater Treatment on a Cubic Meter Basis at the Plant Level.....	85
4.5	Total Annual Air Pollutant Emissions from FGD Wastewater Treatment at U.S. CFPPs.....	90
4.6	National Annual HEC Damages from Air Emissions Associated with FGD Wastewater Treatment at U.S. CFPPs.....	91
4.7	Air-Water Emissions Tradeoffs from FGD Wastewater Treatment.....	93
4.8	Implications for Regulatory Analysis of Air and Water Emissions Controls at CFPPs.....	96
4.9	Acknowledgements.....	98
4.10	Nomenclature.....	98
4.11	References.....	100

### **Part II – Avoiding Air-Water Tradeoffs Associated with CFPP Wastewater Treatment**

#### **5.0 Quantity, Quality, and Availability of Waste Heat from United States Thermal Power Generation.....106**

5.1	Abstract.....	106
5.2	Introduction.....	106
5.3	Methods.....	109
5.3.1	Quantity and Quality of Residual Heat.....	109

5.3.2	Temporal Availability of Residual Heat.....	114
5.3.3	Spatial Availability of Residual Heat.....	115
5.3.4	Residual Heat Forecasts.....	116
5.4	Results and Discussion.....	117
5.4.1	Quantity and Quality of Residual Heat.....	117
5.4.2	Recovering Residual Heat.....	121
5.4.3	Spatial-Temporal Availability of Residual Heat.....	122
5.4.4	Residual Heat Forecasts.....	125
5.4.5	Potential Applications of Residual Heat.....	127
5.5	Implications.....	128
5.6	Acknowledgements.....	129
5.7	Nomenclature.....	129
5.8	References.....	130

## **6.0 Water Treatment Capacity of Forward Osmosis Systems Utilizing Power Plant Waste Heat.....139**

6.1	Abstract.....	139
6.2	Introduction.....	140
6.3	Methods.....	143
6.3.1	CO <sub>2</sub> -NH <sub>3</sub> -H <sub>2</sub> O Separation Models in DSR Systems.....	143
6.3.2	Evaluating Separation Processes for DSR.....	144
6.3.3	Mathematical Model of Distillation for DSR System.....	147
6.3.4	Mathematical Model of FO Membrane Separation System.....	151
6.3.5	Comprehensive Model of FO Desalination System.....	154
6.3.6	Notes on Numerical Solution.....	156
6.3.7	FO Treatment Capacity of US Power Plants by Fuel Cycle and Size.....	156
6.4	Results and Discussion.....	156
6.4.1	Comparison of CO <sub>2</sub> -NH <sub>3</sub> -H <sub>2</sub> O Separation Models.....	156
6.4.2	Comparison of DSR Methods.....	159
6.4.3	Model Comparisons Between ASPEN and Mathematical Model.....	159
6.4.4	Description of Full Process Model.....	159
6.4.5	Modeling the FO Water Treatment Process to Minimize Heat Duty.....	162
6.4.6	FO Treatment Capacity of US Power Plants by Fuel Cycle and Size.....	163
6.4.7	Potential Applications of FO Treatment Capacity at US Power Plants...	165
6.5	Conclusions.....	166
6.6	Acknowledgements.....	167
6.7	Nomenclature.....	167
6.8	References.....	170

## **7.0 Technoeconomic Assessment of Waste Heat Driven Forward Osmosis Systems for Onsite Wastewater Treatment.....174**

7.1	Abstract.....	174
7.2	Introduction.....	174
7.3	Process Description and Modeling.....	176
7.3.1	FGD and Gasification Wastewater.....	176
7.3.2	Process Modeling.....	177

7.3.3	Benchmark Technologies.....	184
7.3.4	Case Studies.....	184
7.3.5	Sensitivity Analyses.....	185
7.4	Results and Discussion.....	186
7.4.1	Cost Minimized FO System Designs.....	186
7.4.2	Sensitivity Analyses.....	188
7.5	Conclusions.....	190
7.6	Acknowledgements.....	191
7.7	Nomenclature.....	191
7.8	References.....	193
<b>8.0</b>	<b>Redesigning the Regulated Power Plant: Optimizing Energy Allocation to Electricity Generation, Water Treatment, and Carbon Capture Processes at Coal-Fired Generating Facilities.....</b>	<b>201</b>
8.1	Abstract.....	201
8.2	Introduction.....	202
8.3	Materials and Methods.....	204
8.3.1	550 MW CFPP Base Model.....	204
8.3.2	Quantification of Plant Energy Sources.....	206
8.3.3	Energy Consumption of Carbon Capture Processes.....	207
8.3.4	Energy Consumption of Water Treatment.....	208
8.3.5	Revenue Impacts of Steam Allocation.....	210
8.4	Results and Discussion.....	212
8.4.1	Tradeoffs between Steam for Electricity Generation and MEA Carbon Capture Solvent Regeneration.....	213
8.4.2	Tradeoffs between Steam for Electricity Generation and Water Treatment.....	214
8.4.3	Revenue Tradeoffs in Steam Allocation.....	215
8.5	Implications.....	218
8.6	Acknowledgements.....	220
8.7	Nomenclature.....	220
8.8	References.....	221
<b>9.0</b>	<b>Summary and Recommendations.....</b>	<b>227</b>
9.1	Summary of Work.....	227
9.2	Contributions.....	231
9.3	Recommendations.....	232
9.3.1	Recommendations for Regulators.....	232
9.3.2	Recommendations for Municipal Water Utilities.....	234
9.3.3	Recommendations for Coal-Fired Power Plants.....	234
9.3.4	Recommendations for Researchers.....	235
9.4	References.....	237

## **Appendices**

Appendix 1: Supporting Information for Chapter 2.....	A2
Appendix 2: Supporting Information for Chapter 3.....	A24
Appendix 3: Supporting Information for Chapter 4.....	A46
Appendix 4: Supporting Information for Chapter 5.....	A47
Appendix 5: Supporting Information for Chapter 6.....	A48
Appendix 6: Supporting Information for Chapter 7.....	A49
Appendix 7: Supporting Information for Chapter 9.....	A72

## LIST OF TABLES

Table 2.1 Rules and compliance technologies.....	21
Table 2.2 Benefit-cost analysis for the six drinking water regulations after accounting for estimated air emission damages.....	29
Table 3.1 Uncertain parameters, values, and ranges.....	55
Table 5.1 Efficiency, energy and exergy of U.S. power plants.....	111
Table 5.2 Quantity, quality, and temporal availability of residual heat generated at power plants with capacity greater than 10 MW in 2012.....	118
Table 6.1 Model comparison.....,	144
Table 6.2 Specifications of the DSR system in this case study.....	151
Table 6.3 Parameters important for DSR systems design and corresponding design aspects....	155
Table 6.4 Comparison of distillation, steam stripping, and air stripping (DDS flowrate = 18 m <sup>3</sup> /hr).....	159
Table 6.5 Minimum normalized heat duty of each fuel cycle.....	163
Table 7.1 Optimization parameters for our four case studies.....	185
Table 8.1 Minimum estimated energy consumption associated with meeting chemical precipitation and biological treatment (CPBT) standard or the zero liquid discharge (ZLD) standard.....	215



## LIST OF FIGURES AND ILLUSTRATIONS

Figure 1.1 Environmental compliance decision making.....	2
Figure 2.1 Method for calculating the drinking water air emission damages and net benefits or net costs for the regulations included in this analysis.....	20
Figure 2.2 Per capita air emission damages associated with operating drinking water treatment processes under current and future regulatory scenarios.....	27
Figure 2.3 Air emission damages from reverse osmosis and granular activated carbon treatment for PFOA/PFOS removal at 58,000 drinking water facilities across the US.....	30
Figure 2.4 Projected air emission damages from electricity generated to treat US drinking water with the baseline treatment train and the additional air emissions that result from drinking water compliance.....	32
Figure 3.1 Methods for calculating the benefits from biogas-fueled electricity generation and the damages resulting from biogas heat generation.....	51
Figure 3.2 Air emission damages in 2012 from wastewater treatment from installed wastewater treatment and sludge digestion processes.....	57
Figure 3.3 Potential for biogas-fueled electricity generation to reduce net electricity demand at wastewater treatment plants in the CWNS database.....	59
Figure 3.4 Changes in air emissions associated with wastewater treatment resulting from biogas-fueled heat and electricity generation at wastewater treatment facilities in the continental United States.....	61
Figure 3.5 Uncertainty analyses for air emission damages from wastewater treatment and energy self-sufficiency of wastewater treatment.....	63
Figure 4.1 Process trains, auxiliary electricity consumption, and chemical consumption associated with treating 1 m <sup>3</sup> of FGD wastewater.....	85
Figure 4.2 Average air emissions per m <sup>3</sup> of FGD wastewater treatment using CPBT or ZLD processes.....	88
Figure 4.3 Estimated annual HEC damages associated with transition from FGD wastewater impoundment to FGD wastewater treatment by CPBT or ZLD processes.....	92
Figure 4.4 Estimated benefits and costs of CPBT and ZLD technologies for FGD treatment on a per cubic meter basis.....	94
Figure 5.1 Methods and data sources for calculating residual heat quantity and availability.....	110

Figure 5.2 Residual heat production and capacity factor by fuel source.....	119
Figure 5.3 Spatial distribution of techno-economically feasible residual heat in the U.S.....	123
Figure 5.4 Forecasted residual heat generation based on EIA fuel consumption projections under 21 different scenarios.....	126
Figure 6.1 Generalized process flow diagram of the forward osmosis process.....	141
Figure 6.2 Schematic diagram of the FO membrane.....	154
Figure 6.3 Input and output of parameter networks connecting the process equipment.....	155
Figure 6.4 Comparison of the predicted heat duty of the draw solute regeneration process for three different CO <sub>2</sub> -NH <sub>3</sub> -H <sub>2</sub> O separation models.....	157
Figure 6.5 Parametric analyses of heat duty of the FO process under various operating parameters.....	161
Figure 6.6 Upper bound estimates of the residual heat driven FO water treatment capacity of US power plants.....	165
Figure 7.1 The forward osmosis and crystallization process modeled in this paper.....	177
Figure 7.2 Optimization model.....	178
Figure 7.3. Optimization results for wastewater treatment requiring zero liquid discharge.....	186
Figure 7.4 Sensitivity analyses on the cost of FO with crystallization for the NETL sub-critical coal case without carbon capture.....	188
Figure 8.1 Energy balance for the NETL 550 MW turbines.....	205
Figure 8.2 Parasitic losses from (A) carbon capture and (B) FGD wastewater treatment processes.....	212
Figure 8.3 Revenue per hour as a function of steam, residual heat, and electricity used for environmental compliance.....	217

# CHAPTER 1: INTRODUCTION

## 1.1 Context

The federal government first started to meaningfully address environmental regulations for water quality in the late 1960s and early 1970s. Until then, the nation's environmental waters had been left unfishable and unswimable by decades of industrial and municipal wastewater discharges.<sup>1</sup> The nation's drinking water was no better, as a 1969 study by the US Public Health Service found that more than 40% of drinking water systems did not comply with state and federal standards.<sup>2</sup> This state of affairs launched a flurry of regulatory activity to clean up water in the US. These activities were codified by Congress in two landmark pieces of legislation, the Clean Water Act (CWA) and the Safe Drinking Water Act (SDWA). Both pieces of legislation have led to significant impact on the quality of environmental waterbodies and drinking water.<sup>3-4</sup>

The regulations promulgated by the Environmental Protection Agency (EPA) under the CWA and SDWA drive utilities, municipalities, industry, and private citizens to make decisions about water treatment technologies to install or infrastructure to build (Figure 1.1). More than 15,000 publicly operated treatment works (POTWs) in the United States treat domestic, commercial, and industrial wastewater in order to protect receiving waterbodies under Clean Water Act regulations.<sup>5</sup> Industries often install on-site wastewater treatment systems in order to comply with the nearly 60 Effluent Limitation Guidelines (ELGs) promulgated by the EPA under the auspices of the Clean Water Act.<sup>6</sup> Finally, 52,000 community water systems across the country treat and supply water to 286 million people in a manner compliant with Safe Drinking Water Act standards.<sup>7</sup>

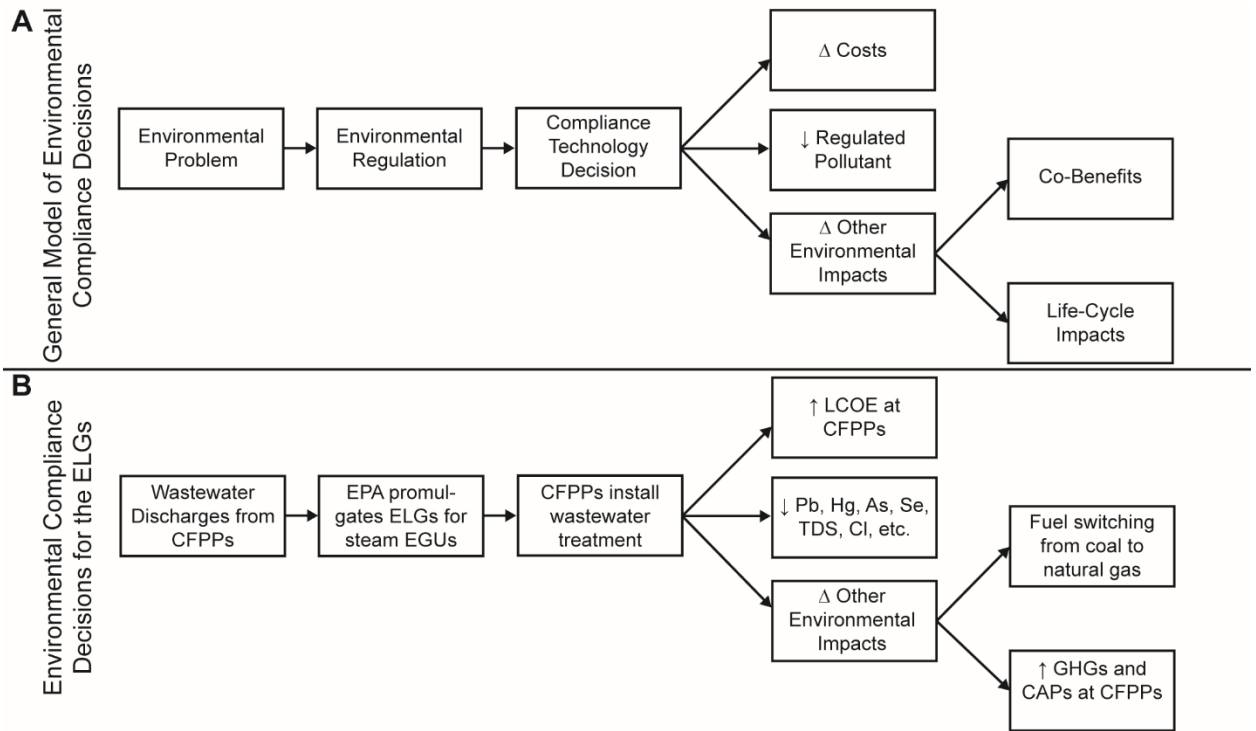


*Figure 1.1 – Environmental compliance decision making for a (A) generic compliance decision and (B) example for coal-fired power plants (CFPPs) decisions to comply with the effluent limitation guidelines (ELGs). In general, an environmental problem rises to the policy agenda, a regulation is promulgated, and the regulated sector makes a decision about how to comply with the new regulation. As a result of the compliance decision, discharges of the regulated pollutant decrease. Compliance decisions also change the costs to the regulated industry and lead to other environmental changes.*

Water infrastructure requires the use of electricity and chemicals. The average electricity consumption for water treatment in the United States is approximately 0.05-0.1 kWh/m<sup>3</sup>.<sup>8</sup> This is likely to increase as regulations target more difficult to remove contaminants and water suppliers have to move to more saline sources of water. Energy consumption for municipal wastewater varies between 0.25-0.6 kWh/m<sup>3</sup>, mostly due to the electricity consumption for pumping air in

activated sludge processes.<sup>8-9</sup> Treatment also requires chemicals such as alum for coagulation, sodium hypochlorite for disinfection, fluorosilicic acid for fluoridation, and activated carbon for adsorption processes.<sup>9-11</sup>

The emissions produced by electricity generation and chemical manufacturing result in a public health tradeoff. Emissions of criteria air pollutants lead to human health and environmental damages.<sup>12-15</sup> Emissions of greenhouse gases contribute to climate change.<sup>16</sup> If the compliance technologies that municipalities or industries choose to install are energy- or chemical-intensive, emissions of air pollutants can set up risk tradeoffs that potentially lead to damages greater than the benefits.

In a few cases, policy makers and regulators have considered risk tradeoffs while setting regulatory levels. In the water area, the most notable example of the EPA considering risk tradeoffs is that of pathogens and disinfection byproducts.<sup>17-18</sup> While promulgating the Long-Term Enhanced Surface Water Treatment Rules, the EPA explicitly balanced the risks of microbial contamination in drinking water and cancer from disinfection byproducts. In only one recent regulation, however, did the EPA consider air emission damages in setting a regulation about water quality, the Effluent Limitation Guidelines for steam electric generating units.<sup>19-20</sup> Even in this case, the EPA only considered air emissions from electricity generation and did not include air emissions from chemical manufacturing.

While regulators have quantified risk tradeoffs for these rules, there are a multitude of other cases where they have not. Often these overlooked risk tradeoffs are scenarios where the risks cross environmental media or cross sector boundaries. A handful of examples from the literature of overlooked risk tradeoffs include the pesticide atrazine,<sup>21</sup> the gasoline additive

methyl tert-butyl ether (MTBE),<sup>22</sup> and the use of brominated activated carbon for mercury removal in coal-fired power plants (CFPPs).<sup>23-24</sup>

Members of the policy<sup>25-26</sup> and environmental engineering<sup>27</sup> communities have acknowledged a need to move away from a single-media or single-sector approaches. Instead they advocate for the adoption of a *one environment* framework. Whereas a traditional regulatory framework is based upon regulating an individual sector or single environmental media at a time, the one environment framework recognizes that all sectors impact the environment and that the environment consists of all media. Using a one environment framework requires taking into account how rules impact all environmental media and the impacts on all sectors of the economy simultaneously.<sup>25</sup> Adopting a one environment framework challenges the current structure of regulatory agencies of bounded oversight, which is the tendency of regulatory bodies to have responsibility for only one media or sector.<sup>25</sup> While the structure of regulatory bodies would need to change to accommodate this framework, a tool for performing one environment regulatory analyses already exists – benefit-cost analysis (BCA).

Benefit-cost analysis is a frequently used tool for policy analysis. Its use in the United States dates back to the Army Corps of Engineers in the 1930s. It became a cornerstone of the regulatory process after it was mandated by Executive Order 12291 in 1981.<sup>28</sup> As BCA is already used in setting water and wastewater regulations, using BCA to address one environment considerations is an attractive proposal. However, there is still a need to develop the methods required to quantify one environment thinking analyses so that they can be incorporated into BCAs.

## **1.2 Towards a One Environment Approach in Water Treatment**

There are three main barriers impeding the adoption of a one environment framework for water treatment decisions. First, as mentioned above there is a lack of methods and tools for quantifying tradeoffs across environmental media and sectors in order to include tradeoffs in BCAs. Second, most conventional water treatment processes require chemicals or electricity, so there is a need to develop new technologies that reduce or eliminate reliance on chemicals and electricity. Finally, there is a need for tools to support treatment system operators in making compliance decisions that reflect a one environment approach.

First, life-cycle assessment (LCA) is a widely used tool for modeling the environmental impacts of a good or process across environmental media and sectors.<sup>29</sup> However, many LCA practitioners have been hesitant to place dollar values on these environmental impacts.<sup>30</sup> This reluctance is often due to a desire to promote analytical transparency and for analysts to not impose their values onto an analysis. But, choosing between options in a comparative LCA without valuing the environmental impacts of different options is a challenging, if not impossible, task.<sup>30</sup> Valuing LCA impacts using conventional, well-known and frequently used metrics would allow LCA to more easily contribute to one environment decision making.

Second, it may be impossible to avoid cross-sector and cross-media impacts without water treatment technologies that rely on chemicals or electricity. Fortunately, engineers are developing a variety of water treatment technologies that can run on low-temperature waste heat and are suitable for a variety of applications.<sup>31-36</sup> However, when used in the real world many of these systems rely on the combustion of primary fuel for energy.<sup>37</sup> As a result, they do not avoid the tradeoffs between air and water. Understanding the availability of waste heat and the

feasibility of waste heat driven water treatment systems is critical to avoid air and water risk tradeoffs.

Finally, there is also a need for the development of decision support tools for holistic regulatory compliance. This gap is most evident in the electricity generating sector, as it is the largest source of air<sup>38</sup> and industrial water pollution<sup>39</sup> in the United States. Driven by frequent regulatory activity on air pollution from power plants, tools such as the Integrated Environmental Compliance Model<sup>40</sup> exist to support power plant decision making for evaluating compliance strategies with air emission regulations. The large gap between the 1982 and 2015 EPA Effluent Limitation Guidelines on Steam Electric Generating Units (ELGs) means that there has not been a regulatory driver to create similar tools to support compliance decisions for wastewater treatment, let alone tools to facilitate complying with both air and water regulations in a cost-effective manner.

### **1.3 Overview**

Replacing the current regulatory environment of piecemeal, single-sector and single media regulations with a one environment regulatory framework is a critical step in protecting human health and ensuring that the nation's water infrastructure does not inadvertently increase health risks. This thesis contributes to the one environment approach by developing a model to quantify the air emissions and damages that result from water treatment. I then use this model in a variety of contexts. These air emission damages are then used in a benefit-cost analysis for water and wastewater treatment decisions. In this thesis, I also examine the technologies and choices that CFPPs face in making compliance decisions that take into account multiple regulations targeting pollutants in different environmental media.



This work is separated into two parts. In Part I, I develop and use a tool to quantify and value the damages from air emissions associated with water and wastewater treatment. This tool is then used in three different case studies: municipal drinking water, municipal wastewater, and CFPP wastewater. In Part II, I focus on applying one environment thinking to environmental compliance decision-making at CFPPs. This entails modeling holistic energy and technology choices for CFPP compliance with the ELGs and the Clean Power Plan.

Chapter 2 develops a model for quantifying air emissions associated with water treatment. I then use this model to quantify the health, environment, and climate (HEC) damages from air emissions associated with six regulations that have already been promulgated or are currently under consideration. These drinking water standards are for arsenic, lead and copper, disinfection byproducts, strontium, hexavalent chromium, and the perfluoroalkyls PFOA and PFOS. This model quantifies the air emissions, and the resulting damages are then integrated into a benefit-cost analysis framework. I find that while air emissions are unlikely to reverse the signs of the BCAs for these regulations, different compliance technology options can impose radically different air emission damages. As a result, the EPA should account for these differences in air emission damages when they identify the best available technology for drinking water regulations.

Chapter 3 adapts this model to municipal wastewater treatment and uses it to quantify the HEC benefits of widespread adoption of anaerobic biogas-fueled electricity generation. In this chapter, I first quantify the air emission damages associated with wastewater treatment at POTWs in the United States. I then calculate the potential air emission reductions from substituting grid electricity with on-site biogas fueled electricity generation. I find that biogas-

fueled electricity generation has the potential to reduce air emission damages associated with wastewater treatment by \$310 million annually or 25% of the total damages.

Chapter 4 applies this model to the treatment of flue gas desulfurization (FGD) wastewater in order to demonstrate the need for highly resolved, spatial data in making regulatory decisions. This study incorporates emissions from CFPP electricity and chemical manufacturing into the BCA for FGD wastewater treatment performed by the EPA. I also quantify the differences in using spatially-resolved data versus average process or nation-level data. Using this model, I find that there is an order of magnitude difference in air emission damages associated with FGD wastewater treatment and the EPA reported benefits of reduced FGD wastewater pollution.

In Part I of this thesis, I demonstrate that the use of electricity to treat drinking water and wastewater sets up the potential for air emission damages in excess of the benefits that result from water treatment. Avoiding these tradeoffs is a critical task for environmental engineers as they protect human health<sup>27</sup> and will require new, creative approaches for selecting compliance technologies and designing regulations. In Part II of this thesis, I examine the techno-economic feasibility of one solution for avoiding air-water tradeoffs at CFPPs – the use of waste heat, instead of electricity, to drive treatment processes.

Chapter 5 starts Part II of this thesis by examining the quantity, quality, and spatio-temporal availability of waste heat from thermal power generation facilities. I quantify the recoverable heat from the exhaust gas and cooling water by combining energy balance models with EIA data on coal, nuclear, and natural gas power plants in the United States. I also perform an economic assessment to model the maximum distance away from power plants where waste heat transport is economically viable. I find that the off-site applications of waste heat that are

often discussed in the literature (e.g. district heating<sup>41-42</sup> or desalination<sup>43-45</sup>) are unlikely to occur due to spatio-temporal constraints. On-site applications of waste heat however are technically viable and hold the potential to improve power plant efficiency.

Chapter 6 develops a model of forward osmosis (FO), a technology that has shown promise in using waste heat for water treatment.<sup>45-46</sup> I use this model to identify general trends in the design and operation of waste heat driven FO systems. I use these trends in order to develop engineering rules of thumb that reduce the energy consumption of the system. Finally, I use this model to create first order estimates of waste heat driven FO treatment capacity from the US coal and natural gas power generation fleet. I find that for all but five coal- and natural gas-fired power plants in the US, waste heat driven FO can theoretically meet FGD wastewater and boiler feedwater treatment needs.

Chapter 7 extends the model of FO developed in Chapter 6 and uses it for a techno-economic assessment of FO's feasibility. I perform optimization for four different case studies of FO, of which three are for flue gas desulfurization wastewater treatment and one is for gasification wastewater treatment system. I then benchmark FO against the EPA identified best available technology, mechanical vapor recompression and crystallization (MVCC), to determine if FO is economically competitive. I find that waste-heat driven FO is a competitive way for coal-fired and gasification power plants to achieve compliance with the ELGs.

Chapter 8 creates a model to support regulatory compliance at CFPPs by identifying revenue optimal solutions for energy dispatch to electricity generation, carbon capture, and wastewater treatment. I apply this model to the National Energy Technology Laboratory's 550 MW pulverized CFPPs without carbon capture model and include five different water treatment technologies (four thermal and one electric) and four different carbon capture technologies (three

thermal and one electric). I use this model in order to determine the revenue optimal energy allocation strategy under six different regulatory regimes. Critically, I find that regulatory uncertainty surrounding carbon capture prevents power plants from making energy-efficient choices surrounding flue gas desulfurization wastewater treatment.

Finally, Chapter 9 synthesizes the preceding chapters and provides recommendations to four different audiences: regulators, municipal water utilities, coal-fired power plants, and researchers.

## 1.4 References

1. Rosenbaum, W. A., *Environmental Politics & Policy*. 7th ed.; CQ Press: Washington, D.C., 2007; p 369.
2. Bureau of Water Hygiene, Community Water Supply Study: Analysis of National Survey Findings. U.S. Department of Health, Education, and Welfare, Public Health Service: Washington, D.C., 1970.
3. Keiser, D. A.; Shapiro, J. S. *Consequences of the Clean Water Act and the Demand for Water Quality*; National Bureau of Economic Research: Cambridge, MA, 2017.
4. Roberson, J. A., What's next after 40 years of drinking water regulations? *Environ Sci Technol* **2011**, *45*, 154-160.
5. U.S. Environmental Protection Agency About the Clean Watersheds Needs Survey (CWNS). <https://www.epa.gov/cwns/about-clean-watersheds-needs-survey-cwns> (accessed June 10).
6. U.S. Environmental Protection Agency Effluent Guidelines. <https://www.epa.gov/eg> (accessed July 3, 2017).

7. U.S. Environmental Protection Agency Safe Drinking Water Information System (SDWIS). <https://www3.epa.gov/enviro/facts/sdwis/search.html> (accessed March 25, 2017).
8. Plappally, A. K.; Lienhard V, J. H., Energy requirements for water production, treatment, end use, reclamation, and disposal. *Renewable and Sustainable Energy Reviews* **2012**, *16* (7), 4818-4848.
9. Stokes, J. R.; Horvath, A., Supply-chain environmental effects of wastewater utilities. *Environmental Research Letters* **2010**, *5* (1), 014015.
10. Stokes, J. R.; Hovarth, A., Energy and Air Emission Effects of Water Supply *Environmental Science & Technology* **2009**, *43* (2680-2687).
11. Stokes, J.; Horvath, A., Life-Cycle Assessment of Urban Water Provision: Tool and Case Study in California *Journal of Infrastructure Systems* **2011**, *17* (1), 15-24.
12. Muller, N. Z.; Mendelsohn, R., Measuring the damages of air pollution in the United States. *Journal of Environmental Economics and Management* **2007**, *54* (1), 1-14.
13. Apte, J. S.; Marshall, J. D.; Cohen, A. J.; Brauer, M., Addressing Global Mortality from Ambient PM<sub>2.5</sub>. *Environmental Science & Technology* **2015**, *49* (13), 8057-66.
14. Heo, J.; Adams, P. J.; Gao, H. O., Public Health Costs of Primary PM<sub>2.5</sub> and Inorganic PM<sub>2.5</sub> Precursor Emissions in the United States. *Environmental Science & Technology* **2016**, *50* (11), 6061-70.
15. Caiazzo, F.; Ashok, A.; Waitz, I. A.; Yim, S. H. L.; Barrett, S. R. H., Air pollution and early deaths in the United States. Part I: Quantifying the impact of major sectors in 2005. *Atmospheric Environment* **2013**, *79*, 198-208.

16. Interagency Working Group on the Social Cost of Carbon, Technical Support Document: Technical Update of the Social Cost of Carbon for Regulatory Impact Analysis. Washington, D.C., 2015.
17. Richardson, S. D., Water Analysis: Emerging Contaminants and Current Issues. *Analytical Chemistry* **2009**, 81 (12), 4645-4677.
18. Putnam, S. W.; Wiener, J. B., Seeking Safe Drinking Water. In *Risk vs. Risk*, Graham, J. D.; Wiener, J. B., Eds. Harvard University Press: Cambridge, Massachusetts, 1995.
19. U.S. Environmental Protection Agency, Benefit and Cost Analysis for the Effluent Limitations Guidelines and Standards for the Steam Electric Power Generating Point Source Category. U.S. Environmental Protection Agency: Washington, D.C., 2015.
20. U.S. Environmental Protection Agency, Regulatory Impact Analysis for the Effluent Limitations Guidelines and Standards for the Steam Electric Power Generating Point Source Category; U.S. Environmental Protection Agency: Washington, D.C., 2015.
21. Tesfamichael, A. A.; Caplan, A. J.; Kaluarachchi, J. J., Risk-cost-benefit analysis of atrazine in drinking water from agricultural activities and policy implications. *Water Resources Research* **2005**, 41 (5).
22. Stickers, D., The Unintended Consequence of Reformulated Gasoline. In *Improving Regulation: Cases in Environment, Health, and Safety*, Fischbeck, P. S.; Farrow, R. S., Eds. Resources for the Future Washington, D.C., 2001.
23. Wang, Y.; Small, M. J.; VanBriesen, J. M., Assessing the Risk Associated with Increasing Bromine in Drinking Water Sources in the Monongahela River, Pennsylvania. *Journal of Environmental Engineering* **2017**, 143 (3).

24. Good, K. D.; VanBriesen, J. M., Current and Potential Future Bromide Loads from Coal-Fired Power Plants in the Allegheny River Basin and Their Effects on Downstream Concentrations. *Environmental Science & Technology* **2016**, *50* (17), 9078-88.
25. Wiener, J. B.; Graham, J. D., Resolving Risk Tradeoffs. In *Risk vs. Risk: Tradeoffs in Protecting Health and the Environment*, Graham, J. D.; Wiener, J. B., Eds. Harvard University Press: Cambridge, MA, 1995.
26. Gray, W. B. S.; Ronald J, Multimedia Pollution Regulation and Environmental Performance: EPA's Cluster Rule. Resources for the Future: Washington, D.C., 2015.
27. Daigger, G. T.; Murthy, S.; Love, N. G.; Sandino, J., Transforming Environmental Engineering and Science Education, Research, and Practice. *Environmental Engineering Science* **2017**, *34* (1), 42-50.
28. Morgan, M. G., *Theory and Practice in Policy Analysis: Including Applications in Science and Technology*. Cambridge University Press: New York, NY, 2017.
29. Matthews, H. S.; Hendrickson, C. T.; Matthews, D. H., *Life Cycle Assessment: Quantitative Approaches for Decisions That Matter*. Carnegie Mellon University: Pittsburgh, PA, 2015.
30. Klopffer, W.; Grahl, B., *Life Cycle Assessment (LCA) A Guide to Best Practice*. Wiley-VCH: Weinheim, Germany, 2014.
31. Chen, Q.; Li, Y.; Chua, K. J., On the thermodynamic analysis of a novel low-grade heat driven desalination system. *Energy Conversion and Management* **2016**, *128*, 145-159.
32. Thiel, G. P.; Tow, E. W.; Banchik, L. D.; Chung, H. W.; Lienhard, J. H., Energy consumption in desalinating produced water from shale oil and gas extraction. *Desalination* **2015**, *366*, 94-112.

33. Subramani, A.; Jacangelo, J. G., Emerging desalination technologies for water treatment: a critical review. *Water Res* **2015**, 75, 164-87.
34. Shannon, M. A.; Bohn, P. W.; Elimelech, M.; Georgiadis, J. G.; Marinas, B. J.; Mayes, A. M., Science and technology for water purification in the coming decades. *Nature* **2008**, 452 (7185), 301-10.
35. Shahzad, M. W.; Ng, K. C.; Thu, K., Future sustainable desalination using waste heat: kudos to thermodynamic synergy. *Environ. Sci.: Water Res. Technol.* **2016**, 2 (1), 206-212.
36. Khawaji, A. D.; Kutubkhanah, I. K.; Wie, J.-M., Advances in seawater desalination technologies. *Desalination* **2008**, 221 (1-3), 47-69.
37. Pendergast, M. M.; Nowosielski-Slepowron, M. S.; Tracy, J., Going big with forward osmosis. *Desalination and Water Treatment* **2016**, 57 (55), 26529-26538.
38. National Research Council, *Hidden Costs of Energy: Unpriced Consequences of Energy Production and Use*. The National Academies Press: Washington, D.C., 2010.
39. U.S. Environmental Protection Agency *Environmental Assessment for the Effluent Limitations Guidelines and Standards for the Steam Electric Power Generating Point Source Category*; U.S. Environmental Protection Agency: Washington, D.C., 2015.
40. Rubin, E. S.; Zhai, H. About IECM. <https://www.cmu.edu/epp/iecm/about.html> (accessed July 5,2017).
41. Chae, K.-J.; Kang, J., Estimating the energy independence of a municipal wastewater treatment plant incorporating green energy resources. *Energy Conversion and Management* **2013**, 75, 664-672.



42. Erdem, H. H.; Dagdas, A.; Sevilgen, S. H.; Cetin, B.; Akkaya, A. V.; Sahin, B.; Teke, I.; Gungor, C.; Atas, S., Thermodynamic analysis of an existing coal-fired power plant for district heating/cooling application. *Applied Thermal Engineering* **2010**, *30* (2-3), 181-187.
43. Ghalavand, Y.; Hatamipour, M. S.; Rahimi, A., A review on energy consumption of desalination processes. *Desalination and Water Treatment* **2014**, *54*, 1526-1541.
44. Elimelech, M.; Phillip, W. A., The future of seawater desalination: energy, technology, and the environment. *Science* **2011**, *333* (6043), 712-7.
45. McGinnis, R. L.; Elimelech, M., Global Challenges in Energy and Water Supply: The Promise of Engineered Osmosis. *Environmental Science & Technology* **2008**, *42* (23), 8625-8629.
46. McGinnis, R.; Elimelech, M., Energy requirements of ammonia-carbon dioxide forward osmosis desalination. *Desalination* **2007**, *207*, 370-382.

## **PART I**

# **QUANTIFYING AIR-WATER TRADEOFFS ASSOCIATED WITH WATER TREATMENT**

## **CHAPTER 2: AIR EMISSIONS DAMAGES FROM MUNICIPAL DRINKING WATER TREATMENT UNDER CURRENT AND PROPOSED REGULATORY STANDARDS<sup>1</sup>**

### **2.1 Abstract**

Water treatment processes present inter-sectoral and cross-media risk trade-offs that are not presently considered in Safe Drinking Water Act regulatory analyses. This paper develops a method for assessing the air emission implications of common municipal water treatment processes used to comply with recently promulgated and proposed regulatory standards for arsenic, lead and copper, disinfection byproducts, chromium (VI), strontium, and PFOA/PFOS. Life-cycle models of electricity and chemical consumption for individual drinking water unit processes are used to estimate embedded NO<sub>x</sub>, SO<sub>2</sub>, PM<sub>2.5</sub>, and CO<sub>2</sub> emissions on a cubic meter basis. We estimate air emission damages from currently installed treatment processes at US drinking water facilities to be on the order of \$500 million USD annually. Fully complying with six promulgated and proposed rules would increase baseline air emission damages by approximately 50%, with three-quarters of these damages originating from chemical manufacturing. Despite the magnitude of these air emission damages, the net benefit of currently implemented rules remains positive. For some proposed rules, however, the promise of net benefits remains contingent on technology choice.

### **2.2 Introduction**

The Safe Drinking Water Act (SDWA) provides regulatory authority to the US federal government to create enforceable standards for drinking water quality and safety.<sup>1</sup> These standards have enabled extraordinary gains in public health,<sup>2</sup> and retrospective analyses of

---

<sup>1</sup> This chapter is based on a paper co-authored with Prof. Meagan Mauter that was submitted to at Environmental Science & Technology.

historic drinking water quality regulations indicate that the benefits have far exceeded any compliance costs.<sup>2, 3</sup> Fully assessing these benefits and costs for emerging drinking water contaminants is more challenging, particularly when contaminant removal processes impose systemic risk tradeoffs.<sup>4</sup>

The most notable example of these risk trade-offs in drinking water regulatory analyses is for disinfection and disinfection byproducts. In establishing the Long-Term Enhanced Surface Water Treatment Rules,<sup>5</sup> the EPA set regulatory standards to balance the competing risks of acute illness from microbial contamination with the risks of cancer from disinfection byproducts.<sup>6</sup> There is also a growing body of research on inter-sectoral risk trade-offs involving drinking water, including the use of methyl *tert*-butyl ether (MTBE) as a gasoline additive,<sup>7</sup> bromide for mercury control at power plants,<sup>8, 9</sup> and atrazine as a pesticide.<sup>10</sup> But the incorporation of inter-sectoral and inter-media (e.g. water and air or water and soil) trade-offs into regulatory analyses is often limited by the “bounded oversight” of the regulators responsible for designing drinking water regulations.<sup>7, 11</sup> Researchers have argued that benefit-cost analysis can address bounded oversight to express the benefits and damages to a variety of media.<sup>12, 13</sup> Even with benefit-cost analysis, however, an analyst must make a deliberate choice to include cross-media impacts in the scope.

Drinking water regulatory analyses have also neglected to consider trade-offs that occur over the life-cycle of the water treatment system, most notably the operation phase. Drinking water systems comply with SDWA rules by installing separation processes that rely on electricity and chemicals.<sup>14, 15</sup> Life-cycle assessments (LCAs) of drinking water systems have demonstrated that the majority of impacts associated with drinking water treatment occur as a result of electricity and chemical consumption during plant operation.<sup>15-18</sup> These impacts include

emissions of greenhouse gasses (GHGs) and the criteria air pollutants (CAPs) NO<sub>x</sub>, SO<sub>2</sub>, and particulate matter from electricity generation and chemical manufacturing. These indirect emissions of GHGs and CAPs produced over the life cycle of water treatment impose human health, environmental, and climate (HEC) damages.<sup>19-23</sup>

While there are a multitude of drinking water treatment LCAs that quantify the energy intensity or GHG and CAP emissions from water treatment,<sup>15-17, 24-29</sup> we are unaware of any that quantify the human health damages associated with these emissions. Furthermore, the vast majority of these LCAs were performed for a single treatment train, rather than for the diverse set of processes currently installed at drinking water treatment facilities around the US. Performing an accurate estimate of the air emission damages from US water treatment plants under current and future regulatory scenarios is further confounded by the high regional variability in the emissions factors associated with chemical and electricity process inputs. In the absence of quantitative methods for estimating air emission damages from existing and emerging water treatment processes, rulemaking activities have been unable to consider competing risks from diminished air or water quality.

This work fills the air-water risk tradeoff gap by developing and applying a quantitative method for evaluating the life-cycle air emission damages from drinking water treatment. We build life-cycle models of electricity and chemical consumption for drinking water unit processes, estimate the embedded emissions of NO<sub>x</sub>, SO<sub>2</sub>, PM<sub>2.5</sub>, and CO<sub>2</sub>, and provide spatially resolved estimates of associated damages to human health and the environment. We apply this method to estimate the air emission damages from installed water treatment processes at all US drinking water facilities. Finally, we evaluate the air-water risk tradeoffs for six proposed and promulgated drinking water regulations.

## 2.3 Methods

### 2.3.1 Estimating Air Emission Damages from Drinking Water Treatment

To calculate the air emission damages associated with drinking water treatment processes we combine treatment level-facility data with state-level data on electricity consumption, chemical manufacturing, and air emission damages (Figure 2.1).

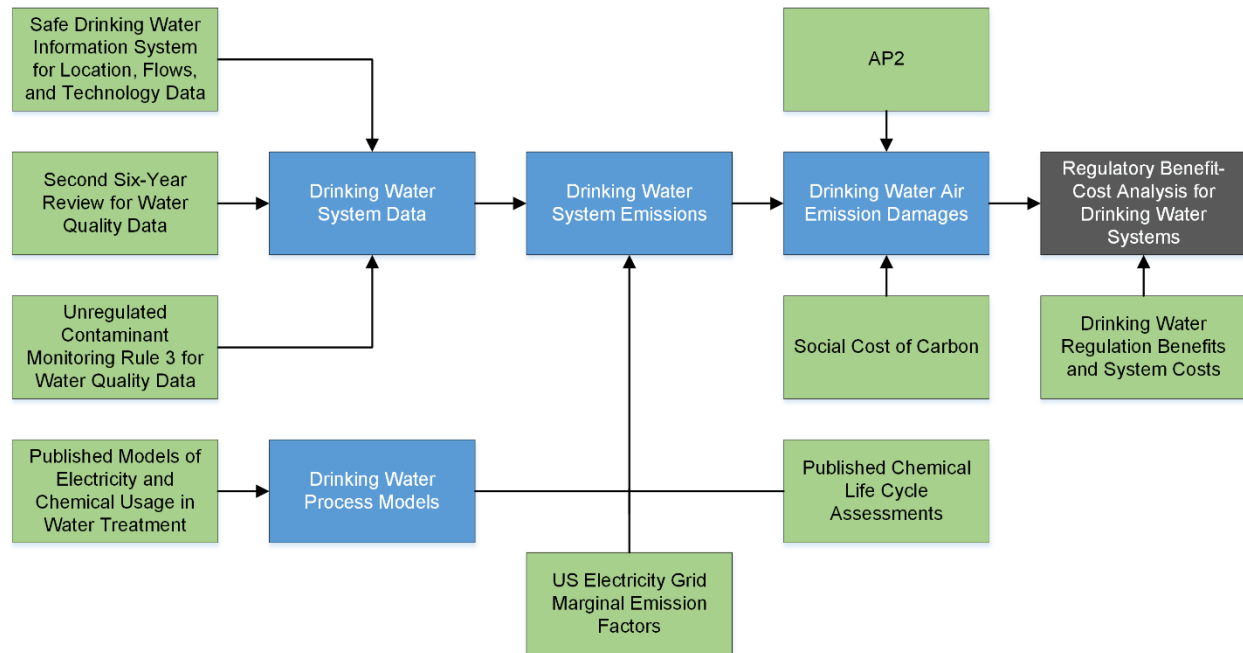


Figure 2.1. Method for calculating the drinking water air emission damages and net benefits or net costs for the regulations included in this analysis.

For this analysis, we focus on six different contaminant/regulations and compliance technologies: Arsenic,<sup>30</sup> Lead and Copper,<sup>31</sup> Disinfectant By-Products (DBPs),<sup>5</sup> Hexavalent Chromium,<sup>32</sup> Strontium,<sup>33</sup> and Perfluorooctanoic Acid (PFOA) and Perfluorooctyl Sulfonate (PFOS)<sup>34</sup> (Table 2.1, Supporting Information in Appendix 1Section 1.0). Three of these rules (Arsenic, Lead and Copper, and DBP) are finalized. The other three rules, Hexavalent Chromium, Strontium, and PFOA/PFOS, are at various stages in the regulatory process. These

rules will require the installation of new treatment processes at non-compliant facilities. Our analysis of the air emission impacts of regulations considers only the effects of installing new processes at non-compliant plants to meet proposed standards. If a facility already has a compliance technology installed and is compliant with the standard, we do not consider it in evaluating the air emissions associated with complying with that rule.

*Table 2.1. Rules and Compliance Technologies*

Rule	Compliance Technologies	Standard	Number of Non-Compliant Systems
Arsenic	Iron Co-Precipitation	10 ug/L	1,086
Lead and Copper	Corrosion Inhibitor	Lead 15 ug/L Copper 1.3 mg/L	2,757
DBP	GAC Adsorption	TTHM 80 ug/L HAA5 60 ug/L	1,697
Chromium (VI)	Reverse Osmosis	10 ug/L	25
Strontium	Lime Soda Ash Softening	1.5 mg/L	113
PFOS/PFOA	Reverse Osmosis / GAC Adsorption	Total 70 ng/L	27,000

*Drinking Water System Data.* We use data from the Safe Drinking Water Information System (SDWIS),<sup>35</sup> Unregulated Contaminant Monitoring Rule (UCMR),<sup>36</sup> and Information Collecting Rule (ICR)<sup>37</sup> (SI Section 2.0) to identify the (1) state, (2) installed treatment technologies (SI Section 3.0), and (3) volume of water for each of 47,500 drinking water systems serving 288 million people.

We use the location of each facility reported in SDWIS to identify the appropriate state-level marginal emissions factor<sup>38</sup> for generating electricity used during water treatment. SDWIS also identifies currently installed treatment processes that we use in developing a model of baseline emissions from drinking water treatment. SDWIS does not report water production, and so we estimate total annual water production for system  $i$ ,  $\forall_i$  [m<sup>3</sup>/yr], as the product of SDWIS

reported population served,  $Pop_{served}$  [person], and the average per capita water consumption per year,  $A_{pc}$  [ $m^3$ /person·yr], of  $124 m^3$ /person·yr<sup>39</sup> as shown in Equation 2.1.

$$\Psi_i = A_{PC} Pop_{i,served} \quad (2.1)$$

We determine facilities that will need to install additional treatment technologies to comply with the six water quality rules (Table 2.1) by comparing the MCL for each rule to water quality data reported in the UCMR and the ICR. If water quality data are not available for a facility, we apply state-averaged water quality data for that facility. We assume that any compliance technologies that are installed are operated to in order to achieve compliance with the regulation.

*Life-Cycle Inventory of Air Emissions from Drinking Water Systems.* For each facility in our dataset, we use SDWIS<sup>35</sup> to inventory the water treatment technologies currently installed in the “baseline” treatment train. For non-compliant systems, we also inventory technologies necessary to bring a “regulated” treatment train into compliance with each of the six pending or proposed water quality rules (SI Section 1.0). Average electricity<sup>27, 40</sup> and chemical inputs<sup>15, 27, 41</sup> for each of these treatment processes is obtained from the published literature and reported in SI Sections 2.0 and 3.0 and Tables S1-S3. Finally, we estimate the air emissions embedded in these electricity and chemical inputs in the year 2014.

The mass of annual air emissions associated with electricity consumption,  $M_{h,i,j}^{Elec}$  [g/yr] is calculated for each pollutant  $j$  from drinking water facility  $i$  under scenario  $h$  of either the baseline scenario or new regulation scenario using Equation 2.2. Emissions are the product of the volume of water produced at facility  $i$ ,  $\Psi_i$  [ $m^3$ /yr], the total electricity consumption of the unit processes,  $g$ , that are installed in the baseline or newly-regulated scenario,  $h$ ,  $E_{g,h}^W$  [kWh/ $m^3$ ], and the marginal emissions factors per kWh for air pollutant  $j$  in state  $l$ ,  $emf_{j,l}$  [g/kWh].<sup>38, 42</sup> The



emissions factors for CO<sub>2</sub>, NO<sub>x</sub>, and SO<sub>2</sub> are marginal emission factors, as only a small percentage of US electricity generation is consumed by water treatment processes.<sup>43, 44</sup> Marginal emission factors are not available for PM<sub>2.5</sub> and so we use state-level average emission factors from the EPA Emission Inventories.<sup>42</sup> Electricity is assumed to be generated in the state where the drinking water facility is located.

$$M_{h,i,j}^{Elec} = \forall_i E_{g,h}^W e_{mf,j,l} \quad (2.2)$$

$$M_{h,i,j}^C = \sum_f \forall_i Q_{i,f,j} (e_{cm,f,h}^C + \sum_d E_{d,f}^D e_{d,h}^D + E_f^W \sum_l e_{mf,l,h} \frac{V_l}{\sum_l V_l}) \quad (2.3)$$

Similarly, the mass of annual air emissions associated with chemical consumption by each water treatment facility,  $M_{h,i,j}^C$  in [g/yr], is calculated using Equation 2.3. Air emissions from chemical manufacturing originate from three sources. The first source is emissions released directly during the manufacturing of chemical  $f$ ,  $e_{cm,f,h}^C$  in [g-emissions/g-chemicals]. The second source of emissions is from the combustion of thermal energy to drive chemical manufacturing, which is the product of the energy consumed from fuel source  $d$ ,  $E_{d,f}^D$  in [MJ/g-chemical], and emission per unit of thermal energy,  $e_{d,h}^D$  in [g-pollutant/MJ]. The final source is emissions from electricity consumed in chemical manufacturing which is the weighted average of the grid emissions,  $\sum_l e_{mf,l,h} \frac{V_l}{\sum_l V_l}$  in [g-emissions/kWh] multiplied by the electricity consumed to produce a unit of chemicals,  $E_f^C$  in [kWh/g-chemical]. This weighting is done according to a state's chemical manufacturing sector size and we assume chemical manufacturing follows the nationwide distribution in chemical production.<sup>45</sup> The sum of these emissions per unit of chemical is then multiplied by the water required to be treated at facility  $i$ ,  $\forall_i$  in [m<sup>3</sup>/yr], and the chemical dosage,  $Q_{i,f}$  [g-chemical/m<sup>3</sup>]. Additional detail about the methods used to calculate chemical emissions can be found in our published work.<sup>46</sup> We also perform sensitivity

analyses (SI Section 4.0) on assumptions about the geographic distribution of chemical manufacturing and binding air pollution regulations.

*Damages from Drinking Water Systems.* To calculate the associated air emission damages from drinking water systems at the facility-level, we use AP2,<sup>21</sup> EASIUR,<sup>47</sup> and the social cost of carbon<sup>23</sup> to estimate the damages per ton of additional pollutant  $j$  occurring in state  $l$ ,  $d_{j,l}$  in [\$/g]. In this chapter we report damages from CAPs using AP2 with EASIUR results reported in the SI (SI Section 5.2, Tables S10 and S11, and Figure S1). Our results are sensitive to the assumed value of a statistical life (\$8.3M in 2012\$) and social cost of carbon (\$42/short ton in 2012\$). To first order, the impact of alternative values of a statistical life or social costs of carbon can be assessed by linearly scaling our damages.

Air emission damages associated with electricity consumption are calculated at the facility-level,  $D_{i,h}^{Elec}$  in [\$/yr], by multiplying the amount of electricity consumed at facility  $i$  by  $d_{j,l}$  (Equation 2.4). Air emission damages associated with the production of chemicals consumed in water treatment are calculated for each state  $l$  as the product of  $d_{j,l}$  and estimated mass of air emissions from chemical manufacturing in that state (Equation 2.5).

$$D_{h,l}^{Elec} = \sum_j d_{j,l} M_{h,l,j}^{Elec} \quad (2.4)$$

$$D_{h,l}^C = \sum_j d_{j,l} M_{h,i,j}^C \frac{V_{l=L}}{\sum_l V_l} \quad (2.5)$$

The total damages nationwide for treatment train  $h$ ,  $D_h$  in [\$/yr], is given by Equation 2.6.

$$D_h = \sum_i D_{i,h}^{Elec} + \sum_l D_{h,l}^C \quad (2.6)$$

### 2.3.2 Benefit-Cost Analysis of Drinking Water Regulations

We compare the damages calculated using Equation 2.6 to the benefits reported in the regulatory documentation for Arsenic, the Lead and Copper Rules, and the Disinfection Byproduct Rules. Costs (C) considered in these regulatory analyses include technology

installation and regulatory oversight. The costs do not include damages from embedded air emissions, as the EPA did not calculate them during the BCA process. Benefits (B) include health benefits and other environmental benefits. The net benefits (N) of a rule are calculated using Equation 2.7.

$$N = B - C - D_h \quad (2.7)$$

For the three rules that are still in development, we use published estimates of compliance technology costs to calculate the health benefits from improved water quality necessary for the rule to provide a net benefit to society.<sup>48</sup>

### 2.3.3 Evaluating Regulatory Compliance Options

The EPA recommends two compliance technology options for PFOA/PFOS: reverse osmosis or granular activated carbon. In the main analysis laid out in Section 2.1, we model plants installing granular activated carbon adsorption processes to comply with the PFOA/PFOS health advisory. We repeat the calculations in Section 2.1 using reverse osmosis as the compliance technology to explore the difference in damages resulting from selecting an alternative technology.

### 2.3.4 Forecasting Emissions from Electricity Consumption

The marginal emission factors from electricity generation are expected to decrease as coal fired power plants are replaced by natural gas plants and renewable energy sources. This transition may, in turn, reduce the embedded air emission damages from drinking water treatment. We use EIA Annual Energy Outlook 2017<sup>49</sup> forecasts of electricity generation,  $G_{k,m}$  [kWh], to calculate national average shares of electricity from fuel  $m$  (coal, natural gas, diesel, and zero operating emission energy sources) in year  $k$  between 2015-2050. We then calculate national average emission factor forecasts,  $e_{af,m}$  [g/kWh], over this interval for SO<sub>2</sub>, NO<sub>x</sub>, PM<sub>2.5</sub>,

and CO<sub>2</sub> using average emission factors from fuel source coal, natural gas, and diesel.<sup>50</sup> We then multiply national average emission factor forecasts by the amount of electricity consumed to drive baseline and regulatory treatment trains and average damages per mass of air pollution values in order to calculate expected damages through 2050 (Equation 2.8).

$$D_{k,h} = \sum_j (d_j \sum_i \forall_t \sum_g (E_{g,h}^W * \frac{G_{k,m}^{eaf,m}}{\sum_l G_{k,m}})) \quad (2.8)$$

Because we use marginal emission factors for the main analysis and average emission factors for forecasting, Equation 2.8 overestimates the damages. We correct for this overestimation,  $\widetilde{D}_{k,h}$  [\$/yr], by multiplying the ratio of calculated results for 2014 from Equation 2.5,  $D_h$  [\$/yr], forecasted results for 2014 from Equation 2.8,  $D_{k,h}$  [\$/yr] (Equation 2.9).

$$\widetilde{D}_{k,h} = \frac{D_h}{D_{h,k=2014}} D_{k,h} \quad (9)$$

## 2.4 Results and Discussion

### 2.4.1 Air Emission Damages from Operating Baseline and Compliant Treatment Trains

We estimate that baseline operation of water treatment plants consumed 2500 GWh of electricity, consumed 1.5 million tons of chemicals, and generated \$500 million dollars in air emission damages in 2014 (expressed in 2014 dollars and using a value of a statistical life of \$9 million) (Figure 2.2A, 2.2C, and 2.2E). Emissions from chemical manufacturing contribute 73% of the damages in the baseline treatment train. The damages associated with operating baseline water treatment are several orders of magnitude lower than the benefits of avoided illness and death from untreated drinking water.<sup>2</sup>

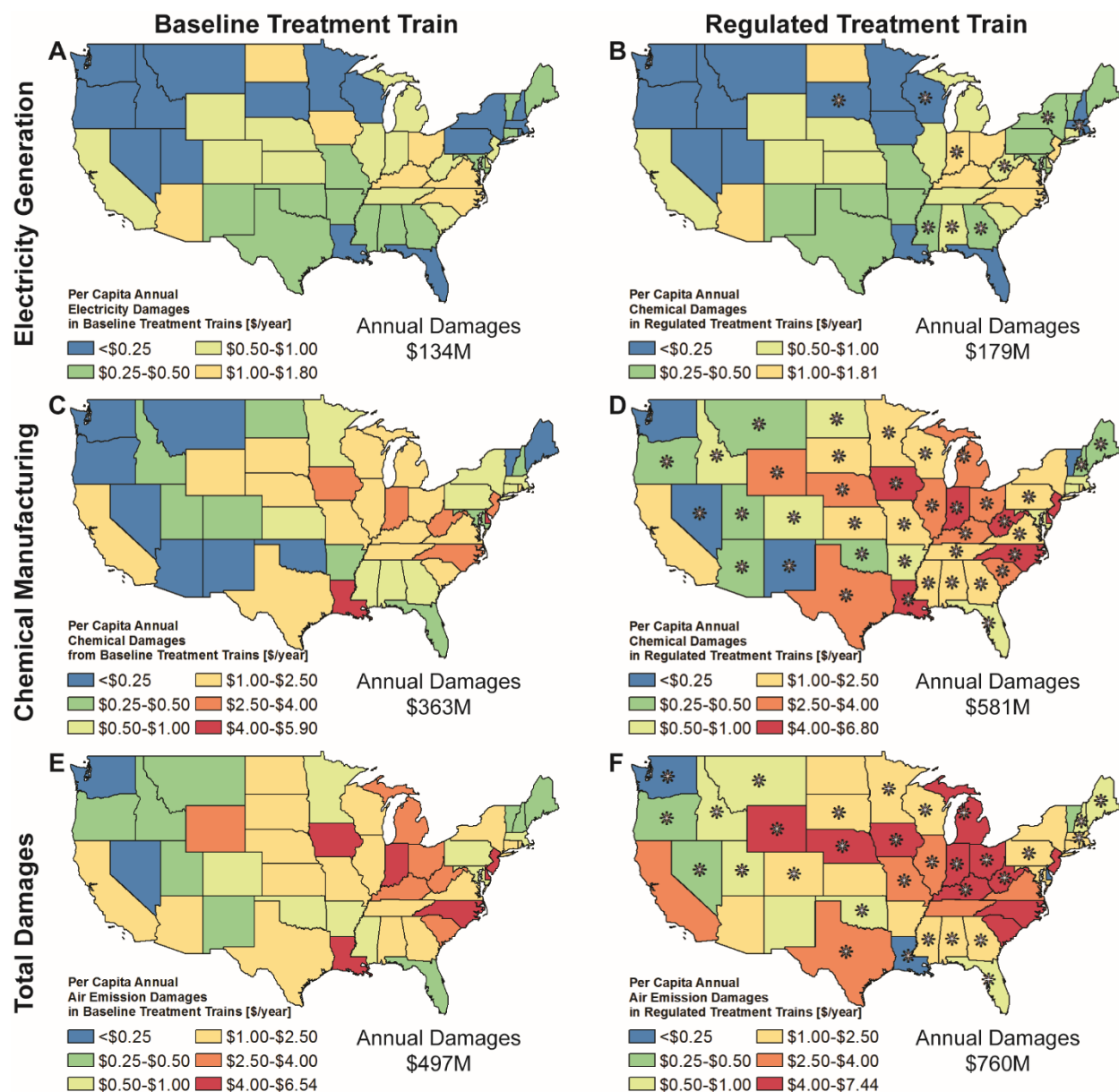


Figure 2.2. Per capita air emission damages associated with operating drinking water treatment processes under current and future regulatory scenarios. State-level damages embedded in electricity consumption by water treatment processes for the (A) baseline treatment train and the (B) regulated treatment train assuming compliance with all promulgated and proposed SDWA regulations. State-level damages embedded in chemical consumption by water treatment processes for the (C) baseline treatment train and the (D) regulated treatment train. Total air

*emissions damages for the (E) baseline treatment train and the (F) regulated treatment train. In panels (B), (D), and (F) the asterisk indicates a > 50% increase in air emission damages for the regulated treatment train that is compliant with the six drinking water regulations studied in this paper relative to the baseline train. Emissions and damages are tabulated in SI Tables S8 and S9 and SI Section 5.1. Results calculated using EASIUR to price CAP damages can be found in SI Section 5.2 and Tables S10 and S11.*

Achieving compliance with the six drinking water regulations increases air emission damages by \$260 million (in 2014\$) annually (Figure 2.2B, 2.2D, and 2.2F). This represents an increase of 53% from the emissions associated with the baseline treatment train. Of this \$260 million in damages, 76% are damages from chemical manufacturing. Over 85% of these damages, \$230 million (in 2014\$), stem from compliance with the PFOA/PFOS Health Advisory at 27,000 drinking water facilities nationwide. Emissions and damages increases estimated for compliance with each of the six regulations are broken down in SI Section 6.0, Tables S12-S17, and Figures S2-S7.

The state-level damages presented in Figure 2.2 are based on a nationwide average of per capita water consumption. Per capita water consumption, however, varies across states.<sup>39</sup> Accounting for this variability in water consumption may lead to differences in damages, especially in western states where water consumption is higher on a per capita basis.<sup>51</sup>

### 2.4.2 Benefit-Cost Analysis of Drinking Water Regulations

Table 2.2 Benefit-cost analysis for the six drinking water regulations after accounting for estimated air emission damages.

Contaminant	Benefits	Costs/Damages			Net
		Compliance	Electricity	Chemical	
		Costs	Damages	Damages	
(\$/m <sup>3</sup> in 2014\$)					
Finalized Rules					
Arsenic	0.14	0.16	0.0006	0.000002	-0.024
DBP	2.70	0.94	0.0012	0.0080	1.80
Lead and Copper	7.70	1.25	0.0006	0.0003	6.50
Rules Under Consideration					
Chromium (VI)	≥0.23*	0.20 <sup>48</sup>	0.025	0.0014	≥0
Strontium	≥0.44*	0.40 <sup>52</sup>	0.0008	0.042	≥0
PFOA/PFOS**	≥0.61*	0.60 <sup>48</sup>	0.0017	0.0080	≥0

\*Rules that are under consideration do not have published estimates for their benefits and compliance costs.

\*\*Using Granular Activated Carbon as the compliance technology.

For the three finalized rules (Arsenic, DBPs, and Lead and Copper), the signs on the benefit-cost analysis do not change with the inclusion of air emission damages (Table 2.2). The DBP and Lead and Copper rules had large benefits to society, and accounting for air emissions damages does not change this conclusion. The arsenic rule was a net cost to society without incorporating air emissions from drinking water; including air emissions in the benefit-cost analysis only increases the cost.

For the three rules that are not yet finalized, Table 2.2 presents the minimum benefits required given estimates of air emission damages from this analysis and literature-based compliance technology costs.<sup>48, 52</sup> On a per cubic meter basis, air emission damages contribute 2-11% of the total costs to society for these rules. Air emissions are therefore a small, but non-

negligible contributor to these overall costs. The benefits required for these rules to impart net social benefits range from \$0.23/m<sup>3</sup> to \$0.61/m<sup>3</sup> (in 2014\$).

There are several unquantifiable co-benefits of adopting the six drinking water regulations that are not accounted for in this analysis. These include the reduction of unregulated contaminant concentrations associated with the advanced treatment technologies that are installed to comply with these rules. There is also the possibility that, in the process of complying with new water quality regulations, monitoring and enforcement of existing water quality regulations is improved.

#### 2.4.3 Evaluating Regulatory Compliance Options

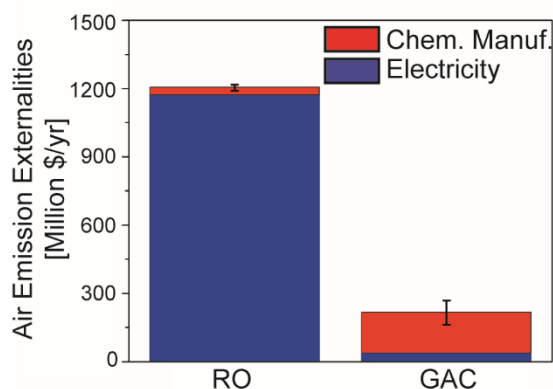


*Figure 2.3. Air emission damages from reverse osmosis and granular activated carbon treatment for PFOA/PFOS removal at 58,000 drinking water facilities across the US. The error bars show the uncertainty in the location and presence of binding regulations affecting emissions from the chemical manufacturing sector (SI Section 4.0) and Tables S4-S7.*

Quantifying the air emission externalities of drinking water treatment processes can also assist in compliance technology selection. Of the two compliance options for PFOA/PFOS removal, reverse osmosis is the highest damage alternative (Figure 2.3). Using reverse osmosis



to comply with the PFOA/PFOS standards imposes air emission damages of \$1.2 billion annually (in 2014\$). The use of GAC to achieve compliance with PFOA/PFOS imposes air emission damages of \$220 million/yr (in 2014\$), a sixth of the damages from reverse osmosis. The primary source of air emission damages from RO is the electricity used to drive the process, rather than from emissions embedded in chemical consumption. In contrast, granular activated carbon leads to more damages from chemical manufacturing than reverse osmosis, with subsequently more uncertainty.

Reverse osmosis and granular activated carbon have different removal efficiencies for PFOA/PFOS, with RO producing higher quality water. This sets up a trade-off between reducing health risks from PFOA/PFOS in drinking water and minimizing the environmental and health risks from criteria air pollutants and greenhouse gasses. To account for this additional \$1.0 billion in air emission damages annually, reverse osmosis would need to save an additional 124 statistical lives through PFOA/PFOS concentration reduction. These additional statistical lives could also be saved by the co-benefits of RO by producing higher quality water.

#### *2.4.4 Future Air Emission Damages from Electricity Consumed in Drinking Water Treatment*

As the grid evolves to rely less on fossil fuel sources, damages from air emissions are expected to decrease (Figure 2.4). By 2050, annual damages associated with emissions from electricity generation that result from compliance with these six standards decreases by \$36 million per year from the 2015 level of \$97 million. This reduction in damages from electricity will lower the required benefits presented in Table 2.2 to achieve net benefits from these drinking water rules.

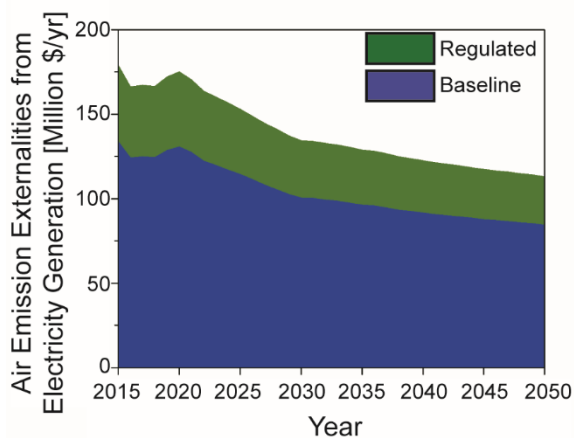


*Figure 2.4. Projected air emission damages from electricity generated to treat US drinking water with the baseline treatment train and the additional emissions that result from drinking water compliance. N.B. That this figure does not include damages resulting from the electricity consumed during chemical manufacturing.*

#### 4.0 Implications

Stronger epidemiological evidence of health impacts from contaminated water, enhanced public awareness of water quality issues, and improved analytical techniques for detecting aqueous contaminants are each drivers for stricter water quality regulations.<sup>1, 53</sup> While the counter-argument to installing the advanced treatment technologies necessary for compliance has historically been cost, we proposed that the very real risks of air emission externalities of water treatment should also be considered. On the order of 100,000 deaths from air emissions occur annually in the US.<sup>54</sup> We advocate a regulatory assessment process that explicitly considers the life-cycle tradeoffs between improved water quality and reduced air emissions.

Adapting the regulatory assessment process for the six water quality regulations evaluated in this analysis would be unlikely to significantly change the assessment of net benefits or the regulatory standards. However, as demonstrated for the PFOA/PFOS rule, it may influence the selection of the best available technology for regulatory compliance.

Adapting the regulatory assessment process to include life-cycle air emissions may also broaden the scope of environmental justice analyses. This analysis demonstrates that spatial distribution of the damages, and not simply the water quality benefits, varies across the United States and should be considered in evaluating regulations. Areas with high-levels of coal-fired electricity generation or chemical manufacturing may experience damages from air emissions in excess of benefits from improved drinking water quality. Performing spatially-resolved air emissions analyses allows the EPA to quantify these trade-offs as part of their standard environmental justice analyses.

Finally, this analysis supports the ongoing transition from single-media focused regulations (e.g. drinking water) towards more holistic analyses that account for the countervailing risks analyzed in this paper. Previous examples of the EPA moving to holistic regulatory activity includes the cluster rules for the pulp and paper industry<sup>55</sup> and Executive Order (EO) 13211 mandating that all regulations, including drinking water regulations, undergo an energy inventory if they are deemed “economically significant.”<sup>43</sup> Unfortunately, it is not standard practice for analyses performed under EO 13211 to assess emissions associated with this electricity generation or incorporate the damages into benefit-cost analyses performed under EO 12866. Even if damages from the emissions associated with electricity generation were included in EPA BCAs for drinking water treatment, the emissions from chemical manufacturing would be overlooked. As chemical manufacturing damages contribute roughly three times as much as electricity generation, their inclusion is important in ensuring a comprehensive analysis of these trade-offs.

In short, more rapid adoption of environmental regulatory frameworks that account for inter-sectoral and cross-media risk trade-offs should be a priority at both the national and state levels.

## 2.6 Acknowledgements

This work was supported by the National Science Foundation under award number CBET-1554117.

## 2.7 Nomenclature

### Symbols

<i>A</i> :	Per capita annual water consumption [ $\text{m}^3/\text{person}\cdot\text{yr}$ ]
<i>B</i> :	Benefits from a drinking water regulation [ $\$/\text{yr}$ ]
<i>C</i> :	Compliance costs from a drinking water regulation [ $\$/\text{yr}$ ]
<i>D</i> :	Air emission damages for drinking water treatment [ $\$/\text{yr}$ ]
$\tilde{D}$ :	Corrected damages forecast [ $\$/\text{yr}$ ]
<i>d</i> :	Damages per unit of $\text{NO}_x$ , $\text{SO}_2$ , $\text{PM}_{2.5}$ , and $\text{CO}_2$ [ $\$/\text{g}$ ]
<i>E</i> :	Energy consumption [ $\text{kWh}/\text{m}^3$ ], [ $\text{kWh}/\text{g-chemical}$ ], or [ $\text{MJ}/\text{g-chemical}$ ]
<i>e</i> :	Emissions factor per unit of energy [ $\text{g}/\text{kWh}$ ] or [ $\text{g}/\text{MJ}$ ]
<i>G</i> :	Annual electricity generation [ $\text{kWh}$ ]
<i>M</i> :	Annual mass of $\text{NO}_x$ , $\text{SO}_2$ , $\text{PM}_{2.5}$ , or $\text{CO}_2$ emissions [ $\text{g}/\text{yr}$ ]
<i>N</i> :	Net benefits or costs from a drinking water regulation [ $\$/\text{yr}$ ]
<i>Pop</i> :	Population served by a facility [people]
<i>Q</i> :	Chemical dosage [ $\text{g-chemical}/\text{m}^3$ ]
<i>V</i> :	Annual value of products from the chemical manufacturing sector [ $\$$ ]
$\Psi$ :	Annual water production [ $\text{m}^3/\text{yr}$ ]

$W$ : Electricity consumption for water treatment process [kWh/m<sup>3</sup>]

### Subscripts

$af$ : Average emissions factor

$cm$ : Chemical manufacturing

$d$ : Thermal fuel

$f$ : Chemical

$g$ : Unit process

$h$ : Treatment train (baseline or newly-regulated)

$i$ : Drinking water facility

$j$ : Air pollutant (NO<sub>x</sub>, SO<sub>2</sub>, PM<sub>2.5</sub>, or CO<sub>2</sub>)

$k$ : Year

$l$ : State

$m$ : Fuel source for electricity generation

$mf$ : Marginal emissions factor

$PC$ : per capita

$served$ : Population served by a facility

### Superscripts

$C$ : From chemical manufacturing

$D$ : From thermal fuel combustion

$Elec$ : From electricity generation

$W$ : Electricity consumption

## 2.8 References

1. Roberson, J. A., What's next after 40 years of drinking water regulations? *Environmental Science & Technology* **2011**, *45*, 154-160.
2. Craun, G. F.; Craun, M. F.; Calderon, R. L.; Beach, M. J., Waterborne outbreaks reported in the United States. *Journal of Water and Health* **2006**, *04*, (Suppl 2), 19-30.
3. Gurian, P. L.; Tarr, J. A., The origin of federal drinking water quality standards. *Proceedings of the Institution of Civil Engineers - Engineering History and Heritage* **2011**, *164*, (1), 17-26.
4. Putnam, S. W.; Wiener, J. B., Seeking Safe Drinking Water. In *Risk vs. Risk*, Graham, J. D.; Wiener, J. B., Eds. Harvard University press: Cambridge, Massachusetts, 1995.
5. U.S. Environmental Protection Agency, Stage 1 and Stage 2 Disinfectants and Disinfection Byproducts Rules <https://www.epa.gov/dwreginfo/stage-1-and-stage-2-disinfectants-and-disinfection-byproducts-rules> (March 25, 2017).
6. Richardson, S. D., Water Analysis: Emerging Contaminants and Current Issues. *Analytical Chemistry* **2009**, *81*, (12), 4645-4677.
7. Stickers, D., The Unintended Consequence of Reformulated Gasoline. In *Improving Regulation: Cases in Environment, Health, and Safety*, Fischbeck, P. S.; Farrow, R. S., Eds. Resources for the Future Washington, D.C., 2001.
8. Wang, Y.; Small, M. J.; VanBriesen, J. M., Assessing the Risk Associated with Increasing Bromine in Drinking Water Sources in the Monongahela River, Pennsylvania. *Journal of Environmental Engineering* **2017**, *143*, (3) 04016089.

9. Good, K. D.; VanBriesen, J. M., Current and Potential Future Bromide Loads from Coal-Fired Power Plants in the Allegheny River Basin and Their Effects on Downstream Concentrations. *Environmental Science & Technology* **2016**, *50*, (17), 9078-9088.
10. Tesfamichael, A. A.; Caplan, A. J.; Kaluarachchi, J. J., Risk-cost-benefit analysis of atrazine in drinking water from agricultural activities and policy implications. *Water Resources Research* **2005**, *41*, (5) W05015.
11. Wiener, J. B.; Graham, J. D., Resolving Risk Tradeoffs. In *Risk vs. Risk: Tradeoffs in Protecting Health and the Environment*, Graham, J. D.; Wiener, J. B., Eds. Harvard University Press: Cambridge, MA, 1995.
12. Arrow, K. J.; Cropper, M. L.; Eads, G. C.; Hahn, R. W.; Lave, L. B.; Noll, R. G.; Portney, P. R.; Russell, M.; Schmalensee, R.; Smith, V. K. S., Robert N., Is There a Role for Benefit-Cost Analysis in Environmental, Health, and Safety Regulation? *Science* **1996**, *272*, 221-222.
13. Lave, L. B., Benefit-Cost Analysis: Do the Benefits Exceed the Costs? In *Risks, Costs, and Lives Saved: Getting Better Results from Regulation*, Hahn, R. W., Ed. The AEI Press: Washington, D.C., 1996; pp 104-134.
14. Santana, M. V.; Zhang, Q.; Mihelcic, J. R., Influence of water quality on the embodied energy of drinking water treatment. *Environmental Science & Technology* **2014**, *48*, (5), 3084-3091.
15. Stokes, J. R.; Hovarth, A., Energy and Air Emission Effects of Water Supply *Environmental Science & Technology* **2009**, *43*, 2680-2687.
16. Stokes, J.; Horvath, A., Life-Cycle Assessment of Urban Water Provision: Tool and Case Study in California *Journal of Infrastructure Systems* **2011**, *17*, (1), 15-24.

17. Mo, W.; Wang, H.; Jacobs, J. M., Understanding the influence of climate change on the embodied energy of water supply. *Water Research* **2016**, *95*, 220-229.
18. Fang, A. J.; Newell, J. P.; Cousins, J. J., The energy and emissions footprint of water supply for Southern California. *Environmental Research Letters* **2015**, *10*, (11), 114002.
19. Muller, N. Z.; Mendelsohn, R., Efficient Pollution Regulation: Getting the Prices Right. *American Economic Review* **2009**, *99*, (5), 1714-1739.
20. Muller, N. Z.; Mendelsohn, R.; Nordhaus, W., Environmental Accounting for Pollution in the United States Economy. *American Economic Review* **2011**, *101*, (5), 1649-1675.
21. Muller, N. Z., Using index numbers for deflation in environmental accounting. *Environment and Development Economics* **2013**, *19*, (04), 466-486.
22. Heo, J.; Adams, P. J.; Gao, H. O., Public Health Costs of Primary PM<sub>2.5</sub> and Inorganic PM<sub>2.5</sub> Precursor Emissions in the United States. *Environmental Science & Technology* **2016**, *50*, (11), 6061-6070.
23. Interagency Working Group on the Social Cost of Carbon, Technical Support Document: Technical Update of the Social Cost of Carbon for Regulatory Impact Analysis. Washington, D.C., 2015.
24. Stokes, J. R.; Hendrickson, T. P.; Horvath, A., Save water to save carbon and money: developing abatement costs for expanded greenhouse gas reduction portfolios. *Environmental Science & Technology* **2014**, *48*, (23), 13583-135891.
25. Lam, K. L.; Kenway, S. J.; Lant, P. A., Energy use for water provision in cities. *Journal of Cleaner Production* **2016**, *143*, 699-709.



26. Qi, C.; Chang, N.-B., Integrated carbon footprint and cost evaluation of a drinking water infrastructure system for screening expansion alternatives. *Journal of Cleaner Production* **2013**, *60*, 170-181.
27. Bonton, A.; Bouchard, C.; Barbeau, B.; Jedrzejak, S., Comparative life cycle assessment of water treatment plants. *Desalination* **2012**, *284*, 42-54.
28. Capitanescu, F.; Ahmadi, A.; Benetto, E.; Marvuglia, A.; Tiruta-Barna, L., Some efficient approaches for multi-objective constrained optimization of computationally expensive black-box model problems. *Computers & Chemical Engineering* **2015**, *82*, 228-239.
29. Wakeel, M.; Chen, B.; Hayat, T.; Alsaedi, A.; Ahmad, B., Energy consumption for water use cycles in different countries: A review. *Applied Energy* **2016**, *178*, 868-885.
30. U.S. Environmental Protection Agency, Chemical Contaminant Rules.  
<https://www.epa.gov/dwreginfo/chemical-contaminant-rules> (March 25).
31. U.S. Environmental Protection Agency, Lead and Copper Rule.  
<https://www.epa.gov/dwreginfo/lead-and-copper-rule> (March 25).
32. U.S. Environmental Protection Agency, Chromium in Drinking Water.  
<https://www.epa.gov/dwstandardsregulations/chromium-drinking-water> (March 25, 2017).
33. U.S. Environmental Protection Agency, Regulatory Determination 3.  
<https://www.epa.gov/ccl/regulatory-determination-3> (March 25, 2017).
34. U.S. Environmental Protection Agency, Basic Information about Per- and Polyfluoroalkyl Substances (PFASs). <https://www.epa.gov/pfas/basic-information-about-and-polyfluoroalkyl-substances-pfass> (March 25, 2017).

35. U.S. Environmental Protection Agency, Safe Drinking Water Information System (SDWIS). <https://www3.epa.gov/enviro/facts/sdwis/search.html> (March 25, 2017).
36. U.S. Environmental Protection Agency, Occurrence Data for the Unregulated Contaminant Monitoring Rule. <https://www.epa.gov/dwucmr/occurrence-data-unregulated-contaminant-monitoring-rule#3> (March 25, 2017).
37. U.S. Environmental Protection Agency, Information Collection Rule. <https://archive.epa.gov/enviro/html/icr/web/html/index.html> (March 25, 2017).
38. Siler-Evans, K.; Azevedo, I. L.; Morgan, M. G., Marginal emissions factors for the U.S. electricity system. *Environmental Science & Technology* **2012**, *46*, (9), 4742-4748.
39. United States Geological Survey, Water Use in the United States. (March 3, 2017).
40. Plappally, A. K.; Lienhard V, J. H., Energy requirements for water production, treatment, end use, reclamation, and disposal. *Renewable and Sustainable Energy Reviews* **2012**, *16*, (7), 4818-4848.
41. Crittenden, J. C.; Trussell, R. R.; Hand, D. W.; Howe, K. J.; Tchobanoglous, G., *Water Treatment: Principles and Design*. John Wiley & Sons, Inc.: Hoboken, New Jersey, 2012.
42. U.S. Environmental Protection Agency, Emission Inventories. <https://www3.epa.gov/ttn/chief/eiinformation.html> (October 9, 2015).
43. Reiling, S. J.; Roberson, J. A.; Cromwell III, J. E., Drinking water regulations: Estimated cumulative energy use and costs. *Journal American Water Works Association* **2009**, *101*, (3), 42-53.

44. Liu, Y.; Hejazi, M.; Kyle, P.; Kim, S. H.; Davies, E.; Miralles, D. G.; Teuling, A. J.; He, Y.; Niyogi, D., Global and Regional Evaluation of Energy for Water. *Environmental Science & Technology* **2016**, *50*, (17), 9736-9745.
45. United States Census Bureau, Annual Survey of Manufacturers 2013.  
<https://www.census.gov/manufacturing/asm/index.html> (October 11, 2015).
46. Gingerich, D. B.; Sun, X. B., A. Patrick; Azevedo, I. M. L.; Mauter, M. S., Spatially resolved air-water emissions tradeoffs improve regulatory impact analyses for electricity generation. *Proceedings of the National Academy of Science* **2017**, *114*, (8), 1862-1867.
47. Heo, J.; Adams, P. J.; Gao, H. O., Reduced-form modeling of public health impacts of inorganic PM<sub>2.5</sub> and precursor emissions. *Atmospheric Environment* **2016**, *137*, 80-89.
48. Plappally, A. K.; Lienhard, J. H., Costs for water supply, treatment, end-use and reclamation. *Desalination and Water Treatment* **2013**, *51*, (1-3), 200-232.
49. U.S. Energy Information Administration, *Annual Energy Outlook 2017 with Projections to 2050*; U.S. Energy Information Administration: Washington, D.C., 2017.
50. National Renewable Energy Laboratory, National Renewable Energy Laboratory - Life-Cycle Inventory Database. . <https://www.lcacommons.gov/nrel/process/show/50158> (October 3, 2015).
51. Maupin, M. A.; Kenny, J. F.; Huston, S. S.; Lovelace, J. K.; Barber, N. L.; Linsey, K. S., Estimtaed Use of Water in the United States in 2010. In Survey, U. S. G., Ed. United States Geological Survey: Washington, D.C., 2014.
52. Bergman, R. A., Membrane softening versus lime softening in Florida. *Desalination* **1995**, *103*, (1), 11-24.

53. Roberson, J. A., The middle-aged Safe Drinking Water Act *Journal American Water Works Association* **2014**, *106*, (8), 96-106.
54. U.S. Burden of Disease Collaborators, The state of US health, 1990-2010: burden of diseases, injuries, and risk factors. *Journal of the American Medical Association* **2013**, *310*, (6), 591-608.
55. Gray, W. B. S., Ronald J, Multimedia Pollution Regulation and Environmental Performance: EPA's Cluster Rule. In *Resources for the Future*: Washington, D.C., 2015.

## **CHAPTER 3: AIR EMISSION BENEFITS OF BIOGAS ELECTRICITY GENERATION AT MUNICIPAL WASTEWATER TREATMENT PLANTS<sup>2</sup>**

### **3.1 Abstract**

Conventional processes for municipal wastewater treatment facilities are energy intensive. This work quantifies the air emission implications of energy consumption, chemical use, and direct pollutant release at municipal wastewater treatment facilities across the US and assesses the potential for biogas combustion for heat and electricity generation to offset these damages. We find that embedded and on-site air emissions from municipal wastewater treatment imposed human health, environmental, and climate (HEC) damages on the order of \$1.26 billion USD in 2012, with 83% of these damages attributed to electricity consumption by treatment processes. An additional 9,800,00 tons of biogenic CO<sub>2</sub> are directly emitted by wastewater treatment and sludge digestion processes currently installed at plants. Retrofitting existing wastewater treatment facilities with anaerobic sludge digestion for biogas production and biogas-fueled heat and electricity generation would reduce HEC damages by 22.8% relative to the baseline electricity emissions, or \$241 million annually. These findings reinforce the importance of accounting for use-phase embedded air emissions and spatially-resolved marginal damage estimates when designing sustainable infrastructure systems.

### **3.2 Introduction**

Aging systems, tighter regulatory standards, and expanding demand are driving significant growth in the construction of publicly operated treatment works (POTWs) in the US.<sup>1</sup> These facilities are likely to operate for several decades, a time during which the US electricity sector will likely undergo radical change. Next generation wastewater treatment processes must

---

<sup>2</sup> This chapter is based on a manuscript co-authored with Prof. Meagan Mauter and is in preparation for submission to Sustainable Chemistry & Engineering.

meet standards for pathogen and nutrient control,<sup>2-3</sup> while also creating opportunities for nutrient recovery,<sup>4-8</sup> minimizing electricity demand, buffering against intermittency in electricity supply, and reducing direct and embedded air emissions from the treatment process.

Biological wastewater treatment generates direct emissions of volatile organic compounds (VOCs) and greenhouse gasses (GHGs), including CO<sub>2</sub>, CH<sub>4</sub>, and N<sub>2</sub>O. These emissions stem from the biodegradation of organics in secondary treatment processes.<sup>9-20</sup> Past efforts to quantify these emissions through direct monitoring<sup>9, 16, 21-23</sup> or modeling<sup>10, 14, 18, 24</sup> have been limited to individual plants. As a result, we lack a spatially-resolved national emissions inventory of GHGs from wastewater treatment facilities that is critical to informing climate policy. We also lack tools for valuing the broader human health, environmental, and climate (HEC) damages that result from VOC and GHG emissions. Indeed, previous assessments of VOC emission damages have focused exclusively on health impacts to workers.<sup>22, 25</sup>

In addition to direct emissions from biological wastewater treatment, there are embedded air emissions from the consumption of electricity and chemicals in the treatment process.<sup>26-32</sup> Electricity and chemical consumption has been evaluated for both conventional and emerging treatment processes, including small scale systems for decentralized wastewater treatment.<sup>28-29, 31-36</sup> Studies that translate these electricity and chemical inputs into air emissions use national grid average emissions factors,<sup>5</sup> and thus do not account for the marginal or regional variability in the emissions intensity of the grid. Finally, there are no studies that monetize the air emission damages from wastewater treatment, which stymies the inclusion of air emission damages in benefit-cost analyses used in regulatory and planning processes.

Despite limited quantitative information on direct or embedded emissions from US wastewater treatment facilities or their associated damages, energy recovery and emissions reductions from wastewater treatment are a priority for many states.<sup>37-38</sup> Anaerobic sludge digestion for biogas generation is a particularly cost-effective approach to energy recovery, as it does not require modification of the primary and secondary treatment processes.<sup>39-41</sup> The biogas production rate is approximately 0.07 m<sup>3</sup> per m<sup>3</sup> of wastewater,<sup>42</sup> and the recovered biogas can be combusted to help meet the thermal and electrical energy requirements at the plant. The life cycle emissions reduction benefits of displacing electricity consumption are likely to be highest in regions with a coal-dependent grid.

This paper quantifies the air emission benefits of anaerobic sludge digestion at municipal wastewater treatment facilities in three steps. First, we develop a model of the life-cycle emissions of criteria air pollutants (CAPs) and greenhouse gasses (GHGs) from electricity generation, chemical manufacturing, and on-site emissions associated with municipal wastewater treatment at all wastewater treatment facilities in the continental US. We then use this model to evaluate the HEC externalities from air pollution associated with wastewater treatment using AP2<sup>43</sup> and the social cost of carbon.<sup>44</sup> Finally, we evaluate the potential of biogas-fueled heat and electricity to reduce emissions relative to natural gas combustion and local grid supplied electricity.

### **3.3 Methods**

#### *3.3.1 Air Emission Damages from Municipal Wastewater Treatment*

We use methods for calculating air emission damages associated with currently installed municipal wastewater treatment processes that are similar to our previous work on calculating air emission damages associated with drinking water treatment in Chapter 2.<sup>26</sup> We make three

changes to that method for an analysis of emissions associated with wastewater treatment. First, we source data on installed wastewater treatment processes at 14,693 publicly operated treatment works (POTWs) within the continental US from the Clean Watersheds Needs Survey (CWNS).<sup>45-46</sup> Second, in addition to emissions from electricity generation and chemical manufacturing, we incorporate on-site emissions of greenhouse gasses and VOCs from microbial activity, natural gas combustion to heat bioreactors, biogas combustion, and fugitive biogas emissions from wastewater and sludge digestion processes. Third, we account for emissions and damages of VOCs that result from electricity generation and chemical manufacturing using the US EPA's National Emissions Inventory<sup>47</sup> (for electricity generation) and from the life-cycle assessment literature<sup>48-49</sup> (for chemical manufacturing). Details of the methods for calculating air emissions and damages associated with electricity generation and chemical manufacturing can be found in Chapter 2.<sup>26</sup> The treatment technologies included in our analysis, data inputs, and a summary of the methods can be found in SI Sections 1.0-3.0 in Appendix 2.

*Wastewater Treatment System Data.* We use the CWNS results for data on POTWs. For 47 of the 48 continental US states and the District of Columbia, we use 2012 CWNS data.<sup>46</sup> South Carolina did not participate in the 2012 CWNS and so we use 2008 CWNS data<sup>45</sup> for that state. This combined CWNS dataset includes 14,693 POTWs, or 99.6% of the nation's wastewater treatment facilities. CWNS data includes (1) installed technologies, (2) treatment flow, and (3) the state and county of the facility. We use this data to estimate the electrical and chemical inputs for each facility and to compute location-specific emission factors and emission damages.



*Life-Cycle Air Emissions for Wastewater Treatment Systems.* We evaluate the life-cycle air emissions of four CAPs (SO<sub>2</sub>, NO<sub>x</sub>, PM<sub>2.5</sub>, and VOCs) and three GHGs (CO<sub>2</sub>, CH<sub>4</sub>, and N<sub>2</sub>O). There are three sources of CAP and GHG emissions associated with wastewater treatment. First, there are on-site emissions. On-site emissions of pollutant  $j$  at facilities  $i$  include emissions from biodegradation in activated sludge processes,  $M_{i,j}^{Aer}$ , emissions from biogas combustion at facilities with anaerobic digestion and biogas combustion,  $M_{i,j}^{Comb}$ , fugitive emissions of biogas at facilities with anaerobic digestion but no biogas combustion,  $M_{i,j}^{Fugitive}$ , and emissions from natural gas combustion to supplement biogas combustion heating of the anaerobic digester. There are also emissions of pollutant  $j$  from generating the electricity used to drive wastewater processes at facility  $i$ ,  $M_{i,j}^{Elec}$ . Finally, there are emissions of pollutant  $j$  from manufacturing the chemicals used in wastewater treatment processes at facility  $i$ ,  $M_{i,j}^{Chem}$ . As noted above, the details on the calculation methods for these last two sources can be found in our previous work<sup>26</sup> and are summarized in SI Section 3.0.

For each wastewater treatment facility with activated sludge processes or aerobic digestion installed, we calculate the direct emissions of VOCs and GHGs resulting from wastewater treatment,  $M_{i,j}^{Aer}$  [g/yr], using Equation 3.1 and emission factors listed in Table S4.

$$M_{i,j}^{Aer} = V_{i,influent} e_{treat,j}^{Aer} \quad (3.1)$$

Emissions are the product of water treated,  $V_{i,influent}$  [m<sup>3</sup>/yr], and average literature reported emissions per cubic meter,  $e_{treat,j}^{Aer}$  [g/m<sup>3</sup>],<sup>50-56</sup> listed in Table S4.

For anaerobic sludge digestion, we assume that the biogas is either captured and combusted or released to the atmosphere as fugitive biogas. For facilities with anaerobic sludge digestion and that report having biogas combustion, we calculate combustion emissions,  $M_{i,j}^{Comb}$

[g/yr], using Equation 3.2. We assume that 99% of biogas is combusted with the remaining 1% released to the environment, and scale the emissions factors listed in Table S4 accordingly to calculate the biogas combustion emission factor,  $e_j^{Comb}$  [g/m<sup>3</sup>]. We multiply the resulting emission factors by the volume of influent wastewater,  $V_{i,influent}$  [m<sup>3</sup>/yr].

$$M_{i,j}^{Comb} = V_{i,influent} e_j^{Comb} \quad (3.2)$$

For facilities with anaerobic sludge digestion that do not report biogas combustion, we assume that roughly 82% of biogas is flared without the heat being used by the plant, with the remaining 18% released as fugitive emissions. This assumption is based on past reviews of biogas generation in the US.<sup>57</sup> As shown in Equation 3.3, we calculate fugitive emissions,

$M_{i,j}^{Fugitive}$  [g/yr], by multiplying influent wastewater volume,  $V_{i,influent}$  [m<sup>3</sup>/yr], and scale the emissions factors listed in Table S4 accordingly to calculate the fugitive biogas emissions factor,  $e_j^{Fugitive}$  [g/m<sup>3</sup>] listed in Table S4.

$$M_{i,j}^{Fugitive} = V_{i,influent} e_j^{Fugitive} \quad (3.3)$$

Finally, we calculate emissions from natural gas combustion for anaerobic digester heating at facilities with an anaerobic digester but insufficient amounts of biogas combusted to heat the digester. We calculate emissions of pollutant  $j$  at facility  $i$  resulting from natural gas combustion,  $M_{i,j}^{NG}$ , using Equation 3.5. We do this by first calculating the amount of thermal energy required to heat the sludge. The amount of heat required is the product of the flow rate of sludge into the anaerobic digester,  $V_{i,sludge}$  [m<sup>3</sup>/yr], the density of wastewater,  $\rho$  [g/m<sup>3</sup>], which we assume to be 1000 g/m<sup>3</sup>,<sup>42</sup> the heat capacity of wastewater,  $c_p$  [J/g·°C], which we assume to be 4.18 J/g·°C,<sup>42</sup> and the required temperature to raise the sludge temperature from the average temperature in activated sludge processes of 30°C to achieve an optimal temperature of 38°C.<sup>42</sup>

The amount of heat produced from biogas is the product of the influent wastewater,  $V_{i,influent}$  [m<sup>3</sup>/yr], production of biogas per cubic meter of influent wastewater,  $P$  [m<sup>3</sup>-biogas/m<sup>3</sup>-influent wastewater],<sup>42</sup> and the higher heating value of biogas,  $HHV_{biogas}$  [J/m<sup>3</sup>-biogas].<sup>58</sup> The difference between heat required and heat produced from biogas generation is the amount of heat that needs to come from natural gas,  $Q_{NG}$  [J/yr] (Equation 3.4). We then divide by the higher heating value of natural gas,  $HHV_{NG}$  [J/m<sup>3</sup>-natural gas],<sup>59</sup> and multiply by the emissions factor for pollutant  $j$  for natural gas combustion in an industrial boiler,  $e_{NG,j}$  [g/m<sup>3</sup>] (Equation 3.5).<sup>48</sup>

$$Q_{NG} = V_{i,sludge} \rho C_p \Delta T - V_{i,influent} P HHV_{biogas} \quad (3.4)$$

$$M_{i,j}^{NG} = e_{NG,j} \left( \frac{Q_{NG}}{HHV_{NG}} \right) \quad (3.5)$$

*Damages for Wastewater Treatment Systems.* Using Equations 3.6-3.9, we calculate damages from direct emissions from aerobic processes,  $D_i^{Bio}$  [\$]/yr; biogas combustion,  $D_i^{Comb}$  [\$]/yr; fugitive emissions,  $D_i^{Fugitive}$  [\$]/yr; and natural gas combustion,  $D_i^{NG}$  [\$]/yr, at the facility-level. The damages are the product of damages per marginal gram of emissions from county  $k$ ,  $d_{j,k}$  [\$]/g, and the emissions from aerobic processes,  $M_{i,j}^{Aer}$  [g]/yr; biogas combustion,  $M_{i,j}^{Comb}$  [g]/yr; fugitive emissions,  $M_{i,j}^{Fugitive}$  [g]/yr; and from natural gas combustion,  $M_{i,j}^{NG}$  [g]/yr.

$$D_i^{Aer} = \sum_j d_{j,k} M_{i,j}^{Aer} \quad (3.6)$$

$$D_i^{Comb} = \sum_j d_{j,k} M_{i,j}^{Comb} \quad (3.7)$$

$$D_i^{Fugitive} = \sum_j d_{j,k} M_{i,j}^{Fugitive} \quad (3.8)$$

$$D_i^{NG} = \sum_j d_{j,k} M_{i,j}^{NG} \quad (3.9)$$

We use the social cost of carbon to estimate the damages from GHG emissions and county-level marginal damages from AP2 to estimate damages from CAPs emissions. We use 100-year global warming potentials to convert CH<sub>4</sub> and N<sub>2</sub>O into CO<sub>2</sub> equivalents.<sup>44</sup> In keeping with the

IPCC's determination that CO<sub>2</sub> emissions from wastewater treatment are biogenic in origin, we report CO<sub>2</sub> emissions associated with biodegradation separately from damages associated with VOC, CH<sub>4</sub>, and N<sub>2</sub>O emissions and do not include them in our total damage results.

Damages from chemical manufacturing and electricity generation are calculated using Equations S2 and S4.

### *3.3.2 Evaluating the Energy Self-Sufficiency of Wastewater Treatment Plants*

As shown in Figure 3.1, we calculate the air emission reduction benefits of installing biogas-fueled heat and electricity generation at all 14,693 wastewater treatment facilities in the contiguous United States in three steps. These steps include calculating the potential heat and electricity generation of biogas production and combustion, calculating the difference in emissions between a natural gas and biogas combustion scenario and a baseline grid electricity scenario and biogas-fueled electricity generation scenario, and pricing the damages resulting in these different air emission scenarios.

*Biogas Heat Generation Potential.* Anaerobic digestion requires heating to raise the temperature of the sludge to higher temperatures than secondary treatment processes. Literature reports that biogas has a heat density of 22.4 MJ/m<sup>3</sup> of biogas.<sup>42</sup> We allocate heat produced by biogas combustion to heating the anaerobic digester. If there is additional heat needed for the anaerobic digester, we use Equation 3.4 to calculate the heat required from natural gas combustion.

*Biogas-Fueled Electricity Generation Potential.* We estimate electricity generation potential from biogas,  $G_i$  [kWh/yr], using Equation 3.10.<sup>60</sup> Anaerobic digestion requires, on average, 0.09 kWh per cubic meter of sludge treated and we allocate any electricity generated from biogas combustion to cover this difference. Any biogas-fueled electricity generation above

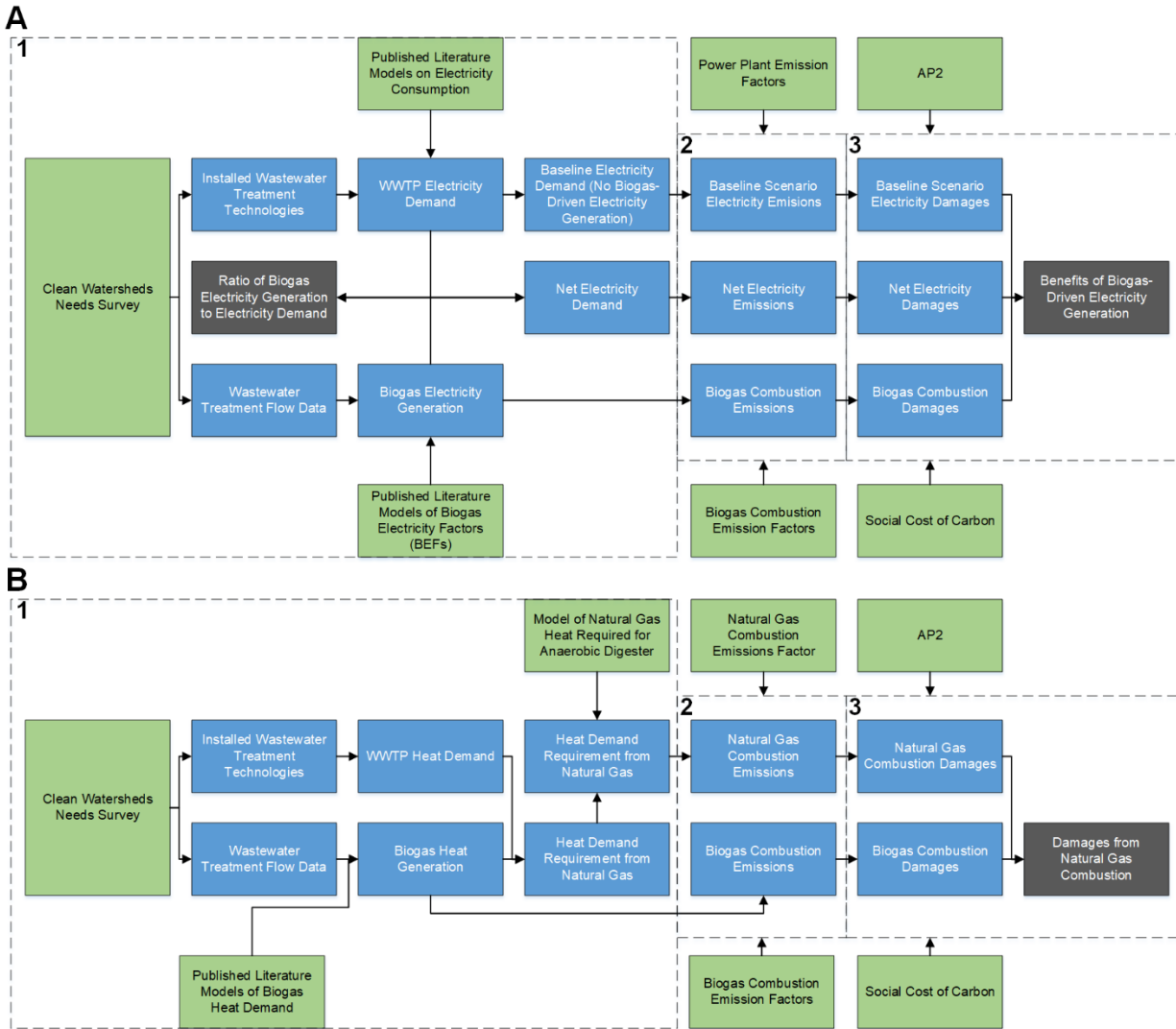


*Figure 3.1. Methods for calculating the benefits from biogas-fueled electricity generation and the damages resulting from biogas heat generation. There are three primary steps in this analysis: (1) calculating electricity based on installed treatment technologies and with biogas-fueled electricity generation using anaerobic digestion and the heat demand that needs to be supplemented from natural gas combustion; (2) calculating emissions based on grid electricity demand, natural gas combustion in an industrial boiler, and biogas generation; and (3) calculating the benefits of biogas-fueled electricity generation and damages resulting from natural gas combustion.*

the demand can be sold to the grid or used for non-process needs on-site. The biogas electricity factor,  $BEF$  [kWh/m<sup>3</sup>], is the amount of electricity that can be generated based on the influent wastewater flow rate,  $V_{i,influent}$  [m<sup>3</sup>/yr]. We select a BEF of 0.113 kWh/m<sup>3</sup>, consistent with a review performed by the Electric Power Research Institute.<sup>61</sup> We also perform sensitivity analysis on the BEF by using a high (0.139 kWh/m<sup>3</sup>) and low (0.0925 kWh/m<sup>3</sup>) BEF.

$$G_i = BEF * V_{i,influent} \quad (3.10)$$

We use the electricity generated from biogas combustion to calculate the self-sufficiency of wastewater treatment facilities and the net electricity demand at these facilities after installation of anaerobic sludge digestion. We define the self-sufficiency of wastewater treatment at facility  $i$ ,  $R_i$ , as the ratio of biogas-fueled electricity generated to the electricity demand at a POTW upgraded with biogas usage. Electricity demand at the POTW is the product of treated water volume,  $V_{i,influent}$  [m<sup>3</sup>/yr], and the sum of electricity consumption for all treatment processes  $g$  installed at the plant,  $\sum_g W_g^{Elec}$  [kWh/m<sup>3</sup>] (Equation 3.11).

$$R_i = \frac{G_i}{\sum_g V_{i,influent} \sum_g W_g^{Elec}} \quad (3.11)$$

The net electricity demand,  $E_{net,i}$  [kWh/yr], at these facilities is the baseline electricity demand minus the biogas-fueled electricity generated (Equation 3.12).

$$E_{net,i} = V_{i,influent} (\sum_g W_g^{Elec} + W_{anaerobic}^{Elec}) - G_i \quad (3.12)$$

We model the installation of anaerobic sludge digestion at all facilities and assume that plants with aerobic sludge digestion no longer operate those systems in favor of an anaerobic digester.

### 3.3.3 Air Emissions from Biogas Collection and Combustion.

Biogas-fueled electricity generation affects air emissions in four ways. First, there is an increase in biogas combustion emissions. Second, with the addition of biogas usage, there are reduced fugitive emissions of biogas from facilities that were previously emitting biogas to the

environment without flaring. Third, there is an increase in emissions from natural gas combustion to heat the anaerobic digester. Finally, there is a decrease in emissions due to the reduction in grid electricity consumption.

First, we calculate increases in emissions resulting from increases in biogas combustion at upgraded facilities that previously did not have anaerobic digestion or flare biogas that was produced in anaerobic digesters. To do this, we use Equation 3.2.

We calculate the reduced emissions from controlling and combusting fugitive emissions of biogas,  $M_{i,j,anaerobic}^{fugitive}$  [g/yr], using Equation 3.13. These emission changes are calculated by multiplying the wastewater influent flow rate,  $V_{i,influent}$  [m<sup>3</sup>/yr], by the difference in emissions factors between fugitive emissions factor,  $e_j^{fugitive}$  [g/m<sup>3</sup>] and combustion emissions factor,  $e_j^{comb}$  [g/m<sup>3</sup>]. As noted above, we assume that 18% of biogas that is produced at facilities that do not report biogas combustion are directly emitting biogas to the atmosphere.<sup>57</sup> Equation 3.13 therefore calculates the estimates of emissions,  $M_{i,j,anaerobic}^{fugitive}$  [g/yr], from these remaining facilities.

$$M_{i,j,anaerobic}^{fugitive} = V_{i,influent}(e_j^{fugitive} - e_j^{comb}) \quad (3.13)$$

There are also additional emissions associated with combusting natural gas to heat the anaerobic digester if not enough biogas is produced to completely meet the demand calculated in Equation 3.2. We allocate heat produced from biogas combustion to heat the digester rather than other needs on site that are outside the scope of our analysis (e.g. space heating for buildings, use in CHP systems). We calculate emissions resulting from natural gas combustion to supplement heat from biogas combustion,  $M_{anaerobic,i,j}^{NG}$  [g/yr], using Equation 3.5.

Finally, we calculate emissions associated with reduced grid electricity usage using Equation 3.14. We first calculate the net generation of electricity after accounting for the pre-anaerobic digester train by subtracting energy required to drive the pre-anaerobic digester train,

$V_{i,influent} \sum_g W_g^{Elec}$  [kWh/yr], from the amount of generated electricity,  $G_i$  [kWh/yr]. We then subtract the net electricity generated from the amount required to power the anaerobic digester,  $V_{i,influent} W_{anaerobic}^{Elec}$  [kWh/yr]. We multiply the resulting grid electricity demand by the electricity emissions factor for pollutant  $j$ ,  $e_{mf,j,l}$  [g/kWh], which is the marginal emissions factor<sup>62</sup> for CO<sub>2</sub>, NO<sub>x</sub>, and SO<sub>2</sub> and the average emissions factor for VOCs and PM<sub>2.5</sub><sup>63</sup> for state  $l$ .

$$M_{i,j,anaerobic}^{elec} = e_{mf,j,l} [V_{i,influent} W_{anaerobic}^{Elec} - (G_i - V_{i,influent} \sum_g W_g^{Elec})] \quad (3.14)$$

*Air Emissions Benefits Associated with Biogas-Fueled Electricity Generation.* Changes in air emission damages associated with electricity generation from biogas are the benefits of reductions in grid electricity usage and damages associated with natural gas and biogas combustion to operate the anaerobic digester. For facility-level benefits of grid electricity reduction, we use Equation S2 to calculate damages associated with the baseline grid electricity,  $D_{i,baseline}^{Elec}$  [\$/yr], and the biogas electricity,  $D_{i,net}^{Elec}$  [\$/yr], scenarios. The benefits of reductions in grid electricity usage are the difference between these two scenarios. We calculate the increase in damages from combustion emissions at facility  $i$ ,  $D_{i,anaerobic}^{Comb}$  [\$/yr]; the benefits of controlling and combusting fugitive biogas emissions,  $B_{i,anaerobic}^{Fugitive}$  [\$/yr]; the increase in damages from natural gas combustion,  $D_{anaerobic,i}^{NG}$  [\$/yr]; and the damages for grid electricity generation,  $D_{anaerobic,i}^{Elec}$  [\$/yr], using Equations 3.15-3.18, which are similar to Equations 3.6-3.9.

$$D_{i,anaerobic}^{Comb} = \sum_j d_{j,k} M_{anaerobic,i,j}^{Comb} \quad (3.15)$$

$$B_{i,anaerobic}^{Fugitive} = \sum_j d_{j,k} M_{anaerobic,i,j}^{Fugitive} \quad (3.16)$$

$$D_{i,anaerobic}^{NG} = \sum_j d_{j,k} M_{anaerobic,i,j}^{NG} \quad (3.17)$$

$$D_{i,anaerobic}^{Elec} = \sum_j d_{j,k} M_{anaerobic,i,j}^{Elec} \quad (3.18)$$



The net benefits from biogas-fueled electricity generation at facility  $i$ ,  $B_i$  [\$/yr], are calculated using Equation 3.19.

$$B_i = (D_{i,baseline}^{Elec} - D_{i,net}^{Elec}) + B_{i,anaerobic}^{Fugitive} - D_{i,anaerobic}^{Comb} - D_{i,anaerobic}^{NG} \quad (3.19)$$

### 3.3.4 Uncertainty Analysis

Table 3.1 Uncertain parameters, values and ranges.

Variable	Value in Main Text	Uncertainty Analysis Ranges	SI Section
<i>Uncertainty in Air Emissions and Damages Calculation</i>			
Electricity Consumption for Unit Processes	Literature-Based Averages	Literature Minimums and Maximums	S5.2
Chemical Consumption for Unit Processes	Literature-Based Averages	Literature Minimums and Maximums	S5.3
Influent Flow	CWNS Average Flow	CWNS Design Flow	S5.4
Biogas Flaring at Facilities that Produce but Do Not Use Biogas	82% Flare/18% Emit <sup>57</sup>	100% Flare/0% Emit 0% Flare/100% Emit	S5.5
Chemical Manufacturing Location	Revenue Distribution of Chemical Manufacturing Sector	(a) In-State (b) Evenly Distributed (c) In Lowest Damage State (d) In Highest Damage State (e) Off-Shore	S6.0
Value of a Statistical Life	\$8.6M (2014 USD) <sup>43</sup>	\$2M-\$10M	Manuscript
Social Cost of Carbon	\$43/short ton <sup>44</sup>	\$0-\$60/short ton	Manuscript
<i>Uncertainty in Biogas-Fueled Electricity Generation</i>			
Influent Flow	CWNS Average Flow	CWNS Design Flow	S7.1
Biogas Electricity Factors	0.113 kWh/m <sup>3</sup>	0.0925 kWh/m <sup>3</sup> (low) 0.139 kWh/m <sup>3</sup> (high)	Manuscript
Electricity Consumption for Unit Processes	Literature-Based Averages	Literature Minimums and Maximums	S7.2

There are several uncertain parameters in our analysis listed in Table 3.1. These include uncertainty in calculating air emissions, damages, and biogas-fueled electricity generation. For the results presented in the main manuscript, we rely on average values based on literature sources and data. For sensitivity analyses, we run a Monte Carlo analysis on the total damages

resulting from electricity generation, chemical manufacturing, and on-site emissions. The probability distributions for flow rate, electricity consumption, and chemical dosage, as well as the results of the Monte Carlo Analysis can be found in SI Section 5.1. We also perform one-at-a-time analysis for each of these variables by recalculating Equations 3.1-3.9 and S1-S4 to create ranges for air emissions damages and biogas-fueled electricity generation, using the range of values identified in Tables 1 and S1 in SI Section 1.0. Results of the one-at-a-time uncertainty analyses can be found in the SI Sections listed in Table 3.1.

There is also uncertainty about the location of chemical manufacturing. In the main manuscript, we assume that chemical manufacturing follows the national distribution of revenue from chemical manufacturing based on the Annual Survey of Manufacturers data set.<sup>64</sup> This is the same assumption we made in our previous work.<sup>26-27</sup> We also perform sensitivity analyses based on several alternative chemical manufacturing distributions as discussed in SI Section 6.0.

Finally, we also perform sensitivity analyses on the electricity self-sufficiency of biogas-fueled electricity generation. To do this, we calculate a minimum and maximum self-sufficiency scenario using Equation 3.6. The minimum self-sufficiency scenario is a scenario with the low BEF value and the maximum electricity consumption for treatment processes. The maximum self-sufficiency scenario is a scenario with the high BEF value and the minimum electricity consumption for treatment processes.

## **3.4 Results**

### *3.4.1 Damages from Municipal Wastewater Treatment*

We use the 2012 CWNS to estimate the air emission damages associated with operating installed wastewater treatment processes. As such, all damage values are specific to 2012 and reported in 2012 USD.<sup>65</sup> In 2012, wastewater treatment generated air emission damages of \$1,300 million.

The geographic distributions of damages associated with electricity generation, chemical manufacturing, and direct emissions are shown in Figure 3.2. Electricity generation accounts for 83%, or \$1.05 billion, of these air emission damages. There are an additional \$190 million annually (15% of total damages) in on-site emissions. The largest drivers of these direct damages include VOCs released during secondary treatment (\$84 million annually) and \$64 million in fugitive methane emissions from facilities with existing anaerobic digesters but without gas capture or flaring. Damages from chemical manufacturing contribute \$16 million.

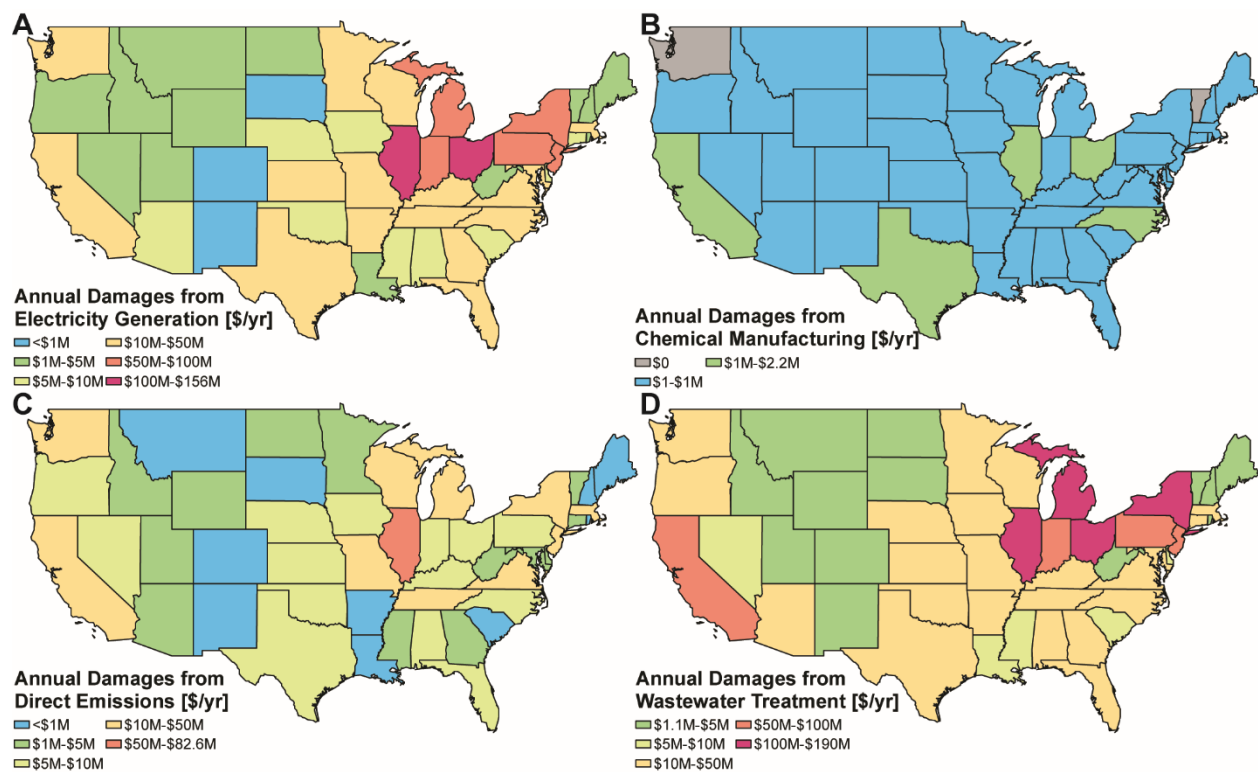


*Figure 3.2. Air emission damages in 2012 from installed wastewater treatment and sludge digestion processes due to (A) electricity generation (\$1.05 billion in 2012 USD), (B) chemical manufacturing (\$16 million in 2012 USD), (C) direct emissions (\$190 million in 2012 USD), and (D) total damages (\$1.3 billion in 2012 USD). N.B. Damages from on-site emissions of biogenic CO<sub>2</sub> are not shown in Panel C, and would add an additional \$430 million (in 2012 USD) if valued at the social cost of carbon.*

Air emissions and damages from wastewater treatment are tabulated in SI Section 4.0 and Tables S5 and S6.

### *3.4.2 Energy Self-Sufficiency of POTWs*

Anaerobic sludge digestion and biogas combustion have the potential to offset a meaningful fraction of the air emission damages from electricity consumption at wastewater treatment facilities. Nationwide, we estimate biogas-fueled electricity generation potential of 3700 GWh (3000-4400 GWh) annually (Figure 3.3A). This amounts to 19-28% of the electricity consumed in operating wastewater treatment facilities. At POTWs that completely meet their electricity need using biogas-fueled electricity generation, there is an excess 1,700 GWh of electricity produced that could be used for non-treatment needs on-site or potentially sold to the grid if facilities were to upgrade.

While the potential for biogas-fueled electricity generation is significant, the technical potential for biogas-fueled electricity generation to displace grid-sourced electricity depends upon the energy intensity of the installed treatment processes. The maximum potential electricity demand could be met by biogas-fueled generation potential is plotted in Figure 3.3B, with the regions of the curve generally corresponding to different wastewater treatment process intensity. Region 1 includes facilities operating energy intensive processes including primary treatment for solids removal, activated sludge, disinfection, and tertiary treatment for nitrogen or phosphorous removal. POTWs in Region 2 are more likely to use trickling biofilters in place of energy intensive activated sludge processes, and less likely to employ tertiary treatment technologies. Regions 3 and 4 have either a lagoon plus disinfection (Region 3) or primary treatment, aeration, and disinfection (Region 4). Finally, Region 5 contains POTWs with only solids removal and disinfection processes installed.

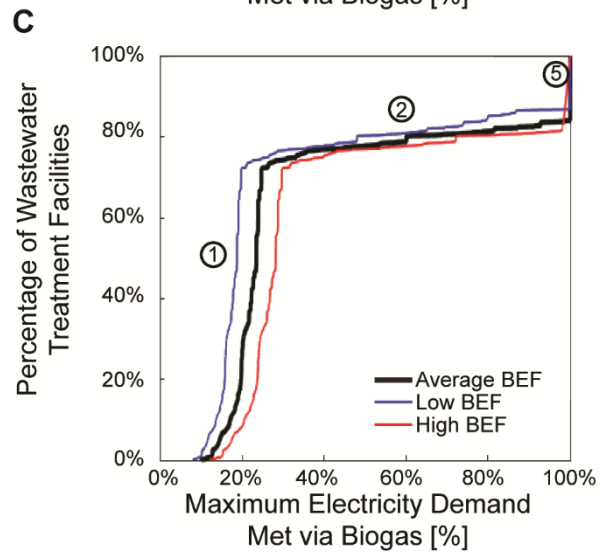
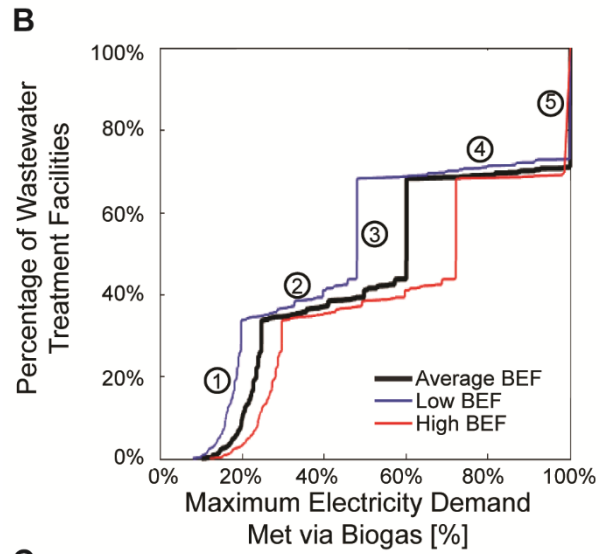
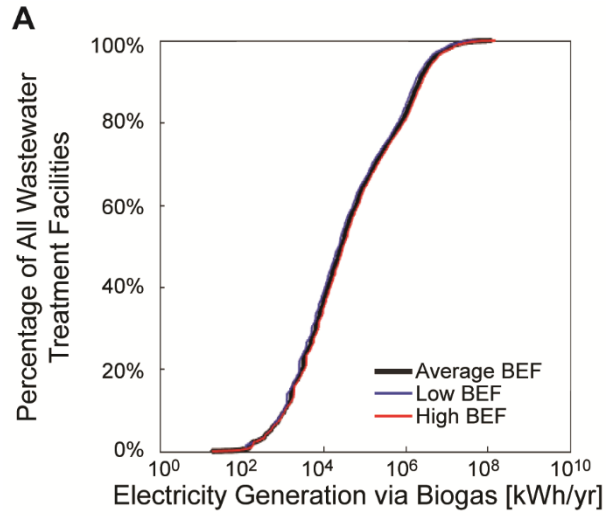


*Figure 3.3. Potential for biogas-fueled electricity generation to reduce net electricity demand at wastewater treatment plants in the CWNS database. Panel (A) shows the treatment facility level estimates of electricity generation via biogas combustion using an average, low, and high biogas electricity factor (BEF). Panels (B) and (C) show the ratio of electricity generation via biogas to the electricity demand at all facilities and at large (>5 MGD capacity) facilities, respectively. The circled numbers indicate different levels of treatment intensity, as described in the text, with more intense levels of treatment (e.g. nutrient control and tertiary treatment) installed at lower levels.*

Biogas combustion from the plant could completely meet the thermal needs of heating the anaerobic digestion. The excess biogas that is not used to heat the anaerobic digester contains 18 million GJ of thermal energy. This excess biogas could be used for other on-site heating needs or further processed and fed into the natural gas grid.<sup>57</sup>

In addition to the technical feasibility of offsetting heat and electricity generation, there are economic and operational challenges to operating anaerobic sludge digesters and biogas-fueled generators. As there may not be sufficient biosolids produced at facilities that treat less than 5 MGD to make biogas-fueled combined heat and power technically feasible,<sup>66</sup> we have replotted the potential for biogas to meet electricity demand at large facilities with inflows of >5 MGD in Figure 3.3C. While large facilities tend to operate more energy intensive process and have lower offset potentials, they also process more wastewater and have larger biogas generation potential on a per facility basis.

### 3.4.3 Air Emission Benefits from Biogas-Fueled Electricity Generation

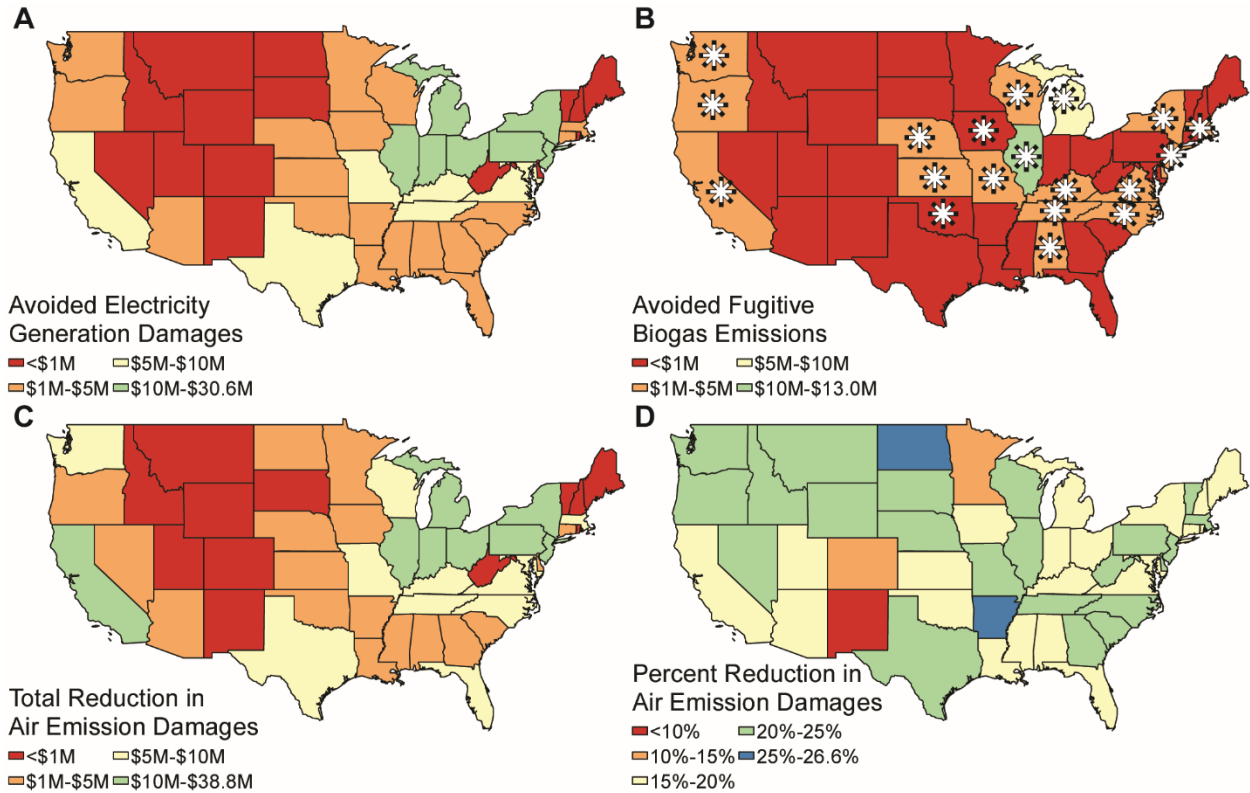


*Figure 3.4. Changes in air emissions associated with wastewater treatment resulting from*

*biogas-fueled heat and electricity generation at wastewater treatment facilities in the continental United States. (A) The changes in air emissions are driven by avoided damages from electricity generation (\$240 million in benefits in 2012 USD). However, there are \$390,000 (in 2012 USD) additional damages occurring from facilities upgraded to combust biogas. Combusting fugitive emissions and using it to heat the anaerobic digesters at these facilities would also reduce natural gas combustion emissions by \$8 million (in 2012 USD). The asterisks in Panel B indicate states where reduced natural gas combustion produce at least \$100,000 (in 2012 USD) in benefits annually. The total benefits of upgrading all POTWs to anaerobic digestion and biogas-fueled CHP are (C) \$310 million annually (in 2012 USD) or (D) a 25% reduction in air emission damages. Benefits are tabulated in SI Section 4.2 and Tables S7-S8.*

Installing anaerobic digestion and biogas usage for heat and electricity generation at all POTWs that do not currently have these processes installed would produce air emission benefits of \$310 million (in 2012 USD) annually or a 25% reduction in air emission damages from wastewater treatment (Figure 3.4). Nationwide, biogas-fueled electricity generation offsets \$240 million in damages from the grid. As shown in Figure 3.4A, these benefits are greatest in states with grids that are heavily-reliant on coal (e.g. Pennsylvania and Ohio) or with large populations (e.g. New York and California). There are \$64 million (in 2012 USD) in benefits to controlling and combusting fugitive biogas emissions (Figure 3.4B). There are also small benefits in avoided natural gas combustion resulting from using combusted biogas (\$8.0 million in 2012 USD) and even smaller additional damages resulting from biogas combustion emissions at upgraded facilities (\$390,000 in 2012 USD).

#### *3.4.4 Uncertainty Analyses*

To assess the uncertainty in our air emission damage results we performed Monte Carlo analyses by assigning a distribution of values to influent wastewater flow rate, electricity demand of the unit processes, chemical dosing required for operating these processes, and on-site emissions from wastewater treatment processes. Total damages are robust to uncertainty in these input parameters (Figure 3.5A). The primary contribution to this uncertainty originates from uncertainty in the electricity consumption, which itself is a function of the influent flow rate and the demand from unit processes. The results of the one-at-a-time analyses are reported in SI Sections 5.2-5.4, SI Section 6.0 and Table S10-S18.



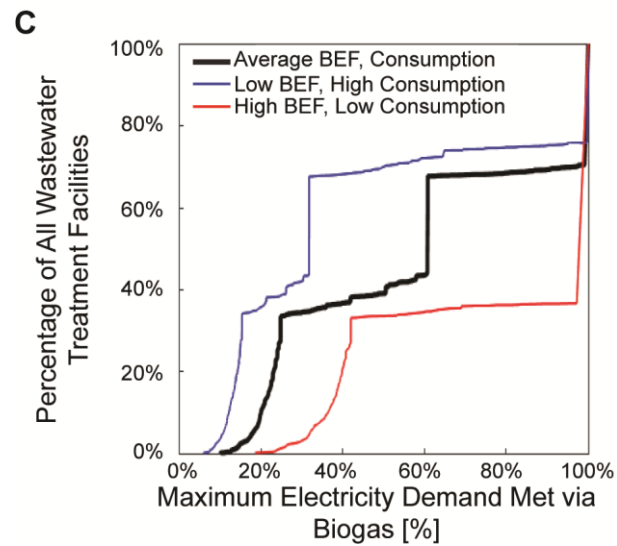
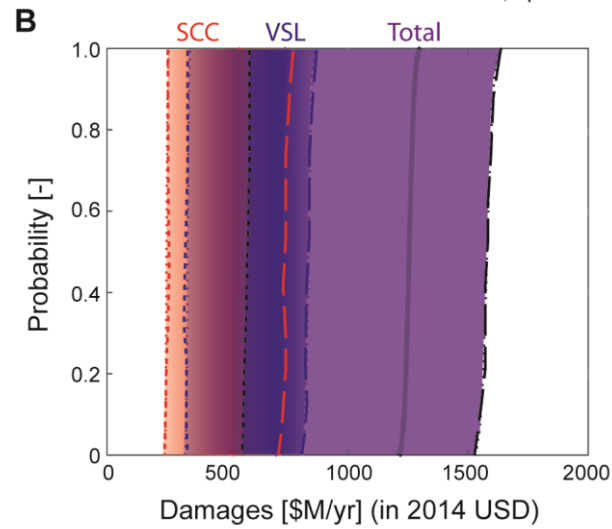
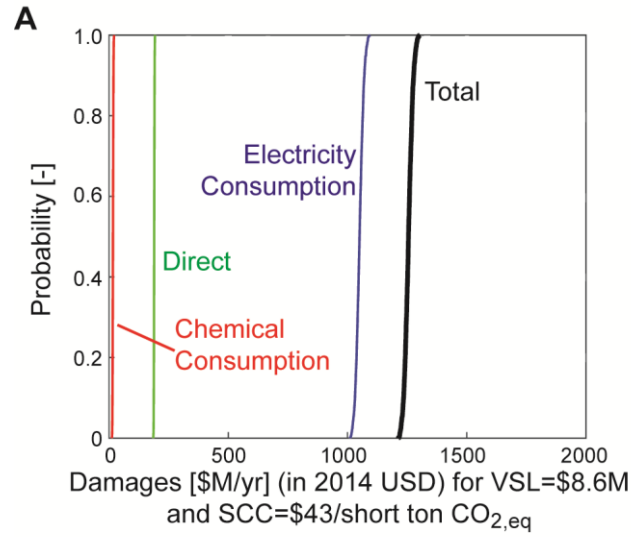


*Figure 3.5. Uncertainty analyses for (A) air emission damages from wastewater treatment at the default assumptions for the value of a statistical life (\$8.6M in 2014USD) and social cost of carbon (\$43/short ton in 2014USD), (B) the value of a statistical life (ranging from 4-10M in 2014 USD) shown in blue and social cost of carbon shown in red (ranging from \$20-\$60/short ton CO<sub>2,eq</sub>), and (C) energy self-sufficiency of wastewater treatment. In panel (B), the dotted and dashed lines represents the minimum and maximum VSL and SCC considered, respectively.*

These results are also sensitive to the value of a statistical life (VSL) and social cost of carbon (SCC) (Figure 3.5 B). In the baseline analysis, we used a VSL of \$8.6M (in 2014 USD) to value damages of criteria air pollutants. Varying the from \$4M-\$10M (in 2014 USD) produces the range shown in blue with damages from \$330M/yr (VSL of \$4M) to \$840M/yr (VSL of \$10M). The SCC used in the base case analysis was \$43/short ton of CO<sub>2</sub> (in 2014 USD). The damages are approximately \$250M/yr and \$740M/yr when the SCC is \$20/short ton and \$60/short ton, respectively. The assumed VSL and SCC are significant determiners of the final air emission damages associated with municipal wastewater treatment, and therefore the benefits of anaerobic digestion installation.

Finally, we performed sensitivity analyses on the electricity self-sufficiency of POTWs (Figure 3.5C) and the amount of electricity generated from biogas (SI Section 7.1 and Figure S1). The electricity self-sufficiency and electricity generated are dependent on several variables, including the wastewater flowrate, the BEF, and the unit electricity consumption. The low and high self-sufficiency cases are shown in blue and red in Figure 3.5B and have a different shape than the baseline assumptions. The most significant difference is the number of plants capable of achieving complete self-sufficiency. In the high electricity self-sufficiency case, 60% of systems

generate enough electricity from biogas-fueled electricity generation to meet all of their electricity needs. In the low self-sufficiency case, only about 30% are capable of achieving complete energy self-sufficiency. Analysis on the impact of wastewater flowrate on biogas-fueled electricity generation can be found in SI Section 7.0 and Figure S1.

### **3.5 Discussion**

In 2012, wastewater treatment processes in the United States generated \$1.3 billion in air emission damages. Electricity consumption is the largest source of these damages, contributing \$1.05 billion in damages resulting from the consumption of 16,000 GWh of electricity. As the US demand for wastewater treatment is expected to increase by 20-25% by 2032,<sup>1</sup> the electricity consumption of wastewater treatment and air emission damages is going to increase as well.

Biogas generation has the potential to make municipal wastewater treatment more sustainable. Biogas combustion for electricity generation can displace grid electricity, reducing the environmental impact of wastewater treatment in areas with a coal-dependent grid. Despite this potential for environmental benefit, biogas usage in combined heat and power systems occurs at less than 1% of the nation's POTWs with a capacity of 440 MW.<sup>58</sup> Anaerobic digestion, with or without biogas usage, is much more widespread with 43% of the volume of US wastewater treated at facilities with anaerobic digesters.<sup>57</sup> Installing biogas-fueled electricity generation at facilities with anaerobic digestion that currently do not have it thus appears an obvious opportunity to reduce the environmental impact of wastewater treatment throughout the United States.<sup>58</sup>

Despite this opportunity, there are several barriers to the widespread adoption of biogas-fueled electricity generation. Given limited budgets for capital investments, POTWs have frequently identified the large upfront capital costs for installing biogas-fueled electricity

generation as a major barrier to adoption.<sup>67</sup> Improving the quality of biogas, i.e. increasing the CH<sub>4</sub> concentration, by removing impurities (e.g. CO<sub>2</sub> or H<sub>2</sub>S) is another substantial challenge for making biogas combustion and sale to the natural gas grid more attractive.<sup>58, 67</sup>

Another barrier for implementation, especially for systems that treat less than 5 MGD, is inadequate biosolids production.<sup>66</sup> However, 89% of the systems in our analysis have a capacity of less than 5 MGD, but only contribute 17% of the total biogas-fueled electricity generation potential. Co-digestion of other organic wastes (e.g. food and animal waste) can lower the minimum size to 1 MGD,<sup>57-58</sup> allowing generation of electricity at additional POTWs.

Developing new technologies to lower the size at which energy recovery is economically viable is a vital area of research that would reduce the electricity consumption and air emissions associated with wastewater treatment. Small, decentralized wastewater treatment systems would also enable other environmental benefits, including source separation, gray water reuse, and the ability to design systems to target specific pollutants.<sup>28, 68</sup>

Finally, there are several policy interventions that could support POTW implementation of biogas-fueled electricity generation. First, as noted above the most significant barrier to implementation is the upfront capital costs and long payback periods associated with the equipment required. Policies that offer financial assistance or that internalize the air emission benefits for POTWs for installing biogas-fueled electricity generation would make the process more economically attractive. There is also some uncertainty around the net national benefits from GHG reduction resulting from installing biogas-fueled electricity generation. Policies that expand data collection and reporting could help quantify this benefit and justify policy interventions.

### 3.6 Conclusions

For infrastructure to be sustainable it has to achieve its mission while balancing its costs, social impacts, and environmental impacts. For wastewater treatment, the largest source of environmental impacts are the air emissions associated with electricity generation.<sup>29, 33, 51</sup> Building sustainable POTWs in the future therefore means increasing POTW energy efficiency and reducing the air emissions associated with consumed electricity. The latter will happen slowly over the coming decades, as the grid reduces its reliance on coal.

In the short term, biogas-fueled electricity generation holds potential to reduce these air emission damages. Our work has shown that the air emission reductions from electricity generation benefits amount to \$240 million (in 2012\$) annually. Furthermore, as many states<sup>37-</sup><sup>38</sup> move to reduce the climate impacts of water and wastewater treatment, capturing and using fugitive biogas offers a relatively straightforward solution. The US may realize approximately \$64 million (in 2012 USD) in benefits from avoided emissions of 1.5 million tons CO<sub>2,eq</sub> of methane in biogas.

This paper quantified the damages from air emissions using marginal air emission damage models, but similar marginal damage models for water pollution do not exist. As a result, past attempts to perform benefit-cost analysis on wastewater treatment by regulators and researchers have relied on contingent valuation models. Contingent valuation approaches are often insufficient for developing accurate estimates of environmental goods (e.g. reduced water pollution).<sup>69</sup> As a consequence of this gap, our work has only quantified one-half of these air-water tradeoffs that result from wastewater treatment. Holistic “one environment” analyses and decisions for wastewater systems will require an ability to quantify both.

### 3.7 Acknowledgements

This work was supported by the National Science Foundation under award number CBET-1554117.

### 3.8 Nomenclature

#### Symbols

BEF: Biogas Electricity Factor [ $\text{kWh/m}^3$ ]

$c_p$ : Heat capacity [ $\text{J/g} \cdot ^\circ\text{C}$ ]

$d$ : Marginal damages per short ton of air emissions [ $\text{\$/ton}$ ]

$D$ : Nationwide damages from air emissions [ $\text{\$/yr}$ ]

$e$ : Unit emissions [ $\text{g/m}^3$ ], [ $\text{g/kWh}$ ], [ $\text{g/g-chemical}$ ]

$E$ : Electricity demand [ $\text{kWh/yr}$ ]

$G$ : Electrical energy production from biogas generation [ $\text{kWh/yr}$ ]

HHV: Higher Heating Value [ $\text{J/m}^3$ ]

$M$ : Mass of pollutants [ $\text{g/yr}$ ]

$R$ : Ratio of biogas-fueled electricity generation to electricity demand [-]

$\rho$ : Density [ $\text{g/m}^3$ ]

$T$ : Temperature [ $^\circ\text{C}$ ]

$\forall$  Volume of wastewater treated [ $\text{m}^3/\text{yr}$ ]

$W$ : Electricity consumed during wastewater treatment process [ $\text{kWh/m}^3$ ]

#### Subscripts

anaerobic: Anaerobic digester

baseline: Baseline scenario (no additional biogas-fueled electricity generation)

biogas: Biogas generation scenario

g: Unit process

i: POTW

influent: Influent wastewater

j: Air pollutant (i.e. NO<sub>x</sub>, SO<sub>2</sub>, PM<sub>2.5</sub>, VOC, CO<sub>2</sub>, CH<sub>4</sub>, N<sub>2</sub>O)

k: County

l: State

mf: Electricity emissions factor

net: Net baseline electricity demand

NG: Natural gas

sludge: Sludge

treat: Emissions from the treatment facility that are released during wastewater treatment

### **Superscripts**

Bio: Emissions of biodegradation of organics in wastewater

Comb: Emissions from combustion of biogas

Elec: Emissions from generating electricity consumed to drive wastewater treatment

NG: Emissions from natural gas combustion

### **3.9 References**

1. American Society of Civil Engineers 2017 Infrastructure Report Card - Wastewater.  
<https://www.infrastructurereportcard.org/cat-item/wastewater/> (accessed May 27, 2017).
2. Hendriks, A.; Langeveld, J. G., Rethinking Wastewater Treatment Plant Effluent Standards: Nutrient Reduction or Nutrient Control? *Environ Sci Technol* **2017**.

3. Molinos-Senante, M.; Hernandez-Sancho, F.; Sala-Garrido, R., Economic feasibility study for wastewater treatment: a cost-benefit analysis. *Sci Total Environ* **2010**, *408* (20), 4396-402.
4. Thong, Z.; Cui, Y.; Ong, Y. K.; Chung, T.-S., Molecular Design of Nanofiltration Membranes for the Recovery of Phosphorus from Sewage Sludge. *ACS Sustainable Chemistry & Engineering* **2016**, *4* (10), 5570-5577.
5. Mihelcic, J. R.; Ren, Z. J.; Cornejo, P. K.; Fisher, A.; Simon, A. J.; Snyder, S. W.; Zhang, Q.; Rosso, D.; Huggins, T. M.; Cooper, W.; Moeller, J.; Rose, B.; Schottel, B. L.; Turgeon, J., Accelerating Innovation that Enhances Resource Recovery in the Wastewater Sector: Advancing a National Testbed Network. *Environ Sci Technol* **2017**.
6. Sutton, P. M.; Rittman, B. E.; Schraa, O. J.; Banaszak, J. E.; Tonga, A. P., Wastewater as a resource: a unique approach to achieving energy sustainability. *Water Science & Technology* **2011**, *63* (9), 2004-2009.
7. Xie, M.; Shon, H. K.; Gray, S. R.; Elimelech, M., Membrane-based processes for wastewater nutrient recovery: Technology, challenges, and future direction. *Water Res* **2016**, *89*, 210-21.
8. Khiewwijit, R.; Temmink, H.; Rijnaarts, H.; Keesman, K. J., Energy and nutrient recovery for municipal wastewater treatment: How to design a feasible plant layout? *Environmental Modelling & Software* **2015**, *68*, 156-165.
9. Hamoda, M. F., Air pollutants emissions from waste treatment and disposal facilities. *J Environ Sci Health A Tox Hazard Subst Environ Eng* **2006**, *41* (1), 77-85.



10. Mikosz, J., Analysis of greenhouse gas emissions and the energy balance in a model municipal wastewater treatment plant. *Desalination and Water Treatment* **2016**, 57 (59), 28551-28559.
11. Basu, S.; Gu, Z. C.; Shilinsky, K. A., Application of Packed Scrubbers for Air Emissions Control in Municipal Wastewater Treatment Plants. *Environmental Progress* **1998**, 17 (1), 9-18.
12. Sahely, H. R.; MacLean, H. L.; Monteith, H. D.; Bagley, D. M., Comparison of on-site and upstream greenhouse gas emissions from Canadian municipal wastewater treatment facilities. *Journal of Environmental Engineering and Science* **2006**, 5 (5), 405-415.
13. Kyung, D.; Kim, M.; Chang, J.; Lee, W., Estimation of greenhouse gas emissions from a hybrid wastewater treatment plant. *Journal of Cleaner Production* **2015**, 95, 117-123.
14. Bani Shahabadi, M.; Yerushalmi, L.; Haghighat, F., Estimation of greenhouse gas generation in wastewater treatment plants--model development and application. *Chemosphere* **2010**, 78 (9), 1085-92.
15. Mihelcic, J. R.; Baillod, C. R.; Crittenden, J. C.; Rogers, T. N., Estimation of VOC Emissions from Wastewater Facilities by Volatilization and Stripping. *Air & Waste* **1993**, 43 (1), 97-105.
16. Bani Shahabadi, M.; Yerushalmi, L.; Haghighat, F., Impact of process design on greenhouse gas (GHG) generation by wastewater treatment plants. *Water Res* **2009**, 43 (10), 2679-87.
17. Oshita, K.; Okumura, T.; Takaoka, M.; Fujimori, T.; Appels, L.; Dewil, R., Methane and nitrous oxide emissions following anaerobic digestion of sludge in Japanese sewage treatment facilities. *Bioresour Technol* **2014**, 171, 175-81.

18. Jones, D. L.; Burklin, C. E.; Seaman, J. C.; Jones, J. W.; Corsi, R. L., Models to Estimate Volatile Organic Hazardous Air Pollutant Emissions from Municipal Sewer Systems. *J Air Waste Manag Assoc* **1996**, *46* (7), 657-666.
19. Noyola, A.; Paredes, M. G.; Morgan-Sagastume, J. M.; Güereca, L. P., Reduction of Greenhouse Gas Emissions From Municipal Wastewater Treatment in Mexico Based on Technology Selection. *CLEAN - Soil, Air, Water* **2016**, *44* (9), 1091-1098.
20. Tansel, B.; Eyma, R. R., Volatile Organic Contaminant Emissions from Wastewater Treatment Plants During Secondary Treatment. *Water, Air, and Soil Pollution* **1999**, *112*, 315-325.
21. Guz, L.; Lagod, G.; Jaromin-Glen, K.; Suchorab, Z.; Sobczuk, H.; Bieganski, A., Application of gas sensor arrays in assessment of wastewater purification effects. *Sensors (Basel)* **2014**, *15* (1), 1-21.
22. Yang, W. B.; Chen, W. H.; Yuan, C. S.; Yang, J. C.; Zhao, Q. L., Comparative assessments of VOC emission rates and associated health risks from wastewater treatment processes. *J Environ Monit* **2012**, *14* (9), 2464-74.
23. Ding, W.; Li, L.; Liu, J., Investigation of the effects of temperature and sludge characteristics on odors and VOC emissions during the drying process of sewage sludge. *Water Sci Technol* **2015**, *72* (4), 543-52.
24. Corsi, R. L.; Card, T. R., Estimation of VOC Emissions Using the BASTE Model. *Environmental Progress* **1991**, *10* (4), 290-299.
25. Yeh, S.-H., Estimating Cancer Risk Increment from Air Pollutant Exposure for Sewer Workers Working in an Industrial City. *Aerosol and Air Quality Research* **2011**, 120-127.

26. Gingerich, D. B.; Mauter, M. S., Life-Cycle Air Emissions Damages of Municipal Drinking Water Treatment Under Current & Proposed Regulatory Standards. **in preparation.**
27. Gingerich, D. B.; Sun, X. B., A. Patrick; Azevedo, I. M. L.; Mauter, M. S., Spatially resolved air-water emissions tradeoffs improve regulatory impact analyses for electricity generation. *Proceedings of the National Academy of Science* **2017**, 1862–1867.
28. Opher, T.; Friedler, E., Comparative LCA of decentralized wastewater treatment alternatives for non-potable urban reuse. *J Environ Manage* **2016**, 182, 464-76.
29. Pasqualino, J. C.; Meneses, M.; Abella, M.; Castells, F., LCA as a Decision Support Tool for the Environmental Improvement of the Operation of a Municipal Wastewater Treatment Plant. *Environmental Science & technology* **2009**, 43 (9), 3300-3307.
30. Shehabi, A.; Stokes, J. R.; Horvath, A., Energy and air emission implications of a decentralized wastewater system. *Environmental Research Letters* **2012**, 7 (2), 024007.
31. Stokes, J. R.; Horvath, A., Supply-chain environmental effects of wastewater utilities. *Environmental Research Letters* **2010**, 5 (1), 014015.
32. Giménez, J.; Bayarri, B.; González, Ó.; Malato, S.; Peral, J.; Esplugas, S., Advanced Oxidation Processes at Laboratory Scale: Environmental and Economic Impacts. *ACS Sustainable Chemistry & Engineering* **2015**, 3 (12), 3188-3196.
33. Rodriguez-Garcia, G.; Molinos-Senante, M.; Hospido, A.; Hernandez-Sancho, F.; Moreira, M. T.; Feijoo, G., Environmental and economic profile of six typologies of wastewater treatment plants. *Water Res* **2011**, 45 (18), 5997-6010.
34. Alyaseri, I.; Zhou, J., Towards better environmental performance of wastewater sludge treatment using endpoint approach in LCA methodology. *Heliyon* **2017**, 3 (3), e00268.

35. Vassallo, P.; Paoli, C.; Fabiano, M., Energy required for the complete treatment of municipal wastewater. *Ecological Engineering* **2009**, *35* (5), 687-694.
36. Lundin, M.; Bengtsson, M.; Molander, S., Life Cycle Assessment of Wastewater Systems: Influence of System Boundaries and Scale on Calculated Environmental Load. *Environmental Science & Technology* **2000**, *43* (1), 180-186.
37. California Department of Water Resources, California Department of Water Resources Climate Action Plan. Resources, C. D. o. W., Ed. California Department of Water Resources: Sacramento, CA, 2012.
38. Massachusetts Department of Environmental Protection *Massachusetts Energy Management Pilot Program for Drinking Water and Wastewater Case Study*; Massachusetts Department of Environmental Protection: Boston, MA, December 2009, 2009; p 8.
39. Berktaý, A.; Nas, B., Biogas Production and Utilization Potential of Wastewater Treatment Sludge. *Energy Source, Part A: Recovery, Utilization, and Environmental Effects* **2008**, *30* (2), 179-188.
40. Smith, A. L.; Stadler, L. B.; Cao, L.; Love, N. G.; Raskin, L.; Skerlos, S. J., Navigating wastewater energy recovery strategies: a life cycle comparison of anaerobic membrane bioreactor and conventional treatment systems with anaerobic digestion. *Environ Sci Technol* **2014**, *48* (10), 5972-81.
41. van Leeuwen, R. P.; Fink, J.; de Wit, J. B.; Smit, G. J. M., Upscaling a district heating system based on biogas cogeneration and heat pumps. *Energy, Sustainability and Society* **2015**, *5* (1).

42. Metcalf & Eddy, I.; Tchobanoglous, G. B., Franklin L.; Stensel, H. D., *Wastewater Engineering: Treatment and Reuse*. 4th ed.; McGraw Hill Higher Education: New York, NY, 2002.
43. Muller, N. Z., Using index numbers for deflation in environmental accounting. *Environment and Development Economics* **2013**, 19 (04), 466-486.
44. Interagency Working Group on the Social Cost of Carbon, Technical Support Document: Technical Update of the Social Cost of Carbon for Regulatory Impact Analysis. Washington, D.C., 2015.
45. U.S. Environmental Protection Agency Clean Watersheds Needs Survey (CWNS) - 2008 Report and Data. <https://www.epa.gov/cwns/clean-watersheds-needs-survey-cwns-2008-report-and-data> (accessed June 10).
46. U.S. Environmental Protection Agency Clean Watersheds Needs Survey (CWNS) - 2012 Report and Data. <https://www.epa.gov/cwns/clean-watersheds-needs-survey-cwns-2012-report-and-data#access> (accessed June 10).
47. U.S. Environmental Protection Agency Emissions Inventories. <http://www3.epa.gov/ttn/chief/eiinformation.html> (accessed October 9, 2015).
48. National Renewable Energy Laboratory National Renewable Energy Laboratory - Life-Cycle Inventory Database. . <https://www.lcacommons.gov/nrel/process/show/50158> (accessed October 3, 2015).
49. Althaus H-J, e. a., *Life Cycle Inventories of Chemicals No. 8*, v. 2.0. Dusseldorf, Switzerland, 2007.

50. Tata, P.; Witherspoon, J.; Lue-Hing, C., *VOC Emissions from Wastewater Treatment Plants: Characterization, Control and Compliance*. Lewis Publishers: Boca Raton, FL, 2016.
51. Hospido, A.; Moreira, M. T.; Fernandez-Couto, M.; Feijoo, G., Environmental Performance of a Municipal Wastewater Treatment Plant *International Journal of Life Cycle Assessment* **2004**, 9 (4), 261-271.
52. Monteith, H. D.; Sahely, H. R.; MacLean, H. L.; Bagley, D. M., A Rational Procedure for Estimation of Greenhouse-Gas Emissions from Municipal Wastewater Treatment Plants. *Water Environment Research* **2005**, 77 (4), 390-403.
53. Doorn, M. R. J.; Towprayoon, S.; Vieira, S. M. M.; Irving, W.; Palmer, C.; Pipatti, R.; Wang, C., Chapter 6: Wastewater Treatment and Discharge. In *2006 IPCC Guidelines for National Greenhouse Gas Inventories*, Change, I. P. o. C., Ed. Intergovernmental Panel on Climate Change: Geneva, Switzerland, 2006.
54. Czepiel, P.; Crill, P.; Harriss, R., Nitrous Oxide Emissions from Municipal Wastewater Treatment. *Environmental Science & Technology* **1995**, 29, 2352-2356.
55. California Air Resource Board; California Climate Action Registry; ICLEI - Local Governments for Sustainability; Registry, T. C. *Local Government Operations Protocol: For the quantification and reporting of greenhouse gas emissions inventories*; California Air Resources Board: Sacramento, CA, 2010.
56. U.S. Environmental Protection Agency *Inventory of U.S. Greenhouse Gas Emissions and Sinks 1990-2015*; U.S. Environmental Protection Agency: Washington, D.C., 2017.
57. Shen, Y.; Linville, J. L.; Urgun-Demirtas, M.; Mintz, M. M.; Snyder, S. W., An overview of biogas production and utilization at full-scale wastewater treatment plants (WWTPs)

- in the United States: Challenges and opportunities towards energy-neutral WWTPs. *Renewable and Sustainable Energy Reviews* **2015**, 50, 346-362.
58. US Environmental Protection Agency CHP Partnership *Opportunities for Combined Heat and Power at Wastewater Treatment Facilities: Market Analysis and Lessons from the Field*; U.S. Environmental Protection Agency: Washington, D.C., 2011.
59. The Engineering Toolbox Fuel Gases Heating Values.  
[http://www.engineeringtoolbox.com/heating-values-fuel-gases-d\\_823.html](http://www.engineeringtoolbox.com/heating-values-fuel-gases-d_823.html) (accessed July 12, 2017).
60. Stillwell, A. S.; Hoppock, D. C.; Webber, M. E., Energy Recovery from Wastewater Treatment Plants in the United States: A Case Study of the Energy-Water Nexus. *Sustainability* **2010**, 2 (4), 945-962.
61. Burton, F. L. *Water and Wastewater Industries: Characteristics and Energy Management Opportunities*; Burton Environmental Engineering Electric Power Research Institute: Los Altos, CA, 1996.
62. Siler-Evans, K.; Azevedo, I. L.; Morgan, M. G., Marginal emissions factors for the U.S. electricity system. *Environmental Science & Technology* **2012**, 46 (9), 4742-8.
63. U.S. Environmental Protection Agency National Emissions Inventory (NEI).  
<https://www.epa.gov/air-emissions-inventories/national-emissions-inventory-nei> (accessed May 23, 2017).
64. United States Census Bureau Annual Survey of Manufacturers 2013.  
<https://www.census.gov/manufacturing/asm/index.html> (accessed October 11, 2015).
65. United States Bureau of Labor Statistics. CPI Inflation Calculator.  
[https://www.bls.gov/data/inflation\\_calculator.htm](https://www.bls.gov/data/inflation_calculator.htm) (accessed January 28, 2017).

66. Eastern Research Group, I.; U.S. Environmental Protection Agency *Opportunities for and Benefits of Combined Heat and Power at Wastewater Treatment Facilities*; U.S. Environmental Protection Agency: Washington, D.C., 2007.
67. Willis, J. L. *Barriers to Biogas Use for Renewable Energy*; Water Environment & Resue Foundation: Alexandria, VA, 2012.
68. Garibay-Rodriguez, J.; Rico-Ramirez, V.; Ponce-Ortega, J. M., Mixed Integer Nonlinear Programming Model for Sustainable Water Management in Macroscopic Systems: Integrating Optimal Resource Management to the Synthesis of Distributed Treatment Systems. *ACS Sustainable Chemistry & Engineering* **2017**, 5 (3), 2129-2145.
69. Diamond, P. A.; Hausman, J. A., Contingent Valuation: Is Some Number Better than No Number? *Journal of Economic Perspectives* **1994**, 8 (4), 45-64.



## CHAPTER 4: SPATIALLY RESOLVED AIR-WATER EMISSIONS TRADEOFFS IMPROVE REGULATORY IMPACT ANALYSES FOR ELECTRICITY GENERATION<sup>3</sup>

### 4.1 Abstract

Coal-fired power plants (CFPPs) generate air, water, and solids emissions that impose substantial human health, environmental, and climate (HEC) damages. This work demonstrates the importance of accounting for cross-media emissions tradeoffs, plant and regional emissions factors, and spatially variation in the marginal damages of air emissions when performing regulatory impact analyses for electric power generation. As a case study, we assess the benefits and costs of treating wet flue gas desulfurization (FGD) wastewater at U.S. CFPPs using the two best available treatment technology options specified in the 2015 Effluent Limitation Guidelines (ELG). We perform a life-cycle inventory of electricity and chemical inputs to FGD wastewater treatment processes and quantify the marginal HEC damages of associated air emissions. We combine these spatially resolved damage estimates with EPA estimates of water quality benefits, fuel switching benefits, and regulatory compliance costs. We estimate that the ELGs will impose net costs of \$3.00/m<sup>3</sup> for chemical precipitation and biological wastewater treatment and \$11.00/m<sup>3</sup> for zero-liquid discharge wastewater treatment (expected cost-benefit ratios of 1.8 and 1.7, respectively), with damages concentrated in regions containing a high fraction of coal generation or a large chemical manufacturing industry. Findings of net cost for FGD wastewater treatment are robust to uncertainty in auxiliary power source, location of chemical

---

<sup>3</sup> This chapter is based on a paper co-authored with Prof. Meagan Mauter, Prof. Ines Azevedo, Xiaodi Sun, and A. Patrick Behrer in Proceedings of the National Academy of Sciences. It can be found at Gingerich, D. B.; Sun, X. B., A. Patrick; Azevedo, I. M. L.; Mauter, M. S., Spatially resolved air-water emissions tradeoffs improve regulatory impact analyses for electricity generation. *Proceedings of the National Academy of Science* **2017**, *114*, (8), 1862-1867.

manufacturing, and binding air emissions limits in non-compliant regions, among other variables. Future regulatory design will minimize compliance costs and HEC tradeoffs by regulating air, water, and solids emissions simultaneously and performing regulatory assessments that account for spatial variation in emissions impacts.

## **4.2 Introduction**

An important recent driver of the U.S. transition away from coal-fired electricity generation has been the implementation of new air and water emission regulations, including the Cross State Air Pollution Rule,<sup>1</sup> the Mercury and Air Toxics Standards,<sup>2</sup> the Clean Power Plan,<sup>3</sup> and the Final Effluent Limitation Guidelines (ELGs) for Steam Electric Power Generation Facilities.<sup>4</sup> While each of these rules targets the human health, environmental, and climate change (HEC) externalities of coal-fired power generation, there has been little work characterizing the interactions between these regulations at the plant or regional levels. In particular, the control systems plants use to meet air and water regulations are interconnected, with wastewater being produced in air pollution control systems and air pollution being produced by water pollution control systems.

For example, the most prevalent SO<sub>2</sub> air emission control technology is wet flue gas desulfurization (FGD), which uses an aqueous slurry to scrub SO<sub>2</sub> from CFPP flue gas.<sup>5-7</sup> In 2014, wet FGD systems prevented emission of 2.7 million short tons of SO<sub>2</sub>, with tens of billions of dollars in benefits to human health.<sup>5</sup> These same wet FGD systems produced an estimated 210 million m<sup>3</sup> of wastewater contaminated with chloride, bromide, mercury, arsenic, boron, selenium, and other aqueous toxicants scrubbed from the flue gas.<sup>8,9</sup> Release of these aqueous contaminants poses risks to human health via fish consumption, drinking water disinfection

byproduct formation, and recreational exposure routes. This aqueous pollution also reduces water quality, contaminates sediments in receiving water bodies, and threatens wildlife.<sup>10</sup>

On the other hand, treating or eliminating this wastewater discharge will increase auxiliary power consumption at CFPPs, decrease generation efficiency, and increase air emissions per unit of energy that is effectively delivered to the grid. These processes will also consume chemical precipitants, nutrients, soda ash, and anti-scalants manufactured off-site, the production of which results in additional air emissions that are outside the scope of the ELG regulatory analyses.<sup>7, 11</sup> The extent of air-water emissions tradeoffs will vary with the composition of the wastewater, the treatment process, the energy inputs, and the location of the plant.

Benefit-cost analysis (BCA) is the institutionalized method for assessing tradeoffs stemming from regulatory decisions.<sup>4, 12-15</sup> Systematic BCA facilitates accounting across a diverse set of outcomes and may reduce the influence of special interests or political pressure on regulatory decisions.<sup>16-18</sup> On the other hand, narrowly conceived regulatory assessments that rely exclusively on BCA tend to undervalue non-market goods,<sup>17</sup> simplistically assess risks, disproportionately prioritize the here and now, and promote efficiency over equity.<sup>17</sup> These shortcomings of BCA may be exacerbated by national-level analyses that obscure the distribution of net benefits at the regional or local levels.<sup>16</sup>

Over the past decade, several interdisciplinary research efforts have produced spatially resolved estimates of the marginal human health and environmental damages of additional air emissions,<sup>19, 20</sup> and have been used to quantify the HEC consequences of policy interventions.<sup>21</sup> Facile approximation of these damages with county-level resolution significantly reduces the barriers to assessing the distribution of B/C ratios for regulation affecting air emissions, but very

few federal BCAs currently employ these methods.<sup>22</sup> There is also a need for comparable tools to assess the spatial distribution of marginal damages from aqueous emissions, allowing BCA to be performed at the local airshed and watershed scales relevant to public health.

Explicitly quantifying air-water emissions tradeoffs at the local scale is particularly important when designing national regulation for distinct regional power grids. A large fraction of the purported benefits of recent air and water regulations at CFPPs are attributed to increases in the levelized cost of electricity (LCOE) and associated decreases in the deployment of coal-based electricity generation at the margin.<sup>10, 12</sup> In North American Electric Reliability Corporation (NERC) regions with a diverse electricity generation mix, fuel switching is likely to lead to large net benefits. Near-term fuel switching is less likely in NERC regions where a large fraction of electricity generation occurs at CFPPs, especially if the best available technologies for regulatory compliance are capital intensive and installing them represents large sunk costs. This heterogeneity in generation infrastructure may lead to unintended local impacts and significant regional inequities in net damages. More broadly, the reliance on criteria air emissions benefits to justify regulatory interventions in CO<sub>2</sub>, solids, and aqueous emissions control<sup>10, 12</sup> raises questions about whether the policy design is most efficiently and effectively targeting high HEC impact pollutants.

Finally, plant-level analysis of air-water emissions tradeoffs is relevant to guiding the selection of emissions control technologies at CFPPs. The slate of forthcoming or promulgated regulations will require implementation of multiple additional processes for gas,<sup>1-3</sup> water,<sup>4</sup> and solids handling.<sup>4, 23</sup> Comprehensive planning and simultaneous implementation of these processes would enable a systems-level redesign of power plants, while staged implementation of capital-intensive infrastructure forced by piecemeal regulatory design will lead to technology

lock-in and reduced flexibility in cost-effectively minimizing air and water emission tradeoffs. Indeed, previous work analyzing the pulp and paper industry suggests that companies make more cost-effective decisions when designing for air and water emissions control simultaneously.<sup>13</sup>

The present work leverages and augments the US Environmental Protection Agency's (EPA) detailed BCA for the final ELG rule<sup>10</sup> to analyze the tradeoffs in air and water emissions associated with the two best available technology options (BATs) for treating wet FGD wastewater at CFPPs. Specifically, we extend the regulatory analysis to include the emissions and HEC damages associated with off-site manufacturing of the chemical inputs to FGD wastewater treatment which is responsible for a substantial fraction of total HEC damages. We also quantify the auxiliary power consumption, emissions, and HEC damages associated with zero liquid discharge (ZLD) processes for FGD wastewater treatment, a BAT option that was not fully evaluated in the ELG regulatory analysis. Finally, we combine plant-level analyses with spatially resolved marginal damage estimates to assess air-water emissions tradeoffs associated with wet FGD wastewater treatment at the state, NERC region, and national scales.

#### **4.3 FGD Wastewater Treatment Process Inventories**

Under the finalized ELGs, CFPPs are required to eliminate or treat wastewater discharge from fly ash transport waters, bottom ash transport waters, flue gas mercury control wastewater, coal gasification wastewater, combustion residual leachate, and FGD wastewater.<sup>7, 10</sup> Wastewater from most processes will be eliminated through dry-handling techniques, but for FGD wastewater, CFPPs are provided a choice between two different BAT wastewater treatment approaches with significantly different air and water emissions profiles.<sup>7</sup> Under the first option, plants will comply with effluent water quality standards starting in 2018 using chemical precipitation and biological treatment (CPBT). Under the second, plants may delay

implementation of water treatment capacity starting until 2023, but are required to comply with a more stringent zero liquid discharge (ZLD) plan using a combination of chemical precipitation and softening pre-treatment followed by mechanical vapor compression (MVC) and crystallization technologies that will further reduce metal emissions and eliminate dissolved solids discharges unaddressed by CPBT technology. While existing plants have a mix of installed FGD wastewater management approaches (e.g. impoundments, chemical precipitation, anaerobic biological treatment, distillation, and constructed wetlands), the present analysis is performed relative to a baseline of impoundment management. Detailed descriptions of FGD installations, water quality standards, and BAT options are provided in the Supporting Information (SI) Section 1.0, Tables S1 and S2, and Figure S1 available in Appendix 3.

We develop process models of the ELGs' two BATs options for FGD wastewater treatment: CPBT (Figure 4.1A) and ZLD (Figure 4.1B) as described in SI Section 2.1.<sup>7</sup> These process models are drawn from peer reviewed literature and regulatory documentation and include estimates of electricity consumption,<sup>24, 25</sup> water entrainment,<sup>11</sup> and chemical inputs<sup>11</sup> (Tables S3-S5 of SI Section 3.0) for each unit process in the treatment train. We estimate FGD wastewater treatment will consume an average 0.71 kWh/m<sup>3</sup> of auxiliary power using CPBT processes and 37.4 kWh/m<sup>3</sup> of auxiliary power using ZLD processes. Detailed estimates of soda ash, lime, hydrochloric acid, and nutrient mix consumption are provided in SI Section 2.0. Additional methodological details associated with developing the process inventories are reported in SI Section 2.1.

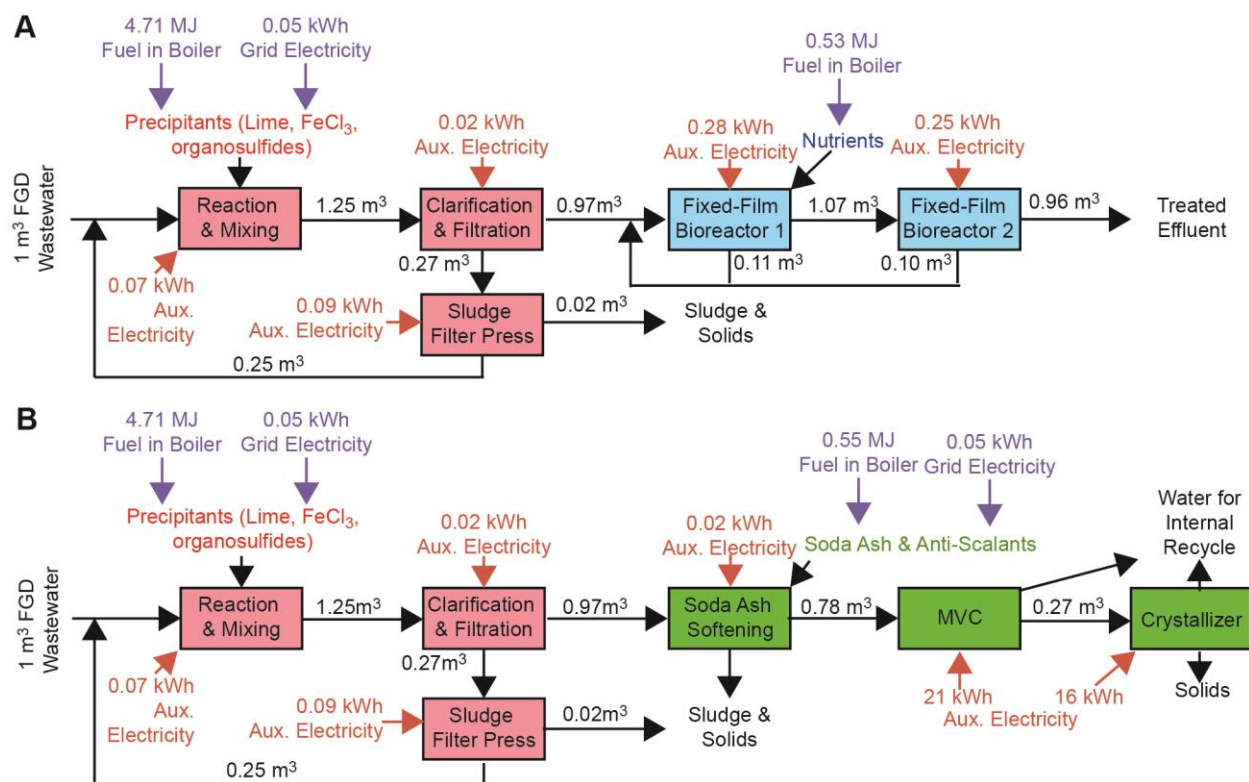


Figure 4.1. Process trains, auxiliary electricity consumption, and chemical consumption associated with treating 1 m<sup>3</sup> of FGD wastewater. Water lost during treatment reduces the volumetric flow between processes, and this reduction is accounted for in the quantified electricity and chemical inputs. (A) chemical precipitation (with four reaction & mixing tanks) followed by biological treatment, and (B) chemical precipitation (with four reaction & mixing tanks) followed by soda ash softening, mechanical vapor compression (MVC), and crystallization.

#### 4.4 Air Emissions from FGD Wastewater Treatment on a Cubic Meter Basis at the Plant Level

We estimate the NO<sub>x</sub>, SO<sub>2</sub>, PM<sub>2.5</sub>, and CO<sub>2</sub> emissions associated with auxiliary electricity consumption<sup>24, 25</sup> and the manufacturing of chemical inputs<sup>26, 27</sup> to FGD wastewater treatment

processes at U.S. CFPPs at the plant level. To estimate the air emissions associated with auxiliary electricity consumption per m<sup>3</sup>, we multiply the electricity consumed in the treatment process by the emissions factor for each CFPP with a wet FGD system installed (Equation 4.1).

$$m_{elec,g,i}^W = \sum_h E_{elec,h}^W e_{af,i}^E \quad (4.1)$$

Here,  $m_{elec,g,i}^W$  is the mass of air pollutant  $g$  [g/m<sup>3</sup> of wastewater treated] emitted as a result of auxiliary electricity consumption for each U.S. CFPP with a wet FGD system,  $i$ ;  $h$  is an indicator variable representing the unit process;  $E_{elec,h}^W$  is the electricity consumed by each unit process [kWh/m<sup>3</sup> of wastewater treated]; and  $e_{af,i}^E$  is the emissions factor [g/kWh] at plant  $i$  derived from eGRID<sup>28</sup> and National Emissions Inventory data<sup>29</sup> for the year 2012, the latest year for which eGRID data is available. Further details on the calculation of plant emission factors are provided in SI Section 2.2. We estimate that the generation weighted average emissions factor across all U.S. CFPPs with installed wet FGD capacity,  $\overline{e_{af,g}^E}$ , was 1000 g/kWh for CO<sub>2</sub>, 1.3 g/kWh for SO<sub>2</sub>, 0.82 g/kWh for NO<sub>x</sub>, and 0.32 g/kWh for PM<sub>2.5</sub> in 2012.

In addition to air emissions from auxiliary electricity consumption, there are embedded emissions associated with the manufacture of chemical inputs to FGD treatment processes,  $m_g^C$  [g/m<sup>3</sup>]. These air emissions are a function of the quantity of chemical used in each unit process and the sum of 1) direct emissions produced during manufacturing (i.e. emissions released during chemical production) reported in NREL's Life-Cycle Inventory database<sup>26</sup> and in EcoInvent 2.0<sup>27</sup> (SI Section 3.0); 2) indirect emissions from thermal energy consumption (i.e. boiler emissions) derived from the same NREL database; and 3) emissions from electricity consumption in chemical manufacturing determined by multiplying state-level grid marginal emissions factors<sup>30</sup> by the fraction of U.S. chemical production that occurs in state  $l$ <sup>31</sup> (Equation 4.2).



$$m_g^C = \sum_h \sum_j Q_{j,h} (e_{cm,j}^C + \sum_k E_{k,j}^C e_k^J + E_{elec,j}^C \sum_l e_{mf,l}^E \frac{V_l}{\sum_l V_l}) \quad (4.2)$$

Where  $m_g^C$  is the mass of pollutant  $g$  per  $m^3$  of wastewater treated [ $g/m^3$  of wastewater treated] from chemical manufacture;  $Q_{h,i}$  is the mass of chemical  $j$  used in process  $h$  per  $m^3$  of wastewater [ $kg\text{-chemical}/m^3$  of wastewater treated];  $e_{cm,j}^C$  are the direct emissions produced during manufacturing [in  $g\text{-pollutant}/kg\text{-chemical}$ ];  $E_{k,j}^C$  is the thermal energy input from fuel source  $k$  (bituminous coal, lignite, petroleum, residual fuel oil, natural gas, diesel) [ $MJ/kg\text{-chemical}$ ];  $e_k^J$  is the emission factor from combustion of fuel  $k$  [ $g\text{-pollutant}/MJ$  fuel];  $E_{elec,j}^C$  is the electrical energy consumed in the manufacturing process [ $kWh/kg\text{-chemical}$ ];  $V_l$  is the value of chemical products from U.S. state  $l$  [\$]; and  $e_{mf,l}^E$  is the marginal emissions factors for  $CO_2$ ,  $NO_x$ , and  $SO_2$ ,<sup>32</sup> and average emissions factors for  $PM_{2.5}$ <sup>29</sup> from the electricity generated in state  $l$  [ $g\text{-pollutant}/kWh$ ]. The methods used to calculate direct, thermal energy, and electrical energy emissions factors for chemical manufacturing are reported in SI Section 2.2.

We assume that chemical inputs are commodities purchased on the national market and that the spatial distribution of chemical manufacturing for wastewater treatment follows that of U.S. chemical production as reported in the 2013 Annual Survey of Manufacturers.<sup>31</sup> Using this approach, we estimate a single value for the embedded air emissions from chemical manufacturing on a  $m^3$  basis and determine the effective air emission impacts at the plant level by adjusting for the volume of FGD wastewater treatment. Sensitivity analysis on the spatial distribution of chemical manufacturing is provided in SI Section 4.0, including cases where we assume that 1) chemicals are manufactured evenly throughout the 48 contiguous states, 2) that chemicals are manufactured in the states where the chemicals are used, that chemicals are manufactured 3) only in Nebraska (the state with the lowest marginal damages) or 4) only in New Jersey (the state with the marginal highest damages), and 5) manufactured offshore (Figure

S2, and Tables S6-S10). While the total mass of emissions does not change significantly under these alternative cases, the spatial distribution of the emissions and the populations exposed to those emissions vary widely. As a result, subsequent monetization of incurred damages varies by 32%-310% of total chemical damages incurred by CPBT treatment and 34%-470% incurred by ZLD treatment.

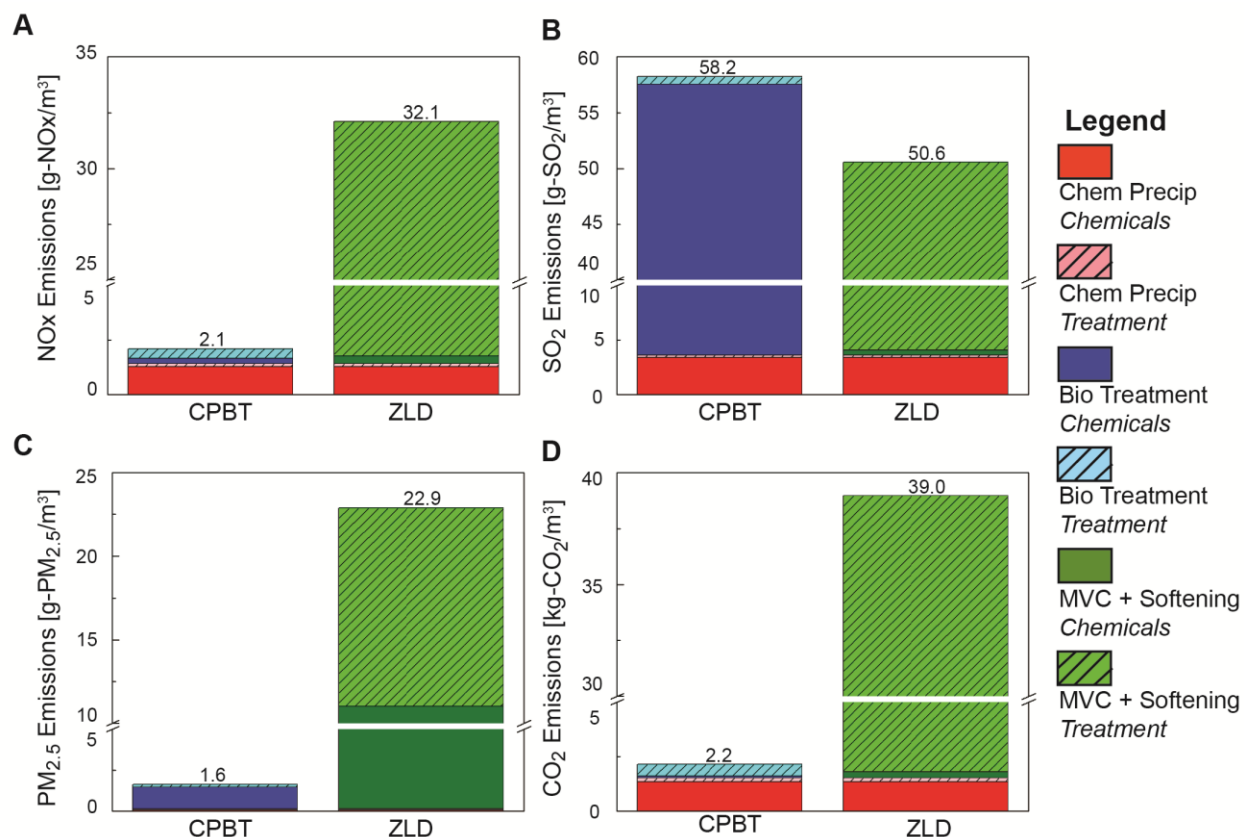


Figure 4.2. Average air emissions per m<sup>3</sup> of FGD wastewater treatment using CPBT or ZLD processes. Emissions are determined at the plant level and the averages reported here are normalized to plant generation in 2014. (A) NO<sub>x</sub>, (B) SO<sub>2</sub>, (C) PM<sub>2.5</sub>, and (D) CO<sub>2</sub> emissions generated due to auxiliary power consumption and chemical manufacturing. Processes correspond to those detailed in Figure 4.1. Results are tabulated in Table S11 of SI Section 5.0, and the distribution of air emissions at the plant, state, and NERC region levels is reported in SI Figure S3.

We sum emissions from auxiliary electricity consumption and chemical manufacturing ( $m_{elec,g,i}^W + m_g^C$ ) to obtain net air emissions per m<sup>3</sup> for CPBT and ZLD processes at the plant level. Figure 4.2 reports average net air emissions per cubic meter of CPBT and ZLD wastewater treatment,  $\overline{m_g}$ , at U.S. CFPPs normalized by plant generation ( $W_i$  [kWh]) in 2014 (Equation 4.3), while Table S11 of SI Section 5.0 tabulates these same values. Plant-level emission factors vary significantly by age, boiler efficiency, coal quality, and installed air emissions control technologies, and the distribution of these emissions factors for CFPPs with wet FGD systems is provided in SI Figure S3.

$$\overline{m_g} = \frac{\sum_i m_{elec,g,i}^W W_i}{\sum_i W_i} + m_g^C \quad (4.3)$$

Additional electricity for operating wastewater treatment processes could also be drawn from the grid, where the marginal emissions factors are lower due to the mix of coal, natural gas, nuclear, and renewable sources. We report state and NERC region marginal air emissions distributions in SI Figure S3. Using a state-level grid reduces the median emissions per cubic meter of wastewater to 1.6 g/m<sup>3</sup> of NO<sub>x</sub>, 49.3 g/m<sup>3</sup> of SO<sub>2</sub>, and 1.5 kg CO<sub>2</sub>/m<sup>3</sup> for CPBT and to 20 g/m<sup>3</sup> of NO<sub>x</sub>, 35 g/m<sup>3</sup> of SO<sub>2</sub>, and 20 kg CO<sub>2</sub>/m<sup>3</sup> for ZLD. Using the NERC-level grid reduces the median emissions per cubic meter of wastewater to 1.6 g/m<sup>3</sup> of NO<sub>x</sub>, 49.2 g/m<sup>3</sup> of SO<sub>2</sub>, and 1.8 kg CO<sub>2</sub>/m<sup>3</sup> for CPBT and to 20 g/m<sup>3</sup> of NO<sub>x</sub>, 29 g/m<sup>3</sup> of SO<sub>2</sub>, and 20 kg CO<sub>2</sub>/m<sup>3</sup> for ZLD.

Most emissions from CPBT processes stem from chemical inputs to the treatment process, while emissions from ZLD processes are dominated by auxiliary electricity consumption at the plant. Air pollutant emissions from CPBT processes are an order of magnitude lower than from ZLD processes for pollutants other than SO<sub>2</sub>. In this case, manufacturing of nutrient inputs to biological processes has a significant SO<sub>2</sub> footprint, while SO<sub>2</sub> emission factors at plants with FGD control technology are relatively small.

#### 4.5 Total Annual Air Pollutant Emissions from FGD Wastewater Treatment at U.S. CFPPs

We estimate the total annual air emissions from FGD wastewater treatment,  $M_g$  [kg/yr], under each ELG option by multiplying the volumetric emissions factors ( $m_{elec,g,i}^W + m_g^C$ ) of pollutant [kg] by estimated FGD wastewater volume at the plant level (Equation 4.4).

$$M_g = \sum_i \left[ (m_{elec,g,i}^W + m_g^C) (\sum_i Capacity_i * G_{scrubbed,i}) \left( \frac{G_{scrubbed,i} * W_i}{\sum_i G_{scrubbed,i} * W_i} \right) \right] \quad (4.4)$$

Here, the second term is the national annual wastewater production volume determined by multiplying EPA's estimate of the national average annual volume of wastewater produced per unit of wet FGD scrubbed nameplate capacity,<sup>11</sup>  $\varnothing$  [m<sup>3</sup>/kW.yr], by the sum of plant capacity,  $Capacity_i$  [kW], and percent of the plant exhaust gas scrubbed via wet FGD,  $G_{scrubbed,i}$ , over all U.S. CFPPs. Finally, the third term,  $\left( \frac{G_{scrubbed,i} * W_i}{\sum_i G_{scrubbed,i} * W_i} \right)$ , represents the fraction of national scrubbed electricity generation at plant  $i$ . Sensitivity analysis on the volume of FGD wastewater produced per kWh of generation is provided in SI Section 1.0. A detailed description of the methods is reported in SI Section 2.3.

There are several policies and regulations that may limit emissions increases. Clean Air Act (CAA) Title V requires operating permits for large point source emitters<sup>33</sup> and MATS establishes a total PM limit for existing CFPPs.<sup>2</sup> In addition, National Air Quality Standards (NAAQS) mandate State Implementation Plans (SIPs) for realizing emissions reductions in non-compliant regions. SIPs may limit emissions from both existing sources<sup>34</sup> and new facilities.<sup>35</sup> While our base case analysis assumes no binding air emission regulation limits, we consider the effect of limited emissions increases in our sensitivity analysis by evaluating scenarios with no additional emissions of SO<sub>2</sub>, NO<sub>x</sub>, and PM<sub>2.5</sub> from electricity generation, from chemical

manufacturing in states containing a non-attainment area, or from both electricity and chemical manufacturing.

#### **4.6 National Annual HEC Damages from Air Emissions Associated with FGD Wastewater Treatment at U.S. CFPPs**

Monetizing the HEC damages associated with air emissions from FGD wastewater treatment facilitates efficient policy design. We estimate human health and environmental damages at the plant level using marginal damages from the AP2 model,<sup>19</sup> a widely implemented integrated assessment model that estimates the human health and ecological damages associated with a marginal change in the emissions of SO<sub>2</sub>, NO<sub>x</sub>, and PM<sub>2.5</sub> from point sources in U.S. counties (detailed in SI Sections 2.4 and 6.0 and Figure S4). To estimate damages associated with CO<sub>2</sub> emissions, we adopt the average social cost of carbon (SCC) estimate at a 3% discount rate provided by the Interagency Working Group of \$43 per short ton CO<sub>2</sub> in 2014 dollars based on a pulse in 2020.<sup>36</sup>

To account for significant disagreement in the methodological approach and numerical assumptions used in valuing carbon emissions reductions, we perform a sensitivity analysis by varying the SCC between \$0 and \$100 per short ton (SI Section 7.0, Table S12, and Figure S6). Low CO<sub>2</sub> emissions factors for CBPT processes (Figure 4.2) mean that the total damages change by only 12% over this SCC range. The CO<sub>2</sub> emissions of ZLD processes are substantially greater, leading to a change of 55% in the total damages over the SCC range. In neither case does a \$0/short ton CO<sub>2</sub> SCC price impact the conclusion of the BCA.

We estimate annual HEC damages from air emissions associated with FGD wastewater treatment at each U.S. CFPP at the county level. The distribution of downwind damages for the G.G. Allen CFPP, for which precise FGD wastewater volumes are available,<sup>11</sup> is provided in SI

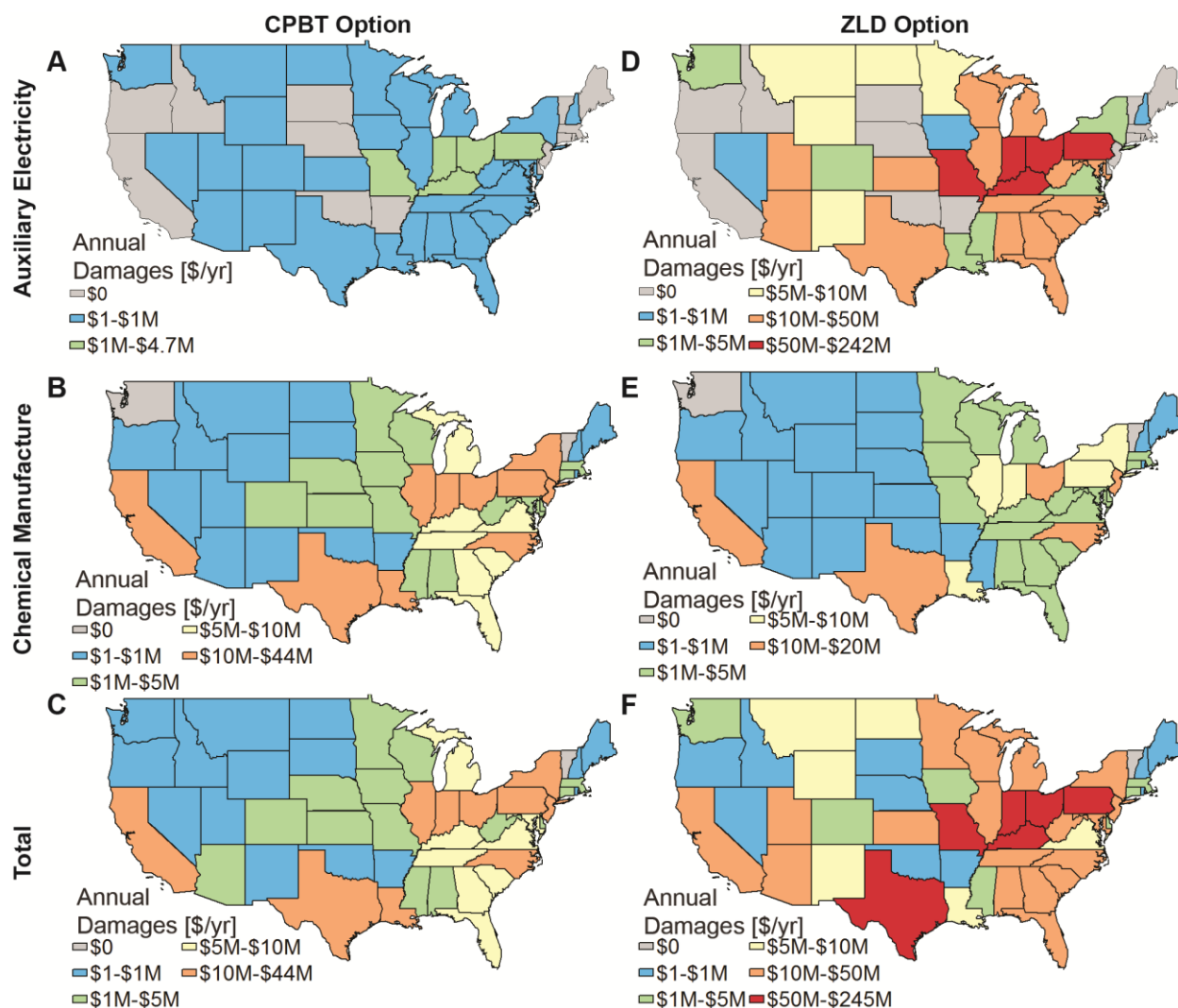


Figure 4.3. Estimated annual HEC damages associated with transitioning from FGD wastewater impoundment to FGD wastewater treatment by CPBT or ZLD processes. Damages downwind of power plant and chemical manufacturing are aggregated to the state in which the emissions were generated. HEC damages from CPBT wastewater treatment accounting for (A) only auxiliary electricity generation, (B) only chemical manufacture, and (C) both auxiliary electricity generation and chemical manufacture. HEC damages from ZLD wastewater treatment accounting for (D) only auxiliary electricity generation, (E) only chemical manufacture, and (F) both auxiliary electricity generation and chemical manufacture. Damages are tabulated in Table S13 of SI Section 8.0. This analysis is performed relative to a baseline of no advanced FGD

*wastewater treatment (i.e. wastewater impoundment) and uses estimated wastewater volumes from 2014. We assume that chemical manufacturing follows the 2013 chemical sector distribution, that auxiliary power is generated onsite, a value for the social cost of carbon of \$43 per short ton of CO<sub>2</sub>, a value of a statistical life of \$8.5 million, and non-binding NO<sub>x</sub> and SO<sub>2</sub> regulations. Sensitivity analyses on these assumptions are detailed in SI Section 14.*

Section 6.2 and Figure S5. The estimated HEC damages are \$320 million for CPBT treatment processes and \$1,100 million for ZLD treatment processes, with expected cost-benefit ratios of 1.8 (range of 1.5 to 2.5) for CPBT and 1.7 (range of 1.4 to 1.9) for ZLD treatment processes (Figure 4.3, SI Section 8.0, and Table S13). Note that while the costs of FGD wastewater treatment exceed the benefits of FGD wastewater treatment, the HEC benefits of FGD processes are at least an order of magnitude higher than the costs of FGD wastewater treatment.<sup>10</sup> Annual emissions from chemical manufacturing will add significantly to total air emission damages for the CPBT treatment process, especially in states with large chemical manufacturing bases (e.g. California, Texas). The air emission damages from chemical manufacturing will be much smaller for ZLD processes, where the majority of emissions are associated with auxiliary electricity generation. Under this option, states with large amounts of coal generation capacity (e.g. Ohio, Pennsylvania) would be responsible for the majority of air emission damages.

#### **4.7 Air-Water Emissions Tradeoffs from FGD Wastewater Treatment**

Comprehensive assessment of air and water emissions tradeoffs for FGD wastewater treatment requires comparing the HEC and technology implementation costs against the human health, ecosystem, and fuel switching benefits of installing aqueous emission control technologies. *Ex ante* estimates of future costs and benefits are highly uncertain<sup>37</sup> and improving these estimates is

an active area of research. Nevertheless, this work adapts and extends the EPA's analysis regulatory analysis of the full ELG rule<sup>10</sup> to estimate the stand-alone benefits and costs of FGD wastewater treatment. We disaggregate the benefits and costs of FGD wastewater treatment from those of other wastewater streams covered under the ELG regulation and we reference our analysis to a baseline of impoundment water management. Detailed descriptions of methods, assumptions, and sensitivity analysis on these assumptions are provided in SI Sections 4 (Tables S6-S10 and Figure S2), and SI Sections 7-14 (Tables S12-S24 and Figures S6-S12).

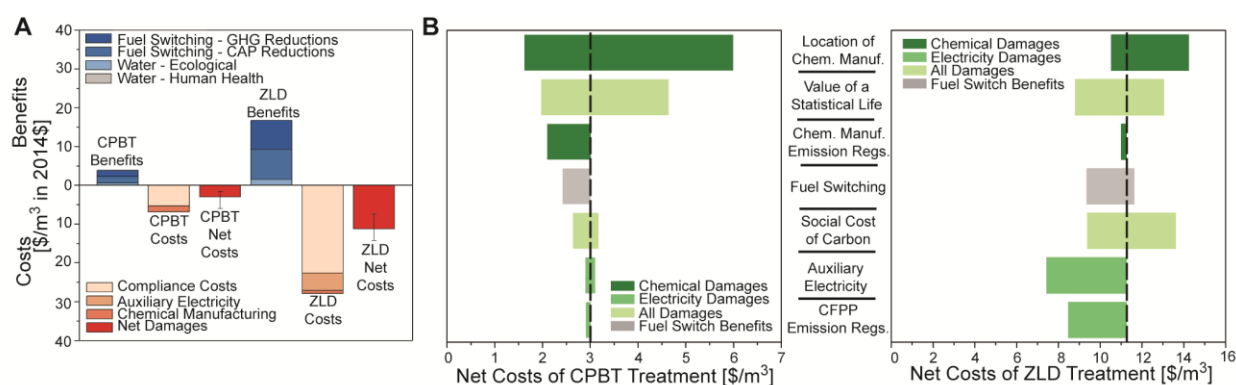


Figure 4.4. (A) Estimated benefits and costs of chemical precipitation and biological treatment (CPBT) and zero liquid discharge (ZLD) technologies for FGD treatment on a per cubic meter basis. Benefit estimates are derived from the EPA's regulatory analysis of the ELG rule and include reduced greenhouse gas (GHG) and criteria air pollution (CAP) emissions that stem from fuel switching and reduced water emissions leading to improved human and ecological health. Damage estimates are derived through a combination of EPA's regulatory analysis for compliance costs and the analysis described in this work for damages associated with auxiliary electricity and chemical manufacturing emissions. The error bars on the net cost value represent the extremes of the sensitivity analysis for seven key variables reported in (B) and detailed in SI Tables S17, S23, and S24.



The social costs of FGD wastewater treatment under the assumptions detailed above exceed the estimated social benefits for CPBT and ZLD by a factor of 1.8 and 1.7, respectively (Figure 4.4A, SI Table S17). The largest costs are the capital and operational costs of the technology, while the largest source of benefits stem from fuel switching, and the associated reductions in CO<sub>2</sub> and criteria air emissions, resulting from these increased electricity generation costs. Since these costs and benefits are directly related (SI Figure S8), reducing the cost of technology operation is also expected to reduce the fuel switching benefits.

Our conclusion that FGD wastewater treatment imposes net costs is robust to sensitivity analyses reported in Figure 4.4B and SI Tables S17, S23, and S24, including the distribution of FGD wastewater treatment technologies currently installed at CFPPs and assumptions about the location of chemical manufacturing, the value of a statistical life, the presence of binding regulations limiting NO<sub>x</sub>, SO<sub>2</sub>, and PM<sub>2.5</sub> emissions from power plants and chemical manufacturing facilities in non-attainment areas, the compliance cost to fuel switching relationship, the social cost of carbon, and the origin of auxiliary power supplied for wastewater treatment. Even in scenarios where we assume no additional marginal emissions of SO<sub>2</sub>, NO<sub>x</sub>, and PM<sub>2.5</sub> from electricity generation or from chemical manufacturing in states containing a non-attainment area, treating FGD wastewater using BATs recommended by the EPA still imposes net costs as a result of compliance costs, chemical manufacturing emissions in states without non-attainment areas, and CO<sub>2</sub> emissions damages (Table S22).

This sensitivity analysis also highlights the importance of using plant or location-specific emissions factors and spatially resolved marginal damage values in regulatory analysis of the national electricity grid. Replacing regional or national average emissions factors with plant or location-specific emissions factors increases estimates of total emissions and resulting damages

from auxiliary electricity generation for FGD wastewater treatment by 26-36% (\$3.9-\$5.5 million dollars annually for CPBT and \$200-\$280 million dollars annually for ZLD) (SI Section 8.2). Similarly, assumptions about the location of chemical manufacturing influence the associated estimates of air emissions damages by an order of magnitude (SI Section 4.0).

Replacing national average marginal damage estimates with spatially resolved marginal damage values has comparable implications. We compare results using county-level marginal damage estimates provide by AP2 to results computed using 1) national average marginal damage determined by averaging all county-level marginal damages and 2) using national average marginal damage estimates provided by the EPA. The first case underestimates the air emissions damages of FGD wastewater treatment by 4% for CPBT and 10% for ZLD. In contrast, the national average marginal damage estimates provided by the EPA overestimates air emissions damages by 25% for CPBT and 7% for ZLD. Additional details of these calculations are available in SI Section 15 and Table S25.

#### **4.8 Implications for Regulatory Analysis of Air and Water Emissions Controls at CFPPs**

Though market conditions and regulatory pressure have reduced the fraction of electricity generation by CFPPs to 33% in 2015,<sup>38</sup> a full transition to low-carbon electricity generation will take several decades.<sup>35-37</sup> In the interim, CFPPs are likely to make significant capital investments in emissions control technologies. Quantifying the air-water emissions tradeoffs of these capital improvements will be critical to avoiding unintended HEC consequences, to mitigating these consequences through technology innovation, and to maximizing the value of investments emissions control technologies.

This work adopted a life-cycle emissions inventory framework to assess air-water emissions tradeoffs of treating FGD wastewater. As previously noted, damage estimates from

wet FGD wastewater treatment are at least one to two orders of magnitude smaller than the health and environmental benefits of removing SO<sub>2</sub> emissions via wet FGD processes. This analysis does not reconsider implementing SO<sub>2</sub> controls, or evaluate options for replacing wet FGD systems with dry FGD alternatives. Instead, we assess only the air emission implications of a recent policy shift—regulation of wet FGD wastewater discharge—under two different wastewater treatment technology options.

When accounting for emissions from chemical manufacturing processes that occur off-site, using the appropriate plant or regional level emissions factors, and applying spatially resolved marginal damage estimates, we estimate that the costs of FGD wastewater treatment by BAT treatment processes exceed the benefits by a factor of 1.7 to 1.8 for our base-case analysis. Sources of systematic error in this estimate exist due to the absence of models that spatially resolve the marginal benefits of reduced aqueous pollution, the difficulty of accurately capturing the ecosystem benefits of higher water quality, methodological issues associated with valuing the SCC, and the difficulty of projecting improvements in the energy and chemical efficiency of FGD wastewater treatment technology. Despite these limitations, this BCA aids comprehensive decision making processes that include non-monetary benefits of FGD wastewater treatment by establishing priorities for plant retrofit, identifying wastewater treatment technologies that maximize HEC benefits, and highlighting the need for improved energy and chemical efficiency of wastewater treatment technologies.

This analysis also highlights the magnitude of HEC benefits available from reducing criteria air emissions from the electricity generation sector. The largest benefits of FGD wastewater treatment are the reduced HEC damages associated with fuel switching, rather than the averted damages caused by reduced water pollution. While it is desirable that CFPPs reduce

their environmental impacts from both water and air pollution, the most efficient pathway toward reducing air pollution damages is to directly regulate greenhouse gas and criteria air emissions.

Minimizing sustainability tradeoffs and reducing the compliance costs of emissions control requires future regulatory design to address air and water emissions control processes simultaneously. This work reinforces the need for comprehensive regulation that allows plants to strategically redesign the electricity generation process to minimize costs and HEC damages across all emissions control processes. Spatially resolved water emission marginal damage models to complement those for estimating air emissions marginal damages would greatly facilitate that effort.

#### **4.9 Acknowledgements**

This work was supported by the National Science Foundation under award numbers SEES-1215845 and CBET 1554117. This work was funded in part by the Center for Climate and Energy Decision Making (SES-0949710 and SES-1463492), through a cooperative agreement between the National Science Foundation and Carnegie Mellon University.

#### **4.10 Nomenclature**

##### **Symbols**

Capacity:	Generator Nameplate Capacity [kW]
$E^W$ :	Auxiliary Electricity Consumed for Water Treatment [kWh/m <sup>3</sup> ]
$E^C$ :	Energy Inputs for Chemical Manufacturing [MJ/kg], [MJ/L], [kWh/kg], [kWh/L]
$e^C$ :	Emissions Factor per Unit of Chemical [g-pollutant/kg-chemical], [g-pollutant/L-chemical]
$e^I$ :	Emissions per MJ of Thermal Energy Input for Chemical Manufacturing [g/MJ]

$e^E$ :	Emissions per kWh of Electricity Input to Water Treatment or Chemical Manufacturing [g/kWh]
$G_{\text{scrubbed}}$ :	Percent of a Plant's Exhaust Gas Scrubbed with a Wet FGD unit [%]
$M$ :	Total Annual Air Emissions from Chemical Manufacturing and Auxiliary Electricity Consumption [g/yr]
$m^C$ :	Mass of Air Emissions from Chemical Manufacturing per $m^3$ of Wastewater Treated [g/ $m^3$ ]
$m^W$ :	Mass of Air Emissions from FGD Wastewater Treatment per $m^3$ of Wastewater Treated [g/ $m^3$ ]
$\bar{m}$ :	Average Emissions from Chemical Manufacturing and Auxiliary Electricity Consumption per $m^3$ of Wastewater Treated [g/ $m^3$ ]
$Q$ :	Dose of Chemical in a Unit Process [kg/ $m^3$ ] or [L/ $m^3$ ]
$V$ :	Annual Value of Products from the Chemical Manufacturing Sector [\$]
$W$ :	Annual Net Electricity Generation [kWh/yr]

### **Subscripts**

$af$ :	Average Emissions Factor
$cm$ :	Direct Emissions from Chemical Manufacturing
$elec$ :	Auxiliary Electricity Consumption in Water Treatment or Chemical Manufacturing
$g$ :	Pollutant
$h$ :	Unit Process for Wastewater Treatment
$i$ :	Coal-Fired Power Plant
$j$ :	Chemical

k: Thermal Fuel Source  
i: U.S. State  
mf: Marginal Emissions Factor

#### 4.11 References

1. U.S. Environmental Protection Agency Cross-State Air Pollution Rule.  
<https://www3.epa.gov/airtransport/CSAPR/index.html> (July 21,2015),
2. U.S. Environmental Protection Agency Mercury and Air Toxics Standards.  
<http://www.epa.gov/mats/index.html> (July 20),
3. U.S. Environmental Protection Agency Clean Power Plan.  
<http://www2.epa.gov/cleanpowerplan> (July 20, 2015),
4. U.S. Environmental Protection Agency Steam Electric Power Generating Effluent Guidelines - 2015 Final Rule. <http://www.epa.gov/eg/steam-electric-power-generating-effluent-guidelines-2015-final-rule> (September 30, 2015),
5. U.S. Energy Information Administration Form EIA-860 Detailed Data.  
<http://www.eia.gov/electricity/data/eia860/>
6. U.S. Environmental Protection Agency *Steam Electric Power Generating Point Source Category 2007/2008 Detailed Study Report*; U.S. Environmental Protection Agency: Washington, DC, 2008.
7. U.S. Environmental Protection Agency, Technical Development Document for the Effluent Limitations Guidelines and Standards for the Steam Electric Generating Point Source Category. In Washington, D.C., 2015.
8. Rubin, E. S., Toxic Releases from Power Plants. *Environmental Science & Technology* **1999**, 33, (18), 3062-3067.

9. U.S. Environmental Protection Agency, Environmental Assessment for the Effluent Limitation Guidelines and Standards for the Steam Electric Power Generating Point Source Category. In Washington, D.C., 2015.
10. U.S. Environmental Protection Agency, Benefit and Cost Analysis for the Effluent Limitations Guidelines and Standards for the Steam Electric Power Generating Point Source Category. In Washington, D.C., 2015.
11. Eastern Research Group Inc. *Final Power Plant Monitoring Data Collected Under Clean Water Act Section 308 Authority*; Chantilly, VA, 2012.
12. U.S. Environmental Protection Agency, Regulatory Impact Analysis for the Clean Power Plan Final Rule. In Washington, D.C., 2015.
13. Gray, W. B. S., Ronald J, Multimedia Pollution Regulation and Environmental Performance: EPA's Cluster Rule. In *Resources for the Future*: Washington, D.C., 2015.
14. National Center for Environmental Economics, Guidelines for Preparing Economic Analyses. In Agency, U. S. E. P., Ed. Washington, D.C., 2014.
15. Budget, O. o. M. a., Circular A-94: Guidelines and Discount Rates for Benefit-Cost Analysis of Federal Programs. In Budget, O. o. M. a., Ed. Washington, D.C., 1992.
16. Arrow, K. J.; Cropper, M. L.; Eads, G. C.; Hahn, R. W.; Lave, L. B.; Noll, R. G.; Portney, P. R.; Russell, M.; Schmalensee, R.; Smith, V. K. S., Robert N., Is There a Role for Benefit-Cost Analysis in Environmental, Health, and Safety Regulation? *Science* **1996**, 272, 221-222.
17. Lave, L. B., Benefit-Cost Analysis: Do the Benefits Exceed the Costs? In *Risks, Costs, and Lives Saved: Getting Better Results from Regulation*, Hahn, R. W., Ed. The AEI Press: Washington, D.C., 1996; pp 104-134.

18. Graham, J. D., Saving Lives Through Administrative Law and Economics. *University of Pennsylvania Law Review* **2008**, *157*, 395-540.
19. Muller, N. Z., Using index numbers for deflation in environmental accounting. *Environment and Development Economics* **2013**, *19*, (04), 466-486.
20. Heo, J.; Adams, P. J.; Gao, H. O., Public Health Costs of Primary PM<sub>2.5</sub> and Inorganic PM<sub>2.5</sub> Precursor Emissions in the United States. *Environmental Science & Technology* **2016**, *50*, (11), 6061-70.
21. Siler-Evans, K.; Azevedo, I. L.; Morgan, M. G.; Apt, J., Regional variations in the health, environmental and climate benefits of wind and solar generation. *Proceedings of the National Academy of Science* **2013**, *110*, (29), 11768-11773.
22. Muller, N. Z.; Mendelsohn, R.; Nordhaus, W., Environmental Accounting for Pollution in the United States Economy. *American Economic Review* **2011**, *101*, (5), 1649-1675.
23. U.S. Environmental Protection Agency Coal Ash (Coal Combustion Residuals, or CCR). <http://www2.epa.gov/coalash> (July 20,2015),
24. Plappally, A. K.; Lienhard V, J. H., Energy requirements for water production, treatment, end use, reclamation, and disposal. *Renewable and Sustainable Energy Reviews* **2012**, *16*, (7), 4818-4848.
25. Subramani, A.; Jacangelo, J. G., Treatment technologies for reverse osmosis concentrate volume minimization: A review. *Separation and Purification Technology* **2014**, *122*, 472-489.
26. National Renewable Energy Laboratory National Renewable Energy Laboratory - Life-Cycle Inventory Database. . <https://www.lcacommons.gov/nrel/process/show/50158> (October 3, 2015),



27. Althaus H-J, e. a., *Life Cycle Inventories of Chemicals No. 8, v. 2.0*. Dusseldorf, Switzerland, 2007.
28. U.S. Environmental Protection Agency eGRID. <http://www.epa.gov/cleanenergy/energy-resources/egrid> (July 11, 2015),
29. U.S. Environmental Protection Agency Emissions Inventories. <http://www3.epa.gov/ttn/chief/eiinformation.html> (October 9, 2015),
30. Siler-Evans, K.; Azevedo, I. L.; Morgan, M. G., Marginal emissions factors for the U.S. electricity system. *Environmental Science & Technology* **2012**, 46, (9), 4742-8.
31. United States Census Bureau Annual Survey of Manufacturers 2013. <https://www.census.gov/manufacturing/asm/index.html> (October 11, 2015),
32. Azevedo, I. M. L.; Siler-Evans, K., Marginal impact factors: estimating the health and environmental impacts of interventions in the US electricity system. *Environmental Science & technology*.
33. U.S. Environmental Protection Agency Title V - Permits. <https://www.epa.gov/clean-air-act-overview/title-v-permits> (August 19, 2016),
34. U.S. Environmental Protection Agency Applying or "Implementing" Sulfur Dioxide Standards - Sulfur Dioxide Pollution. <https://www.epa.gov/so2-pollution/applying-or-implementing-sulfur-dioxide-standards> (August 19, 2016),
35. U.S. Environmental Protection Agency Nonattainment NSR Basic Information - New Source Review Permitting. <https://www.epa.gov/nsr/nonattainment-nsr-basic-information> (August 19, 2016),

36. Interagency Working Group on the Social Cost of Carbon, Technical Support Document: Technical Update of the Social Cost of Carbon for Regulatory Impact Analysis. In Washington, D.C., 2015.
37. Morgenstern, R. D., The RFF Regulatory Performance Initiative: What Have We Learned. In Resources for the Future: Washington, D.C., 2015.
38. U.S. Energy Information Administration Electric Power Monthly Data for August 2016. <http://www.eia.gov/electricity/monthly/> (November 10, 2016),

## **PART II**

### **AVOIDING AIR-WATER TRADEOFFS ASSOCIATED WITH CFPP WASTEWATER TREATMENT**

## **CHAPTER 5: QUANTITY, QUALITY, AND AVAILABILITY OF WASTE HEAT FROM UNITED STATES THERMAL POWER GENERATION<sup>4</sup>**

### **5.1 Abstract**

Secondary application of unconverted heat produced during electric power generation has the potential to improve the life-cycle fuel efficiency of the electric power industry and the sectors it serves. This work quantifies the residual heat (also known as waste heat) generated by U.S. thermal power plants and assesses the intermittency and transport issues that must be considered when planning to use this heat. Combining Energy Information Administration plant-level data with literature-reported process efficiency data, we develop estimates of the unconverted heat flux from individual U.S. thermal power plants in 2012. Together these power plants discharged an estimated 18.9 billion GJ<sub>th</sub> of residual heat in 2012, 4% of which was discharged at temperatures greater than 90 °C. We also characterize the temperature, spatial distribution, and temporal availability of this residual heat at the plant level and model the implications for the technical and economic feasibility of its use. Increased implementation of flue gas desulfurization technologies at coal-fired facilities and the higher quality heat generated in the exhaust of natural gas fuel cycles are expected to increase the availability of residual heat generated by 10.6% in 2040.

### **5.2 Introduction**

In 2012, U.S. electric utilities converted 38 billion GJ<sub>en</sub> of coal, natural gas, and nuclear energy into 12.3 billion GJ<sub>elec</sub> of electricity,<sup>1</sup> an average efficiency of 32%. Electricity generation

---

<sup>4</sup> This chapter is based on a paper co-authored with Prof. Meagan Mauter. It can be found at Gingerich, D.B.; Mauter, M.S., Quantity, Quality, and Availability of Waste Heat from United States Thermal Power Generation. *Environmental Science & Technology* **2015**, 49(14), 8297-8306.

at these plants is performed by combusting fuel (e.g. coal and natural gas) or using nuclear reactions to heat a fluid. The resulting hot fluid drives the blades of a turbine and its associated generator, thereby converting thermal energy into mechanical energy and then electric energy (see Supporting Information (SI) Section 1.0 and Figure S1 for additional detail on power plant operations and thermodynamics).<sup>2,3</sup>

Thermal generation processes are plagued by inefficiencies that leave approximately two-thirds of energy input unused for electricity generation.<sup>4,5</sup> In addition to the thermodynamic limits on power plant efficiency, common sources of inefficiency for power generation include incomplete combustion, inefficient heat transfer from combustion gasses to the steam cycle, heat loss during condensation, heat transfer to the environment, and seasonal temperature changes affecting ideal efficiency. While a portion of the unconverted energy is captured for use in air and fuel pre-heating systems<sup>6,7</sup> or applied in processes downstream of the turbines, significant quantities of heat are passively released during steam conveyance<sup>2,4</sup> or discharged into the environment through cooling water and exhaust streams.<sup>2,5,8</sup> Recoverable energy that is not converted into electricity is henceforth referred to as “residual heat” in this manuscript.

Plant-level efforts to improve power generation efficiency focus on decreasing the heat rate, defined as the fuel input needed to generate a unit of electricity,<sup>9</sup> of a power cycle. This is accomplished through a combination of retrofits to the plant infrastructure,<sup>10–15</sup> mathematical modeling and optimization of thermodynamic operating conditions,<sup>8,16,17</sup> and improved plant maintenance and operation.<sup>10,16,18</sup>

Increasing the efficiency of fuel combustion can also be accomplished by expanding the system boundaries to include applications of heat beyond electricity generation. Common examples include district heating for the residential and commercial sectors,<sup>19</sup> heating and

cooling in the processes of chemical synthesis and metal smelting, or thermal processes for water desalination.<sup>20–24</sup> Common among these diverse applications is the substitution of residual heat (sometimes augmented with high temperature steam) for heat generated through primary fuel sources or electricity.<sup>5</sup>

Increasing power plant efficiency through heat capture and usage also confers environmental benefits. Thermal pollution released in the cooling water has the potential to harm aquatic life,<sup>25</sup> the diversity of aquatic ecosystems,<sup>26</sup> and lake mixing regimes.<sup>27</sup> Finding ways to divert residual heat to practical applications could assist thermal power generators in complying with heat discharge regulations that protect receiving water bodies.<sup>25</sup> Previous studies have shown that waste heat has a non-negligible impact on climate<sup>28</sup> and projected that substituting residual heat for primary energy could reduce net greenhouse gas emissions by 13%.<sup>5</sup>

Studies estimating the quality, quantity, and availability of residual heat are sparse in the literature.<sup>5,29</sup> Those available are focused solely on heat quantity and use data from before the sharp increase in natural gas driven electric power generation and the increased use of post-combustion flue gas desulfurization (FGD) control technologies. Industrial and manufacturing processes, under-exploited geothermal resources, automobiles, waste facilities, and the built environment also discharge significant quantities of heat. An estimate of unconverted heat quantity produced by industrial and manufacturing processes was recently published elsewhere,<sup>5,29</sup> though the granularity of the underlying data preclude careful quantification of spatial distribution, heat quality, and the temporal availability of the heat. The present manuscript focuses exclusively on the residual heat produced by electric power generation facilities.

In this study we estimate the temperature, heat flux, and spatial-temporal availability of residual heat from the U.S. coal, nuclear, and natural gas power generation sectors. We exclude from this analysis petroleum, biomass, geothermal, wind, hydropower, and solar power systems. These estimates are informed by thermodynamic or average process models of power plants, Energy Information Administration (EIA) plant-specific data, and economic models. We also offer novel contributions to the existing literature by incorporating temperature limits imposed by acid gas condensation on the quality of heat extracted, providing estimates for the spatial and temporal availability of residual heat, and estimating future heat availability under EIA projected fuel mix and carbon policy scenarios. These results will help to inform policy objectives for residual heat usage by clarifying the technical and economic viability of extracting and conveying heat from power plants in the U.S.

## **5.3 Methods**

### *5.3.1 Quantity and Quality of Residual Heat*

The methodological steps for modeling the quantity and quality of residual heat are summarized in Figure 5.1. Estimates of power plant efficiencies are reported in the literature<sup>5,13,30–37</sup> and by manufacturers,<sup>38</sup> but actual efficiencies vary significantly based on load, capacity factor, ramping rates, and environmental conditions. To account for these variations, we use plant-level data for electricity generation, fuel consumption, and cycle type reported in EIA Form EIA-923<sup>1</sup> to estimate the quantity of unconverted heat based on the heat input and electricity output from the system. The fuel and cycle types considered in this manuscript include coal, nuclear, natural gas combined cycle (NGCC), natural gas gas turbine (NGGT), and natural gas steam turbine (NGST).

We first divide plant-specific annual generation ( $W_{elec,j,k}$ ) by an average process turbine and generator efficiency ( $\eta_{conv,i}$ ) of 86% for steam cycles and 93% for gas cycles<sup>39</sup> to calculate the heat used for electricity generation. We then calculate power cycle efficiency ( $\eta_{cycle,I,j,k}$ ) by dividing the heat used for electricity generation by the total heat input ( $Q_{fuel,j,k}$ ) in the fuel

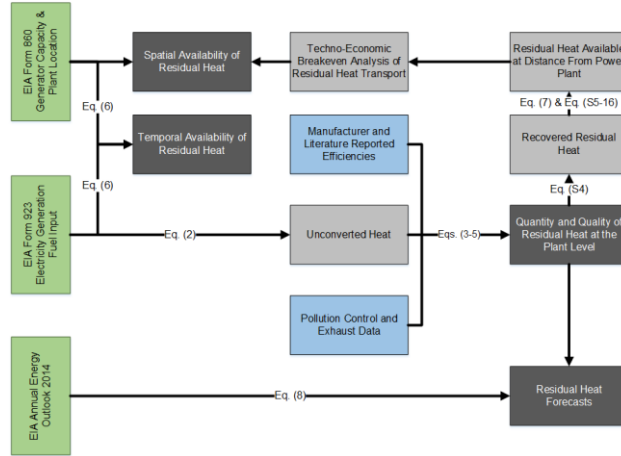


Figure 5.1. Methods and data sources for calculating residual heat quantity and availability.

Green rectangles are plant-specific data sources, blue rectangles are average process data, grey rectangles are intermediate calculations, and black rectangles are final reported values. Using EIA Form 923 plant-specific data, we calculate the unconverted heat at each U.S. power plant. We calculate the recoverable fraction, or total residual heat, by incorporating literature reported average process efficiency data and accounting for limitations on heat recovery imposed by pollution control and exhaust systems at each power plant. Summing plant level residual heat over all U.S. power plants provides residual heat totals for the year 2012. We combine the residual heat totals with EIA Form 860 location data for each generator to perform spatial characterization of residual heat availability using calculations of recovered residual heat and heat losses during transport. Temporal availability, provided by plant capacity factors, is calculated using plant-specific EIA Form 860 and Form 923 data. Residual heat forecasts are estimated using residual heat totals and EIA electricity generation predictions.



(Equation 5.1, Table 5.1), where the power plant fuel/cycle type combination is denoted by  $i$ , the specific generator is denoted by  $j$ , and the power plant is denoted by  $k$ . Finally, we calculate

*Table 5.1 Efficiency, energy, and exergy of U.S. power plants.*

		Residual Heat Source (% of Input)				
Fuel and Power Cycle	Efficiency	Energy	Exergy	$\alpha$		
<b><i>Coal</i></b>						
Steam Turbine <sup>5,13,30,34,37</sup>	29.5%	Exhaust Gas				
		9.3%	4.3%	14.2%		
		Condenser				
		47.0%	2.0%	71.5%		
		Other Losses/Destruction				
		14.2%	62.0%	14.3%		
<b><i>Natural Gas</i></b>						
Combined Cycle <sup>5,33,36</sup>	45.5%	Exhaust Gas				
		7.3%	1.0%	15.5%		
		Condenser				
		34.5%	0.8%	73.2%		
		Other Losses/Destruction				
		12.7%	45.9%	11.3%		
Steam Turbine <sup>5,31</sup>	30%	Exhaust Gas				
		5.7%	*	8.7%		
		Condenser				
		51.0%	3.1%	78.2%		
		Other Losses/Destruction				
		13.3%	45.9%	13.0%		
Gas Turbine <sup>5</sup>	31.0%	Exhaust Gas				
		59.4%	*	89.7%		
		Other Losses/Destruction				
				9.6%	*	10.3%
		<b><i>Nuclear</i></b>				
Steam Turbine <sup>5,32,34,35</sup>	29.0%	Condenser				
		65.5%	2.4%	99.2%		
		Other Losses/Destruction				
		5.5%	63.0%	0.8%		

unconverted heat ( $Q_{unconverted,i,j,k}$ ) by subtracting heat for electricity generation from the heat equivalent of fuel input (Equation 5.2).

$$\eta_{cycle,i,j,k} = \frac{W_{elec,j,k}/\eta_{conv,i}}{Q_{fuel,j,k}} \quad (5.1)$$

$$Q_{unconverted,i,j,k} = Q_{fuel,j,k} - \frac{W_{elec,j,k}}{\eta_{conv,i}} \quad (5.2)$$

Unconverted heat escapes via wall losses, or is discharged in condenser systems and exhaust gasses. Only a portion of this unconverted heat is potentially recoverable, defined throughout this manuscript as residual heat, and including all heat isolated to a controllable process stream that is not otherwise allocated to the prevention of acid mist condensation formation. Functionally, wall losses are considered non-recoverable, while heat discharged in condenser systems is considered recoverable. Operationalizing this definition for exhaust gasses requires consideration of the fuel and the air pollution control technologies present at the plant.

The acid gas mist condensation temperature determines the fraction of recoverable heat in the exhaust of both coal and natural gas fired power plants. For those coal-fired power plants that do not report an operational FGD unit in EIA form 923, we model all exhaust gas heat as unrecoverable. For those coal-fired plants with operating FGD units, and for all natural gas units, we model exhaust heat as recoverable between  $T_{exhaust}$  (Table 2) and the estimated dew point of  $SO_2$  at standard concentrations and pressures in desulfurized exhaust.<sup>40</sup>

Desulfurization systems vary widely in their removal efficiency, but  $SO_2$  concentrations of 75 ppb and  $H_2O$  partial pressures of 0.01 atm are robust estimates for the median FGD process in coal plants.<sup>41</sup> Due to poor data on the range of concentration, as well as the difficulty of capturing heat between 30°C and 50°C, we assume the lower recoverable limit is likely to be closer to 50°C.<sup>42</sup> This corresponds to a partial pressure of  $SO_2$  in the exhaust of around 260 ppb.

The median total sulfur content in pipeline natural gas is 4.58 mg/Nm<sup>3,43</sup> though there is significant variation depending on the source of the gas and the standards set by the company operating the pipeline. Because of this variation we assume that the maximum permissible amount of sulfur in piped natural gas (13.7 mg/Nm<sup>3</sup>)<sup>41</sup> was present in the gas before combustion and then perform a mass balance to obtain an upper bound of 500 ppb on sulfur in the natural gas exhaust. The resulting dewpoint is approximately 49°C, but given the feasible constraints on low temperature heat recovery,<sup>42</sup> we assume a lower recoverable limit for natural gas exhaust to be 50°C. Chemical composition, the heat capacity of the exhaust gasses, and calculations of the acid gas dew point are detailed in SI Sections 2.1 and 2.2 and Table S1.

A portion of the residual heat from the exhaust flue gas is used to improve plant efficiency by preheating and dehumidifying combustion air<sup>6</sup> and fuel.<sup>7</sup> The existing literature does not provide robust estimates of the temperature drop resulting from these processes, thereby limiting our ability to deduct this heat from total estimates of residual heat. The scarcity of reasonable estimates for efficiency gains resulting from preheating and dehumidifying processes also suggests that there may be higher value secondary uses for this heat.

With these limits on exhaust heat capture established, we define a normal distribution of unconverted heat among these streams for each fuel type and power cycle using averages and standard deviations of previously published thermodynamic analyses on real and simulated power plants (Table S2).<sup>5,13,30–38</sup> The fraction of energy content in each unconverted heat stream relative to total unconverted energy is reported in Table 5.1 as  $\alpha$ . Additional methodological details are presented in SI Section 3.0 and Table S2.

We then estimate the residual heat in the condenser and exhaust streams for each power plant in the U.S. We use @Risk (Palisade Corporation, Ithica, NY), a Monte Carlo simulation

software package, to randomly select 1,000 values from a normal distribution describing the percentage of fuel energy in the electricity, condenser, exhaust, and other loss streams. We then multiply these randomly generated  $\alpha$  values by the unconverted heat at each generator (Equations 5.3 and 5.4) yielding estimates for the heat content in each energy stream. We use the results of these 1000 iterations to identify the first, second, and third quartile estimates of residual heat in each energy stream. Additional methodological details are described in SI Section 4.0.

$$Q_{condenser,i,j,k} = \alpha_{condenser,i} Q_{fuel,j,k} \quad (5.3)$$

$$Q_{exhaust,i,j,k} = \frac{(G * c_{p,High,i} * (T_{High,i} + 273.15)) - (G * c_{p,Low,i} * (T_{Low,i} + 273.15))}{1,000,000 \left(\frac{J}{MJ}\right)} \quad (5.4)$$

$$Q_{total,i,j,k} = \alpha_{condenser,i} Q_{fuel,j,k} + \frac{(G * c_{p,High,i} * (T_{High,i} + 273.15)) - (G * c_{p,Low,i} * (T_{Low,i} + 273.15))}{1,000,000 \left(\frac{J}{MJ}\right)} \quad (5.5)$$

We total the residual heat at each U.S. power plant by summing over  $k$ . Finally, we total the amount of residual heat generated in the U.S. and classify it based on the five fuel/cycle combinations studied.

### 5.3.2 Temporal Availability of Residual Heat

The temporal availability of residual heat will determine the range of viable end uses. Although plants produce heat while idling, the bulk of fuel is consumed, and the majority of heat is generated, while the plant is producing electricity. Therefore, we use capacity factor, a 0.0 to 1.0 measure of how frequently a generator is producing electricity, as a conservative estimate for the temporal availability of residual heat. We calculate capacity factor for each generator by dividing the generator's annual electricity production by its total annual capacity (Equation 5.6), both of which are reported in EIA Form EIA-860.<sup>44</sup>

$$CF_j = \frac{W_{elec,j}}{W_{capacity,j}} \quad (5.6)$$

### 5.3.3 Spatial Availability of Residual Heat

The spatial availability of residual heat depends upon generation location and the techno-economic feasibility of heat transport. Geospatial coordinates for generation location are reported in Form EIA-860.<sup>44</sup> Here, we construct a model describing the techno-economic feasibility of heat transport as a function of heat flux, capacity factor, stream temperatures, and primary fuel (i.e. natural gas) prices.

The calculation of plant-level heat flux is described above. The capacity factor of the plant, also described above, significantly influences the plant-level heat flux and therefore the techno-economically feasible waste transport distance. In the absence of highly resolved temporal data on the length of each generating period of each plant over the course of a year, we estimate the influence of capacity factor via two methods. The first, assuming that all plants continuously operate at maximum capacity (equivalent to a capacity factor of 1), provides an upper bound for the techno-economically feasible limit of heat transport. The second, which time-averages the heat flux for each plant over an entire year, approximates a lower bound. An actual lower bound would require the consideration of heat loss associated with starting up and shutting down the heat delivery system for low-capacity plants. Additional details on the calculations of the time-averaged heat flux are presented in SI Section 5.1.

To determine stream temperatures of the condenser heat stream, we assume that condenser water is diverted directly to heat pipes, negating the need for heat exchangers in these systems. In contrast, we model exhaust heat recovery via an aluminum shell-and-tube system (details in SI Section 5.2, 5.3, and Figure S3) that is scaled to capture all heat above the lower recoverable limit temperature of 50°C. The purpose of this model is to identify three inputs into

the heat transport model: the optimal flow rate of water in the pipe, the energy flow in the pipe, and the temperature.

Next, we determine the feasible limits of heat transport given the heat flux provided by the heat exchanger model ( $q_{initial}$ ) at each power plant. Models of thermal losses per unit length ( $\Delta q$ ) are taken from the literature,<sup>45</sup> and the amount of energy,  $q_L$  at distance  $L$  is calculated as shown in Equation 5.7. Additional details are provided in SI Section 5.4 and Figure S4.

$$q_L = q_{initial} - \Delta q * L \quad (5.7)$$

Economically feasible limits of heat transport are determined by comparing the capital costs of the heat exchanger and heat pipe construction to the cost of generating substitute heat onsite using natural gas fired burners. Details on estimating the cost of the heat exchanger are available in SI Section 5.3. We estimate the cost of laying heat pipe a \$1460 per meter of pipe constructed,<sup>19</sup> paid back over 25 years at a discount rate of 7%. To calculate the fuel cost for generating heat on site, we multiply  $q_L$  by the cost for natural gas at a boiler efficiency of 85%. The present model assumes a cost of \$4.62/mcf,<sup>46</sup> or the average of industrial natural gas prices from 2011-2014. Techno-economically feasible heat transport is defined as the point where fuel costs equals the cost of the heat exchanger plus the cost of laying the heat pipe.

#### 5.3.4 Residual Heat Forecasts

EIA projects coal, natural gas, and nuclear fuel consumption for electricity generation out to 2040 under 31 different scenarios.<sup>47</sup> To predict future residual heat production from these EIA projections in 21 of the 31 scenarios relevant to fuel consumption for power generation (Table S3 in SI Section 6.0), we assume that overall plant efficiencies remain constant and that the relative ratio of NGCCs, NGSTs, and NGGTs remains unchanged. Though these assumptions

will overestimate the amount of residual heat generated if the number of NGCC grows faster than other natural gas fired cycles, they are necessary because EIA only reports aggregate projections for natural gas cycles. We calculate the residual heat generation in future years by multiplying the amount of fuel consumed for electricity generation in each year,  $l$ , by the percentage of heat input in each residual stream. Summing the totals from the five cycle types provides annual residual heat generation for a single year (Equation 5.8).

$$Q_{residual,l} = \sum_i Q_{fuel,l} \alpha_i \quad (5.8)$$

## 5.4 Results and Discussion

### 5.4.1 Quantity and Quality of Residual Heat

In 2012, 12.3 billion  $\text{GJ}_{\text{elec}}$  of electricity and 18.9 billion  $\text{GJ}_{\text{th}}$  of residual heat were produced at U.S. coal-fired, nuclear, NGCC, NGST, and NGGT thermal power plants (Table 2, SI Section 7.0). Of this residual heat, 96% is condenser heat discharged to the environment at or below  $41.5^\circ\text{C}$  (Figure 5.2A). The remaining 4%, or 803 million  $\text{GJ}_{\text{th}}$ , is discharged in exhaust streams at temperatures between  $91$  and  $543^\circ\text{C}$ . A total of 640 million  $\text{GJ}_{\text{th}}$  of residual heat was produced from NGGT, NGST, and NGCC system exhaust in 2012, while 163 million  $\text{GJ}_{\text{th}}$  is produced from FGD treated coal-fired system exhaust.

Residual heat production varies significantly across fuel source and power cycle, but this variation is primarily a function of plant size and capacity factor. The median-size nuclear power plant is the largest emitter of residual heat, followed by median-sized coal-fired plants and NGCC plants (Figure 5.2B). This wide distribution, however, reflects the range of electricity production by power plants, rather than significant variation in plant generation efficiencies.

Table 5.2 Quantity, quality, and temporal availability of residual heat generated at power plants with capacity greater than 10 MW in 2012.

Fuel and Prime Mover	Median Capacity Factor	Number of Cycles (% of total)	Net Generation [GWh/yr] (% of total)	Estimated Temp. [°C]	Total Residual Heat <sup>c</sup> [GJ <sub>th</sub> /yr]	Median-Size Plant Residual Heat <sup>c</sup> [GJ <sub>th</sub> /yr]	Median-Size Plant Residual Heat Flux <sup>c</sup> [kJ/s]
<i>Coal</i>							
Steam Turbine	0.468	673 (30%)	1,504,000 (43%)	128.4 <sup>5,13,30,34,37</sup> 40.0 <sup>5,13,30,34,37</sup>	163,000,000 <sup>a</sup> (59-262x10 <sup>6</sup> ) 7,924,000,000 <sup>b</sup> (7.02-8.83x10 <sup>9</sup> )	429,000 (154-690x10 <sup>3</sup> ) 5,040,000 (4.47-5.62x10 <sup>6</sup> )	13,600 (5-22x10 <sup>3</sup> ) 160,000 (117-207x10 <sup>3</sup> )
<i>Natural Gas</i>							
Combined Cycle	0.382	522 (23%)	1,017,000 (29%)	91.1 <sup>5,33,36</sup> 29.0 <sup>5,33,36</sup>	96,000,000 <sup>a</sup> (66-125x10 <sup>6</sup> ) 3,760,000,000 <sup>b</sup> (3.32-4.18 x10 <sup>9</sup> )	90,000 (61-117x10 <sup>3</sup> ) 3,530,000 (3.12-3.92x10 <sup>6</sup> )	2,900 (1,950-3,710) 111,800 (98-124x10 <sup>3</sup> )
Steam Turbine <sup>d</sup>	0.098	711 (31%)	108,000 (3%)	120.0 <sup>5,31</sup> 38.1 <sup>5,31</sup>	21,000,000 <sup>a</sup> 991,000,000 <sup>b</sup>	3,000 150,000	100 4,700
Gas Turbine <sup>d</sup>	0.036	894 (39%)	98,000 (3%)	543.0 <sup>5</sup>	523,000,000 <sup>a</sup>	178,000	5,700
<i>Nuclear</i>							
Steam Turbine	0.858	66 (3%)	769,000 (22%)	41.5 <sup>5,32,34,35</sup>	5,254,000,000 <sup>b</sup> (5.23-5.28x10 <sup>9</sup> )	53,608,000 (53.3-53.9x10 <sup>6</sup> )	1,700,00 (1.69-1.91x10 <sup>6</sup> )
TOTAL		2866	3,496,000		18,878,000,000 (17.8-19.8x10 <sup>9</sup> )		

<sup>a</sup>Heat available in power plant exhaust stream. Final temperature is 50°C to prevent acid gas deposition and provide in heat exchanger.

<sup>b</sup>Heat available in the condenser cooling water.

<sup>c</sup>Parentheses indicate 50% confidence interval on the median in simulations on coal, NGCC, and nuclear. Supporting Information Section 4.0 presents the distributions for simulation results and Figure S2 in the Supporting Information presents simulation result distributions for coal, NGCC, and nuclear cycles.

<sup>d</sup>Sensitivity analysis not performed due to insufficient peer-reviewed studies.



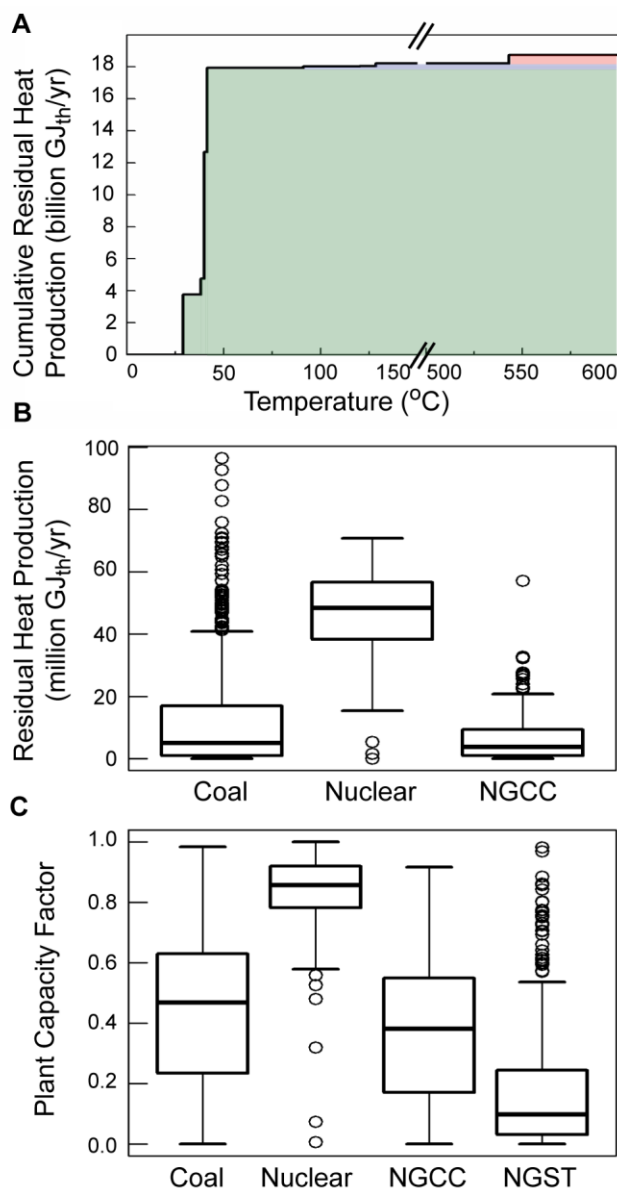


Figure 5.2 Residual heat production and capacity factor by fuel source. (A) Cumulative quantity of residual heat across all fuel cycles as a function of heat quality. Approximately 96% of residual heat is contained in the condenser streams ( $<41.5^{\circ}\text{C}$ ), as represented by the green shaded region. The remaining 4% of residual heat is contained exhaust streams, as represented by the blue ( $91.1\text{--}128.4^{\circ}\text{C}$ ) and red ( $543.0^{\circ}\text{C}$ ) shaded regions. (B) Box plots of residual heat production at U.S. power plants in 2012, with whiskers demarking 1.5 times the interquartile range from the median. Outliers are represented by open circles. Nuclear power plants have

*higher quantities of residual heat production, but the heat available is of low temperature (40°C). Coal and NGCC plants produce less heat, but they discharge higher temperature (128.4°C for coal and 91.1°C for NGCC) exhaust streams. The median NGST plant produces 153,000 GJ<sub>th</sub>/year and the median NGST plant produces 178,000 GJ<sub>th</sub>/year. (C) Box plots of plant capacity factor for U.S. power plants. While all system types have plants that operate at or near capacity, NGGT systems with high quality residual heat (NGGT) have median capacity factors of only 0.036.*

The quality of residual heat produced depends upon the efficiency of the fuel cycle. High quality heat (543°C) is available from the exhaust stream of NGGT systems, because heat in the exhaust is not subsequently used for steam generation in a steam cycle. The presence of steam cycles in coal, NGCC, and NGST systems leads to greater conversion efficiencies and lower temperature residual heat (91.1-128.4°C). Condenser heat (29.0-41.5°C) is available from the systems with a steam cycle: coal, NGCC, NGST, and nuclear systems.

If one were to ignore availability and transport constraints, the quantity and quality of generated residual heat would appear sufficient to meet many of the reported thermal energy needs within the U.S.<sup>48,49</sup> Residual heat from natural gas condensers at an average process temperature of 29.0°C (NGCC) and 38.1°C (NGST) is comparable to the need for water heating in pools, spas, and aquariums (99 million GJ<sub>th</sub> annually).<sup>48,49</sup> Residual heat from coal and nuclear condensers (40.0 and 41.5°C, respectively) exceeds U.S. space heating requirements (8.5 billion GJ<sub>th</sub> annually).<sup>48,49</sup> NGCC exhaust heat is greater than the demand for steam at a temperature of 80-100°C for food and industrial processes (110 million GJ<sub>th</sub> annually).<sup>48,49</sup> And the quantity of residual heat from NGST and coal exhaust is sufficient to meet the 120-140°C steam demands

for industrial cooling (250 million GJ<sub>th</sub> annually).<sup>48,49</sup> Absent availability and transport constraints, application of residual heat for these process could replace between 8.8 and 26 billion GJ<sub>th</sub> of primary fuel combustion for on-site heat generation or electricity generation for subsequent electric heating and cooling (see SI Section 8.0), roughly 2-6 times the natural gas consumption in the residential sector in 2012.<sup>48,49</sup>

#### *5.4.2 Recovering Residual Heat*

Despite reasonable parity between heat demand and residual heat quantity and quality, cost-effectively recovering residual heat remains a technical challenge. This is particularly true of low-temperature residual heat recovery, where a shallow temperature gradient between the heat source and heat sink requires high surface areas and thorough fluid mixing. Heat exchanger design will necessarily depend upon the physical infrastructure of the power plant, the working fluids, and the end-use of the residual heat, but a number of low-temperature designs relevant to heat capture at power plants are covered in a recent report issued by the U.S. Department of Energy.<sup>42</sup> Installing heat recovery systems poses several non-technical challenges that also limit recovery of residual heat from power plants. The Department of Energy reports that physical accessibility of heat sources can prevent recovery in tight spaces by preventing the installation of new equipment.<sup>42</sup> They also note that for smaller systems, upfront capital costs could be prohibitive. The unique challenge of thermal cycling between high and low temperatures during on and off times also poses a limit on the materials that can be used. We consider only traditional shell-in-tube heat exchanger designs to inform subsequent calculations of spatial availability, and we do not limit the area of the heat exchanger since the capital costs of the heat exchanger are significantly lower than that of the heat pipe network (SI Section 5.3).

### *5.4.3 Spatial-Temporal Availability of Residual Heat*

Spatial-temporal variability of residual heat also imposes significant constraints on its application. Temporal availability over the course of the year is reasonably approximated by power plant capacity factors, as significantly greater quantities of residual heat are produced during electricity generation than during plant idling. Power plant capacity factors are plotted against fuel cycles in Figure 5.2C. The median nuclear power plant has a significantly higher capacity factor than the median coal, NGCC, NGST, or NGGT system.

The spatial availability of residual heat, modeled as technical and economic constraints on heat capture, transport, and usage, also limit its viable end uses. We estimate the spatial availability of residual heat of both condenser and exhaust streams using models described in the materials and methods. For the condenser streams from the median NGST, NGCC, and coal power plants, the techno-economically feasible transport distance is less than 100 meters (Figure 5.3). For nuclear plants, which discharge significantly more heat in their condenser streams, the techno-economic limit of heat conveyance is approximately 1.5 km. As a result of these low waste transport distances, Figure 5.3 represents the spatial extent of condenser heat streams schematically rather than precisely.

The medium and high temperature heat associated with exhaust streams, on the other hand, have techno-economically feasible transport distances far beyond the plant boundaries (Figure 5.3). The spatial extents of the red and blue regions indicate the feasible limits of heat transport, while darker shading indicates greater residual heat availability. Figure 5.3 is presented as separate residual heat maps for low condenser heat of  $<41.5^{\circ}\text{C}$ , medium temperature exhaust heat of  $91.1\text{--}128.4^{\circ}\text{C}$ , and high temperature NGGT exhaust heat at  $543^{\circ}\text{C}$  in Figure S5 of SI Section 9.0.

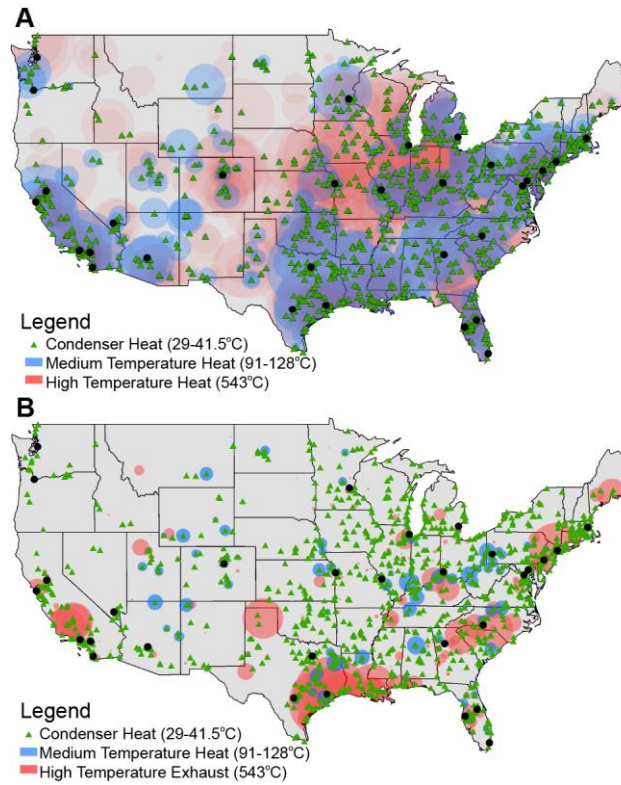


*Figure 5.3 Spatial distribution of techno-economically feasible residual heat in the U.S. Panel (A) depicts the upper bound of the techno-economically feasible transport distance of residual heat. This data simulates the case in which all electric power generation facilities operate at full capacity. Panel (B) depicts the economically feasible transport distance for plants under the assumption that their calculated annual waste heat generation is time-averaged throughout the year. Therefore, this second case neglects additional losses associated with start-up and shut-down of steam conveyance systems. Green triangles denote the availability of condenser heat at the power plant (transport > 0.1 km, economically infeasible). The extent of the blue and red circles indicate the spatial limits of availability for medium temperature exhaust heat (from coal, NGCC, and NGST systems), and higher temperature exhaust heat (from NGGT systems), respectively. The darker the color, the greater the quantity of residual heat available. Black points demarcate the thirty largest metro areas in the United States.*

Techno-economically feasible transport distance is positively correlated with discharged heat temperature, plant size, and capacity factor. Figure 5.3A shows the economically feasible transport distance for all plants operating at full generation capacity throughout the year. Figure 5.3B shows the economically feasible transport distance for plants under the assumption that their calculated annual waste heat generation is time-averaged throughout the year. The difference in the two panels stems from the lower annual generation of waste heat in the time-averaged case and the small capacity factors of many plants, especially NGGT systems. These two cases approximate upper and lower bounds on the feasibility of heat transport, though since the capacity factor is 1 for both cases, these calculations do not account for heat loss associated with start-up and shut-down of heat conveyance systems for low capacity factor plants.

For the time-averaged heat flux case, heat captured from the exhaust streams of median NGST, NGCC, NGGT, and coal plants have economically feasible transport distances of 1.6, 22.8, 89.7, and 104.7 km, respectively. At these upper limits for economically feasible residual heat transport, 41%, 30%, 41%, and 40% of the heat is lost to the environment during transport, respectively.

The economic viability of heat transport is also positively correlated with the price of natural gas. Economically feasible heat transport distances presented in Figure 5.3 assume a natural gas price of \$4.60 per thousand cubic feet, the average industrial price between 2011 and 2014. Details on the sensitivity to natural gas price are reported in SI Section 10.0 and Figure S8.

Temporal availability and spatial availability of heat are not well aligned in the current US power mix. Temporal constraints favor large nuclear systems that produce only low temperature condenser residual heat. This is in direct contrast to the spatial limitations, where

the high temperature of NGGT exhaust significantly enhances the techno-economically feasible transport distance. These results suggest that beneficial application of low temperature heat is most likely to be realized through on-site use or at facilities co-located with power plants, where the cost and pressure requirements of low temperature heat transport are less limiting. Beneficial application of high and medium temperature exhaust heat will likely occur only at plants with sufficiently high capacity factors to meet end-use demands. The proximity of plants to high population density, a proxy for off-site end uses, is discussed in SI Section 9.0 and Figure S6 and S7.

#### *5.4.4 Residual Heat Forecasts*

Substantial changes in the fuel mix for electric power generation are expected between 2013 and 2040. My projections estimate a 10.6% or 1.8 billion GJ<sub>th</sub> increase in residual heat production between 2013 and 2040 in EIA's reference predictions for fuel consumption by power plants. These reference predictions assume the implementation of the Mercury and Air Toxics Standards in 2016. Additionally, Clean Air Act Section 111 proposed carbon pollution standards are represented in scenarios demarcated with a blue line in Figure 5.4A and 5.4B. Total annual residual heat production from scenarios without a price on carbon is plotted in yellow.

Variability in forecasted annual residual heat production stems from assumptions about the price of carbon, the future of US nuclear generation capacity, and the timing of coal fired power plant decommissioning. The dashed blue line denotes the scenario in which a high price on carbon drives the growth of nuclear power as a substitution for coal generation. The effect is to increase the total annual residual heat generation (Figure 5.4A), but to decrease medium and

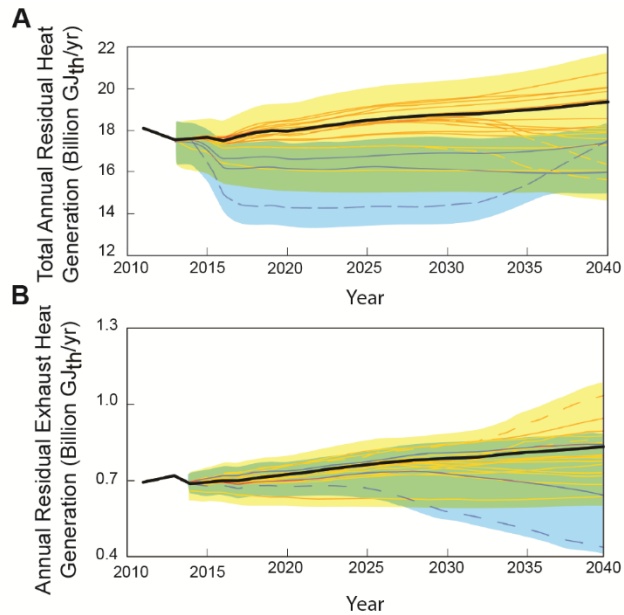


*Figure 5.4 Forecasted residual heat generation based on EIA fuel consumption projections under 21 different scenarios. Panel (A) shows the residual heat production for all heat streams. Panel (B) shows residual heat production for exhaust streams. The thicker black line represents EIA's reference case from the 2014 Annual Energy Outlook. The scenarios represented by other lines can be found in Table S3 of the Supporting Information, with hashed yellow lines indicating accelerated nuclear retirement and hashed blue lines indicating accelerated nuclear construction. Scenarios with a carbon price are shown in blue; those without a price on carbon in yellow. The shaded areas represent 25-75% uncertainty around the forecasts for carbon price scenarios (shaded blue), non-carbon price scenarios (shaded yellow), or both (shaded green).*

high temperature annual heat generation (Figure 5.4B). On the other hand, accelerated nuclear power plant retirements (scenarios denoted by dashed yellow lines) will significantly decrease the availability of low quality heat (Figure 5.4A). As these cases highlight, the generation of nuclear power has a significant impact on the quantity and quality of residual heat.



EIA forecasts do not explicitly account for regulatory or scarcity constraints on cooling water availability. Shifting from once-through and recirculating cooling to dry-cooling will increase the cost of electricity generation and result in heat being discharged to the environment as a warm gas stream.<sup>50,51</sup> The recoverability of the condenser heat may be impacted for some applications.

#### *5.4.5 Potential Applications of Residual Heat*

Typical combined heat and power systems sacrifice some electricity conversion for higher heat in the condenser stream, thereby requiring separate calculations from those detailed here. Here, we evaluate only the techno-economic viability of residual heat capture and transport. The low to moderate quality and quantity of residual heat from nuclear, coal, NGCC, and NGST fuel cycles severely limit heat transport off-site, while the very low capacity factors of NGGT plants are likely to limit the transport of this high temperature exhaust heat.

As a result, we expect that residual heat use will find its primary application at the power plant, including carbon capture from flue-gas and onsite water treatment.<sup>52</sup> Temperature swing CO<sub>2</sub> adsorption systems, such as the monoethanolamine system, are capable of operating at temperatures around 117°C,<sup>53</sup> below the temperature of residual heat in the exhaust of coal fired power plants with FGD units.

Onsite water treatment may also be a viable application for medium temperature residual heat at electric power generation facilities.<sup>54</sup> Forward osmosis, a two-stage process consisting of a membrane separation step followed by a moderate-temperature distillation step,<sup>55,56</sup> may find application in boiler feedwater or wastewater treatment. Similarly, the membrane distillation process, in which the driving force for separation is the difference in vapor pressure (i.e. temperature) across a hydrophobic microporous membrane, may find application in power plant

wastewater treatment.<sup>24,57</sup> Using waste heat, rather than electricity, to drive these processes will reduce auxiliary electricity consumption at the power plant and improve the economical viability of plant water recycle systems and impaired water sourcing.

## 5.5 Implications

From the quantity, quality, and availability of residual heat from the US power sector detailed in this analysis, we conclude that residual heat use provides a small to moderate near-term opportunity for systems-level energy savings in the U.S of 8.8-26 GJ<sub>th</sub>. Residual heat generated by nuclear, coal, NGCC, and NGST condensers and exhaust streams is frequently available, but, the low to moderate temperatures of the heat will limit its applications to on-site processes (e.g. carbon capture,<sup>53,58,59</sup> thermoelectrics,<sup>60–63</sup> heat pumps,<sup>64</sup> or water treatment<sup>55,65</sup>) the efficiency of which varies considerably. High quality heat from NGGT exhaust is less spatially constrained, but its use will be limited to applications that can accommodate high variation in temporal availability, as the median capacity factor of NGGT plants is only 0.036.

From an economic perspective, capturing and transporting residual heat off-site requires significant capital investments in heat exchangers and heat distribution networks. Economic viability is ultimately constrained by the life-cycle cost of heat production via primary fuel combustion. One long-term solution to these economic limitations is enhanced co-location of power generation with viable low-temperature heat end-uses, thereby minimizing the cost of installing the heat distribution system.

Several additional levels of analysis are necessary to assess specific end use applications for power plant residual heat. The residual heat estimates presented here are average annual estimates; seasonal and hourly temporal distribution of the residual heat will also influence the compatibility between power plant residual heat generation and end-use applications. Second,

the system efficiencies we used for this study were for optimized systems or from manufacturing sources, which may cite slightly higher efficiency values than those realized by the current fleet of power plants. Finally, greater information about the geospatial characteristics of specific end-uses is required to understand the actual availability of residual heat at the site.

## **5.6 Acknowledgements**

The authors thank Dr. Haibo Zhai and Dr. Nicholas Siefert for their valuable feedback on the manuscript. This work was supported by the National Science Foundation under award number SEES-1215845. This material is based upon work supported by the Department of Energy under Award Number DE-FE0024008. DG also acknowledges support from The Pittsburgh Chapter of ARCS Foundation (Achievement Rewards for College Scientists), the Steinbrenner Graduate Fellowship, and the Phillips & Huang Family Foundation Fellowship.

## **5.7 Nomenclature**

### **Symbols**

$c_p$ : heat capacity [J/mol·K]

$G$ : exhaust gas flow rate [mol/yr]

$L$ : length of heat pipe [m]

$Q$ : heat flow rate [MJ/yr]

$q$ : heat flow rate in the heat pipe [J/s]

$T$ : stream temperature [°C]

$W$ : electricity generated [MJ]

$\alpha$ : percentage of unconverted energy input in stream

$\eta$ : process efficiency

## **Subscripts**

condenser: condenser

conv: thermal to electrical conversion

cycle: entire power cycle

elec: electricity

ex: exergy

exhaust: exhaust gas

fuel: fuel input

i: fuel and cycle (i.e. Coal, Nuclear, NGCC, NGST, NGGT)

j: generator level

k: plant level

L: distance from power plant

i: year

$L_{\text{ow}}$ : minimum exhaust gas temperature

residual: residual heat

th: thermal

unconverted: heat not converted into electricity

## 5.8 References

1. U.S. Energy Information Agency. Form EIA-923 Detailed Data  
<http://www.eia.gov/electricity/data/eia923/>.
2. Moran, M. J.; Shapiro, H. N. *Fundamentals of Engineering Thermodynamics*; 6th ed.; John Wiley & Sons, Inc.: Hoboken, NJ, 2008.
3. Black & Veatch. *Power Plant Engineering*; Drbal, L. F.; Boston, P. G.; Westra, K. L.; Erickson, R. B., Eds.; Kluwer Academic Publishers: Boston, MA, 1996.
4. Bhatt, M. S. Energy audit case studies I - steam systems. *Appl. Therm. Eng.* **2000**, *20*, 285–296.
5. Rattner, A. S.; Garimella, S. Energy harvesting, reuse and upgrade to reduce primary energy usage in the USA. *Energy* **2011**, *36*, 6172–6183.
6. Wang, H.; Zhao, L.; Zhou, Q.; Xu, Z.; Kim, H. Exergy analysis on the irreversibility of rotary air preheater in thermal power plant. *Energy* **2008**, *33*, 647–656.
7. Liu, M.; Yan, J.; Chong, D.; Liu, J.; Wang, J. Thermodynamic analysis of pre-drying methods for pre-dried lignite-fired power plant. *Energy* **2013**, *49*, 107–118.
8. Rosen, M. A. Assessing and improving the efficiencies of a steam power plant using exergy analysis. Part 1: assessment. *Int. J. exergy* **2006**, *3*, 362–376.
9. Beér, J. M. High efficiency electric power generation: The environmental role. *Prog. Energy Combust. Sci.* **2007**, *33*, 107–134.

10. National Energy Technology Laboratory. *Improving the Thermal Efficiency of Coal-Fired Power Plants Plants in the United States*; 2010.
11. Bezdek, R. H.; Wendling, R. M. Economic, Environmental, and Job Impacts of Increased Efficiency in Existing Coal-Fired Power Plants. *J. Fusion Energy* **2012**, 32, 215–220.
12. Shi, X.; Agnew, B.; Che, D.; Gao, J. Performance enhancement of conventional combined cycle power plant by inlet air cooling, inter-cooling and LNG cold energy utilization. *Appl. Therm. Eng.* **2010**, 30, 2003–2010.
13. Suresh, M. V. J. J.; Reddy, K. S.; Kolar, a. K. Thermodynamic analysis of a coal-fired power plant repowered with pressurized pulverized coal combustion. *Proc. Inst. Mech. Eng. Part A J. Power Energy* **2011**, 226, 5–16.
14. Poullikkas, A. An overview of current and future sustainable gas turbine technologies. *Renew. Sustain. Energy Rev.* **2005**, 9, 409–443.
15. Najjar, Y. S. H. Efficient use of energy by utilizing gas turbine combined systems. *Appl. Therm. Eng.* **2001**, 21, 407–438.
16. Rosen, M. A.; Dincer, I. Survey of thermodynamic methods to improve the efficiency of coal-fired electricity generation. *Proc. Inst. Mech. Eng. Part A J. Power Energy* **2003**, 217, 67–73.
17. Tzolakis, G.; Papanikolaou, P.; Kolokotronis, D.; Samaras, N.; Tzourlidakis, a.; Tomboulides, a. Simulation of a coal-fired power plant using mathematical programming algorithms in order to optimize its efficiency. *Appl. Therm. Eng.* **2012**, 48, 256–267.

18. Ray, T. K.; Datta, A.; Gupta, A.; Ganguly, R. Exergy-based performance analysis for proper O&M decisions in a steam power plant. *Energy Convers. Manag.* **2010**, *51*, 1333–1344.
19. Kapil, A.; Bulatov, I.; Smith, R.; Kim, J.-K. Process integration of low grade heat in process industry with district heating networks. *Energy* **2012**, *44*, 11–19.
20. Li, C.; Goswami, D. Y.; Shapiro, A.; Stefanakos, E. K.; Demirkaya, G. A new combined power and desalination system driven by low grade heat for concentrated brine. *Energy* **2012**, *46*, 582–595.
21. Zhao, S.; Zou, L.; Tang, C. Y.; Mulcahy, D. Recent developments in forward osmosis: Opportunities and challenges. *J. Memb. Sci.* **2012**, *396*, 1–21.
22. Lay, W. C. L.; Zhang, J.; Tang, C.; Wang, R.; Liu, Y.; Fane, A. G. Factors affecting flux performance of forward osmosis systems. *J. Memb. Sci.* **2012**, *394-395*, 151–168.
23. McGinnis, R. L.; Elimelech, M. Global Challenges in Energy and Water Supply: The Promise of Engineered Osmosis. *Environ. Sci. Technol.* **2008**, *42*, 8625–8629.
24. Jansen, A. E.; Assink, J. W.; Hanemaaijer, J. H.; van Medevoort, J.; van Sonsbeek, E. Development and pilot testing of full-scale membrane distillation modules for deployment of waste heat. *Desalination* **2013**, *323*, 55–65.
25. Madden, N.; Lewis, a; Davis, M. Thermal effluent from the power sector: an analysis of once-through cooling system impacts on surface water temperature. *Environ. Res. Lett.* **2013**, *8*, 035006.

26. Teixeira, T. P.; Neves, L. M.; Araújo, F. G. Thermal impact of a nuclear power plant in a coastal area in Southeastern Brazil: effects of heating and physical structure on benthic cover and fish communities. *Hydrobiologia* **2012**, *684*, 161–175.
27. Kirillin, G.; Shatwell, T.; Kasprzak, P. Consequences of thermal pollution from a nuclear plant on lake temperature and mixing regime. *J. Hydrol.* **2013**, *496*, 47–56.
28. Zevenhoven, R.; Beyene, a. The relative contribution of waste heat from power plants to global warming. *Energy* **2011**, *36*, 3754–3762.
29. Ozalp, N. Utilization of Heat, Power, and Recovered Waste Heat for Industrial Processes in the U.S. Chemical Industry. *J. Energy Resour. Technol.* **2009**, *131*, 022401.
30. Erdem, H. H.; Dagdas, A.; Sevilgen, S. H.; Cetin, B.; Akkaya, A. V.; Sahin, B.; Teke, I.; Gungor, C.; Atas, S. Thermodynamic analysis of an existing coal-fired power plant for district heating/cooling application. *Appl. Therm. Eng.* **2010**, *30*, 181–187.
31. Ameri, M.; Ahmadi, P.; Hamidi, A. Energy , exergy and exergoeconomic analysis of a steam power plant : A case study. *Int. J. Energy Res.* **2009**, *33*, 499–512.
32. Durmayaz, A.; Yavuz, H. Exergy analysis of a pressurized-water reactor. *Appl. Energy* **2001**, *69*, 39–57.
33. Shi, X.; Che, D. Thermodynamic analysis of an LNG fuelled combined cycle power plant with waste heat recovery and utilization system. *Int. J. Energy Res.* **2007**, *31*, 975–998.



34. Rosen, M. A. Energy- and exergy-based comparison of coal-fired and nuclear steam power plants. *Exergy* **2001**, *1*, 180–192.
35. Dunbar, W. R.; Moody, S. D.; Lior, N. Exergy analysis of an operating boiling-water-reactor nuclear power station. *Energy Convers. Manag.* **1995**, *36*, 149–159.
36. Hammond, G. P.; Akwe, S. S. O. Thermodynamic and related analysis of natural gas combined cycle power plants with and without carbon sequestration. *Int. J. Energy Res.* **2007**, *31*, 1180–1201.
37. Rosen, M. .; Dincer, I. Exergoeconomic analysis of power plants operating on various fuels. *Appl. Therm. Eng.* **2003**, *23*, 643–658.
38. GE Energy. Heavy Duty Gas Turbine Products <http://www.gepower.com/home/index.htm>.
39. Arrieta, F. R. P.; Lora, E. E. S. Influence of ambient temperature on combined-cycle power-plant performance. *Appl. Energy* **2005**, *80*, 261–272.
40. U.S. Environmental Protection Agency. National Emission Standards for Hazardous Air Pollutants From Coal- and Oil-Fired Electric Utility Steam Generating Units and Standards of Performance for Fossil-Fuel-Fired Electric Utility, Industrial-Commercial-Institutional, and Small Industrial-Commer <http://www.gpo.gov/fdsys/pkg/FR-2012-02-16/pdf/2012-806.pdf>.
41. National Energy Technology Laboratory. *Cost and Performance Baseline for Fossil Energy Plants Volume 1 : Bituminous Coal and Natural Gas to Electricity*; 2013; Vol. 1.

42. U.S. Department of Energy. *Waste Heat Recovery: Technology and Opportunities in U.S. Industry*; Washington, DC, 2008.
43. U.S. Environmental Protection Agency. Emissions Factors & AP 42, Compilation of Air Pollutant Emission Factors <http://www.epa.gov/ttnchie1/ap42/>.
44. U.S. Energy Information Agency. Form EIA-860 Detailed Data <http://www.eia.gov/electricity/data/eia860/>.
45. Dalla Rosa, A.; Li, H.; Svendsen, S. Method for optimal design of pipes for low-energy district heating, with focus on heat losses. *Energy* **2011**, *36*, 2407–2418.
46. U.S. Energy Information Administration. United States Natural Gas Industrial Price <http://www.eia.gov/dnav/ng/hist/n3035us3m.htm>.
47. U.S. Energy Information Agency. *American Energy Outlook 2014 Early Release Report*; Washington, DC, 2013; Vol. 2014.
48. Fox, D. B.; Sutter, D.; Tester, J. W. *The Thermal Spectrum of Low-Temperature Energy Use in the United States*; Ithaca NY, 2011.
49. Fox, D. B.; Sutter, D.; Tester, J. W. The thermal spectrum of low-temperature energy use in the United States. *Energy Environ. Sci.* **2011**, *4*, 3731.
50. National Energy Technology Laboratory. *Water Requirements for Existing and Emerging Thermoelectric Plant Technologies*; Morgantown, WV, 2009; Vol. 2008.

51. National Energy Technology Laboratory. *Estimating Freshwater Needs to Meet Future Thermoelectric Generation Requirements*; Pittsburgh, PA, 2010.
52. Zhai, H.; Rubin, E. S.; Versteeg, P. L. Water use at pulverized coal power plants with postcombustion carbon capture and storage. *Environ. Sci. Technol.* **2011**, *45*, 2479–2485.
53. House, K. Z.; Harvey, C. F.; Aziz, M. J.; Schrag, D. P. The energy penalty of post-combustion CO<sub>2</sub> capture & storage and its implications for retrofitting the U.S. installed base. *Energy Environ. Sci.* **2009**, *2*, 193.
54. Shannon, M. a; Bohn, P. W.; Elimelech, M.; Georgiadis, J. G.; Mariñas, B. J.; Mayes, A. M. Science and technology for water purification in the coming decades. *Nature* **2008**, *452*, 301–310.
55. McGinnis, R. L.; Elimelech, M. Energy requirements of ammonia-carbon dioxide forward osmosis desalination. *Desalination* **2007**, *207*, 370–382.
56. McCutcheon, J. R.; McGinnis, R. L.; Elimelech, M. A novel ammonia-carbon dioxide forward ( direct ) osmosis desalination process. *Desalination* **2005**, *174*, 1–11.
57. Lawson, K. W.; Lloyd, D. R. Membrane distillation. II. Direct contact MD. *J. Memb. Sci.* **1996**, *120*, 123–133.
58. Markewitz, P.; Kuckshinrichs, W.; Leitner, W.; Linssen, J.; Zapp, P.; Bongartz, R.; Schreiber, A.; Müller, T. E. Worldwide innovations in the development of carbon capture technologies and the utilization of CO<sub>2</sub>. *Energy Environ. Sci.* **2012**, *5*, 7281.

59. MacDowell, N.; Florin, N.; Buchard, A.; Hallett, J.; Galindo, A.; Jackson, G.; Adjiman, C. S.; Williams, C. K.; Shah, N.; Fennell, P. An overview of CO<sub>2</sub> capture technologies. *Energy Environ. Sci.* **2010**, *3*, 1645.
60. Abraham, T. J.; MacFarlane, D. R.; Pringle, J. M. High Seebeck coefficient redox ionic liquid electrolytes for thermal energy harvesting. *Energy Environ. Sci.* **2013**, *6*, 2639.
61. Bubnova, O.; Crispin, X. Towards polymer-based organic thermoelectric generators. *Energy Environ. Sci.* **2012**, *5*, 9345.
62. Poehler, T. O.; Katz, H. E. Prospects for polymer-based thermoelectrics: state of the art and theoretical analysis. *Energy Environ. Sci.* **2012**, *5*, 8110.
63. Minnich, A. J.; Dresselhaus, M. S.; Ren, Z. F.; Chen, G. Bulk nanostructured thermoelectric materials: current research and future prospects. *Energy Environ. Sci.* **2009**, *2*, 466.
64. Staffell, I.; Brett, D.; Brandon, N.; Hawkes, A. A review of domestic heat pumps. *Energy Environ. Sci.* **2012**, *5*, 9291.
65. Bajpayee, A.; Luo, T.; Muto, A.; Chen, G. Very low temperature membrane-free desalination by directional solvent extraction. *Energy Environ. Sci.* **2011**, *4*, 1672.

## CHAPTER 6: WATER TREATMENT CAPACITY OF FORWARD OSMOSIS SYSTEMS UTILIZING POWER PLANT WASTE HEAT<sup>5</sup>

### 6.1 Abstract

Forward osmosis (FO) has the potential to improve the energy efficiency of membrane-based water treatment by leveraging waste heat from steam electric power generation as the primary driving force for separation. In this study, we develop a comprehensive FO process model, consisting of membrane separation, heat recovery, and draw solute regeneration (DSR) models. We quantitatively characterize three alternative processes for DSR: distillation, steam stripping, and air stripping. We then construct a mathematical model of the distillation process for DSR that incorporates hydrodynamics, mass and heat transport resistance, and reaction kinetics, and we integrate this into a model for the full FO process. Finally, we use this FO process model to derive a first-order approximation of the water production capacity given the rejected heat quantity and quality available at US electric power facilities. We find that the upper bound of FO water treatment capacity using low-grade heat sources at electric power facilities exceeds process water treatment demand for boiler water make-up and flue gas desulfurization wastewater systems.

---

<sup>5</sup> This chapter is based on a paper co-authored with Prof. Meagan Mauter and Xingshi Zhou in Industrial & Engineering Chemistry Research. It can be found at Zhou, X.; Gingerich, D.B.; Mauter, M.S., Water Treatment Capacity of Forward-Osmosis Systems Utilizing Power-Plant Waste Heat. *Industrial & Engineering Chemistry Research* **2015**, 54, (24), 6378-6389. X.Z. developed the model. D.B.G. applied the model to treating FGD wastewater and performed the FO treatment capacity calculations. Both X.Z. and D.B.G. contributed to writing the manuscript.

## 6.2 Introduction

Proposed effluent limitation guidelines at steam electric power generation facilities will significantly increase the demand for onsite water treatment.<sup>1</sup> One opportunity to minimize the auxiliary power consumption associated with this treatment capacity is to use waste heat available onsite for membrane-based water treatment. One potential technology is forward osmosis (FO), where the draw solution is a thermolytic salt (e.g.  $\text{NH}_4\text{HCO}_3$ ) (Figure 6.1).<sup>2-4</sup> In this two-step process, feedwater is drawn across a semipermeable membrane by a difference in osmotic pressure between the feed solution and the draw solution. The diluted draw solute is then regenerated via thermal decomposition of the thermolytic salt into its constituent gases (i.e.  $\text{NH}_3$  and  $\text{CO}_2$ ).<sup>5</sup> If waste heat is available, this separation process offers significant electricity savings over reverse osmosis.<sup>6,7</sup>

Steam electric power generation facilities are the largest source of waste heat in the U.S.,<sup>8</sup> but the feasibility of using this waste heat to drive FO separation processes has yet to be systematically assessed in the peer-reviewed literature.<sup>5,6,9</sup> Past modeling efforts to evaluate the feasibility of waste heat driven FO assume that heat is available at desired quantities and temperatures,<sup>7</sup> while experimental demonstrations of FO processes in the peer reviewed literature use electricity or fuel to generate heat.<sup>9-11</sup> This significant gap in the literature exists largely because robust estimates of power plant waste heat quantity, quality, and availability are sparse.<sup>12,13</sup> Our recent work provides estimates of quantity, quality, and spatial-temporal availability for the U.S. power sector over the next 30 years.<sup>14</sup> Demonstrating the feasibility of power plant waste heat driven FO requires the integration of these waste heat estimates with heat capture, transport, draw solute regeneration (DSR), and membrane separation models.

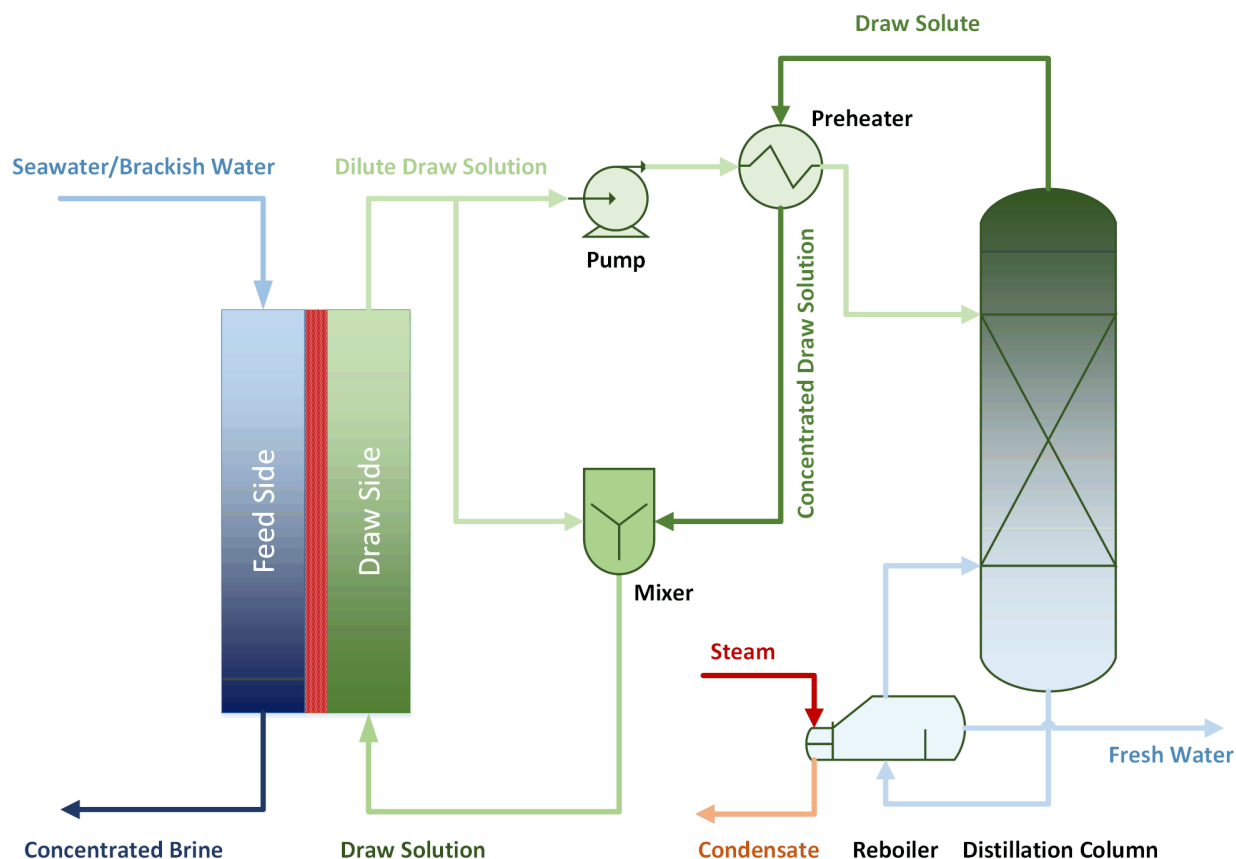


Figure 6.1. Generalized process flow diagram of the forward osmosis process.

Accurate modeling of the DSR system also depends on a robust understanding of draw solute chemistry. Much of the past modeling work fails to report the specific method for evaluating the separation performance of the  $\text{CO}_2\text{-NH}_3\text{-H}_2\text{O}$  ternary system.<sup>7,9,15</sup> Other models underestimate heat consumption per unit of product water or the column height by assuming that the system reaches equilibrium over the column height. For example, Kim et al.'s equilibrium-based simulations underestimate the heating energy by 59% compared to experimental data from their pilot recovery process.<sup>16</sup> Recent efforts to model the ammonia-based  $\text{CO}_2$  capture process provide a potential route for including the influence of hydrodynamics, mass and heat transport resistance, and reaction kinetics into the DSR model.<sup>17–20</sup> The application of these rate-based models to the FO draw solute regeneration system ensures the validity of the DSR process

simulations, but these rate-based models are also computationally intensive and therefore unfavorable for optimization case studies. To overcome this issue, we develop both a rate-based model and a reduced model that simplifies the rate-based model with negligible deviation from predicted values.

Finally, optimizing the water production capacity of waste heat driven FO systems has been hampered by reliance on the ASPEN modeling environment. ASPEN, and associated black box optimization techniques, pose numerical issues (e.g. system convergence, initialization, non-convexity), are time consuming, and do not efficiently perform multi-objective optimization.<sup>7,9</sup> When optimization of DSR systems was performed by past researchers, the objective was to minimize the cost of the system rather than maximize the amount of water constrained by a certain heat input.<sup>7</sup> The distinction is particularly important for systems using waste heat as the energy source. Integrated mathematical models of FO unit processes will ultimately allow for efficient optimization and for a thorough characterization of the trade-offs between operating conditions and cost.

This work evaluates the feasibility of using waste heat rejected from steam electric power generation processes to treat water of moderate salinity (~30,000 ppm TDS), such as flue gas desulfurization wastewater, onsite. In 2012, coal and natural gas generators discharged 900 million GJ of heat to the environment in their exhaust streams.<sup>14</sup> This heat has temperatures ranging from an average of 90°C to 543°C, depending on the fuel cycle (i.e. coal; natural gas combined cycle, NGCC; natural gas steam turbine, NGST; and natural gas gas turbine, NGGT). Using simulation models, we identify the most energy-efficient DSR design given the heat quality available at the median U.S. power plant for each fuel cycle. We then develop a mathematical model of the complete FO process, including the membrane separation step, the



heat recovery step,<sup>14</sup> and the DSR process, in order to evaluate trade-offs between various operating conditions. Finally, we apply solutions from the mathematical model to determine the upper bound of water volume that could feasibly be treated via FO using waste heat from the flue gas streams of power plants. We limit our water production capacity analysis to waste heat available on site, as this waste heat has commonly been cited as an ideal source of energy for FO processes.<sup>6,21</sup>

## 6.3 Methods

### 6.3.1 $\text{CO}_2\text{-NH}_3\text{-H}_2\text{O}$ Separation Models in DSR Systems

We model regeneration of the thermolytic  $\text{CO}_2\text{-NH}_3$  draw solute system. In aqueous solution, complex reversible reactions occur (see Table S1 of Supporting Information (SI) Section S1 for the list of these reactions) and species including bicarbonate, carbonate, and carbamate are formed.<sup>19,20,22</sup> Although Table S1 lists a precipitation/dissolution reaction (R6), we neglect this reaction in the present work since the maximum concentration of the draw solution, 8 M ( $\text{CO}_2$  based), is far below the solubility limit of 13 M.

Previous work in modeling this ternary system for  $\text{CO}_2$  capture suggests that hydrodynamics, thermodynamics, rate-based mass and heat transfer, and reaction kinetics are critical to accurately capturing the energy intensity of the regeneration process.<sup>20</sup> We start modeling the DSR system by developing a rate-based model that considers hydrodynamics, thermodynamics, rate-based mass and heat transfer, and reaction kinetics. Next, we simplify the rate-based model in order to develop an equilibrium state model that considers thermodynamics and reaction kinetics, but neglects mass transport resistance and heat transport resistance. Given a distillation column of infinite residence time, the rate-based model and equilibrium model produce very similar estimates of normalized heat duty. Finally, we develop a basic chemistry

model that assumes instantaneous chemical equilibrium and neglects hydrodynamics and interfacial mass or heat transport resistance in the column. The resulting models and their major differences are listed in Table 6.1.

For all models, we record computational speed and compare heat duty estimates in Table S7 of Section S10 of the SI. While we expect the greatest accuracy from the rate-based model, incorporation of hydrodynamics and rate-based mass and heat transfer increases the complexity of the models and significantly slows the computational speed of the calculations. Therefore, we use the solution from the rate-based model as a reference for evaluating the validity of the basic chemistry and equilibrium state models.

*Table 6.1 Model comparison*

<b>Model Name</b>	<b>Thermodynamics</b>	<b>Reaction Kinetics</b>	<b>Hydrodynamics</b>	<b>Rate-based Mass/ Heat Transfer</b>
<b>Chemistry Model</b>	Yes	No	No	No
<b>Equilibrium Stage Model</b>	Yes	Yes	Yes	No
<b>Rate-based Model</b>	Yes	Yes	Yes	Yes

### 6.3.2 Evaluating Separation Processes for DSR

Though selection of an appropriate DSR process depends upon the properties of the draw solute, the efficiency of upstream membrane processes, size or process constraints imposed by site conditions, cost, and many other factors, in this initial study we consider only the limitations imposed by heat quality and quantity available at electric power generation facilities. The reversible thermal decomposition of the species in the dilute draw solution including the ammonium bicarbonate, ammonium carbonate and ammonium carbamate into  $\text{CO}_2$  and  $\text{NH}_3$  can be achieved either by the addition of heat or the reduction of partial pressure. As a result, both conventional distillation and stripping techniques are potentially viable means of regenerating

the draw solution. We consider three alternative processes, distillation, steam stripping, and air stripping to separate the dilute draw solution into a concentrated  $\text{NH}_3/\text{CO}_2$  stream and a low-salinity product water that meets drinking water standards for ammonia of 1 mg/L.

An overview of the DSR process is provided in Figure 6.1. We model each of the DSR processes using a packed column. The DSR process commences with dilute draw solution preheating, using the thermal energy of hot streams from the top or bottom of a packed column. The dilute draw solution at or above its bubble point, depending on the specific operating pressure, then enters the packed column, where one of the three alternative processes is performed.

In the distillation-based DSR process, a reboiler at the bottom of a conventional distillation column provides the thermal input for distillation. The indirect heating of distillation is likely to be less efficient than stripping methods due to the thermal inefficiency introduced by the heat exchanger, but this process is better suited for low temperature DSR where sub-atmospheric pressures are required to completely recover the draw solution. In the steam stripping process, the latent heat of steam directly heats the sump streams in the column. This process is hindered by steam purity, as condensation may result in impurities in product water and affect its downstream application. The final DSR method considered, hot air stripping, drives the separation by reducing the partial pressure of volatile components in the gas phase, as well as increasing the temperature. According to Henry's law, fractions of the volatile in the liquid phase decrease due to vapor-liquid equilibrium limitations, leading to the separation of  $\text{CO}_2$  and  $\text{NH}_3$  from the clean water.

We build models for the three alternative DSR processes in ASPEN Plus (Aspen Technology, Inc.) using the electrolyte NRTL-RK thermodynamic method. We specify the dilute

draw solution flow rate and concentration, the number of stages, the boilup ratio, and the packing. ASPEN Plus simulates the required heat duty, as well as the column diameter, product water concentration and flow rate, and concentrated draw solution concentration and flow rate.

The rate-based model takes hydrodynamic, thermodynamic, rate-based heat/mass transfer, and chemical reaction into account, as shown in Table S2 of SI Section S2 on the equipment specifications for the ASPEN Model. In order to perform rate-based simulation, the columns are specified to contain Amistco (Goodloe equivalent) structured packing<sup>4</sup> with a void fraction of 0.945, a specific area of 580 ft<sup>2</sup>/ft<sup>3</sup>, a static holdup of 5% and a pressure drop of 0.096 mm Hg/ft. Packing height is approximately 8.3 ft, (equivalent to 25 theoretical stages). We vary the column pressure depending on the specific case (i.e. ambient or sub-atmospheric). Thermal and electrical energy requirements are calculated based on a product water quality specified to contain less than 1 ppm of ammonia (including related species like ammonium and carbamate).

The equilibrium stage model is constructed by switching from “rate-based” mode to “equilibrium” mode in ASPEN Plus and disabling rate-based modeling in packing rating section. The chemistry stage model was constructed by further deleting the reaction section in the column specifications, thereby leveraging the chemistry model without the consideration of rate-based heat/mass transfer and reaction kinetics.

We quantitatively evaluate each DSR method by determining its normalized heat duty in ASPEN Plus. Considering the relatively low energy consumption (as detailed in the “Results and Discussion” Section 1 and 2), potential issues with the steam contaminating the product water in steam stripping processes, and the option of accessing lower quality heat by operating the distillation column at sub-atmospheric pressures, we select distillation as the optimal DSR system for mathematical model formulation.

### 6.3.3 Mathematical Model of Distillation for DSR System

The majority of energy consumption of the FO desalination process lies in the DSR system and further evaluation and optimization of this process in the context of other FO system components is greatly aided by a rigorous mathematical model of the DSR process. We formulate a rate-based model for draw solute recovery based on a comprehensive MERSHQ model<sup>20</sup> including mass balances (M), energy balances (E), rate equations (R), summation equations (S), hydrodynamic equations (H), and equilibrium equations (Q) detailed below. This model assumes that stages are well-mixed and have similar properties (e.g. temperature) throughout the stage as calculated within the model. We model the distillation column to have metal gauze structure packing in the “X” configuration<sup>23</sup> in order to minimize the pressure drop in the column.

**Mass balances.** Material balances the vapor,  $\mathbf{M}_{i,j}^V$ , and liquid,  $\mathbf{M}_{i,j}^L$  phases for component  $i$  at stage  $j$  depend on the flowrate of the vapor ( $V_j$ ), liquid ( $L_j$ ), and feed ( $F_j$ ); the mole fraction in the vapor ( $y_{i,j}$ ) and the liquid ( $x_{i,j}$ ); the molar flux ( $N_{i,j}$ ); the effective interfacial area ( $a_e$ ); the volume of column per stage ( $V_S$ ) and reactions that occur that depend on stoichiometric coefficients ( $v$ ), reaction rates ( $r$ ), and the reaction extent ( $X$ ) for each of the controlled reactions (NRC) and instantaneous reactions (NRE). Details on the calculation of mass and heat transfer behavior can be found in SI Section S3. Information on activity correction using the Electrolyte NRTL model can be found in SI Section S4.

$$\mathbf{M}_{i,j}^V = V_j y_{i,j} - V_{j+1} y_{i,j+1} - F_j^V y_{i,j}^F - N_{i,j}^V a_e(V_S)_j = 0 \quad (6.1)$$

$$\mathbf{M}_{i,j}^L = L_j x_{i,j} - L_{j-1} x_{i,j-1} - F_j^L x_{i,j}^F - N_{i,j}^L a_e(V_S)_j - (V_{LH})_j \left( \sum_{k=1}^{NRC} (v_{i,k} r_{j,k}) + \sum_{k=1}^{NRE} (v'_{i,k} \chi_{j,k}) \right) = 0 \quad (6.2)$$

Total material balances equations at stage  $j$

$$\mathbf{M}_{T,j}^V = V_j - V_{j+1} - F_j^V + N_{T,j}^V a_e(V_S)_j = 0 \quad (6.3)$$

$$\mathbf{M}_{T,j}^L = L_j - L_{j-1} - F_j^L - N_{T,j}^L a_e(V_S)_j - (V_{LH})_j \sum_{i=1}^C (\sum_{k=1}^{NRC} (v_{i,k} r_{j,k}) + \sum_{k=1}^{NRE} (v'_{i,k} \chi_{j,k})) = 0 \quad (6.4)$$

**Energy balances.** Energy balances equations for the vapor ( $\mathbf{E}_j^V$ ), the liquid ( $\mathbf{E}_j^L$ ), and the interface ( $\mathbf{E}_j^I$ ) at stage  $j$  depend on the vapor, liquid, and feed flow rate; the molar enthalpy ( $H$ ); the heat duty added at each stage ( $Q$ ); and the interfacial energy ( $\epsilon$ ).

$$\mathbf{E}_j^V = V_j H_j^V - V_{j+1} H_{j+1}^V - F_j^V H_j^{VF} + Q_j^V + \epsilon_j^V = 0 \quad (6.5)$$

$$\mathbf{E}_j^L = L_j H_j^L - L_{j-1} H_{j-1}^L - F_j^L H_j^{LF} + Q_j^L - \epsilon_j^L = 0 \quad (6.6)$$

Energy balances equations at the interface

$$\mathbf{E}_j^I = \epsilon_j^V - \epsilon_j^L = 0 \quad (6.7)$$

**Rate equations.** The reaction rate for each component  $i$  on each stage  $j$  in the vapor ( $\mathbf{R}_{i,j}^V$ ) and the liquid ( $\mathbf{R}_{i,j}^L$ ) is a function of the molar flux for each component  $I$  on each stage  $j$  in the vapor ( $N_{i,j}^V$ ) and liquid ( $N_{i,j}^L$ ).

$$\mathbf{R}_{i,j}^V = N_{i,j} - N_{i,j}^V = 0 \quad (6.8)$$

$$\mathbf{R}_{i,j}^L = N_{i,j} - N_{i,j}^L = 0 \quad (6.9)$$

**Summation equations.** The summation equation for the vapor phase ( $\mathbf{S}_j^{IV}$ ) and liquid phase ( $\mathbf{S}_j^{IL}$ ) is a function of the molar fraction in the vapor ( $y_{i,j}^I$ ) and the liquid ( $x_{i,j}^I$ ) phases.

$$\mathbf{S}_j^{IV} = \sum_{i=1}^C y_{i,j}^I - 1 = 0 \quad (6.10)$$

$$\mathbf{S}_j^{LL} = \sum_{i=1}^C x_{i,j}^L - 1 = 0 \quad (6.11)$$

**Hydraulic equations.** The hydraulic equation at each stage ( $\mathbf{H}_j$ ) is a pressure balance equation, so that at any stage  $j$  the pressure ( $P_j$ ) minus the drop in each stage ( $\Delta P_{j-1}$ ) is equal to the pressure on the next stage ( $P_{j-1}$ ).

$$\mathbf{H}_j = P_j - P_{j-1} - \Delta P_{j-1} = 0 \quad (6.12)$$

**Vapor-liquid equilibrium equations.** The vapor-liquid equilibrium at the interface equation ( $\mathbf{Q}_{i,j}^I$ ) is a function of the vapor-liquid equilibrium constant ( $K_{i,j}$ ) and the mass fractions in the liquid and vapor phases at the interfaces.

$$\mathbf{Q}_{i,j}^I = K_{i,j} x_{i,j}^L - y_{i,j}^I = 0 \quad (6.13)$$

Similar to the approach that we took in developing the ASPEN models, both the chemistry model and equilibrium stage model are simplified versions of this original rate-based model. In the chemistry model, we assume instantaneous chemical equilibrium for the reactions by neglecting all kinetics terms and replacing the interfacial composition with the composition in the bulk phase. In the equilibrium state model, we do account for kinetics, yielding the following sets of equations:

The material balances the vapor,  $\mathbf{M}_{i,j}^V$ , and liquid,  $\mathbf{M}_{i,j}^L$  phases for component  $i$  at stage  $j$  depend on the flowrate of the vapor ( $V_j$ ), liquid ( $L_j$ ), and feed ( $F_j$ ); the mole fraction in the vapor ( $y_{i,j}$ ) and the liquid ( $x_{i,j}$ ); the volume of column per stage ( $V_s$ ) and reactions that occur that depend on stoichiometric coefficients ( $\nu$ ), reaction rates ( $r$ ), and the reaction extent ( $X$ ) for each of the controlled reactions (NRC) and instantaneous reactions (NRE):

$$\mathbf{M}_{i,j} = L_j x_{i,j} + V_j y_{i,j} - L_{j-1} x_{i,j-1} - V_{j+1} y_{i,j+1} - F_j^V y_{i,j}^F - F_j^L x_{i,j}^F - (V_{LH})_j \left( \sum_{k=1}^{NRC} (\nu_{i,k} r_{j,k}) + \sum_{k=1}^{NRE} (\nu'_{i,k} \chi_{j,k}) \right) = 0 \quad (6.14)$$

The energy balances at stage  $j$ , which depend on the vapor, liquid, and feed flow rate; the molar enthalpy ( $H$ ); the heat duty added at each stage ( $Q$ ) are expressed as:

$$\mathbf{E}_j = L_j H_j^L + V_j H_j^V - L_{j-1} H_{j-1}^L - V_{j+1} H_{j+1}^V - F_j^L H_j^{LF} - F_j^V H_j^{VF} + Q_j = 0 \quad (6.15)$$

The summation equations for both liquid and vapor phase, which are functions of the molar fraction in the vapor ( $y_{i,j}$ ) and the liquid ( $x_{i,j}$ ) phases, are expressed as:

$$\mathbf{S}_j^L = \sum_{i=1}^C x_{i,j} - 1 = 0, \quad \mathbf{S}_j^V = \sum_{i=1}^C y_{i,j} - 1 = 0 \quad (6.16)$$

Vapor-liquid equilibrium still holds, but equilibrium stage model replaces the interfacial composition with the composition in the bulk phase of the liquid ( $x_{i,j}$ ) and the vapor ( $y_{i,j}$ ) phases:

$$\mathbf{Q}_{i,j} = K_{i,j} x_{i,j} - y_{i,j} = 0 \quad (6.17)$$

The expressions for the equilibrium constants ( $K_{j,k}$ ) of the instantaneous reactions are a function of the temperature in the stage ( $T_j$ ) and are considered in the rate-based, equilibrium, and chemistry models:

$$\ln K_{j,k}^{eq} = \frac{A_k}{T_j} + \mathbf{B}_k \ln T_j + \mathbf{C}_k T_j + \mathbf{D}_k = \sum_{i=1}^C v'_{i,k} \ln a_{i,j} \quad (k = 1, NRE) \quad (6.18)$$

The reaction rates ( $r_{j,k}$ ) of the rate-controlled reactions are a function of temperature, energy of activation ( $E_k$ ), the ideal gas constant ( $R$ ), the mass fraction in the liquid, the activity coefficient ( $\gamma_{i,j}$ ) and the liquid phase activity ( $a_{i,k}$ ), but are considered in only the rate-based model:

$$r_{j,k} = k T_j^n \exp\left(-\frac{E_{a,k}}{RT_j}\right) \prod_{i=1}^C (x_{i,j} \gamma_{i,j})^{a_{i,k}} \quad (k = 1, NRC) \quad (6.19)$$

The values for equilibrium constants and reaction rates are listed in Table S3 and Table S4 of SI Section S5 respectively.



The CO<sub>2</sub>-NH<sub>3</sub> system has mixed polar and nonpolar components in its vapor phase. To account for this and the non-ideality of our system, we estimate fugacity, activity, and density of the system using the methods listed in Table S5 in SI Section S6 on parameter estimation for the mathematical model. Table S5 details the parameter estimation methods used in the current work, while Table 6.2 details the input parameters for the simulation study of the DSR. We allow the draw solution entering the column to range from 0.5M-1.5M (CO<sub>2</sub>-based).

*Table 6.2 Specifications of the DSR system in this case study*

<b>Specifications</b>	<b>Values in the Case Study</b>
<b>Dilute DS Column Feed, m<sup>3</sup>/hr</b>	18
<b>C:N Ratio of Draw Solution</b>	0.714
<b>Column Pressure, atm</b>	1
<b>Feed Concentration, M</b>	1
<b>Target NH<sub>3</sub> Content in Product Water</b>	<1 ppm

#### *6.3.4 Mathematical Model of FO Membrane Separation System*

The composition of the dilute draw solution has a significant influence on the DSR separation efficiency and heat consumption. We relate this composition to the upstream membrane process by adapting a finite differences method model of a flat sheet plate-and-frame FO membrane module detailed in SI Sections S7 on the FO membrane model and S8 on the draw and feed solution modeling with parameters for the FO membrane listed in Table S6.<sup>24,25</sup> This model is based on the following assumptions:

- (1) The membrane separation system operates isothermally at 298.15 K.<sup>9</sup>
- (2) The feedwater is similar in composition to seawater (35 g/L) and all existing salts are in the form of NaCl.

(3) The feedwater and the draw solution flow into an FO membrane module in countercurrent mode.

(4) The effective driving force ( $J_w$ ) is reduced due to the presence of dilutive internal concentration polarization and concentrative external concentration polarization.<sup>26</sup> Accounting for this, water flux can be expressed as a function of membrane water permeability ( $A$ ), osmotic pressure ( $\pi_{D,b}$ ), solute resistivity ( $K_m$ ), and mass transport coefficient ( $\kappa$ ):

$$J_w = A \left[ \pi_{D,b} \exp(-J_w K_m) - \pi_{F,b} \exp\left(\frac{J_w}{\kappa}\right) \right] \quad (6.20)$$

The solute resistivity within the porous support layer of the membrane is defined as:

$$K_m = \frac{S}{D} = \frac{t\tau}{D\varepsilon} \quad (6.21)$$

where  $t$ ,  $\tau$ , and  $\varepsilon$  express the thickness, tortuosity, and porosity of the support layer, respectively.

The mass transfer coefficient is correlated to the Sherwood number and it is calculated using:

$$\kappa = \frac{Sh}{d_h} D \quad (6.22)$$

where  $D$  and  $d_h$  are diffusion coefficient of the solute and the hydraulic diameter of the flow channel, respectively.

(5) The salt rejection of the membrane is not 100%, so both feed and draw solute are subjected to permeation. The reverse flux of draw solute ( $J_1$ ) and the forward flux of feed solute ( $J_2$ ), respectively, defined by  $J_w$ , the solute permeabilities ( $B_1$  and  $B_2$ ), concentrations ( $C_1$  and  $C_2$ ) and Peclet's number for the feed and draw side streams ( $Pe^F$  and  $Pe^D$ ) are given by:<sup>27</sup>

$$J_1 = \frac{J_w B_1 (c_1^{F,b} \exp(Pe_1^F + Pe_1^D) - c_1^{D,b})}{(B_1 \exp(Pe_1^F) + J_w) \exp(Pe_1^D) - B_1} \quad (6.23)$$

$$J_2 = \frac{J_w B_2 (c_2^{F,b} \exp(Pe_2^F + Pe_2^D) - c_2^{D,b})}{(B_2 \exp(Pe_2^F) + J_w) \exp(Pe_2^D) - B_2} \quad (6.24)$$

As illustrated in Figure 6.2, the FO membrane has been discretized into finite elements within which we assume constant properties such as velocity, concentration, and diffusivity. The partial differential equations of mass balances describing the velocity and concentration profiles are reformulated using the finite differences method, as described in Equations 25-28.<sup>24</sup> The algorithms for calculating water flux ( $J_w$ ) based on water velocity ( $u_F$  and  $u_D$ ) and solute flux ( $J_s$ ) based on concentration changes ( $C_F$  and  $C_D$ ) using a finite element method of elements with heights  $H$  can be found in the Supporting Information Section S9 and Figure S1.

$$u_{F,i} = u_{F,i-1} - \frac{J_{w,i}\Delta x}{0.5H_o} \quad (6.25)$$

$$C_{F,i} = \frac{C_{F,i-1}u_{F,i-1} - J_{s,i}\left(\frac{\Delta x}{0.5H_o}\right)}{u_{F,i}} \quad (6.26)$$

$$u_{D,i-1} = u_{D,i} + \frac{J_{w,i}\Delta x}{0.5H_i} \quad (6.27)$$

$$C_{D,i-1} = \frac{C_{D,i}u_{D,i} + J_{s,i}\left(\frac{\Delta x}{0.5H_i}\right)}{u_{D,i-1}} \quad (6.28)$$

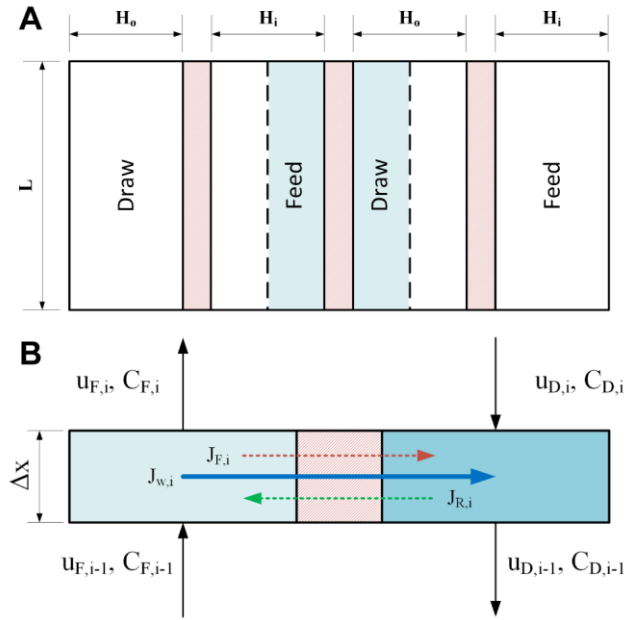


Figure 6.2. A) Schematic diagram of plate-and-frame module; B) A finite element of a counter-current FO membrane module.

### 6.3.5 Comprehensive Model of FO Desalination System

The comprehensive formulation of the FO process using power plant waste heat includes the membrane separation system, the DSR system, and the heat recovery and transport system. The dilute draw solution coming from the draw side of the membrane module enters as the feed to the DSR system, while the heat recovery and transport system provides the thermal energy required to strip  $\text{CO}_2$  and  $\text{NH}_3$  from the dilute draw solution. Figure 6.3 shows the interconnected networks of the input and output variables for each process. The size specification and operation of DSR systems are dependent upon several parameters. Table 6.3 summarizes the most important parameters for DSR system operation.

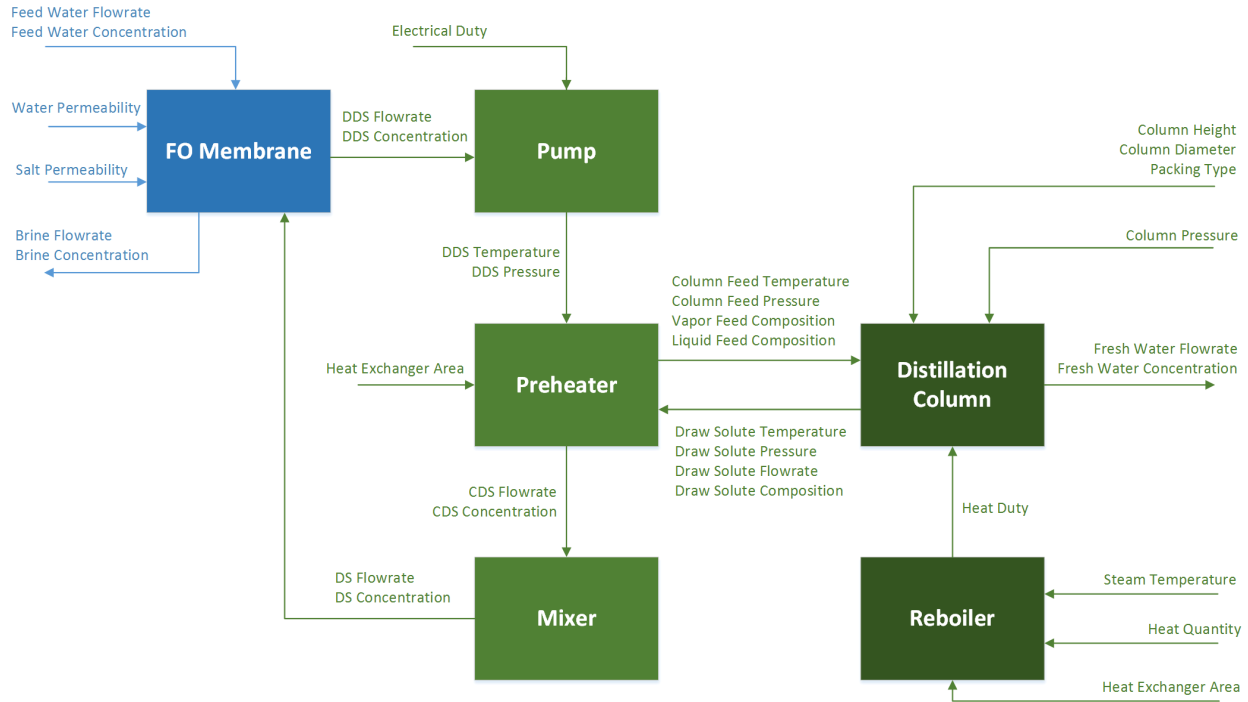


Figure 6.3 Input and output of parameter networks connecting the process equipment.

Table 6.3 Parameters important for DSR systems design and corresponding design aspects.

Parameter	Design Aspects
<b>Height (Stage number)</b>	Height, which refers to the height of structured packing in the column, is determined by height equivalent to theoretical plate (HETP) and the actual stage number in the column.
<b>Pressure</b>	The top and sump temperature requirements decrease as the column pressure drops below atmospheric pressure, thereby enabling the use of a broader range of power plant waste heat quality. We vary the design pressure from 0.1 atm to 1 atm.
<b>Feed Concentration of Diluted Draw Solution</b>	Feed concentration of dilute draw solution is a product of the membrane separation efficiency, but impacts the separation efficiency of the column. A typical range for feed of the DSR system is 0.5-1.5 M.
<b>C:N Ratio</b>	Higher ammonia concentration in draw solute enhances the solubility of CO <sub>2</sub> , increasing the driving force for the FO membrane process. However, excess of either CO <sub>2</sub> or NH <sub>3</sub> can significantly influence the configuration of the process, making the existence of an absorber necessary. A proposed range for C:N ratio is within 0.3-0.71.

### 6.3.6 Notes on Numerical Solution

We built a mathematical model in MATLAB and solved the nonlinear system with a trust-region-dogleg algorithm using MATLAB's `fsolve` function. As some unknowns (e.g., concentrations of  $\text{H}_3\text{O}^+$  and  $\text{OH}^-$ ) are extremely small, the nonlinear problem may be ill-conditioned. To obtain robust convergence, we can either scale the problem or perform transformations on select variables. Here, we adopt the second approach by log transforming very small concentrations to improve the convergence. To further improve the probability of convergence, we use initial guess obtained from the previous simulation in ASPEN Plus for all unknowns.

### 6.3.7 FO Treatment Capacity of US Power Plants by Fuel Cycle and Size

Elsewhere,<sup>14</sup> we estimate the quality and quantity of the waste heat from US coal, natural gas combined cycle (NGCC), natural gas steam turbine (NGST), and natural gas gas turbine (NGGT) plants. These estimates account for both the fuel cycle and the size of the plant. We use these previously reported estimates of heat quality as constraints in the FO model for each fuel cycle. We then arrive at an upper bound of the water treatment capacity for each fuel cycle by dividing the total heat quantity by the normalized heat duty obtained from the FO model.

## 6.4 Results and Discussion

### 6.4.1 Comparison of $\text{CO}_2\text{-NH}_3\text{-H}_2\text{O}$ Separation Models

Past DSR models have relied upon chemistry models to predict the temperature and heat duty of FO separations. The chemistry model omits consideration of hydrodynamics, heat and mass transport limitations, and reaction kinetics, which are imperative in the comprehensive evaluation of DSR systems with finite residence times. Here, we use ASPEN to compare this

chemistry model to equilibrium stage and non-equilibrium (rate-based) approaches in evaluating distillation, steam stripping, and air stripping DSR systems under ambient pressure.

The chemistry, equilibrium stage, and rate-based models estimate similar heat duties for distillation and steam stripping processes at ambient pressures (Figure 6.4 A). The models diverge in the air stripping process, however, where the chemistry model significantly under-predicts the normalized heat duty. This is due to limited reaction rates at low temperature, which prevent the system from reaching equilibrium within the residence time in the stage.

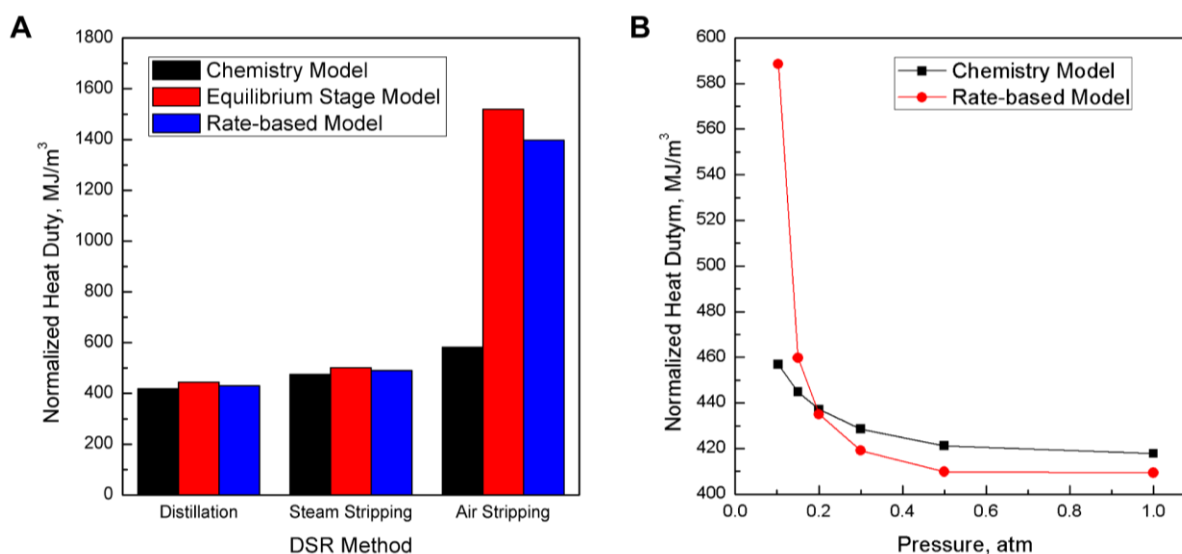


Figure 6.4. Comparison of the predicted heat duty of the draw solute regeneration process for three different  $\text{CO}_2\text{-NH}_3\text{-H}_2\text{O}$  separation models. A) Comparison of the chemistry model, the equilibrium model, and the comprehensive model for the three DSR methods at ambient pressure. Possible heat integration savings are subtracted from the corresponding DSR method. Heat integration does not confer any additional energy savings in air stripping because the temperature difference between the inlet cold dilute draw solution and vapor stream from the top of the column is low; B) Comparison of equilibrium model and comprehensive model under the distillation DSR configuration for different operating pressures.

Additional discrepancies between the chemistry, equilibrium-stage, and rate-based model arise in sub-atmospheric conditions. Figure 6.4B plots the heat consumption per cubic meter of product water against the operating pressure in a distillation column. We observe significant deviation between the chemistry model and the equilibrium and rate-based models at sub-atmospheric pressure, suggesting that it is inappropriate to ignore reaction kinetics when modeling DSR processes for FO systems. As we discuss below, this deviation may significantly skew the results for DSR systems that use waste heat below 60 °C, where sub-atmospheric column conditions are required to maintain the driving force in accordance with Henry's Law.

Modeling normalized heat duty of the DSR process over the set of column pressures and heat temperatures relevant to waste-heat driven distillation also suggests that the equilibrium stage model is a reasonable approximation for the rate-based model. SI Section S12 and Tables S8-S10 compare mass transfer rates and reaction rates at different pressures, and demonstrate that reaction rate dominates under most conditions. Given the significantly lower computational requirements, subsequent calculations are performed using the equilibrium stage model (Table S7).

Finally, at atmospheric pressure the modeled electricity consumption for DSR systems is 0.02 kWh/m<sup>3</sup> (see SI Section S11 for full calculations of electricity consumption in the DSR process and the membrane separation process), or less than 0.5% of the total process energy demand in units of equivalent work. Operating the distillation column at sub-atmospheric pressures would significantly increase electricity consumption, though we do not explicitly address this case in the remainder of this work.



#### 6.4.2 Comparison of DSR Methods

We select distillation as the preferred DSR method. Air stripping had a higher normalized heat duty ( $\text{MJ}/\text{m}^3$ ) and required a significantly larger column to meet the design specifications for  $\text{NH}_3$  in the product water (Table 6.4) than distillation or steam stripping processes. Steam stripping, although comparable to distillation in terms of normalized heat duty, requires an additional compressor that would add to the system cost. Therefore, we selected distillation as the preferred DSR method for subsequent evaluation and mathematical modeling.

*Table 6.4 Comparison of Distillation, Steam Stripping, and Air Stripping (DDS Flowrate =  $18 \text{ m}^3/\text{hr}$ )*

	<i>Distillation</i>		<i>Steam Stripping</i>	<i>Air Stripping</i>
<b>Model Type</b>	ASPEN	Mathematical	ASPEN	ASPEN
<b>Stage Number</b>	25	25	25	80
<b>Column Diameter, m</b>	1.25	1.25	1.25	4.25
<b>Top Temperature, °C</b>	86.4	87.0	86.4	36.8
<b>Sump Temperature, °C</b>	100.6	100.4	100.6	37.7
<b>Normalized Heat Duty, <math>\text{MJ}/\text{m}^3</math></b>	409.37	395.6	405.59	> 680.9

#### 6.4.3 Model Comparisons Between ASPEN and Mathematical Model

Table 6.4 demonstrates that the equilibrium stage mathematical model we developed closely matches the rate-based modeling solutions determined by the ASPEN Plus model. Solving a multi-stage unit with the mathematical model is more time-consuming than solving it in ASPEN Plus, but doing so allows for more thorough sensitivity analysis and process design.

#### 6.4.4 Description of Full Process Model

The complete FO process model, including the membrane system, the heat recovery system, and the distillation-based DSR system, is depicted in Figure 6.3. In this work we perform a sensitivity analysis to clarify the contribution of each key parameter to the overall energy

consumption per cubic meter of clean water produced. Parameters varied in this work are reported in Table 6.3.

**Pressure.** The most important parameter in determining the energy consumption, measured in MJ/m<sup>3</sup> of product water, is the pressure in the column. As pressure decreases, the lower sump temperature enables the integration of a wider range of heat quality (Figure 6.5A). However, a lower pressure also leads to a higher heat duty per unit volume of clean water produced, as discussed in the comparison of alternative DSR processes.

**Column height.** The column size also influences the energy consumption of the process. We analyze the sensitivity of heat duty to the target ammonia concentration in product water for columns of three different heights (Figure 6.5B). We find that, given constraints of <1 ppm ammonia in the product water, taller columns consume less energy.

**Dilute draw solution concentration.** The dilute draw solution concentration is the concentration of carbonate species in the draw solution after it leaves the membrane unit and before it enters the DSR process. Dilute draw solution concentration fed to the column is an indicator of FO membrane performance. Either a larger membrane area or higher water permeability can result in a more dilute draw solution. As shown in Figure 6.5C, the heat duty of the FO process is lower when the diluted draw solution concentration is lower, which implies a trade-off between the membrane process and the DSR process.

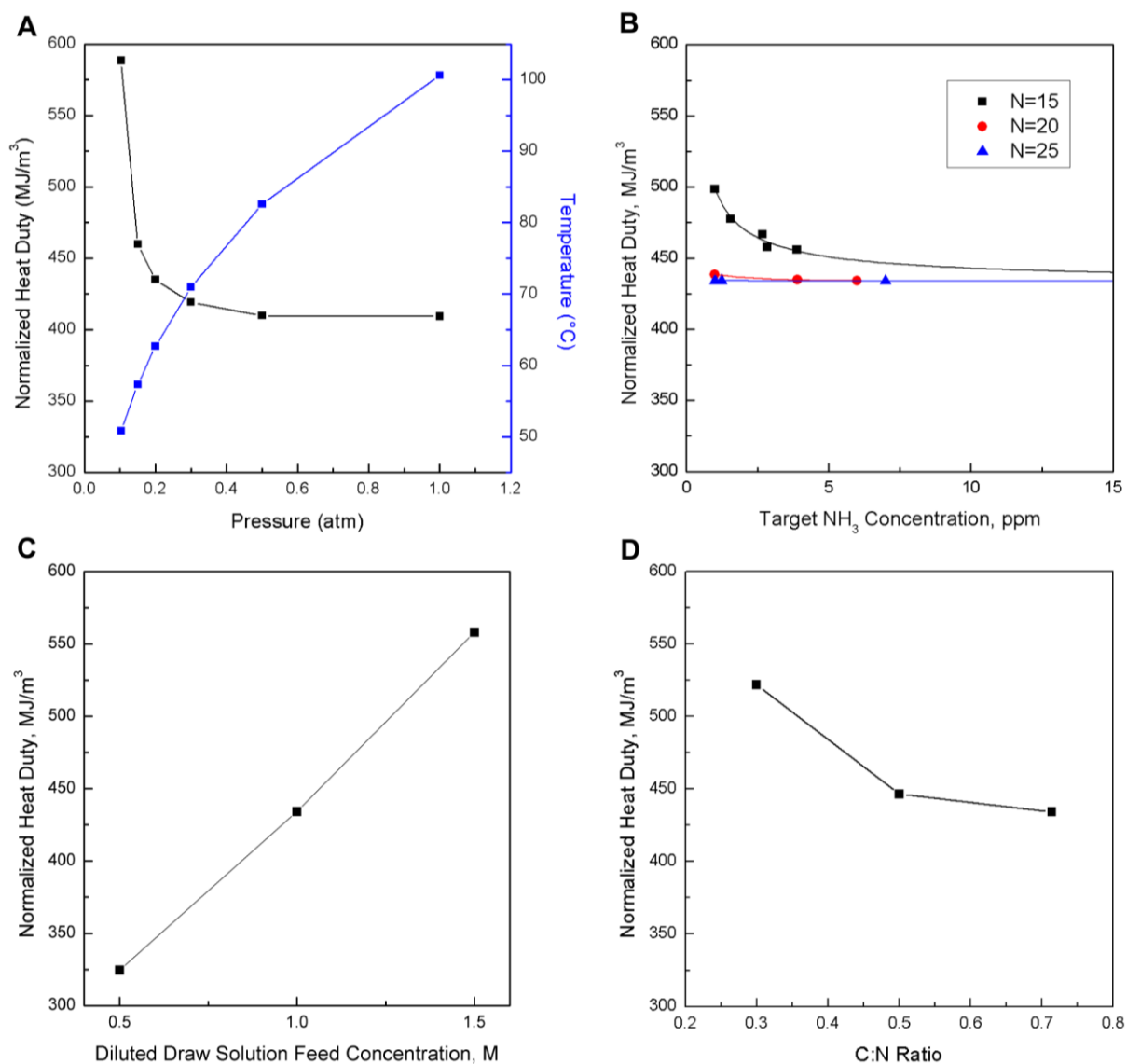


Figure 6.5. Parametric analyses of heat duty of the FO process under various operating parameters. A) Parametric analysis of distillation column operating pressure on energy consumption for 1 M column feed, target NH<sub>3</sub> concentration=1 ppm, stage number=25, C:N ratio=0.714; B) Parametric analysis of target water purity for columns of different sizes on energy consumption for 1 M column feed, pressure=1 atm, C:N ratio=0.714; C) Parametric analysis of dilute draw solution feed on energy consumption for a 25-stage column, pressure=1 atm, target NH<sub>3</sub> concentration=1 ppm, C:N ratio=0.714; D) Parametric analysis of C:N ratio of

*draw solution for the membrane process on energy consumption for a 25-stage column, pressure=1 atm, target  $NH_3$  concentration=1 ppm.*

**C:N ratio.** The C:N ratio of the draw solution influences the osmotic pressure, thus impacting the separation efficiency of the membrane module. On the one hand, more ammonia in the draw solution enhances the solubility of carbon dioxide in water by the association of ammonia with bicarbonate, carbonate, and carbamate species, the latter two of which can hold multiple ammonia ions in solution, and increases the driving force of osmotically driven processes. On the other hand, due to the high solubility of ammonia, additional energy is consumed by stripping the excess ammonia out of the dilute draw solution and the optimal C:N ratio is around 0.714 (Figure 6.5D).

Together these sensitivity analyses suggest that isolated optimization of the DSR process is insufficient. To simultaneously minimize the heat duty and cost of the FO process requires concurrent modeling of the membrane system, the heat capture and transport system, and the DSR system. For instance, we can minimize the energy consumption in DSR process by reducing the concentration of dilute draw solution feed. However, to further dilute the draw solution, a membrane with higher permeability or larger membrane area should be used, which is sub-optimal for a membrane process.

#### *6.4.5 Modeling the FO Water Treatment Process to Minimize Heat Duty*

We use our estimates of normalized heat duty given the quality of potentially recoverable waste heat available in the flue gas streams at US electric power generation facilities. Since normalized heat duty is a monotonic function of the decision variables and in this study there are no constraints on the membrane processes (i.e. maximum membrane area, water recovery rate,

maximum feed stream flow rate), we choose each optimal condition of the decision variable to obtain the minimum normalized heat duty. We do so for coal, NGCC, NGST, and NGGT fuel cycles. The minimum normalized heat duty for each fuel cycle is reported in Table 6.5. There is little variation in the normalized heat duties reported as each fuel cycle generates heat of near identical qualities. This study evaluates only the technical feasibility of performing FO water treatment driven by power plant waste heat. As a result, we maximize water production capacity given the available thermal energy at US power plants, but do not minimize costs, CO<sub>2</sub> emissions, or any other metric relevant to the systems-level performance of the FO water treatment unit.

*Table 6.5 Minimum normalized heat duty of each fuel cycle*

<b>Fuel Cycle</b>	<b>Mean Temperature Quality, °C</b>	<b>Minimized Normalized Heat Duty, MJ/m<sup>3</sup></b>
Coal	119	409.37
NGCC	89	409.8
NGST	119	409.37
NGGT	130	409.37

#### *6.4.6 FO Treatment Capacity of US Power Plants by Fuel Cycle and Size*

We estimate the water treatment capacity of various fuel cycles by dividing waste heat availability by the normalized heat duty obtained from the FO model for each fuel cycle. Resulting water production rates for US power plants by fuel cycle are reported in Figure 6.6. Figure 6.6A depicts the amount of water that can be produced using residual heat driven FO normalized per MWh of electricity generated, with the spread a function of the efficiency of each existing US power plant. Plant efficiency is a function of system design, manufacturer, age, and cooling type, and environmental conditions among other variables.<sup>14</sup> Coal, NGCC, and NGST

fuel cycles have waste heat driven FO water treatment capacities between 0.1 and 10 m<sup>3</sup>/MWh of electricity generated. NGGT systems have a median water treatment capacity of 14 m<sup>3</sup>/MWh, with the range extending from 2 to over 1,000 m<sup>3</sup>/MWh. NGGT systems produce more per MWh because the absence of a steam cycle means that the residual heat content per MWh of their exhaust heat is higher.

Figure 6.6B plots the distribution of annual water treatment capacity at US fossil-fuel power plants. The larger underlying distribution reflects the variation in size and capacity factor across US power plants.<sup>14</sup> If all of the residual heat discharged in the exhaust streams of US plants was allocated for FO water treatment, a theoretical maximum of 1.9 billion m<sup>3</sup>/year of water could be produced. In reality, capital and operational costs, the low size and capacity factors of many plants, and demand for new in-plant water treatment infrastructure are likely to significantly curtail this allocation of waste heat for FO water treatment. NGGT systems contribute 1.2 billion m<sup>3</sup> of this potential water production (63%) because they are large (mean of 1.5 million m<sup>3</sup>) and numerous. Coal systems are larger than NGGT on average (mean of 1.9 million m<sup>3</sup>), but there are fewer of them, and they contribute 500 million m<sup>3</sup> to this total (25%). The remaining production comes from NGCC and NGST (180 and 40 million m<sup>3</sup>, respectively) as they have smaller average production capacities (350,000 and 70,000 m<sup>3</sup>, respectively) compared to coal and NGGT systems.

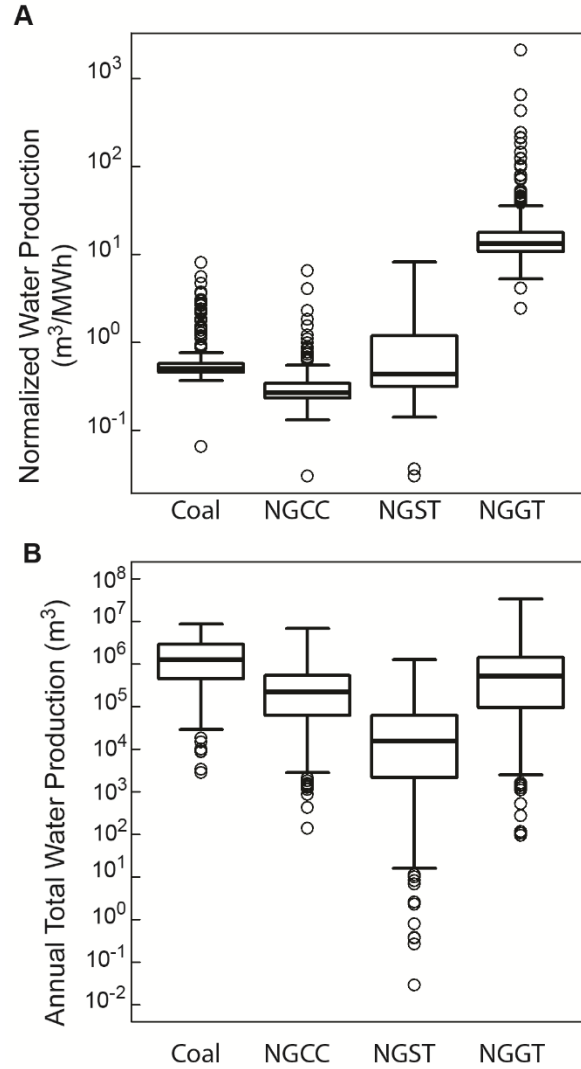


Figure 6.6. Upper bound estimates of the residual heat driven FO water treatment capacity of US power plants in terms of (A)  $\text{m}^3$  of water treatment capacity per MWh of electricity generated and (B) average annual production per plant.

#### 6.4.7 Potential Applications of FO Treatment Capacity at US Power Plants

On average, US power generation facilities withdraw approximately  $87 \text{ m}^3$  of water per MWh of net generation.<sup>28</sup> However, 93% of these water withdrawals are for cooling water, which has lower water quality requirements and is therefore unlikely to be treated via a membrane-based

process. A far more likely candidate for FO treatment is boiler feed water (BFW) make-up or flue gas desulfurization (FGD) water, which collectively accounts for approximately the remaining 7% of water withdrawals,<sup>29</sup> or 0.28, 0.25, and 0.008 m<sup>3</sup>/MWh of water treatment needs at subcritical coal, supercritical coal, and NGCC systems, respectively.<sup>29</sup> While the TDS of this feedwater varies considerably across power plants, the average water quality is approximately 30,000 ppm TDS. Using RO to treat this water would consume approximately 2.5 kWh/m<sup>3</sup>, or 0.7, 0.6, and 0.02 kWh per MWh of generation at subcritical coal, supercritical coal, and NGCC systems. As only about 1.0% of the energy consumed by FO processes is in the form of electricity (for pumping, etc.), adoption of FO has significant potential to reduce the parasitic losses associated with water treatment at power plants.

## **6.5 Conclusions**

This work provides an upper bound on the quantity of water that can be treated via FO processes using only waste heat available at US electric power generation facilities. We demonstrate that distillation is preferable to both steam and air stripping due to process issues with steam purity in steam stripping and the inefficiency of pre-heating in the case of air stripping processes. We also demonstrate that failing to consider reaction kinetics when evaluating the DSR process leads to significant underestimation of heat duty for sub-atmospheric DSR conditions, such as those required for low-temperature heat driven DSR systems. Omission of hydrodynamics, mass transport resistance, and heat transport resistance in the equilibrium model leads to modest deviations of less than 2% from the rate-based model, sufficient for the first order estimates of normalized heat duty responded here. We perform sensitivity analysis to ascertain the influence of column pressure, the extent of draw solution recovery, draw solution concentration, and draw solution chemistry on the energy consumption and performance of the FO system. And, finally,



we demonstrate that waste heat driven FO water treatment processes are capable of meeting the boiler make-up water treatment demands at US power plants.

## 6.6 Acknowledgements

This work was supported by the National Science Foundation (SEES-1215845) and Department of Energy (DE-FE0024008). DG also acknowledges support from The Pittsburgh Chapter of ARCS Foundation (Achievement Rewards for College Scientists), the Steinbrenner Graduate Fellowship, and the Phillips & Huang Family Foundation Fellowship.

## 6.7 Nomenclature

### Symbols

$A$	Water permeability [m/(s·Pa)]
$A, B, C, D$	Equilibrium constant coefficients
$a$	Liquid phase activity
$a_e$	Effective interfacial area [m <sup>2</sup> /m <sup>3</sup> ]
$B$	Solute permeability [m/s]
$C$	Number of species
$c$	Concentration [M]
$D$	Diffusivity [m <sup>2</sup> /s]
$d_h$	Hydraulic diameter [m]
<b>E</b>	Energy balances
$E_a$	Activation energy, [kJ/mol]
$F$	Feed flowrate, [mol/s]
<b>H</b>	Hydraulic equations

$H$	Molar enthalpy [kJ/mol]
$H_i$	Height of the rectangle channel at draw side [m]
$H_o$	Height of the rectangle channel at feed side [m]
$J_s$	Solute flux [mol/(m <sup>2</sup> .s)]
$J_w$	Water flux [m <sup>3</sup> /(m <sup>2</sup> .s)]
$J_1$	Reverse flux of draw solute [mol/(m <sup>2</sup> .s)]
$J_2$	Forward flux of feed solute [mol/(m <sup>2</sup> .s)]
$K$	Vapor-liquid equilibrium constant
$K^{eq}$	Chemical equilibrium constant
$K_m$	Solute resistivity [s/m]
$k$	Pre-exponential factor
$L$	Liquid flowrate [mol/s]
<b>M</b>	Mass balances
$N$	Molar flux [mol/(m <sup>2</sup> .s)]
$NRC$	Number of controlled reactions
$NRE$	Number of instantaneous reactions
$P$	Pressure [atm]
$Pe$	Peclet Number
<b>Q</b>	Liquid-vapor equilibrium equations
$Q$	Heat duty [kW]
<b>R</b>	Rate equations
$R$	Rate of mass transport
$\bar{R}$	Ideal gas constant

$r$	Reaction rate [mol/(m <sup>3</sup> .s)]
<b>S</b>	Summation equations
$S$	Structural parameter of FO membrane [m]
$Sh$	Sherwood Number
$t$	Thickness of FO membrane [m]
$u$	Flow velocity [m/s]
$V$	Vapor flowrate [mol/s]
$V_{LH}$	Liquid holdup [m <sup>3</sup> ]
$V_s$	Volume of column per stage [m <sup>3</sup> ]
$x$	Liquid species mole fraction
$y$	

### **Greek symbols**

$\gamma$	Activity coefficient
$\varepsilon$	Porosity of FO membrane
$\epsilon$	Interfacial energy
$\kappa$	Mass transport coefficient, m/s
$\nu$	Stoichiometric coefficient
$\pi$	
$\tau$	Tortuosity of FO membrane
$\chi$	Reaction extent [mol/(m <sup>3</sup> .s)]

### **Subscript**

$b$	At bulk solution
-----	------------------

## 6.8 References

1. US Environmental Protection Agency. Proposed Effluent Guidelines for the Steam Electric Power Generating Category.
2. Cath, T.; Childress, A.; Elimelech, M. Forward osmosis: principles, applications, and recent developments. *J. Memb. Sci.* **2006**, *281* (1–2), 70–87.
3. Chung, T.-S.; Zhang, S.; Wang, K. Y.; Su, J.; Ling, M. M. Forward osmosis processes: Yesterday, today and tomorrow. *Desalination* **2012**, *287*, 78–81.
4. Zhao, S.; Zou, L.; Tang, C. Y.; Mulcahy, D. Recent developments in forward osmosis: Opportunities and challenges. *J. Memb. Sci.* **2012**, *396*, 1–21.
5. McCutcheon, J.; McGinnis, R.; Elimelech, M. A novel ammonia—carbon dioxide forward (direct) osmosis desalination process. *Desalination* **2005**, *174* (1), 1–11.
6. McGinnis, R. L.; Elimelech, M. Global Challenges in Energy and Water Supply: The Promise of Engineered Osmosis. *Environ. Sci. Technol.* **2008**, *42* (23), 8625–8629.
7. Kim, T.; Kim, Y.; Yun, C.; Jang, H.; Kim, W.; Park, S. Systematic approach for draw solute selection and optimal system design for forward osmosis desalination. *Desalination* **2012**, *284*, 253–260.
8. US Energy Administration. *Annual Energy Review 2009*; Washington, D.C., 2010.
9. McGinnis, R. L.; Elimelech, M. Energy requirements of ammonia—carbon dioxide forward osmosis desalination. *Desalination* **2007**, *207* (1–3), 370–382.
10. McGinnis, R. L.; Hancock, N. T.; Nowosielski-Slepowron, M. S.; McGurgan, G. D. Pilot demonstration of the NH<sub>3</sub>/CO<sub>2</sub> forward osmosis desalination process on high salinity brines. *Desalination* **2013**, *312*, 67–74.

11. Kim, Y. C.; Park, S.-J. Experimental study of a 4040 spiral-wound forward-osmosis membrane module. *Environ. Sci. Technol.* **2011**, *45* (18), 7737–7745.
12. Rattner, A.; Garimella, S. Energy harvesting, reuse and upgrade to reduce primary energy usage in the USA. *Energy* **2011**, *36* (10), 6172–6183.
13. Ozalp, N. Utilization of Heat, Power, and Recovered Waste Heat for Industrial Processes in the U.S. Chemical Industry. *J. Energy Resour. Technol.* **2009**, *131* (2), 22401.
14. Gingerich, D. B.; Mauter, M. S. Quantity, Quality, and Availability of Residual Heat from United States Thermal Power Generation. *Environ. Sci. Technol.* **2015**, *49*, 8297–8306.
15. Kim, T.; Park, S.; Yeh, K. Cost-effective design of a draw solution recovery process for forward osmosis desalination. *Desalination* **2013**, *327*, 46–51.
16. Que, H.; Chen, C.-C. Thermodynamic Modeling of the  $\text{NH}_3\text{--CO}_2\text{--H}_2\text{O}$  System with Electrolyte NRTL Model. *Ind. Eng. Chem. Res.* **2011**, *50* (19), 11406–11421.
17. Darde, V.; van Well, W. J. M.; Stenby, E. H.; Thomsen, K. Modeling of Carbon Dioxide Absorption by Aqueous Ammonia Solutions Using the Extended UNIQUAC Model. *Ind. Eng. Chem. Res.* **2010**, *49* (24), 12663–12674.
18. Niu, Z.; Guo, Y.; Zeng, Q.; Lin, W. Experimental Studies and Rate-Based Process Simulations of  $\text{CO}_2$  Absorption with Aqueous Ammonia Solutions. *Ind. Eng. Chem. Res.* **2012**, *51* (14), 5309–5319.
19. Niu, Z.; Guo, Y.; Zeng, Q.; Lin, W. A novel process for capturing carbon dioxide using aqueous ammonia. *Fuel Process. Technol.* **2013**, *108*, 154–162.
20. Zhang, M.; Guo, Y. A comprehensive model for regeneration process of  $\text{CO}_2$  capture

- using aqueous ammonia solution. *Int. J. Greenh. Gas Control* **2014**, 29, 22–34.
21. Edwards, T. J.; Maurer, G.; Newman, J.; Prausnitz, J. M. Vapor-liquid equilibria in multicomponent aqueous solutions of volatile weak electrolytes. *AIChE J.* **1978**, 24 (6), 966–976.
  22. Brewer, L. *Flue Gas Desulfurization*; Hudson, J. L., Rochelle, G. T., Eds.; ACS Symposium Series; American Chemical Society: Washington, D.C., 1982; Vol. 188.
  23. Soave, G. Application of a Cubic Equation of State to Vapor-liquid Equilibria of Systems Containing Polar Compounds. *Inst. Chem. Eng. Symp. Ser.* **1979**, 56 (1.2), 1–1.
  24. Pitzer, K. S. Thermodynamics of electrolytes. I. Theoretical basis and general equations. *J. Phys. Chem.* **1973**, 77 (2), 268–277.
  25. Pitzer, K. S.; Mayorga, G. Thermodynamics of electrolytes. II. Activity and osmotic coefficients for strong electrolytes with one or both ions univalent. *J. Phys. Chem.* **1973**, 77 (19), 2300–2308.
  26. Zaytsev, I. D.; Aseyev, G. G. *Properties of Aqueous Solutions of Electrolytes*; CRC Press, 1992.
  27. Gu, B.; Kim, D. Y.; Kim, J. H.; Yang, D. R. Mathematical model of flat sheet membrane modules for FO process: Plate-and-frame module and spiral-wound module. *J. Memb. Sci.* **2011**, 379 (1–2), 403–415.
  28. Jung, D. H.; Lee, J.; Kim, D. Y.; Lee, Y. G.; Park, M.; Lee, S.; Yang, D. R.; Kim, J. H. Simulation of forward osmosis membrane process: Effect of membrane orientation and flow direction of feed and draw solutions. *Desalination* **2011**, 277 (1–3), 83–91.
  29. McCutcheon, J.; Elimelech, M. Influence of concentrative and dilutive internal

- concentration polarization on flux behavior in forward osmosis. *J. Memb. Sci.* **2006**, 284 (1–2), 237–247.
30. Hancock, N. T.; Phillip, W. A.; Elimelech, M.; Cath, T. Y. Bidirectional permeation of electrolytes in osmotically driven membrane processes. *Environ. Sci. Technol.* **2011**, 45 (24), 10642–10651.
31. Badr, L.; Boardman, G.; Bigger, J. Review of Water Use in U.S. Thermoelectric Power Plants. *J. Energy Engineering* **2012**, 138, 246–257.
32. National Energy Technology Laboratory. *Water Requirements for Existing and Emerging Thermoelectric Plant Technologies*; Morgantown, WV, 2009; Vol. 2008.

## **CHAPTER 7: TECHNOECONOMIC ASSESSMENT OF WASTE HEAT DRIVEN FORWARD OSMOSIS SYSTEMS FOR ON-SITE WASTEWATER TREATMENT<sup>6</sup>**

### **7.1 Abstract**

Recently promulgated effluent limitation guidelines will require power generators to treat their flue gas desulfurization (FGD) and gasification wastewaters. Forward osmosis (FO) is an emerging water treatment technology capable of using low-temperature waste heat from power plants to treat water in a cost-effective manner. In this work, we perform a techno-economic assessment of FO and crystallization to achieve zero liquid discharge of FGD and gasification wastewater. We build an optimization framework for the use of waste heat driven FO, and we apply this model to minimize the cost of FO and crystallization systems for treating wastewater at four different power plants. Waste heat driven FO and crystallization treats FGD wastewater at a cost of \$2.01-\$2.02/m<sup>3</sup> and gasification wastewater at a cost of \$2.33/m<sup>3</sup>, excluding pre-treatment, labor, and installation costs. This cost for waste heat driven FO and crystallization is cheaper than the EPA's best available technology for treating these wastewaters, mechanical vapor recompression and crystallization. This conclusion is robust over a range of flows and wastewater concentrations, indicating the suitability of FO for treating wastewater from coal-fired and gasification power plants.

### **7.2 Introduction**

Environmental regulations continue to drive reductions in air and water emissions from the electricity sector. In order to comply with these standards, power plants are installing

---

<sup>6</sup> This chapter is based on a manuscript co-authored with Prof. Meagan Mauter and Tim Bartholomew that is currently in preparation for submission to Sustainable Chemistry & Engineering. T.V.B. developed the optimization model. D.B.G. applied this optimization model to the FGD and gasification wastewater cases and wrote the manuscript.



controls for carbon capture<sup>1-4</sup> and criteria<sup>5-10</sup> and hazardous<sup>11-12</sup> air pollutants. In addition, the recently promulgated Effluent Limitation Guidelines<sup>13</sup> (ELGs) will require installation of additional wastewater control technologies to reduce emissions of lead, arsenic, selenium, mercury, and other aqueous pollutants.<sup>14-16</sup>

One technology being considered for compliance with the ELGs is forward osmosis (FO).<sup>17-21</sup> Forward osmosis is a two-step process. In the first step, a feed stream is separated from a concentrated draw stream by a semi-permeable membrane. Water from the feed stream permeates the membrane, concentrating the feed stream and diluting the draw solution. For certain draw solutes, such as ammonium bicarbonate, the reconcentration of the dilute draw solution is performed in a distillation column driven by low temperature heat.<sup>22-25</sup> This heat can potentially be recovered from the exhaust gas of a power plant<sup>24, 26-27</sup> and our past work has shown that there is enough waste heat to meet flue gas desulfurization (FGD) wastewater and boiler feedwater (BFW) treatment needs at almost all US coal-fired power plants (CFPPs).<sup>26</sup>

Currently, FO is moving from conceptual design and bench-scale systems to pilot scale operation<sup>28-29</sup> for desalination,<sup>28, 30-32</sup> municipal wastewater treatment,<sup>32-37</sup> and treating wastewaters from the oil and gas sector.<sup>38-39</sup> FO is also being piloted in China for FGD wastewater treatment at CFPPs.<sup>40</sup> Past work on optimization of FO systems has focused on reducing the overall energy consumption of the FO process.<sup>21, 26</sup> To date, however, FO systems have used heat from fuel combustion or the low pressure turbines, rather than using recovered waste heat. Furthermore, to the best of our knowledge, there is only one published cost model of FO systems.<sup>41</sup> That model evaluates costs between different draw solutes, rather than analyzing the costs of the entire system. Finally, the lack of a cost model for FO prevents technoeconomic assessment and system optimization for cost minimization.

The objective of this work is to develop a cost model of FO and to assess the technoeconomic feasibility of FO processes for wastewater treatment at steam electric power plants. To do this, we combine a performance model of FO from our previous work<sup>26</sup> with estimates of the quantity and quality of waste heat for several model plants. Our non-linear programming model encompasses five processes within the FO and crystallization system: 1) a FO membrane process, 2) heat exchangers, 3) a distillation column for draw solute regeneration, 4) a stripper for ammonia recovery, and 5) a crystallizer. The NLP model calculates the size of system components, the overall thermal and electrical energy use of the system, and the cost of water treatment on a cubic meter basis. We then use this optimization framework on four case studies for on-site treatment of flue gas desulfurization wastewater at three coal-fired power plants and gasification wastewater at an integrated gasification combined cycle plant. Finally, we compare the combined heat recovery and FO system cost against the EPA's identified best available technology of mechanical vapor recompression and crystallization (MVCC).<sup>42</sup>

### **7.3 Process Description and Modeling**

#### *2.1 FGD and Gasification Wastewater*

We investigate two wastewater streams that are created by air pollution control processes at power plants: FGD wastewater and gasification wastewater. Flue gas desulfurization wastewater is purged from the wet FGD slurry stream. Gasification wastewater is the sour water produced in the process of converting coal into cleaner burning synthetic gas. These waste streams are complex mixtures of organic and inorganic components<sup>13</sup> and have compositions and concentrations that vary within and between plants. The average total dissolved solids for these wastewater streams are 33,300 mg/L for FGD wastewater and 4,400 mg/L for gasification wastewater.<sup>42</sup> We simplify the stream composition for our model by assuming that it is

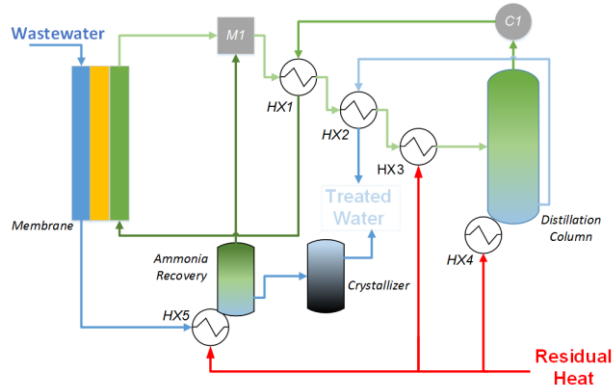


*Figure 7.1 The forward osmosis and crystallization process modeled in this paper. Wastewater enters the FO membrane module. The dilute draw solution exiting the membrane enters a mixer and preheaters before entering the distillation column for the draw solute recovery process. The brine from the membrane enters the ammonia recovery unit and a crystallizer to produce a solid product and treated water.*

composed of an equivalent molar concentration of NaCl. This solution has an osmotic strength roughly 10-15% higher than what would be expected of real world streams. This approximation is justified by the osmotic driving force in FO and the low fouling-propensity of the process.<sup>43</sup>

### 7.3.2 Process Modeling

We create a mathematical model of the FO system described in the introduction with three additional components (Figures 7.1 and 7.2). First, we add two heat exchangers in order to recover heat from the streams leaving the distillation column (HX 1 and 2) and three heat exchangers in order to recover the waste heat from power plant exhaust (HX 3-5).<sup>23, 41</sup> Second, we include an ammonia recovery unit for the concentrated brine stream from the FO process in order to recover the back permeated ammonium bicarbonate. Third, we add a crystallizer after

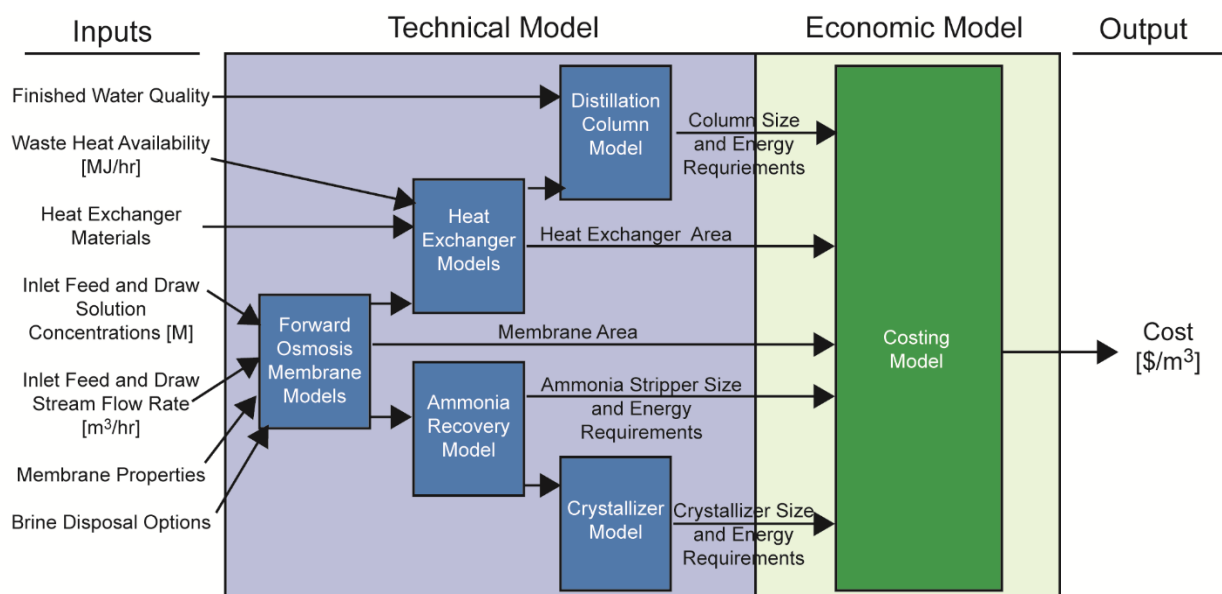


*Figure 7.2 Optimization Model. The optimization uses several inputs about the wastewater, the power plant, and the materials used in the system in order to minimize the system costs on a per cubic meter basis.*

the ammonia recovery process to achieve ZLD and produce a treated water stream for internal recycling.

*Pretreatment.* Modeling the pretreatment needs for FGD and gasification wastewater treatment systems requires a detailed understanding of the composition of the wastewater. Unfortunately, the detail about the wastewater streams required to accurately identify and model pretreatment needs to avoid scaling and fouling is not available. As a result, we do not model pretreatment for FO or MVCC systems for FGD or gasification wastewater systems. This inability to model pretreatment limits our analysis in two ways. First, we do not have the ability to include the impact of pretreatment decision on system costs and so we cannot optimize pretreatment systems. Second, we cannot quantify how the difference in pretreatment

requirements between FO and MVCC will impact the cost competitiveness of FO. Regardless, we expect pretreatment for both systems to include removal of divalent cations with a high scaling propensity.<sup>42</sup> This pretreatment step would lead to a decrease in the osmotic pressure of the FGD wastewater, increasing the recovery in the FO membrane unit and reducing our cost estimates.

*Forward Osmosis Unit.* We develop a discrete element model of the FO membrane module to determine the water recovery and salt rejection. We model the FO membrane as a CTA flat-sheet module operating in counter-current mode. As discussed above, the wastewater feed is assumed to be a sodium chloride solution at the osmotic pressure as a simplification. The deviation between Transport across the membrane is modeled using the flux equations given in Equations 7.1 and 7.2. These equations account for concentration polarization effects, the salt concentration and osmotic pressure gradient across the membrane, membrane properties, and solution properties.

$$J_w = A \left[ \left( \pi_{f,b} \exp\left(\frac{J_w}{k}\right) - \pi_{d,b} \exp(-J_w K) \right) \right] \quad (7.1)$$

$$J_s = B [C_{f,b} - C_{d,b}] \quad (7.2)$$

In Equation 7.1,  $J_w$  is the water flux from the feed to the draw,  $A$  is the pure water permeability coefficient of the membrane, and  $\pi$  is the feed ( $f$ ) and draw ( $d$ ) osmotic pressure in the bulk ( $b$ ) solution,  $k$  is the feed mass transfer coefficient, and  $K$  is the solute resistivity for diffusion in the draw side porous support. In Equation 7.2,  $J_s$  is salt flux across the membrane,  $B$  is the salt permeability coefficient, and  $C$  is the feed ( $f$ ) and draw ( $d$ ) concentrations in the bulk ( $b$ ) solution. We assume that salts that permeate from the feed into the draw solution are non-volatile and therefore remain in the treated water. The ammonium bicarbonate draw solute back permeates into the feed stream. We do not account for fouling of the membrane that would

reduce the flux, an assumption that is reasonable because FO is operated at atmospheric pressure.<sup>43</sup> Furthermore, past work on gypsum scaling for CTA membranes in FO systems has found flux reductions of 10-20%.<sup>44</sup> This is roughly equivalent to the flux increases we expect due to the difference between the osmotic pressure in our simplified NaCl stream and the actual composition stream in our modeled NaCl feed stream and FGD wastewater. The FO membrane model requires five inputs: 1) flow rate of the wastewater at the inlet, 2) concentration of the wastewater at the inlet, 3) draw solution flow rate at the inlet (which we assume to be half of the flow rate of the feed stream flow rate), 4) draw solution concentration at the inlet, 5) and membrane area. This model outputs: 1) brine flow rate at the outlet, 2) brine concentration at the outlet, 3) dilute draw solution flow rate at the outlet, and 4) dilute draw solution concentration at the outlet. More details of the discrete element FO model can be found in Supporting Information (SI) Section 1.1 and Figure S1.

We integrate the discrete element FO model into our optimization framework using a meta-model that relates water recovery and salt rejection to the membrane area. The use of a meta-model significantly reduces the computational intensity of our optimization model, allowing us to approximate the global minimum. The meta-model estimates the water recovery (Equation 7.3) and salt rejection (Equation 7.4) based on a linear regression with fixed inlet flow rates and wastewater.

$$W_{R,FO} = \beta_1 (Area_m)^2 + \beta_2 Area_m + \beta_3 + \epsilon \quad (7.3)$$

Equation 7.3 is the meta-model for water recovery, where  $W_{R,FO}$  is the water recovery in the FO module,  $Area_m$  is the membrane area, and  $\beta_1$ ,  $\beta_2$ , and  $\beta_3$  are regression parameters reported in SI Section 1.1 and Tables S1-S3. We include a quadratic term to account for the marginal changes in the driving force that occurs at higher recoveries (Figure S2).

$$S_{R,FO} = \beta_1 Area_m + \beta_2 + \epsilon \quad (7.4)$$

Equation 7.4 is the meta-model for salt rejection, where  $S_{R,FO}$  is the salt rejection in the FO module, and  $\beta_1$  and  $\beta_2$  are regression parameters reported in SI Section 1.1 and Tables S1-S3.

The regressions these models are based upon have an  $R^2$  value greater than 0.99.

*Heat Recovery.* The dilute draw solution enters several heat exchangers to preheat the draw solution and reduce the energy demand of the distillation column. These heat exchangers also reduce the total energy consumption of the system through heat integration and recovering thermal energy in the treated water stream that would otherwise be lost to the environment.

These preheaters raise the temperature of the dilute draw solution from 50 °C to 100 °C.

We use Equations 7.5 and 7.6 as a basic model to determine stream temperatures, size, and heat duty in the stainless steel, shell and tube heat exchangers associated with preheating the dilute draw solution. We assume a fixed specific heat capacity of 4.18 kJ/kg·°C for the liquid streams in the heat exchanger. We do not account for fouling in the heat exchanger that would reduce its performance. Application of these models to an actual system would need to account for heat exchanger fouling. The heat duty in a heat exchanger,  $Q_{ex}$ ; is a function of the overall heat transfer coefficient,  $U_{ex}$ ; Chen's temperature difference approximation,  $\Delta T_{chen}$ , (calculated using Equation 7.5); and surface area of the heat exchanger,  $Area_{ex}$  (Equation 7.6).

$$\Delta T_{chen} = \left( \frac{\Delta T_1 + \Delta T_2}{2} \right)^{\frac{1}{3}} (\Delta T_1 \Delta T_2)^{\frac{1}{3}} \quad (7.5)$$

$$Q_{ex} = U_{ex} Area_{ex} \Delta T_{chen} \quad (7.6)$$

For Chen's approximation in a counter-current heat exchanger,  $\Delta T_1$  is the temperature difference between the cold stream inlet and hot stream outlet,  $\Delta T_2$  is the temperature difference between the cold stream outlet and the hot stream inlet. The overall heat transfer coefficient  $U_{ex}$  for each heat exchanger<sup>45</sup> varies based on the fluid combinations in the heat exchanger (i.e. gas-liquid,

liquid-liquid, and gas-evaporating liquid). In each heat exchanger we set a minimum approach temperature of 5° C. For those heat exchangers where flue gas serves as the heating medium, we assume the temperature of the flue gas decreases by 10°C. We select this approach temperature because it allows for heat recovery upstream of the FGD unit without causing acid gas mist condensation. We ensure that the resulting heat duty can be satisfied by the flue gas flow rate at the plant.

*Distillation Column.* We model our distillation column as a packed-bed column with waste heat from flue gas providing the energy input into the reboiler. We assume the distillation column operates at one atmosphere of pressure because our previous work<sup>26</sup> demonstrated that at this pressure the electrical and thermal energy inputs are minimized.

Our distillation column model also includes the condenser for the distillate. We estimate the cooling demand in the condenser (in kW) using distillate flow rate and assuming a distillate heat of vaporization of 2257 kJ/kg. We simulate in ASPEN Plus<sup>46</sup> the performance of the distillation column over a range of inlet feed flow rates, inlet concentrations, number of trays, and heat duties in order to meet a standard of less than 1 mg/L ammonia in the treated water. Details of the Aspen model can be found in SI Section 1.2 and Table S4. We assume the column has a height equivalent of a theoretical plate of 0.3 m, and has a diameter of 0.5 m for the gasification wastewater cases and 1.0 m for the FGD wastewater treatment cases. The column is packed with a generic Goodloe structured packing.<sup>26</sup>

We develop a meta-model to determine the size and energy demand of the packed distillation column in order to reduce the computational intensity. The number of trays in the distillation column,  $N_{dis}$ , is a function of the water recovery,  $W_{R,dis}$ , and regression parameters  $\beta_1$  and  $\beta_2$  (Equation 7.7).



$$N_{dis} = \beta_1 (W_{R,dis})^{\beta_2} + \epsilon \quad (7.7)$$

The heat duty in the distillation column,  $Q_{dis}$ , is also a function of the water recovery and regression parameters  $\beta_1$ ,  $\beta_2$ , and  $\beta_3$  (Equation 7.8).

$$Q_{dis} = \beta_1 (W_{R,dis})^2 + \beta_2 W_{R,dis} + \beta_3 + \epsilon \quad (7.8)$$

The parameters in Equation 7.7 and 7.8 can be found in SI Section 1.2 and Tables S5 and S6.

Both models have an  $R^2$  greater than 0.98.

*Ammonia Recovery.* A non-negligible mass of ammonium back permeates across the membrane in FO systems. This necessitates the inclusion of an ammonia recovery system to treat the brine stream exiting the FO module to concentrations less than 1 mg/L.<sup>26, 28</sup> This is done in order to reduce the costs of replenishing lost draw solute and because ammonium bicarbonate can corrode the FGD or gasification system if the product water is reused. Conventional ammonia recovery is done with a stripper.<sup>40</sup> We use a multiple-effect distillation as a stripper in order to model the energy consumption and cost. The energy source for the stripper is waste heat recovered from the exhaust flue gas and the heat exchanger is modeled as described above.

We develop a simple performance model for the ammonia recovery stripper. We use the median simulation value from our ASPEN models of 90% ammonium bicarbonate recovery and 30% water recovery in the stripper distillate (SI Section 1.3). The energy consumed in this process is approximately 320 kJ per kg of distillate. Finally, the stripper distillate is fed into a mixer with the dilute draw solution before the distillation column preheating.

*Crystallization.* Following ammonia recovery, the brine is then fed into an electricity-driven crystallizer to achieve ZLD and produce treated water for reuse. The crystallizer electricity consumption is 59 kWh/m<sup>3</sup> of inlet wastewater.<sup>47</sup> The treated product water can be reused at several locations within the plant in order to comply with the ZLD voluntary incentive

program in the ELGs. These reuse locations include in the FGD scrubber, gasification system, and cooling systems

*Costs.* Finally, we build a model for the cost of the overall FO and crystallization system using NETL's ICARUS model<sup>48</sup> and standard engineering references.<sup>49</sup> We annualize the resulting operating and capital costs at a discount rate of 10% and a life span of 20 years. We then divide the annual cost by the total volume of water produced in order to calculate water treatment cost per cubic meter. The formulation for the optimization problem and costing model are reported in SI Section 2.0, Figure S3, and Tables S7 and S8.

### *7.3.3 Benchmark Technologies*

We compare the costs for FO treatment to the EPA's identified best available technology for achieving ZLD treatment of power plant wastewater – mechanical vapor recompression and crystallization (MVCC).<sup>42</sup> We use a literature-based value of \$2.99/m<sup>3</sup> for this process.<sup>50</sup> This value is based on an assumption of 65% water recovery in the mechanical vapor recompression step<sup>51</sup> and an electricity price to the plant of \$0.05/kWh.<sup>52-53</sup>

### *7.3.4 Case Studies*

We use the optimization model to determine the minimum wastewater treatment costs for ZLD at four different case study plants (Table 7.1). Three of these plants are baseline models of coal and gasification power plants developed by the National Energy Technology Laboratory (NETL).<sup>52-53</sup> We also include Plant Bowen, a coal-fired power plant located in Eulerhee, Georgia, because of access to actual power plant operating data. Three of these plants (Plant Bowen and two of the NETL baseline models) are coal fired power plants that produce a flue gas desulfurization stream. The fourth facility is an NETL integrated gasification model plant that produces a gasification wastewater to be treated.

*Table 7.1 Parameters for Our Four Case Studies*

	Case Study			
	NETL Sub PC	NETL Super PC	NETL	Plant Bowen
	without CCS	with CCS	IGCC	
Available Waste Heat	170,000	205,000	308,000	46,000
[kJ/s]				
Temperature [°C]	153	153	132	128
Water Demand [m <sup>3</sup> /hr]	111.6	134.4	1.2	268
Concentration [M]	0.6	0.6	0.075	0.6

### *7.3.5 Sensitivity Analyses*

We perform sensitivity analyses for three variables: the concentration of the draw solution, the flow rate of the draw solution, and the concentration of the FGD wastewater. The driving force for FO is the concentration gradient between the feed and draw stream. As a result, we expect that an increase in the draw solution concentration will reduce the cost of FO and that an increase in the wastewater concentration will increase the cost of FO. Water flux across the membrane (calculated using Equation 7.1) is independent of flow rate and so we expect that changes in flow rate are unlikely to affect costs on a per cubic meter basis. We run these sensitivity analyses for FO and crystallization treatment of FGD wastewater from the NETL 550 MW subcritical PC plant without carbon capture case.

## 7.4 Results and Discussion

### 7.4.1 Cost Minimized FO System Designs

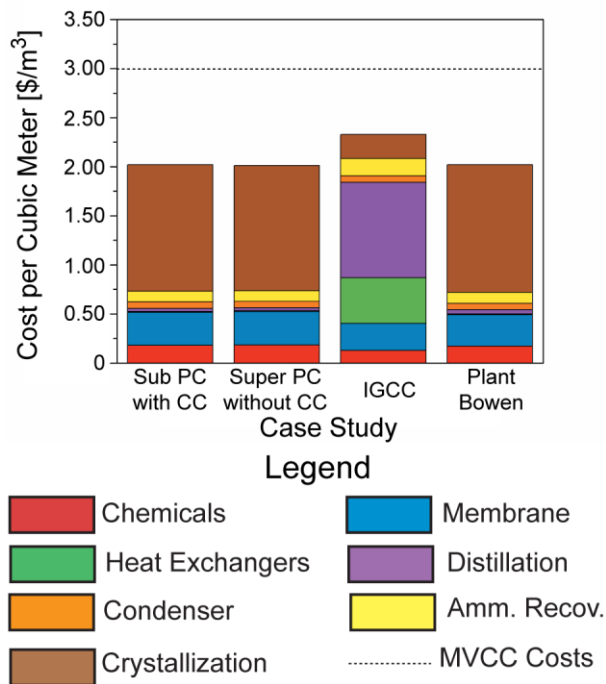


Figure 7.3 Optimization results for wastewater treatment requiring zero liquid discharge. The cost for FO is less than the cost of MVCC (dashed line) for all four cases studied. The case studies are as follows: Sub PC w/o CC, subcritical pulverized coal without carbon capture; Super PC w/ CC, supercritical pulverized coal with carbon capture; IGCC, integrated gasification carbon capture; and the pulverized CFPP Plant Bowen. Results are tabulated in SI Section 3.1 and Table S9 and S10.

The minimum costs for FO and crystallization systems are presented in Figure 7.3. Using our meta-models ( $R^2$ -values greater than 0.98) and excluding pretreatment, installation and labor costs, the costs for the flue gas desulfurization wastewater cases range from  $\$2.01/\text{m}^3$ - $\$2.02/\text{m}^3$ . The largest portion of this cost is the brine crystallizer, which accounts for approximately

\$1.30/m<sup>3</sup> of the total FGD wastewater cost. This cost for crystallization is lower than conventional industrial wastewater systems crystallizers because of the volume reduction that takes place in the FO system and a lower internal electricity price CFPPs pay themselves compared to the price for grid electricity. The cost in the gasification wastewater case is \$2.33/m<sup>3</sup>, again excluding pretreatment, installation, and labor costs. The heat exchanger (\$0.49/m<sup>3</sup>) and distillation column (\$0.96/m<sup>3</sup>) contribute more to the overall system costs in the IGCC case. Costs for the chemicals, membranes, condenser, and the ammonia recovery system are relatively consistent across all cases studied, although they are slightly lower for the IGCC case study.

The FGD wastewater treatment and IGCC wastewater treatment costs are different because of the wastewater concentration for each case. Gasification wastewater has a lower concentration than FGD wastewater.<sup>42</sup> As a result gasification wastewater has a higher osmotic pressure gradient and a water flux. The water recovery in the optimized IGCC wastewater treatment system is 90%, nearly twice the 48-49% water recovery seen in the FGD wastewater treatment cases. As a result of this need for higher water recovery, the heat exchangers and distillation columns used for gasification wastewater treatment are larger and costlier. For the gasification wastewater case, the heat exchangers and distillation column costs on a per cubic meter basis are 28-37 times the FGD wastewater treatment cases. In addition to the difference in concentration, there is a two order of magnitude difference in the flow rate between gasification wastewater and FGD wastewater systems. FGD wastewater systems can therefore take advantage of economies of scale to reduce the costs for these components. The higher recovery in the gasification wastewater membrane module also means less brine is sent to the crystallizer

in gasification wastewater treatment. This leads to a 70% reduction in the ammonia recovery and crystallizer costs relative to the costs in FGD wastewater.

For all four cases, the cost of wastewater treatment using FO and crystallization is lower than the cost of MVCC (the dashed line in Fig. 2). The benchmark cost for MVCC of \$2.99/m<sup>3</sup> is higher than the cost of FO and crystallization.<sup>50</sup> The difference between MVCC and FO is \$0.97-\$0.98/m<sup>3</sup> for the FGD wastewater cases and \$0.66/m<sup>3</sup> for the gasification wastewater case. This indicates that, FO plus crystallization is economically competitive for wastewater treatment. Neither the cost estimate for FO nor for MVCC includes required pretreatment costs to remove heavy metals and divalent cations.<sup>42</sup> It is unlikely, however, that incorporating pretreatment costs will make MVCC less costly than FO and crystallization.

#### *7.4.2 Sensitivity Analyses*

The results of our sensitivity analyses for FGD wastewater treatment at the sub-critical PC plant without carbon capture and sequestration are shown in Figure 7.4. As would be expected from Equation 7.1, an increase in draw solution concentration decreases the cost of product water per cubic meter (Fig 3A). The higher draw solution concentration increases the recovery in the membrane and less brine is therefore sent to the costly crystallizing process. The cost increases by 14% (\$0.27/m<sup>3</sup>) when the concentration of the draw solution decreases from 3M to 2M. The cost decreases by 12% (\$0.25/m<sup>3</sup>) as the draw solution concentration increases from the base case of 3M to 5M. The NETL power plant would therefore minimize the cost for FO and crystallization by increasing the concentration of the draw solute to its upper bound. The upper bound draw solution concentration is typically determined by the solubility limit, but may be lowered in order to avoid corrosion and reactions with salts that permeate into the draw solution from the wastewater, to maintain low viscosity, and to protect worker safety.

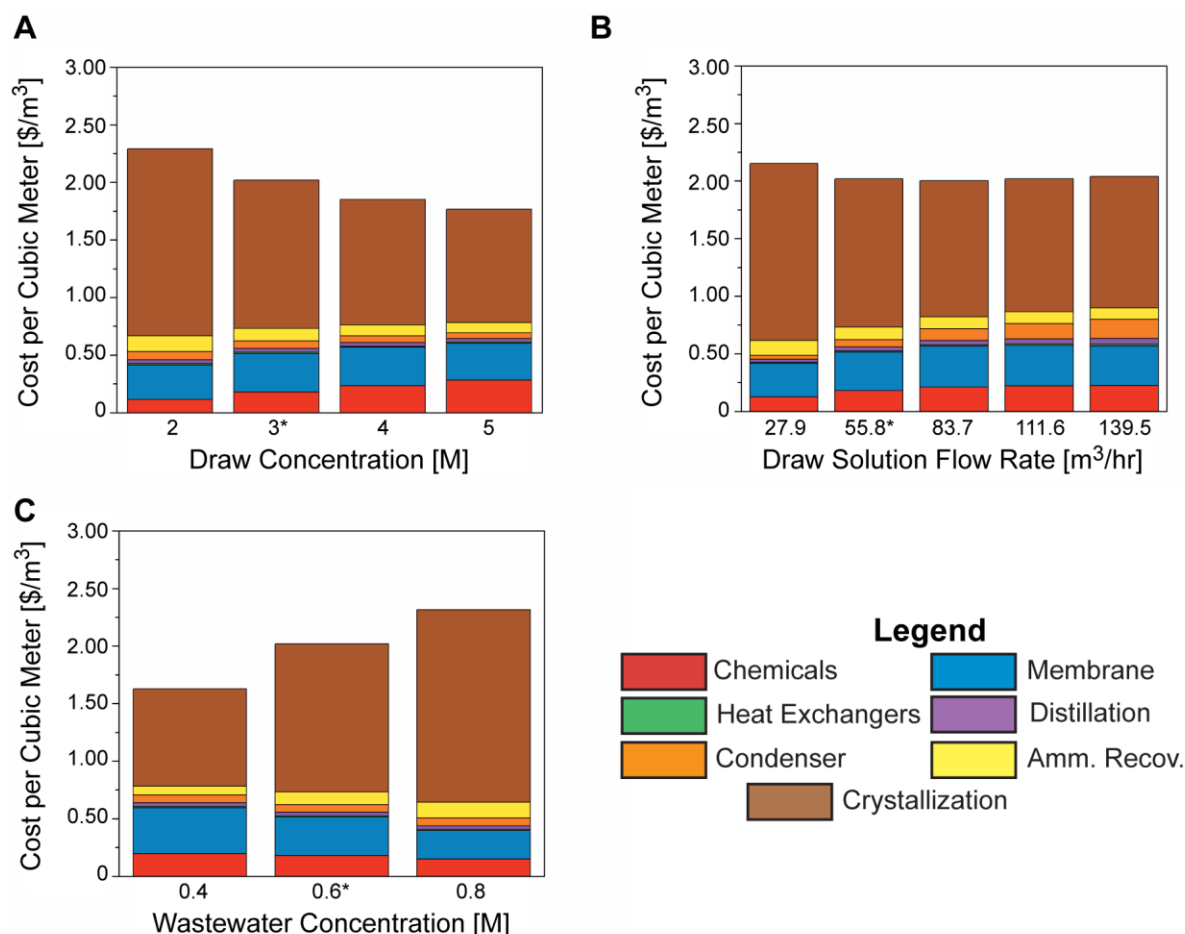


Figure 7.4 Sensitivity analyses on the cost of FO with crystallization for the NETL sub-critical coal case without carbon capture. The variables that are varied include (A) draw solution concentration, (B) draw solution flow rate, and (C) wastewater concentration. The results of the sensitivity analyses are tabulated in SI Section 3.2 and Tables S11-S13

As the draw solution flow rate increases, cost per cubic meter changes non-monotonically (Figure 7.4B). When the draw flow rate is decreased by 50%, from 55.8 m³/hr to 27.9 m³/hr, the cost increases by about 7% (\$0.13/m³). The low flow rate case increases cost because there is less water recovery in the FO module, which diverts more wastewater to the relatively more expensive crystallizer. When the draw flow rate is increased by 50% to 139.5 m³/hr, the costs

negligibly increase by 1% ( $\$0.02/\text{m}^3$ ). The high flow rate case increases cost because the higher flow rate greatly increases the cost of the condenser and offsets any of the increases in the water recovery of the FO module. It is evident from these results that draw solution flow rate has a relatively small effect on the costs of the system.

Whereas the first two sensitivity analyses were variables under the control of a designer, Figure 7.4C shows the impact of a non-design variable on the cost of the system - wastewater concentration. As the concentration of the FGD wastewater increases, the cost per cubic meter increases. Increasing the feed concentration from 0.6M to 0.8M increases the cost by 15% ( $\$0.30/\text{m}^3$ ). Decreasing the concentration to 0.4 M, decreases the cost by 19% ( $\$0.39/\text{m}^3$ ). As predicted by Equation 7.1 higher concentration of the FGD wastewater and a fixed concentration in the draw stream reduces the osmotic pressure difference across the membrane. There is subsequently less recovery in the membrane. This reduction in recovery slightly decreases the cost of the heat exchangers and distillation, but doubles the cost of the most expensive component of the system, the crystallizer. The cost optimal system design is therefore highly dependent on wastewater quality. As FGD wastewater concentration can vary significantly depending on coal quality, air pollution control device operation, and purge frequency this can pose a significant challenge to the design of FO systems for treating FGD wastewater.

## **7.5 Conclusions**

Based on these results, FO and crystallization shows significant promise to reduce the costs of power plant wastewater treatment in comparison to MVCC. Furthermore, our previous work has shown that MVCC at coal fired power plants imposes larger human health damages from air pollution than environmental damages averted from water pollution.<sup>15</sup> Using waste heat to drive FGD wastewater reduces the environmental damages from air pollution by reducing



auxiliary electricity demand at CFPPs and gasification plants. Forward osmosis and crystallization therefore plays a critical role in minimizing the environmental burden of coal-fired power plants in a cost-effective manner.

In developing FO systems for power plant wastewater treatment, several advances need to be made in membrane technology. Researchers should continue to focus on developing membranes with higher permeability and lower structural parameters in order to reduce the required area for membranes.<sup>54</sup> Furthermore, since FGD wastewater treatment systems do not continuously operate and wastewater is purged intermittently<sup>55</sup> researchers should also continue to develop membranes and membrane systems that can handle this intermittent operation. Finally, with FO membranes susceptible to gypsum scaling,<sup>44</sup> research should focus on creating membranes that are scaling resistant and designing anti-scaling treatment to increase the life span of FO membranes.

Finally, this work demonstrates the need to develop models that are capable of assessing different water treatment technologies and energy sources for environmental regulatory compliance at power plants. Power plant operators and utilities need to make compliance decisions in an evolving regulatory environment. These results show that conventional energy sources to drive “best” available technologies may lead to suboptimal economic decisions. By considering emerging technologies and alternative energy sources, power plants can reduce their environmental burden in a cost-effective manner.

## **7.6 Acknowledgements**

This work was supported by the Department of Energy (DE-FE0024008). DG and TB also individually acknowledge support from The Pittsburgh Chapter of the ARCS Foundation

(Achievement Rewards for College Scientists). DG acknowledges support from the Phillips & Huang Family Foundation Fellowship.

## 7.7 Nomenclature

### Symbols

A: Pure water permeability coefficient [m/Pa s]

Area: Area [m<sup>2</sup>]

B: Salt permeability coefficient [m/s]

$\beta$ : Meta-model coefficient [-]

C: Concentration [M]

$\epsilon$ : Meta-model error term [-]

J: Flux across the membrane [m/s]

K: Solute resistivity for diffusion [s/m]

$\kappa$ : Feed mass transfer coefficient [m/s]

N: Number of trays [-]

$\pi$ : Osmotic pressure [atm]

Q: Heat Duty [kJ/s]

S<sub>R</sub>: Salt Rejection [%]

T: Temperature [K]

U: Overall heat Transfer Coefficient [kW/m<sup>2</sup> °C]

W<sub>R</sub>: Water recovery [%]

### Subscripts

b: Bulk solution

chen: Chen's Approximation

d: Draw stream  
dis: Distillation column  
ex: Heat exchanger  
f: Feed stream  
FO: Forward osmosis membrane  
m: Membrane  
s: Salt  
w: Water

## 7.8 References

1. Zhou, Z.; Zhou, X.; Jing, G.; Lv, B., Evaluation of the Multi-amine Functionalized Ionic Liquid for Efficient Postcombustion CO<sub>2</sub>Capture. *Energy & Fuels* **2016**, *30* (9), 7489-7495.
2. Zhao, T.; Guo, B.; Li, Q.; Sha, F.; Zhang, F.; Zhang, J., Highly Efficient CO<sub>2</sub>Capture to a New-Style CO<sub>2</sub>-Storage Material. *Energy & Fuels* **2016**, *30* (8), 6555-6560.
3. Mantripragada, H. C.; Rubin, E. S., Performance Model for Evaluating Chemical Looping Combustion (CLC) Processes for CO<sub>2</sub>Capture at Gas-Fired Power Plants. *Energy & Fuels* **2016**, *30* (3), 2257-2267.
4. Gao, H.; Xu, B.; Liu, H.; Liang, Z., Effect of Amine Activators on AqueousN,N-Diethylethanolamine Solution for Postcombustion CO<sub>2</sub>Capture. *Energy & Fuels* **2016**, *30* (9), 7481-7488.
5. Yang, J.; Gao, H.; Hu, G.; Wang, S.; Zhang, Y., Novel Process of Removal of Sulfur Dioxide by Aqueous Ammonia–Fulvic Acid Solution with Ammonia Escape Inhibition. *Energy & Fuels* **2016**, *30* (4), 3205-3218.

6. Xu, Y.; Liu, X.; Zhang, Y.; Sun, W.; Zhou, Z.; Xu, M.; Pan, S.; Gao, X., Field Measurements on the Emission and Removal of PM<sub>2.5</sub> from Coal-Fired Power Stations: 3. Direct Comparison on the PM Removal Efficiency of Electrostatic Precipitators and Fabric Filters. *Energy & Fuels* **2016**, *30* (7), 5930-5936.
7. Liu, X.; Xu, Y.; Fan, B.; Lv, C.; Xu, M.; Pan, S.; Zhang, K.; Li, L.; Gao, X., Field Measurements on the Emission and Removal of PM<sub>2.5</sub> from Coal-Fired Power Stations: 2. Studies on Two 135 MW Circulating Fluidized Bed Boilers Respectively Equipped with an Electrostatic Precipitator and a Hybrid Electrostatic Filter Precipitator. *Energy & Fuels* **2016**, *30* (7), 5922-5929.
8. Liu, X.; Xu, Y.; Zeng, X.; Zhang, Y.; Xu, M.; Pan, S.; Zhang, K.; Li, L.; Gao, X., Field Measurements on the Emission and Removal of PM<sub>2.5</sub> from Coal-Fired Power Stations: 1. Case Study for a 1000 MW Ultrasupercritical Utility Boiler. *Energy & Fuels* **2016**, *30* (8), 6547-6554.
9. Chen, H.; Wu, W.; Liang, C.; Wu, X., Removal of Fine Particulate Matter by Spraying Attapulgate Suspending Liquid. *Energy & Fuels* **2016**, *30* (5), 4150-4158.
10. Chen, M.; Deng, X.; He, F., Removal of SO<sub>2</sub> from Flue Gas Using Basic Aluminum Sulfate Solution with the Byproduct Oxidation Inhibition by Ethylene Glycol. *Energy & Fuels* **2016**.
11. Wang, H.; Duan, Y.; Li, Y.-n.; Liu, M., Experimental Study on Mercury Oxidation in a Fluidized Bed under O<sub>2</sub>/CO<sub>2</sub> and O<sub>2</sub>/N<sub>2</sub> Atmospheres. *Energy & Fuels* **2016**, *30* (6), 5065-5070.

12. Tang, R.; Yang, W.; Wang, H.; Zhou, J.; Zhang, Z.; Wu, S., Preparation of Fly-Ash-Modified Bamboo-Shell Carbon Black and Its Mercury Removal Performance in Simulated Flue Gases. *Energy & Fuels* **2016**, *30* (5), 4191-4196.
13. U.S. Environmental Protection Agency, Technical Development Document for the Effluent Limitations Guidelines and Standards for the Steam Electric Generating Point Source Category. Washington, D.C., 2015.
14. Gingerich, D. B.; Mauter, M. S., Redesigning the Regulated Power Plant: Optimizing Energy Allocation to Electricity Generation, Water Treatment, and Carbon Capture Processes at Coal-Fired Generating Facilities.
15. Gingerich, D. B.; Sun, X. B., A. Patrick; Azevedo, I. M. L.; Mauter, M. S., Spatially resolved air-water emissions tradeoffs improve regulatory impact analyses for electricity generation. *Proceedings of the National Academy of Science* **2017**, 1862–1867.
16. Zhao, S.; Duan, Y.; Tan, H.; Liu, M.; Wang, X.; Wu, L.; Wang, C.; Lv, J.; Yao, T.; She, M.; Tang, H., Migration and Emission Characteristics of Trace Elements in a 660 MW Coal-Fired Power Plant of China. *Energy & Fuels* **2016**, *30* (7), 5937-5944.
17. Cath, T.; Childress, A.; Elimelech, M., Forward osmosis: Principles, applications, and recent developments. *Journal of Membrane Science* **2006**, *281* (1-2), 70-87.
18. Chung, T.-S.; Zhang, S.; Wang, K. Y.; Su, J.; Ling, M. M., Forward osmosis processes: Yesterday, today and tomorrow. *Desalination* **2012**, *287*, 78-81.
19. Hoover, L. A.; Phillip, W. A.; Tiraferri, A.; Yip, N. Y.; Elimelech, M., Forward with osmosis: emerging applications for greater sustainability. *Environ Sci Technol* **2011**, *45* (23), 9824-30.

20. Zhao, S.; Zou, L.; Tang, C. Y.; Mulcahy, D., Recent developments in forward osmosis: Opportunities and challenges. *Journal of Membrane Science* **2012**, *396*, 1-21.
21. Gazzani, M.; Hartmann, T.; Sutter, D.; Pérez-Calvo, J.-F.; Mazzotti, M., On the optimal design of forward osmosis desalination systems with NH<sub>3</sub>-CO<sub>2</sub>-H<sub>2</sub>O solutions. *Environ. Sci.: Water Res. Technol.* **2017**.
22. McGinnis, R.; Elimelech, M., Energy requirements of ammonia-carbon dioxide forward osmosis desalination. *Desalination* **2007**, *207*, 370-382.
23. McGinnis, R. L.; Elimelech, M., Global Challenges in Energy and Water Supply: The Promise of Engineered Osmosis. *Environmental Science & Technology* **2008**, *42* (23), 8625-8629.
24. McCutcheon, J. R.; McGinnis, R. L.; Elimelech, M., A novel ammonia-carbon dioxide forward (direct) osmosis desalination process. *Desalination* **2005**, *174*, 1-11.
25. Park, M. Y.; Shin, S.; Kim, E. S., Effective energy management by combining gas turbine cycles and forward osmosis desalination process. *Applied Energy* **2015**, *154*, 51-61.
26. Zhou, X.; Gingerich, D. B.; Mauter, M. S., Water Treatment Capacity of Forward-Osmosis Systems Utilizing Power-Plant Waste Heat. *Industrial & Engineering Chemistry Research* **2015**, *54* (24), 6378-6389.
27. Elimelech, M.; Phillip, W. A., The future of seawater desalination: energy, technology, and the environment. *Science* **2011**, *333* (6043), 712-7.
28. McGinnis, R. L.; Hancock, N. T.; Nowosielski-Slepowron, M. S.; McGurgan, G. D., Pilot demonstration of the NH<sub>3</sub>/CO<sub>2</sub> forward osmosis desalination process on high salinity brines. *Desalination* **2013**, *312*, 67-74.

29. Kim, Y. C.; Park, S. J., Experimental study of a 4040 spiral-wound forward-osmosis membrane module. *Environ Sci Technol* **2011**, *45* (18), 7737-45.
30. Blandin, G.; Verliefde, A. R. D.; Tang, C. Y.; Le-Clech, P., Opportunities to reach economic sustainability in forward osmosis–reverse osmosis hybrids for seawater desalination. *Desalination* **2015**, *363*, 26-36.
31. Kim, Y.; Lee, J. H.; Kim, Y. C.; Lee, K. H.; Park, I. S.; Park, S.-J., Operation and simulation of pilot-scale forward osmosis desalination with ammonium bicarbonate. *Chemical Engineering Research and Design* **2015**, *94*, 390-395.
32. Valladares Linares, R.; Li, Z.; Sarp, S.; Bucs, S. S.; Amy, G.; Vrouwenvelder, J. S., Forward osmosis niches in seawater desalination and wastewater reuse. *Water Res* **2014**, *66*, 122-39.
33. Zhang, X.; Ning, Z.; Wang, D. K.; Diniz da Costa, J. C., Processing municipal wastewaters by forward osmosis using CTA membrane. *Journal of Membrane Science* **2014**, *468*, 269-275.
34. Wang, Z.; Zheng, J.; Tang, J.; Wang, X.; Wu, Z., A pilot-scale forward osmosis membrane system for concentrating low-strength municipal wastewater: performance and implications. *Sci Rep* **2016**, *6*, 21653.
35. Chen, L.; Gu, Y.; Cao, C.; Zhang, J.; Ng, J. W.; Tang, C., Performance of a submerged anaerobic membrane bioreactor with forward osmosis membrane for low-strength wastewater treatment. *Water Res* **2014**, *50*, 114-23.
36. Xie, M.; Shon, H. K.; Gray, S. R.; Elimelech, M., Membrane-based processes for wastewater nutrient recovery: Technology, challenges, and future direction. *Water Res* **2016**, *89*, 210-21.

37. Sun, Y.; Tian, J.; Zhao, Z.; Shi, W.; Liu, D.; Cui, F., Membrane fouling of forward osmosis (FO) membrane for municipal wastewater treatment: A comparison between direct FO and OMBR. *Water Res* **2016**, *104*, 330-339.
38. Coday, B. D.; Xu, P.; Beaudry, E. G.; Herron, J.; Lampi, K.; Hancock, N. T.; Cath, T. Y., The sweet spot of forward osmosis: Treatment of produced water, drilling wastewater, and other complex and difficult liquid streams. *Desalination* **2014**, *333* (1), 23-35.
39. Hickenbottom, K. L.; Hancock, N. T.; Hutchings, N. R.; Appleton, E. W.; Beaudry, E. G.; Xu, P.; Cath, T. Y., Forward osmosis treatment of drilling mud and fracturing wastewater from oil and gas operations. *Desalination* **2013**, *312*, 60-66.
40. Pendergast, M. M.; Nowosielski-Slepowron, M. S.; Tracy, J., Going big with forward osmosis. *Desalination and Water Treatment* **2016**, *57* (55), 26529-26538.
41. Kim, T.-W.; Kim, Y.; Yun, C.; Jang, H.; Kim, W.; Park, S., Systematic approach for draw solute selection and optimal system design for forward osmosis desalination. *Desalination* **2012**, *284*, 253-260.
42. U.S. Environmental Protection Agency *Technical Development Document for the Effluent Limitations Guidelines and Standards for the Steam Electric Power Generating Point Source Category*; U.S. Environmental Protection Agency: Washington, D.C., 2015.
43. Mi, B.; Elimelech, M., Chemical and physical aspects of organic fouling of forward osmosis membranes. *Journal of Membrane Science* **2008**, *320* (1-2), 292-302.
44. Wang, Y.-N.; Järvelä, E.; Wei, J.; Zhang, M.; Kyllönen, H.; Wang, R.; Tang, C. Y., Gypsum scaling and membrane integrity of osmotically driven membranes: The effect of membrane materials and operating conditions. *Desalination* **2016**, *377*, 1-10.



45. The Engineering Toolbox Heat Transfer Coefficients in Heat Exchangers.  
[http://www.engineeringtoolbox.com/heat-transfer-coefficients-exchangers-d\\_450.html](http://www.engineeringtoolbox.com/heat-transfer-coefficients-exchangers-d_450.html)  
(accessed January 26, 2017).
46. Aspen Technology, I. Aspen Plus.  
<http://www.aspentech.com/products/engineering/aspen-plus/> (accessed July 16, 2017).
47. Subramani, A.; Jacangelo, J. G., Treatment technologies for reverse osmosis concentrate volume minimization: A review. *Separation and Purification Technology* **2014**, *122*, 472-489.
48. Loh, H. P.; Lyons, J.; White III, C. W. *Process Equipment Cost Estimation Final Report*; National Energy Technology Laboratory: Morgantown, WV, 2002, 2002.
49. Towler, G.; Sinnott, R., *Chemical Engineering Design: Principles, Practice, and Economics of Plant and Process Design*. 2nd Edition ed.; Elsevier, Ltd.: Oxford, UK, 2013.
50. Plappally, A. K.; Lienhard, J. H., Costs for water supply, treatment, end-use and reclamation. *Desalination and Water Treatment* **2013**, *51* (1-3), 200-232.
51. Eastern Research Group Inc. *Final Power Plant Monitoring Data Collected Under Clean Water Act Section 308 Authority*; Chantilly, VA, 2012.
52. National Energy Technology Laboratory *Cost and Performance Baseline for Fossil Energy Plants: Volume 1B Bituminous Coal (IGCC) to Electricity*; Department of Energy - Office of Fossil Energy: Pittsburgh, PA, 2015.
53. National Energy Technology Laboratory *Cost and Performance Baseline for Fossil Energy Plants: Volume 1A Bituminous Coal (PC) and Natural Gas to Electricity*; Department of Energy - Office of Fossil Energy: Pittsburgh PA, 2015.

54. Park, H. B.; Kameev, J.; Robeson, L. M.; Elimelech, M.; Freeman, B. D., Maximizing the right stuff: The trade-off between membrane permeability and selectivity. *Science* **2017**, 356 (6343).
55. U.S. Environmental Protection Agency *Steam Electric Power Generating Point Source Category: Final Detailed Study Report*; U.S. Environmental Protection Agency: Washington, D.C., 2009.

## **CHAPTER 8: REDESIGNING THE REGULATED POWER PLANT: OPTIMIZING ENERGY ALLOCATION TO ELECTRICITY GENERATION, WATER TREATMENT, AND CARBON CAPTURE PROCESSES AT COAL-FIRED GENERATING FACILITIES<sup>7</sup>**

### **8.1 Abstract**

Minimizing the human health and environmental impacts from electricity generation at existing coal-fired power plants (CFPPs) will require extensive plant retrofit, but the separations technologies for reducing CO<sub>2</sub> and wastewater emissions at CFPPs are energy intensive. This paper quantifies the electricity generation efficiency and revenue implications of allocating electricity, steam, or residual heat to these emission control processes under several different regulatory scenarios. We develop an energy balance model of the National Energy Technology Laboratory's 550 MW CFPP without carbon capture (CC) and add models of four CC technologies (one electricity-driven and three thermal processes) and five wastewater treatment (WT) technologies (one electricity-driven and four thermal processes) to comply with the Clean Power Plan and Effluent Limitation Guidelines emissions regulations. Plant revenue is maximized by using residual heat for WT or CC, but the optimal allocation of limited residual heat resources depends on the current regulatory environment. If both CC and zero liquid discharge WT regulatory standards are in place, the plant maximizes revenue by allocating residual heat and steam to amine-based CC and electricity to mechanical vapor recompression WT.

---

<sup>7</sup> This chapter is based on a paper co-authored with Prof. Meagan Maunder that is currently under review at Environmental Science & Technology.

## 8.2 Introduction

Compliance with recent regulations limiting carbon<sup>1</sup> and aqueous emissions<sup>2</sup> at coal-fired power plants (CFPPs) in the United States will require installation of new carbon capture and wastewater treatment systems. These air and water separations systems require energy, either in the form of heat or electricity,<sup>3-8</sup> and may significantly reduce the generation efficiency and revenue of CFPPs. Though recent work has explored the application of residual heat driven separation processes to reduce auxiliary power loads for carbon capture<sup>9</sup> and water treatment,<sup>10</sup> there is not sufficient residual heat to fully meet all process demands. A systematic reevaluation of the use of all thermal and electricity sources at CFPPs will aid power plant designers in maximizing the efficiency and cost-effectiveness of emissions control retrofits.

Electricity generation from coal combustion produces three potentially usable energy sources. The first is high-quality steam fed to the high pressure (HP), intermediate pressure (IP), and low pressure (LP) turbines, which range in enthalpy from 3,470 kJ/kg to 1,980 kJ/kg.<sup>11</sup> The second source is electricity produced by the generator. The third energy source is residual heat discharged in the exhaust gas of CFPPs with a flue gas desulfurization (FGD) unit at an average temperature of 128°C.<sup>10</sup> Any of these three energy sources could conceivably be allocated to meet the energy demands of carbon capture and wastewater treatment processes.

Although solvents, sorbents, and membranes are all being explored as solutions for carbon capture,<sup>12</sup> the most established technologies are amine solvent adsorption systems, including the well-studied monoethanolamine (MEA) system.<sup>5</sup> In a MEA system, CO<sub>2</sub> absorbs into a lean MEA solution. The CO<sub>2</sub> rich solvent solution is then regenerated in a distillation column, producing streams of concentrated CO<sub>2</sub> and lean MEA solvent.<sup>13</sup> The energy for distillation is typically provided by steam that would otherwise drive the low-pressure turbine.

MEA solvent regeneration imposes a significant energy penalty on CFPPs,<sup>6</sup> and reducing the penalty through heat integration and system analysis remains a fruitful area of research.<sup>14-15</sup>

The EPA expects plants to comply with new regulatory standards for wastewater discharges using a combination of chemical precipitation and biological treatment or electricity-driven mechanical vapor recompression (MVC) and crystallization.<sup>7</sup> In addition to these electricity-driven processes, plants can also choose from a range of thermally driven deionization processes. These thermal processes include evaporative technologies, such as multi-stage flash distillation (MSF),<sup>16</sup> multiple effect distillation (MED),<sup>17</sup> thermal vapor recompression (TVC),<sup>18</sup> and the hybrid thermal-membrane processes forward osmosis (FO).<sup>10, 19</sup> These thermal technologies could be powered with high-quality steam, creating a parasitic loss and a trade-off between electricity generation and wastewater treatment. Alternatively, residual heat from the flue gas may be captured for thermal wastewater treatment processes, though the supply of this heat is limited. A quantitative understanding of the efficiency and water treatment potential of electrical, thermal, and residual heat energy sources will allow power plants to optimize heat allocation and minimize the cost of wastewater treatment.

To the best of our knowledge, tools for making holistic energy and environmental compliance decisions at CFPPs have not been developed. Though models of energy consumption and associated parasitic losses of carbon capture are well studied in the literature,<sup>9, 14, 20-23</sup> similar models for water treatment are limited to either combined electricity generation and desalination systems or tri-generation systems,<sup>24-26</sup> and do not model FGD wastewater treatment. Finally, no models incorporate the potential for waste heat usage or evaluate the optimal allocation of electricity, steam, or waste heat across multiple control processes. As a

result, there is a need for environmental compliance decision support tools that consider multiple emissions control processes and energy sources simultaneously.

This study develops a model to quantitatively evaluate the trade-offs between dispatching the three energy streams available at CFPPs to electricity generation, carbon capture, and wastewater treatment processes in a retrofit of the National Energy Technology Laboratory's 550 MW pulverized coal combustion power plant model.<sup>11</sup> We first build mass- and energy-balance models of the turbines in the model plant. We then vary the allocation of energy sources among three "sinks": the turbine for electricity generation, the solvent regeneration for carbon capture, and the wastewater treatment unit. Using this method, we estimate the maximum amount of electricity generation, carbon capture, and wastewater treatment that can be performed with the available fuel energy. Finally, we employ these estimates to maximize revenue by optimizing the allocation of enthalpy to plant processes under a range of likely prices for electricity delivered to the grid, captured carbon, and treated water.

### **8.3 Materials and Methods**

#### *8.3.1 550MW CFPP Base Model*

We selected the National Energy Technology Laboratory's model of a 550 MW pulverized coal combustion plant without carbon capture as the base model plant for retrofit.<sup>11</sup> Versions of this model are frequently used in the literature<sup>27-29</sup> for studying the impact of carbon capture retrofits and changes in power plant operation. The steam produced in the boilers is used to drive three turbines: a high-pressure turbine (596 GJ/hr of energy fed to the turbine), an intermediate-pressure turbine (590 GJ/hr of energy), and a low-pressure turbine (1,050 GJ/hr of energy). Note that steam leaving the HP turbine is reheated in the boiler before entering the IP turbine. These turbines connect to generators where mechanical energy is converted into

electrical energy at a rate of 550 MW per hour. Details of the turbines, stream flows between the turbines, (enthalpy content, temperature, pressure, and flow rates) and steam extractions from the turbines are published in the original NETL report.<sup>11</sup>

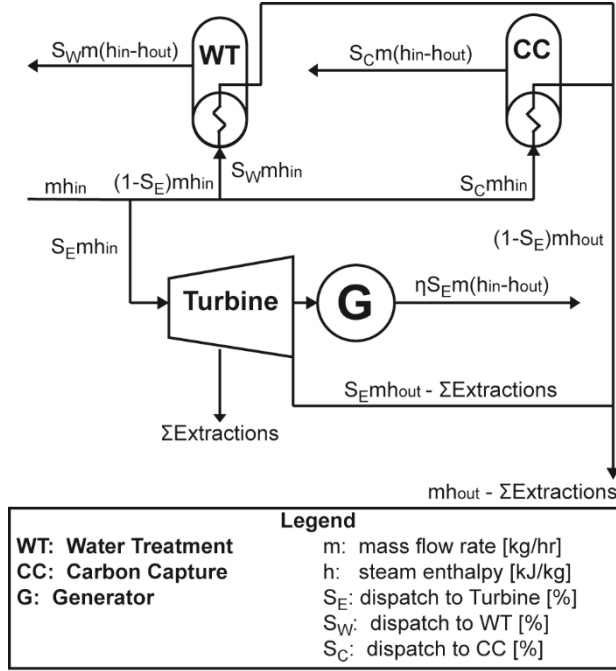


*Figure 8.1. Energy balance for the NETL 550 MW Turbines. This structure of this energy balance is equivalent for the HP and IP turbines. In the LP turbine, exiting steam is diverted to the condenser, whereas the steam leaving the water treatment and carbon capture unit is returned to the steam cycle after the condenser.*

We use an energy balance approach to calculate the electricity generation, carbon capture, and water treatment using high quality steam (Figure 8.1). We first employ this model to evaluate the system trade-offs between dispatching steam for electricity generation,  $S_E$ , or dispatching steam for carbon capture,  $S_C$ , or wastewater treatment,  $S_W$ . Second, we investigate the financial tradeoffs of using steam for electricity generation and environmental controls. Finally, we maximize the revenue of the plant by varying the allocation steam, electricity, and

high-temperature residual heat to comply with carbon capture and effluent limitation guideline (ELG) regulations for FGD wastewater.

### 8.3.2 Quantification of Plant Energy Sources

Three different energy sources can power carbon capture and water treatment emissions control processes: high quality steam dispatched from the turbines, electricity produced at the generator, or residual heat recovered from the exhaust gas. To model steam dispatch for environmental controls, we assume that steam is withdrawn prior to entering the HP, IP, or LP turbines and is returned to the steam cycle after the turbine. In the case of the HP and IP turbines, the enthalpy content of the steam upon return is assumed to equal the steam as it leaves that turbine (Figure 8.1).<sup>30</sup> For the LP turbine, the steam is returned to the steam cycle after the condenser and is assumed to have an enthalpy content equal to the water entering the first preheater.<sup>6</sup>

Next, we calculate the hourly electricity generation by steam that enters the turbine,  $E$  in kWh/hr, by multiplying an assumed efficiency,  $\eta$ , of 90% in converting extracted enthalpy into electricity; the amount of steam sent to the turbines,  $S_E$ ; the mass flow rate of the steam,  $m$  in kg/hr; and the change in enthalpy of the steam,  $h$  in kJ/kg (Equation 8.1).

$$E = \eta S_E m (h_{in} - h_{out}) * \frac{1 \text{ kWh}}{3600 \text{ kJ}} \quad (8.1)$$

The model dispatches enough steam to the IP and LP turbines to meet the feedwater preheating and de-aerator steam extraction requirements. A small fraction of steam is diverted from the IP and LP turbines for boiler water de-aeration (586 GJ/hr) and feedwater preheating (621 GJ/hr). Holding allocation to preheating and the de-aerator constant is a useful and widely used simplifying assumption that eliminates the need to optimize energy flow rates into the initial



turbine.<sup>31</sup> Finally, we calculate the quantity of residual heat that can feasibly be recovered from the exhaust gas before acid mist begins to condense, as reported in previous work.<sup>32</sup>

### 8.3.3 Energy Consumption of Carbon Capture Processes

The case study NETL 550 MW CFPP generates 856 kg/MWh of CO<sub>2</sub>.<sup>11</sup> The plant must capture 221 kg/MWh in order to comply with the maximum CO<sub>2</sub> emissions rate of 1,400 lb/MWh that was to be required of plants under the Clean Power Plan.<sup>1</sup> We assume that the upper bound of CO<sub>2</sub> recovery is 90%, regardless of carbon capture technology.<sup>8, 11</sup>

We first quantify the trade-offs between allocating steam to electricity generation or carbon capture using MEA solvents,<sup>3-6, 8, 33-34</sup> the solid sorbent Zeolite 13X,<sup>5</sup> and the tertiary amine Cansolv.<sup>11</sup> The rate of carbon capture,  $C_j$  in metric tons of CO<sub>2</sub> (tonne CO<sub>2</sub>) per hour, for each technology  $j$ , is determined by dividing the rate of enthalpy diverted to carbon capture by the heat duty requirements of the carbon capture process,  $H_{C,j}$  in kJ/tonne CO<sub>2</sub> (Equation 8.2). We use literature reported values from simulations for  $H_{C,j}$  of 3.54 GJ/tonne CO<sub>2</sub> for MEA,<sup>8, 34</sup> 2.48 GJ/tonne CO<sub>2</sub> for Cansolv,<sup>11</sup> 0.52 GJ/tonCO<sub>2</sub> Zeolite 13X,<sup>5</sup> and the thermodynamic limit of MEA capture of 1.9 GJ/tonne CO<sub>2</sub>.<sup>4</sup> These simulations may exclude inefficiencies present in real-world systems, but their use in this study is necessary for making direct comparisons to technology options that have not been piloted or installed at plants. Table S1 in Supporting Information (SI) Section S1 provides complete descriptions of each process and the calculated values for equivalent electrical energy consumption.

$$C_j = \frac{S_C m(h_{in} - h_{out})}{H_{C,j}} \quad (8.2)$$

These steam dispatch requirements are used to calculate the parasitic losses, or the electricity that would have been generated had the steam been used for electricity generation

rather than diverted to carbon capture. We calculate the average parasitic loss,  $P$  in kWh/tonne  $\text{CO}_2$ , when carbon capture,  $C$ , equals some  $\chi$  tonne  $\text{CO}_2/\text{hr}$  of capture, using Equation 8.3.

$$P = \frac{E_{C=\chi} - E_{C=0}}{\chi} \quad (8.3)$$

Next, we calculate the amount of carbon capture that can be driven by residual heat in the exhaust gas by replacing the numerator of Equation 8.2 with the quantity of waste heat that can be safely recovered. Finally, we calculate the auxiliary loading,  $A_i$  in kWh/hr, for electricity-driven carbon capture by multiplying the estimated electricity consumption of an idealized post-combustion  $\text{CO}_2\text{-N}_2$  membrane separation process,  $a_j$ , modeled at 0.19 MWh/tonne  $\text{CO}_2$ ,<sup>22</sup> by the mass of carbon captured,  $C$  in tonne  $\text{CO}_2/\text{hr}$  (Equation 8.4).

$$A_j = a_j C \quad (8.4)$$

We do not calculate the auxiliary loading associated with pressurizing, transporting, or storage of the captured carbon. We also do not allow multiple carbon capture technologies to be implemented at the same plant, as the capital and operational costs of building parallel adsorption and membrane based carbon capture systems are likely to exceed any revenue gains from allocating a mix of different processes.

#### 8.3.4 Energy Consumption of Water Treatment

Wastewater exits the FGD unit of the case study plant at a volumetric flow rate of 111.6  $\text{m}^3/\text{hr}$  and a temperature of  $56^\circ\text{C}$ .<sup>11</sup> Beyond filtration for gypsum recovery, NETL does not include FGD wastewater treatment in the plant model.<sup>11</sup> However, a survey of plants performed as part of the ELG promulgation found that a majority of CFPPs will need to install additional treatment to comply with the ELGs.<sup>7</sup> As detailed above, plants will either install secondary treatment or zero liquid discharge (ZLD) systems. ZLD treatment trains typically follow primary treatment with water softening; water deionization via thermal, mechanical, or membrane

processes; and crystallization. To cost-effectively crystallize the solids, the water deionization step must achieve approximately 65% recovery. The present work considers only the energy inputs to the water deionization step, which is the greatest contributor to energy consumption in the ZLD treatment train.

We estimate the wastewater deionization capacity,  $W_i$  in m<sup>3</sup>/hr, of steam driven processes by dividing the rate of enthalpy allocated to water deionization by the heat duty requirements for water treatment technology  $i$ ,  $H_{w,i}$  in kJ/m<sup>3</sup> (Equation 8.5). We use simulated heat duties for thermal water deionization at 65% recovery<sup>10, 35-37</sup> and 56°C feed temperatures of 476 MJ/m<sup>3</sup> for multi-effect distillation (MED), 1071 MJ/m<sup>3</sup> for multi-stage flash distillation (MSF), 313 MJ/m<sup>3</sup> for thermal vapor recompression (TVC), and 409 MJ/m<sup>3</sup> for forward osmosis (FO). These simulations may exclude inefficiencies present in real-world systems, but their use in this study is necessary for making direct comparisons to technology options that have not been piloted or installed at plants. The equivalent electrical energy consumption for these technologies is reported in Table S2 of SI Section 2. We use heat exchangers to generate the steam used in the thermal water treatment processes, rather than directly using steam from the turbines. For all turbine-water treatment technology pairs, we set the temperature of working fluid to the temperature that produces the minimum heat duty. This is accomplished by adjusting the mass of the steam used in the heat exchanger loop.

$$W_i = \frac{S_W m(h_{in} - h_{out})}{H_{w,i}} \quad (8.5)$$

These steam dispatch requirements are used to calculate the parasitic losses incurred by allocation steam to wastewater deionization processes. We calculate the average parasitic loss,  $P$  in kWh/m<sup>3</sup>, when water production,  $W$ , equals  $\omega$  m<sup>3</sup>/hr of production, using Equation 8.6.

$$P = \frac{E_{W=\omega} - E_{W=0}}{\omega} \quad (8.6)$$

Next, we estimate the wastewater deionization potential of residual heat by replacing the numerator of Equation 8.5 with the amount of residual heat that can be safely recovered from the exhaust gas. Finally, we calculate the auxiliary electricity consumption of the thermal and electrical wastewater deionization processes,  $A_i$  in kWh/hr, by multiplying electricity consumption per cubic meter of water,  $a_i$  in kWh/m<sup>3</sup>, by the volume of water being treated,  $V$  in m<sup>3</sup>/hr (Equation 8.7). Additional auxiliary electricity consumption of thermal technologies are reported in Table S2 of SI Section 2.<sup>10, 35, 38</sup> In addition, we consider the electricity consumption of the two electrical processes that the EPA identified as best available technologies in the final ELG rule.<sup>2</sup> Chemical precipitation and biological treatment (CBPT) has an estimated electricity requirement of 0.71 kWh/m<sup>3</sup>,<sup>37</sup> while mechanical vapor recompression has an estimated electricity requirement of 21 kWh/m<sup>3</sup> at 65% recovery and feed temperature of 56°C.<sup>37</sup>

$$A_i = a_i V \quad (8.7)$$

Note that while we consider both the thermal and electricity consumption of water deionization processes, we do not allow multiple water deionization processes to be installed at the plant simultaneously. In other words, the plant cannot treat half of the FGD wastewater volume using a thermal process and the other half of the volume using an electricity driven process.

### 8.3.5 Revenue Impacts of Steam Allocation

We evaluate the effects of steam allocation  $S_E$ ,  $S_W$ , and  $S_C$  on hourly revenue,  $R$ , in \$/hr from the retrofitted 550 MW plant. To do so, we multiply the production of electricity,  $E$  [kWh/hr], and water,  $W$  [m<sup>3</sup>/hr], and captured carbon,  $C$  [tonne CO<sub>2</sub>/hr], above the minimum emissions control requirements of the plant,  $W_{required}$  [m<sup>3</sup>/hr] and  $C_{required}$  [tonne CO<sub>2</sub>/hr] by the price for electricity, the price for treated water, and a price of carbon (Equation 8.8).

$$R = eE + w(W - W_{required}) + c(C - C_{required}) \quad (8.8)$$

We assume a constant price for electricity,  $e$ , of \$0.07/kWh. We treat the price of water,  $w$  in \$/m<sup>3</sup>, and the shadow price of carbon,  $c$  in \$/tonne CO<sub>2</sub>, parametrically based on six different regulatory environments. The parametric carbon prices are carbon prices of \$0/tonne CO<sub>2</sub> (for a scenario without carbon regulations) and \$59.44/tonne CO<sub>2</sub> (the social cost of carbon in 2030, when the Clean Power Plan was scheduled to come into effect, with a 3% discount rate).<sup>39</sup> The two wastewater treatment scenarios are for a chemical precipitation and biological treatment (CPBT) standard under the ELGs with an expected  $w$  of \$0.05/m<sup>3</sup> or zero liquid discharge (ZLD) standard under the ELGs with an expected  $w$  of \$2.62/m<sup>3</sup>.<sup>37</sup> To these four scenarios, we add two additional scenarios with wastewater treatment, but no carbon capture.

To simplify the revenue maximization process, we assume the retrofitted plant first allocates residual heat, then assigns steam or electricity to environmental controls. We systematically explore the decision space of our revenue model (Equation 8.8) and alternative values of  $S_E$ ,  $S_W$ , and  $S_C$ . As the model is linear, we then identify the optimal values of  $S_E$ ,  $S_W$ , and  $S_C$  by inspection. This assumption is reasonable as the case study plant maximizes its revenue by generating electricity (as shown in SI Section 3 where this assumption is relaxed), and there are no economically feasible technologies for converting residual heat to electricity.

This analysis is performed only for hourly plant revenue, rather than for profit, for three reasons. First, the costs of carbon capture and water treatment technologies are highly uncertain and will depend largely on the capacity factor of the plant. Second, variability in capital costs between different compliance technologies are likely to be smaller than the differences in operating costs between technologies. Finally, the energy-associated operational costs of these separation technologies are likely to exceed the capital costs.

## 8.4 Results and Discussion

We calculate the trade-offs between electricity generation and carbon capture and between electricity generation and water treatment. For both carbon capture and water treatment we graphically present the trade-offs in allocating steam between electricity generation and

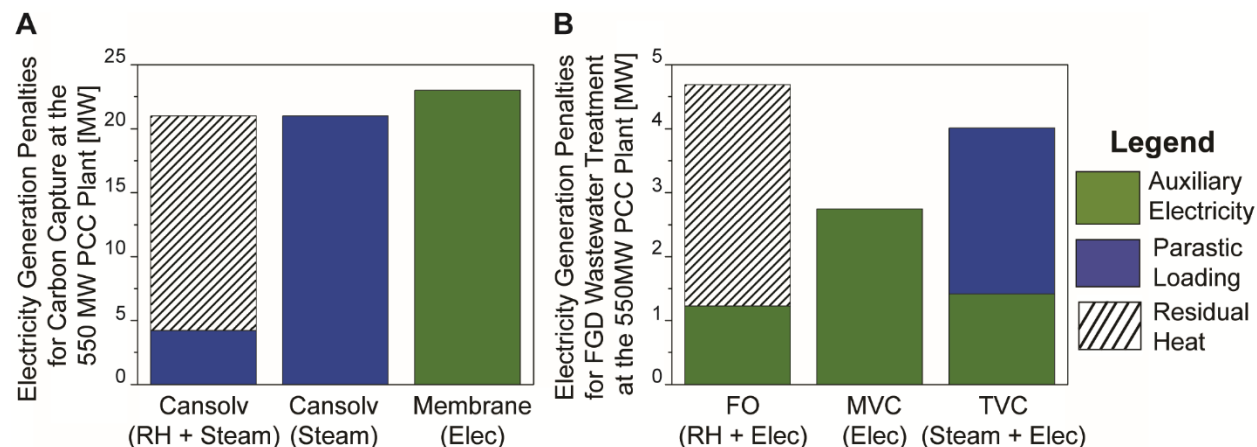


*Figure 8.2. Parasitic losses from (A) carbon capture and (B) FGD wastewater treatment processes. For carbon capture technologies, we compare the most efficient thermal process (Cansolv) to the most efficient electricity driven membrane separation process. (See SI Section 1.3 and Figure S1 for calculations of the relative efficiency of three thermal carbon capture technologies). For wastewater treatment technologies, we compare the parasitic loads of waste heat and electricity driven forward osmosis, electricity driven mechanical vapor recompression, and steam and electricity driven thermal vapor recompression. (See SI Section 2.3 and Figure S3 for calculations of the relative efficiency of four different thermal separation processes). Estimates of electricity generation penalties account for parasitic losses associated with the use of LP steam, electricity consumption imposing an auxiliary electricity load, and residual heat (RH) imposing no electricity generation penalty. N.B. The scale of the y-axis is different in the two graphs.*

environmental controls. Finally, we combine electricity generation, carbon capture, and water treatment into one model and evaluate the revenue implications of energy allocation decisions.

#### *8.4.1 Tradeoffs Between Steam for Electricity Generation and MEA Carbon Capture Solvent Regeneration*

We have calculated the electricity generation penalties for carbon capture at the 550MW PCC plant using a residual heat and steam driven Cansolv process, a steam-only Cansolv process, and an electricity driven membrane-based separation process (Figure 8.2A). Note that this analysis does not include any of the costs or energy consumption associated with CO<sub>2</sub> compression, transport, or underground storage.<sup>8, 34</sup> The Cansolv process captures the most carbon per unit of steam, imposing a parasitic loss of 170 kWh/tonne CO<sub>2</sub> when steam is pulled from the LP turbine (Figure S9A). Meeting the 1,400 lb/MWh standard for coal-fired generators via the Cansolv process uses 301 GJ/hr of LP steam and imposes an equivalent electricity penalty of 21 MW. The equivalent electricity driven membrane separation process consumes 23 MW. The tradeoff between electricity generation and carbon capture for all four carbon capture technologies can be found in Figure S1 of SI Section 1.3. Parasitic losses from the three thermal technologies are shown in Figure S9 of SI Section 4. Alternatively, the plant may reduce this electricity penalty by allocating residual heat for carbon capture processes. There is sufficient residual heat to capture 80% (98 tonne CO<sub>2</sub>/hr) of the CO<sub>2</sub> required for compliance with the Clean Power Plan (122 tonne CO<sub>2</sub>/hr) via the Cansolv process.

For reference, Figure S1 also presents the thermodynamic minimum for MEA solvent adsorption processes and the electricity consumption of membrane-based carbon capture technologies. While the electricity driven membrane separation processes are favorable alternatives to drawing steam from the HP and IP turbines, the thermally driven Cansolv process

is more efficient when allocating steam from the LP turbine. This conclusion is robust, even after accounting for variability in the estimates of energy intensity for amine and membrane based carbon capture processes as shown in SI Section 1.4 and Figure S2. This conclusion stems from the fact that thermal processes recover more of the enthalpy from LP steam than the turbine-generator system.

#### *8.4.2 Tradeoffs between Steam for Electricity Generation and Water Treatment*

We calculated the electricity generation potential for wastewater treatment using forward osmosis, mechanical vapor recompression, and thermal vapor recompression (Figure 8.2B). Thermal water deionization systems impose significant parasitic loads, ranging from 24 kWh/m<sup>3</sup> for thermal vapor recompression (TVC) using steam from the LP turbine to 272 kWh/m<sup>3</sup> for MSF using steam from either the HP or IP turbine (Figure S3 of SI Section 2.3 and Figure S9B of SI Section 4) for 65% water recovery at a feed temperature of 56°C. The auxiliary power for processes with significant vacuum or pumping requirements are reported in Table S2. In each case, the electricity driven MVC process imposes a smaller energy penalty than thermal deionization processes driven by steam diverted from the turbines. Note that the energy consumption of all five deionization water treatment processes exceeds that of chemical precipitation and biological treatment (CPBT) processes, the ELG's minimum treatment standard for FGD wastewater. Also note the additional ZLD treatment train energy requirements for pretreatment of 0.02 kWh/m<sup>3</sup> and crystallization of 16 kWh/m<sup>3</sup> reported in Table 8.1.<sup>37</sup>

For thermal processes using residual heat at 128°C, the most efficient water deionization process is forward osmosis (FO). Extending previous work,<sup>10</sup> we estimate that treatment of 111.6 m<sup>3</sup> of FGD wastewater via FO processes driven by residual heat will consume 29.7 GJ/hr of thermal energy and 0.002 MW of auxiliary electricity. A downside of membrane driven FO



processes is susceptibility to scaling and the potential for membrane damage from suspended gypsum in FGD wastewater.<sup>40</sup> Additional research and piloting is critical to establishing the viability of exhaust heat capture and usage in FO processes for FGD wastewater treatment.

*Table 8.1. Minimum estimated energy consumption associated with meeting chemical precipitation and biological treatment (CPBT) standard or the zero liquid discharge (ZLD) standard by treating 111.6 m<sup>3</sup>/hr of FGD wastewater using steam from the LP turbine, residual heat, or electricity.*

		Energy Requirements of Treating 111.6 m <sup>3</sup> /hr of FGD Wastewater					
		Thermal Energy Input		Electrical Energy Input	Other Electrical Processes in the Treatment Train <sup>37</sup>		
Energy Source and Optimal Technology		Thermal [GJ]	Assoc. Parasitic Losses [MW]	Auxiliary Electricity [MW]	Pre-Treatment [MW]	Crystallization [MW]	Total [MW]
CPBT	Electricity CPBT	0	n/a	0.079	n/a	n/a	0.079
	LP Steam TVC	23.5	2.6	0.19	0.022	1.2	4.0
ZLD	Exhaust Gas FO	29.7	0	0.003	0.022	1.2	1.2
	Electricity MVC	0	n/a	1.52	0.022	1.2	2.74

#### 8.4.3 Revenue Tradeoffs in Steam Allocation

We combine the tradeoff curves shown in SI Figures S1 and S3 with retrofitted NETL plant limits on residual heat availability to identify the revenue maximizing allocation of electricity, steam, and residual heat to meet carbon capture and water treatment requirements under either CPBT or ZLD standards. Note that these tradeoff curves include the auxiliary electricity consumption of the separation processes, but do not include pre-treatment or post-

treatment ancillary processes like brine crystallization or CO<sub>2</sub> compression. The decision to allocate electricity, steam, or residual heat to mandatory environmental control technologies alters the retrofitted NETL 550 MW model plant revenue by approximately \$1,639/hr, from a no environmental control baseline of \$18,174/hr for the LP turbine. Capturing excess CO<sub>2</sub> to bank carbon credits would further widen this revenue window. Conducting this analysis on the basis of hourly revenue reflects the fact that operating costs are the majority of life-cycle costs for many of the technologies we examine and operating costs are likely to be more variable than capital costs. The contours of that decision space as a function of carbon price and the selected level of wastewater treatment (i.e. CPBT standard or ZLD standards set by EPA) are presented in Figure 8.3. The optimal allocations of electricity, LP steam, and residual heat for all five different energy strategies (feasible combinations of electricity, steam, and residual heat) is detailed in SI Section 3 and Figures S4-S8.

The revenue maximizing energy allocation strategy depends on the decision to deploy CPBT or ZLD FGD wastewater treatment trains at the retrofitted model NETL power plant, the date that carbon capture regulations come into effect, and the value of avoided carbon emissions. Under the 2017 regulatory scenario depicted in Figure 8.3A and 8.3B, carbon capture is not required for existing sources. It is more cost effective to treat wastewater using electricity-driven CPBT processes (Figure 8.3A) than residual heat powered FO processes, the most cost effective ZLD option in this scenario.

If the Clean Power Plan were to come into effect in 2030, the retrofitted NETL model plant would maximize revenue by allocating all residual heat (243 GJ) and a small amount of LP steam (59 GJ) to carbon capture processes (Figure 8.3C). Even if changes are made to the plant

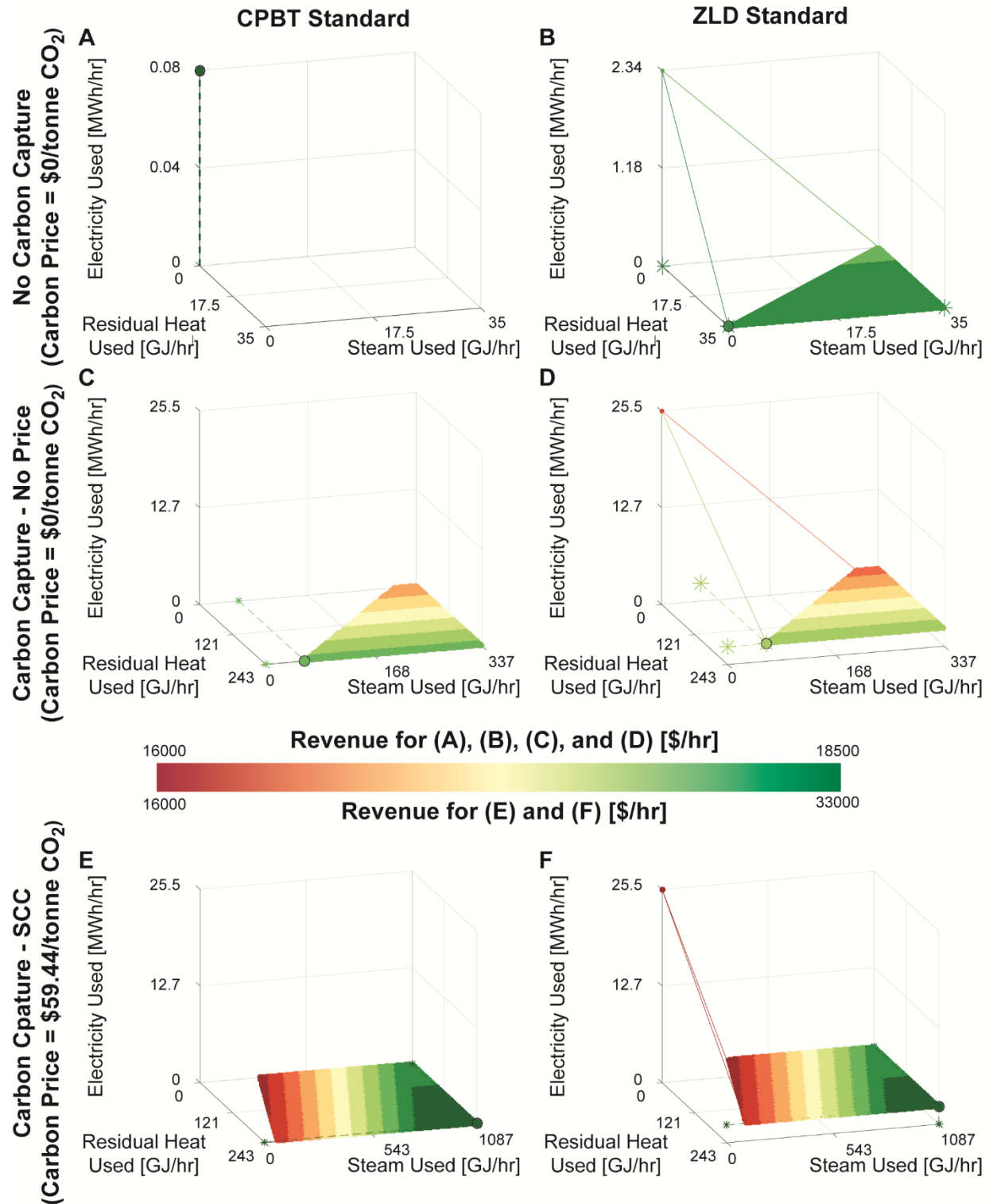


Figure 8.3. Revenue per hour as a function of steam, residual heat, and electricity used for environmental compliance. The price of electricity for all plots is \$70/MWh. In panels (A) and

*(B) carbon is not captured. In panels (C)-(E) carbon is captured. For panels (C) and (D) carbon has no price while in panels (E) and (F) carbon can be sold at the social cost of carbon of \$59.44/tonne. In panels (A), (C), and (E) FGD wastewater is treated to a CPBT standard and in panels (B), (D), and (F) FGD wastewater is treated to a ZLD standard.*

that reduce the amount of residual heat, the optimal allocation solution does not change. In all cases, the optimal solution will first use any available residual heat and second will use LP steam to make up the balance of energy needs. Complying with the CPBT standard is significantly more cost effective than complying with the ZLD one, as all residual heat has been allocated to carbon capture processes. Instead, ZLD is performed using electricity-driven MVC processes that directly reduce plant revenue.

In the final scenario, the retrofitted plant is given the option of capturing carbon in excess of the mandatory minimum capture rate and selling the resulting carbon credits at the Interagency Working Group's social cost of carbon price of \$59.44/tonne in 2030 (in 2015 dollars).<sup>39</sup> Considering only the carbon separation process, it is beneficial to capture excess CO<sub>2</sub> at a price above \$12.12/tonne and so the plant maximizes revenue by capturing excess carbon to sell carbon credits. When considering the CO<sub>2</sub> compression, transport, and underground storage costs, this CO<sub>2</sub> price will need to be significantly higher. Again, residual heat is fully allocated to carbon capture, so the most cost effective technologies for meeting either the CPBT or the ZLD standard are electricity driven processes.

## **8.5 Implications**

Fully transitioning away from high air, water, and carbon emission intensity coal-fired electricity generation is expected to take several decades. In the meantime, regulatory action to

minimize the human health and environmental impacts of coal-fired electricity generation will require extensive retrofit of existing CFPPs. The possible combinations of air and water emissions control technologies that could be installed at plants are vast, and design guidance on optimal retrofit approaches is severely lacking.

Using the NETL 550 MW CFPP as a case study, this work evaluates the energy efficiency and revenue implications of retrofitting a plant to comply with carbon capture and wastewater effluent standards. We evaluate several combinations of carbon capture and wastewater treatment technologies, as well as several different energy sources for driving these separations processes. In so doing, we provide the first estimates of potential energy off-sets associated with using residual heat captured at the power plant to drive carbon capture technologies. We also provide the first estimates of parasitic losses associated with wastewater treatment under the pending deadlines for compliance with newly promulgated ELGs. Finally, this work is the first to evaluate carbon capture and water treatment retrofits simultaneously.

This work demonstrates that plants undergoing retrofit will maximize their revenue by generating as much electricity as possible, while minimizing dispatch of steam and auxiliary electricity to environmental controls. As a result, each revenue maximizing case fully uses residual heat resources for water treatment or carbon capture, though the allocation of this residual heat between end uses depends upon regulatory and market forces. Minimizing the cost of plant compliance with environmental regulations will reduce rate increases experienced by rate payers in the transition to a lower human health and environmental impact electricity system dominated by renewable and natural gas generation.

Evaluating multiple plant retrofits simultaneously is also critical to capturing the effects of regulatory uncertainty in shaping plant decisions about technology adoption. Under a high

uncertainty regulatory future, plants may choose to optimize energy allocation according to near-term compliance requirements. For CFPPs today, this would entail allocating waste heat to FO water treatment to comply with upcoming ELG deadlines. In the long term, however, this capital investment may represent a sub-optimal allocation if carbon capture technologies are eventually mandated. Greater regulatory certainty will improve the probability that plants make optimal technology selections and minimize the costs of emission control.

## 8.6 Acknowledgements

This work was supported by the National Science Foundation under award number SEES-1215845 and CBET-1554117. This material is based upon work supported by the Department of Energy under Award Number DE-FE0024008. DG also acknowledges support from The Pittsburgh Chapter of ARCS Foundation (Achievement Rewards for College Scientists), the Steinbrenner Graduate Fellowship, and the Phillips & Huang Family Foundation Fellowship.

## 8.7 Nomenclature

### Symbols

$A$ :	Hourly Auxiliary Electricity Demand [kWh/hr]
$a$ :	Electricity Demand per m <sup>3</sup> of Water [kWh/m <sup>3</sup> ]
$C$ :	Carbon Captured per Hour [tonne CO <sub>2</sub> /hr]
$c$ :	Social Cost of Carbon [\$/tonne CO <sub>2</sub> ]
$E$ :	Electricity Generation per Hour [kWh/hr]
$e$ :	Electricity Price [\$/kWh]
$H_C$ :	Heat Duty in the MEA Regeneration Column [tonne CO <sub>2</sub> /kJ]
$H_w$ :	Heat Duty for Water Treatment [m <sup>3</sup> /kJ]
$h$ :	Enthalpy of Steam [kJ/kg]

$\eta$ :	Isentropic Efficiency of the Turbine-Generator [-]
$m$ :	Mass Flow Rate of Steam [kg/hr]
$P$ :	Parasitic Loss [kWh/m <sup>3</sup> ] and [kWh/tonne CO <sub>2</sub> ]
$R$ :	Hourly Revenue [\$/hr]
$S$ :	Share of Energy [%]
$\nabla$ :	Volume of FGD Wastewater to be Treated [m <sup>3</sup> /hr]
$W$ :	Water Production per Hour [m <sup>3</sup> /hr]
$w$ :	Water Price [\$/m <sup>3</sup> ]
$\omega$ :	Specified Water Production [m <sup>3</sup> /hr]
$\chi$ :	Specified Carbon Capture [tonne CO <sub>2</sub> /hr]

### Subscripts

$c$ :	Sent to Carbon Capture
$E$ :	Sent to Electricity
$f$ :	Wastewater Treatment Technology
$in$ :	Steam into Turbine, Water Treatment, and MEA Regeneration Column
$f$ :	Carbon Capture Technology
$out$ :	Steam out of Turbine, Water Treatment, and MEA Regeneration Column
$required$ :	Required Water Treatment or Carbon Capture for Environmental Compliance
$w$ :	Sent to Wastewater Treatment

### 8.8 References

1. U.S. Environmental Protection Agency Clean Power Plan.  
<http://www2.epa.gov/cleanpowerplan> (accessed July 20, 2015).

2. U.S. Environmental Protection Agency Steam Electric Power Generating Effluent Guidelines - 2015 Final Rule. <http://www.epa.gov/eg/steam-electric-power-generating-effluent-guidelines-2015-final-rule> (accessed September 30, 2015).
3. Khalilpour, R.; Abbas, A., HEN optimization for efficient retrofitting of coal-fired power plants with post-combustion carbon capture. *International Journal of Greenhouse Gas Control* **2011**, 5 (2), 189-199.
4. Le Moullec, Y., Assessment of carbon capture thermodynamic limitation on coal-fired power plant efficiency. *International Journal of Greenhouse Gas Control* **2012**, 7, 192-201.
5. Lively, R. P.; Chance, R. R.; Koros, W. J., Enabling Low-Cost CO<sub>2</sub> Capture via Heat Integration. *Industrial & Engineering Chemistry Research* **2010**, 49, 7550-7562.
6. Sanpasertparnich, T.; Idem, R.; Bolea, I.; deMontigny, D.; Tontiwachwuthikul, P., Integration of post-combustion capture and storage into a pulverized coal-fired power plant. *International Journal of Greenhouse Gas Control* **2010**, 4 (3), 499-510.
7. U.S. Environmental Protection Agency, Technical Development Document for the Effluent Limitations Guidelines and Standards for the Steam Electric Generating Point Source Category. Washington, D.C., 2015.
8. Zhai, H.; Rubin, E. S., Comparative Performance and Cost Assessments of Coal- and Natural-Gas-Fired Power Plants under a CO<sub>2</sub>Emission Performance Standard Regulation. *Energy & Fuels* **2013**, 27 (8), 4290-4301.
9. House, K. Z.; Harvey, C. F.; Aziz, M. J.; Schrag, D. P., The energy penalty of post-combustion CO<sub>2</sub> capture & storage and its implications for retrofitting the U.S. installed base. *Energy & Environmental Science* **2009**, 2 (2), 193.



10. Zhou, X.; Gingerich, D. B.; Mauter, M. S., Water Treatment Capacity of Forward-Osmosis Systems Utilizing Power-Plant Waste Heat. *Industrial & Engineering Chemistry Research* **2015**, *54* (24), 6378-6389.
11. National Energy Technology Laboratory *Cost and Performance Baseline for Fossil Energy Plants: Volume 1A Bituminous Coal (PC) and Natural Gas to Electricity*; Department of Energy - Office of Fossil Energy: Pittsburgh PA, 2015.
12. Li, B.; Duan, Y.; Luebke, D.; Morreale, B., Advances in CO<sub>2</sub> capture technology: A patent review. *Applied Energy* **2013**, *102*, 1439-1447.
13. Freguia, S.; Rochelle, G. T., Modeling of CO<sub>2</sub> Capture by Aqueous Monethanolamine. *AIChE Journal* **2003**, *49* (7), 1676-1686.
14. Harkin, T.; Hoadley, A.; Hooper, B., Reducing the energy penalty of CO<sub>2</sub> capture and compression using pinch analysis. *Journal of Cleaner Production* **2010**, *18* (9), 857-866.
15. Liu, X.; Chen, J.; Luo, X.; Wang, M.; Meng, H., Study on heat integration of supercritical coal-fired power plant with post-combustion CO<sub>2</sub> capture process through process simulation. *Fuel* **2015**, *158*, 625-633.
16. Junjie, Y.; Shufeng, S.; Jinhua, W.; Jiping, L., Improvement of a multi-stage flash seawater desalination system for cogeneration power plants. *Desalination* **2007**, *217* (1-3), 191-202.
17. Li, C.; Goswami, D. Y.; Shapiro, A.; Stefanakos, E. K.; Demirkaya, G., A new combined power and desalination system driven by low grade heat for concentrated brine. *Energy* **2012**, *46* (1), 582-595.

18. Shakib, S. E.; Hosseini, S. R.; Amidpour, M.; Aghanajafi, C., Multi-objective optimization of a cogeneration plant for supplying given amount of power and fresh water. *Desalination* **2012**, 286, 225-234.
19. Park, M. Y.; Shin, S.; Kim, E. S., Effective energy management by combining gas turbine cycles and forward osmosis desalination process. *Applied Energy* **2015**, 154, 51-61.
20. Supekar, S. D.; Skerlos, S. J., Reassessing the Efficiency Penalty from Carbon Capture in Coal-Fired Power Plants. *Environ Sci Technol* **2015**, 49 (20), 12576-84.
21. Versteeg, P.; Rubin, E. S., A technical and economic assessment of ammonia-based post-combustion CO<sub>2</sub> capture at coal-fired power plants. *International Journal of Greenhouse Gas Control* **2011**, 5 (6), 1596-1605.
22. Ramasubramanian, K.; Verweij, H.; Winston Ho, W. S., Membrane processes for carbon capture from coal-fired power plant flue gas: A modeling and cost study. *Journal of Membrane Science* **2012**, 421-422, 299-310.
23. Hagi, H.; Neveux, T.; Le Moullec, Y., Efficiency evaluation procedure of coal-fired power plants with CO<sub>2</sub> capture, cogeneration and hybridization. *Energy* **2015**, 91, 306-323.
24. González-Bravo, R.; Nápoles-Rivera, F.; Ponce-Ortega, J. M.; El-Halwagi, M. M., Multiobjective Optimization of Dual-Purpose Power Plants and Water Distribution Networks. *ACS Sustainable Chemistry & Engineering* **2016**.
25. González-Bravo, R.; Ponce-Ortega, J. M.; El-Halwagi, M. M., Optimal Design of Water Desalination Systems Involving Waste Heat Recovery. *Industrial & Engineering Chemistry Research* **2017**.

26. Gabriel, K. J.; El-Halwagi, M. M.; Linke, P., Optimization across the Water–Energy Nexus for Integrating Heat, Power, and Water for Industrial Processes, Coupled with Hybrid Thermal-Membrane Desalination. *Industrial & Engineering Chemistry Research* **2016**, *55* (12), 3442-3466.
27. Safari, I.; Walker, M. E.; Hsieh, M.-K.; Dzombak, D. A.; Liu, W.; Vidic, R. D.; Miller, D. C.; Abbasian, J., Utilization of municipal wastewater for cooling in thermoelectric power plants. *Fuel* **2013**, *111*, 103-113.
28. Theregowda, R.; Vidic, R.; Dzombak, D. A.; Landis, A. E., Life cycle impact analysis of tertiary treatment alternatives to treat secondary municipal wastewater for reuse in cooling systems. *Environmental Progress & Sustainable Energy* **2015**, *34* (1), 178-187.
29. Walker, M. E.; Safari, I.; Theregowda, R. B.; Hsieh, M.-K.; Abbasian, J.; Arastoopour, H.; Dzombak, D. A.; Miller, D. C., Economic impact of condenser fouling in existing thermoelectric power plants. *Energy* **2012**, *44* (1), 429-437.
30. Wu, L.; Hu, Y.; Gao, C., Optimum design of cogeneration for power and desalination to satisfy the demand of water and power. *Desalination* **2013**, *324*, 111-117.
31. Zhu, Q.; Luo, X.; Zhang, B.; Chen, Y.; Mo, S., Mathematical modeling, validation, and operation optimization of an industrial complex steam turbine network-methodology and application. *Energy* **2016**, *97*, 191-213.
32. Gingerich, D. B.; Mauter, M. S., Quantity, Quality, and Availability of Waste Heat from United States Thermal Power Generation. *Environ Sci Technol* **2015**, *49* (14), 8297-306.
33. National Energy Technology Laboratory *Cost and Performance Baseline for Fossil Energy Plants Volume 1 Bituminous Coal and Natural Gas to Electricity*; U.S. Department of Energy - Office of Fossil Energy: Pittsburgh, PA, 2013.

34. Ou, Y.; Zhai, H.; Rubin, E. S., Life cycle water use of coal- and natural-gas-fired power plants with and without carbon capture and storage. *International Journal of Greenhouse Gas Control* **2016**, *44*, 249-261.
35. Al-Karaghoul, A.; Kazmerski, L. L., Energy consumption and water production cost of conventional and renewable-energy-powered desalination processes. *Renewable and Sustainable Energy Reviews* **2013**, *24*, 343-356.
36. Bohra, M.; Mauter, M. S., Comparative assessment of waste-heat driven desalination processes: Steam temperature feed salinity, and auxiliary power determinants of water production capacity.
37. Gingerich, D. B.; Sun, X. B., A. Patrick; Azevedo, I. M. L.; Mauter, M. S., Spatially resolved air-water emissions tradeoffs improve regulatory impact analyses for electricity generation. *Proceedings of the National Academy of Science* **2017**.
38. Hausmann, A.; Sanicolo, P.; Vasiljevic, T.; Weeks, M.; Duke, M., Integration of membrane distillation into heat paths of industrial processes. *Chemical Engineering Journal* **2012**, *211-212*, 378-387.
39. Interagency Working Group on the Social Cost of Carbon, Technical Support Document: Technical Update of the Social Cost of Carbon for Regulatory Impact Analysis. Washington, D.C., 2015.
40. Wang, Y.-N.; Järvelä, E.; Wei, J.; Zhang, M.; Kyllönen, H.; Wang, R.; Tang, C. Y., Gypsum scaling and membrane integrity of osmotically driven membranes: The effect of membrane materials and operating conditions. *Desalination* **2016**, *377*, 1-10.

## **CHAPTER 9: SUMMARY AND RECOMMENDATIONS**

### **9.1 Summary of Work**

The main theme of this thesis is that decisions about water treatment need to account for the fact that they are embedded in already existing infrastructure and regulatory regimes. Failing to consider this may lead to outcomes with higher human health, environment, and climate (HEC) damages than what is being avoided by installing water treatment systems. Part I of this thesis focused on quantifying HEC damages from air emissions associated with electricity generation and chemical manufacturing required to treat water and wastewater. Part II examined the feasibility of forward osmosis (FO) as a technique for decoupling the use of electricity from water treatment in order to reduce damages associated with coal-fired power plant (CFPP) wastewater treatment.

Chapter 2 developed a model for incorporating one environment thinking into drinking water treatment in order to quantify the air emissions associated with water treatment. To do this, I built life-cycle models of electricity and chemical consumption for drinking water unit processes, and modeled the associated emissions of  $\text{NO}_x$ ,  $\text{SO}_2$ ,  $\text{PM}_{2.5}$ , and  $\text{CO}_2$ . I estimated air emission damages from currently installed drinking water treatment processes to be on the order of \$500 million USD annually. Fully complying with six recently proposed or finalized rules would increase baseline air emission damages by approximately 50%. Three-quarters of these damages originate from chemical manufacturing. Despite the magnitude of these air emission damages, the net benefit of currently implemented rules remains positive. For some proposed rules, however, the promise of net benefits remains contingent on technology choices.

Chapter 3 applied the model developed in Chapter 2 and used it in the context of one environment thinking to assess biogas-fueled electricity generation at municipal wastewater

treatment facilities. I used this model to calculate the potential damage reductions from installing biogas-fueled electricity generation across the United States to reduce grid electricity usage. I found that nationwide air emission damages in 2012 came to \$1,260 million with \$1,050 million attributed to electricity generation; \$190 million attributed to on-site emissions of VOCs, CH<sub>4</sub>, and N<sub>2</sub>O; and \$16.3 million from chemical manufacturing. Installing biogas-fueled electricity generation would create air emission reduction benefits of \$310 million, or 25% of damages associated with electricity generation. The installation of biogas-fueled electricity generation at the nation's wastewater treatment facilities therefore represents a meaningful way to reduce the air emission impacts of wastewater treatment for *some* facilities and create opportunities for wastewater treatment decentralization.

Chapter 4 leveraged this air-emission damage model to assess the emissions rebound resulting from the installation of flue gas desulfurization (FGD) wastewater treatment for compliance with the Effluent Limitation Guidelines (ELGs). I estimated that the ELGs will impose net costs of \$3.00/m<sup>3</sup> for chemical precipitation and biological wastewater treatment and \$11/m<sup>3</sup> for zero-liquid discharge (ZLD) wastewater treatment, with damages concentrated in regions containing a high fraction of coal generation or a large chemical manufacturing industry. My finding that FGD wastewater treatment imposes a net cost to society is robust to uncertainty in auxiliary power source, location of chemical manufacturing, and binding air emissions limits in non-compliant regions, among other variables. I concluded that future regulatory design will minimize compliance costs and HEC tradeoffs by adopting a one environment framework and regulating air, water, and solids emissions simultaneously while performing regulatory assessments that account for spatial variation in emissions impacts.

Chapter 5 calculated first-order estimates of the quantity, quality and spatio-temporal availability of waste heat from thermal power plants, an energy source that could reduce or eliminate the dependency of water treatment on electricity. By combining Energy Information Administration plant-level data with literature-reported process efficiency data, I developed estimates of the heat flux from individual US thermal power plants in 2012. Together these power plants discharged an estimated 18.9 billion GJ of waste heat in 2012, 4% of which was discharged at temperatures greater than 90 °C. I also characterized the temperature, spatial distribution, and temporal availability of this waste heat at the plant level and modeled the implications for the technical and economic feasibility of its end use. Increased implementation of flue gas desulfurization (FGD) technologies at CFPPs and the higher quality heat generated in the exhaust of natural gas fuel cycles are expected to increase the availability of residual heat generated by 10.6% in 2040.

Chapter 6 built a model of FO and integrated it with the model of waste heat availability at coal and natural gas fired power plants in order to develop first-order estimates of the water treatment capacity of waste heat driven FO. I quantitatively characterized three alternative processes for FO draw solute regeneration (DSR): distillation, steam stripping, and air stripping. I used the FO process model with distillation for the DSR processes to derive a first-order approximation of the water production capacity using waste heat at US electric power facilities. I found that it is possible to produce nearly 1.9 billion cubic meters of water annually using waste heat driven FO. This upper bound of FO water treatment capacity using low-grade heat sources at electric power facilities exceeds process water treatment demand for boiler water makeup and FGD wastewater systems.

Chapter 7 extended the work in Chapter 6 by performing a techno-economic assessment of FO for FGD gasification wastewater treatment under the ELGs. I did this by building a cost minimization framework for waste heat driven FO. I then used this model to develop forward osmosis and crystallization systems at four different case study power plants to treat FGD and gasification wastewaters to achieve ZLD. At a cost of \$2.01-\$2.02/m<sup>3</sup> for FGD wastewater treatment and \$2.33/m<sup>3</sup> for gasification wastewater, waste heat driven FO and crystallization is cheaper than the best available technology, mechanical vapor recompression and crystallization (MVCC). The conclusion that FO is economically competitive is robust over several design and non-design variables. Thus, FO and crystallization holds potential for achieving compliance with the ELGs at CFPPs and gasification plants.

Chapter 8 created an energy balance model for the maximizing the revenue by adjusting the allocation of steam, electricity, and waste heat at CFPPs while achieving compliance with wastewater and carbon capture regulations. I developed an energy balance model of the National Energy Technology Laboratory's 550 MW CFPP without carbon capture and added models of four carbon capture technologies (one electricity-driven and three thermal processes) and five wastewater treatment technologies (one electricity-driven and four thermal processes) to comply with the Clean Power Plan and ELGs. Plant revenue is maximized by using residual heat for wastewater treatment and carbon capture, but the optimal allocation of limited residual heat resources depends on the regulatory environment. If both carbon capture and zero liquid discharge wastewater treatment regulatory standards are in place, the plant maximizes revenue by allocating residual heat and steam to amine-based carbon capture and allocation of electricity to MVCC for water treatment.



Together, the preceding seven chapters and the models that are built in them can fill a crucial gap in one environment regulatory decision-making. The development of these models comes at a critical time as the United States builds a 21<sup>st</sup> century water and electricity infrastructure. Using and building on them will allow utilities and policy makers to make decision that will lead to net risk reductions for society.

## **9.2 Contributions**

In Chapter 1, I identified three gaps impairing the ability of regulators and water treatment professionals from adopting a one environment framework. These gaps were a lack of tools for quantifying tradeoffs across environmental media, a lack of water treatment technologies that decouple water treatment from primary energy sources, and a lack of decision support tools to assist utilities in addressing water and air pollution simultaneously. This thesis makes significant contributions in filling these gaps.

First, Chapters 2-4 expand upon life-cycle assessment (LCA) by creating life-cycle inventories of air emissions associated with water and wastewater treatment processes and assigning a dollar value to the resulting HEC damages. Using this model, I evaluated water treatment decisions for drinking water, municipal wastewater and industrial wastewater. For drinking water and industrial wastewater, I demonstrated how this model can be used for one environment decision making in regulatory analyses by accounting for cross-sector and cross-media impacts in the benefit-cost analyses for six drinking water rules and the ELGs.

Second, Chapters 5-7 examine the availability of waste heat from United States thermal power generators and the feasibility of FO as a waste heat driven water treatment technology. The work in this thesis updated estimates of waste heat quantity and spatio-temporal availability from before the shift to natural gas in the beginning of the current decade. I also explored the

limits of waste heat driven FO to establish upper bounds on the water treatment capacity of it as power plant waste heat driven technologies.

Finally, Chapter 8 developed a method for simultaneously addressing compliance with carbon capture and wastewater treatment regulations at coal-fired power plants. This method provides a framework for CFPPs to holistically consider and minimize the impacts of environmental compliance on their revenue. I also used this method to highlight the impacts of regulatory uncertainty on the ability of CFPPs to make cost-effective and energy-efficient water treatment technologies.

### **9.3 Recommendations**

Several recommendations for different audiences arise from the work presented in this thesis. The first set of recommendations is for regulators and highlights tools to promote a one environment framework in developing environmental regulations. The second set of recommendations is designed for municipal water and wastewater utilities in selecting new technologies to install in order to comply with regulations. The third set of recommendations is for CFPPs on achieving compliance with new and potential environmental regulations. The final set of recommendations for researchers highlights several potential areas of research to support holistic one environment decision-making.

#### *9.3.1 Recommendations for Regulators*

There are three recommendations for improving regulatory analyses and the regulatory process that can be drawn from this work.

1. *Benefits and costs from the entire life-cycle of a process should be accounted for in BCAs.* This was a consistent theme in Part I. Benefit-cost analyses can be designed to promote holistic thinking in regulatory analyses.<sup>1,2</sup> However, the Environmental

Protection Agency (EPA) has not consistently considered life-cycle damages when regulations require additional electricity or chemical inputs. As was shown in this work, adding in damages from electricity generation and chemical manufacturing has the potential to lead to different regulatory and technology choices.

2. *Spatially-resolved data should be used in regulatory analyses rather than average data.*

While I used spatially-resolved data throughout Part I, the difference in using spatially-resolved and non-spatially resolved damage and emissions data is highlighted in Chapter 4. The national average marginal damage estimates used by the EPA in the BCA for the ELGs leads to an overestimate of 25% for air emission damages associated with the CPBT compliance option. As researchers have developed non-computationally intensive, spatially-resolved models for air emission damages and electricity generation, these tools should be used in policy analyses to develop more accurate results with little additional computation burden imposed.

3. *Piecemeal regulatory activity and regulatory uncertainty leads to sub-optimal compliance decisions.* The impact of piecemeal regulatory activity on environmental performance was addressed in Chapter 4 and the impact of regulatory uncertainty was discussed in Chapter 8. When the EPA promulgated rules under the 1990 Clean Air Act Amendments, it effectively required FGD use but did not consider the impacts of FGD wastewater treatment. Considering FGD wastewater treatment may have led to more plants installing dry FGD systems instead of wet FGD systems, protecting public health from harm due to reductions in FGD wastewater production. Finally, the uncertainty surrounding future carbon capture standards prevents plants from making revenue maximizing energy and technology choices for FGD wastewater treatment and carbon

capture. Utilizing cluster rules or “bubble” regulatory frameworks play a vital role in creating this certainty.

### *9.3.2 Recommendations for Municipal Water Utilities*

There are two recommendations for municipal water and wastewater treatment systems that can be drawn from this work.

1. *While the benefits of drinking water treatment may outweigh compliance costs and associated air emission damages, the technology choices for compliance can lead to increases in human health damage.* This point, that compliance technology selection matters, was a key takeaway from Chapter 2. In that Chapter, I found that choosing between either reverse osmosis or granular activated carbon for compliance with the PFOA/PFOS advisory guidelines led to additional air emission damages to society of nearly one billion dollars (in 2014\$) every year. This difference may or may not be compensated for by the higher quality water produced by reverse osmosis.
2. *Biogas-fueled electricity generation can reduce the air emission damages associated with municipal wastewater treatment by 22%.* As shown in Chapter 3, there is a benefit to society from biogas-fueled electricity generation of \$125 million in averted air emissions. These benefits significantly vary across the United States, but are concentrated in areas with a grid that is reliant on coal (e.g. Ohio). Furthermore, biogas-fueled electricity generation can also be used to support distributed wastewater treatment, if the production of biosolids can be improved to allow for implementation at smaller scales.

### *9.3.3 Recommendations for Coal-Fired Power Plants*

There are two recommendations for CFPPs that can be drawn from this work.

1. *Power plants need to make compliance decision technologies holistically, developing compliance solutions for water, air, and solid wastes simultaneously.* Chapter 8 developed a model to facilitate holistic decision making by power plants, which is distinct from past approaches of addressing environmental pollution one contaminant at a time. However, one of the challenges CFPPs face in simultaneously addressing environmental pollutants is regulatory uncertainty. Until power plants have greater clarity surrounding the ELGs and Clean Power Plan, their ability to make cost-effective compliance decisions will be limited.
2. *Waste heat driven forward osmosis is cheaper than conventional technologies for achieving zero liquid discharge of flue gas desulfurization wastewater.* Part II examined the use of waste heat for environmental compliance, with Chapters 6 and 7 focusing on the techno-economic feasibility of waste heat driven forward osmosis for wastewater treatment. Forward osmosis has the potential to save plants \$0.95-\$0.99/m<sup>3</sup> compared to MVCC. More importantly, the use of waste heat can reduce the air-water tradeoffs that were modeled in Part I of this thesis by decoupling water treatment from electricity usage.

#### *9.3.4 Recommendations for Researchers*

There are five recommendations for researchers on future lines of research that can be drawn from this work.

1. *Creating tools for performing triple-bottom sustainability analysis of municipal water systems will allow for more holistic analyses of water treatment decision making.*

As this thesis demonstrates, decisions about water treatment need to be made holistically, and that includes thinking about the economic, environmental, and social sustainability.

Tools for water treatment exist that focus on environmental life-cycle assessment,<sup>3-5</sup> but these tools do not allow for decision makers to quantify trade-offs between environmental impacts, costs, social impacts, and the benefits of water treatment. Developing models and frameworks to facilitate analyses of these tradeoffs will fill a critical gap in the literature and contribute to the national conversation about building a 21<sup>st</sup> century water infrastructure.

2. *Models of compliance options for the effluent limitation guidelines need to be created and incorporated into existing power plant models.* The Integrated Environmental Control Model (IECM)<sup>9</sup> is an already existing model of thermal power plants with air emission control technologies and is frequently used for policy analysis. However, IECM lacks many of the water treatment technologies that plants can choose from in order to comply with the ELGs. Expanding IECM's capacity to model water and wastewater treatment at CFPPs will assist policy makers, industry, and regulators in choosing between alternative system designs.
3. *Marginal water emission damage models need to be developed to complement similar models for marginal air emission damages.* The analysis in Part I used the spatially-resolved marginal air emission damage models AP2<sup>6</sup> and EASIUR.<sup>7</sup> However, similar analyses cannot be performed for water emissions because comparable models do not exist. This lack of a marginal water damage models impedes their inclusion in regulatory analyses, and policy analysts rely on less-accurate contingent valuation or revealed preference models instead.<sup>8</sup> Developing a marginal water emission damage model is crucial for advancing regulatory analysis.

4. *Potential applications for waste heat should be focused on on-site uses.* Researchers have often cited waste heat as a source of energy for water treatment processes.<sup>10-12</sup> However, as shown in Chapter 5, transporting heat far away from plants is economically infeasible and waste heat is only available when the plant operates. This severely limits its potential and means that waste heat usage is unlikely to happen off the power plant site. Development of technologies that use waste heat from power plants should focus on meeting energy needs on-site for achieving environmental compliance or improving the efficiency of the plant.
5. *Incorporate cost into the energy allocation tradeoff model used for environmental compliance at CFPPs.* The model presented in Chapter 8 focused on optimizing revenue, but real power plants are operated to maximize the profit and not just revenue. Integrated costs into the tradeoff model will allow for the analyses to be rerun in a way that finds the revenue maximizing strategy for achieving environmental compliance.

By adopting these twelve recommendations, municipal water systems, CFPPs, regulators, and researchers can work together to create 21<sup>st</sup> century utility sectors that meet society's needs while reducing HEC damages from water *and* air pollution.

## 9.4 References

1. Arrow, K. J.; Cropper, M. L.; Eads, G. C.; Hahn, R. W.; Lave, L. B.; Noll, R. G.; Portney, P. R.; Russell, M.; Schmalensee, R.; Smith, V. K. S., Robert N., Is There a Role for Benefit-Cost Analysis in Environmental, Health, and Safety Regulation? *Science* **1996**, 272, 221-222.

2. Lave, L. B., Benefit-Cost Analysis: Do the Benefits Exceed the Costs? In *Risks, Costs, and Lives Saved: Getting Better Results from Regulation*, Hahn, R. W., Ed. The AEI Press: Washington, D.C., 1996; pp 104-134.
3. Stokes, J. R.; Hovarth, A., Energy and Air Emission Effects of Water Supply *Environmental Science & Technology* **2009**, *43*, (2680-2687).
4. Stokes, J. R.; Horvath, A., Supply-chain environmental effects of wastewater utilities. *Environmental Research Letters* **2010**, *5*, (1), 014015.
5. Mery, Y.; Tiruta-Barna, L.; Benetto, E.; Baudin, I., An integrated "process modelling-life cycle assessment" tool for the assessment and design of water treatment processes. *International Journal of Life Cycle Assessment* **2013**, *18*, 1062-1070.
6. Muller, N. Z., Using index numbers for deflation in environmental accounting. *Environment and Development Economics* **2013**, *19*, (04), 466-486.
7. Heo, J.; Adams, P. J.; Gao, H. O., Reduced-form modeling of public health impacts of inorganic PM<sub>2.5</sub> and precursor emissions. *Atmospheric Environment* **2016**, *137*, 80-89.
8. Morgan, M. G., *Theory and Practice in Policy Analysis: Including Applications in Science and Technology*. Cambridge University Press: New York, NY, 2017.
9. Rubin, E. S.; Zhai, H. About IECM. <https://www.cmu.edu/epp/iecm/about.html> (July 5, 2017),
10. Ghalavand, Y.; Hatamipour, M. S.; Rahimi, A., A review on energy consumption of desalination processes. *Desalination and Water Treatment* **2014**, *54*, 1526-1541.
11. Elimelech, M.; Phillip, W. A., The future of seawater desalination: energy, technology, and the environment. *Science* **2011**, *333*, (6043), 712-7.



12. McGinnis, R. L.; Elimelech, M., Global Challenges in Energy and Water Supply: The Promise of Engineered Osmosis. *Environmental Science & Technology* **2008**, *42*, (23), 8625-8629.

## **APPENDICES**

## **APPENDIX 1: SUPPORTING INFORMATION FOR CHAPTER 2 - AIR EMISSIONS DAMAGES FROM MUNICIPAL DRINKING WATER TREATMENT UNDER CURRENT AND PROPOSED REGULATORY STANDARDS**

### **Supporting Information Summary:**

The supporting information contains descriptions of 1) the six drinking water standards with compliance modeled in this analysis; 2) data sources; 3) drinking water treatment unit process description and inputs; 4) chemical manufacturing location sensitivity analyses; 5) emissions and damages from drinking water treatment using AP2 and EASIUR; and 6) emissions and damages from the individual drinking water standards.

This supporting information is 22 pages long and contains 7 figures (Figures S1-S7) and 17 tables (Tables S1-S17).

## 1.0 Drinking Water Standards

### 1.1 *Arsenic National Primary Drinking Water Regulation*

While implementing the Safe Drinking Water Act, the Environmental Protection Agency (EPA) established a 50 ug/L level for arsenic in drinking water. Congress, in the 1996 Safe Drinking Water Act Amendments, directed the EPA to introduce an arsenic regulation by January 1, 2000. In June 2000, the EPA proposed a 5 ug/L arsenic concentration. The EPA finalized a 10 ug/L regulation for arsenic in drinking water in January 2001.<sup>1</sup>

The 10 ug/L arsenic level serves as the regulatory limit in our analysis.

### 1.2 *Long-Term Enhanced Surface Water Treatment Rule*

In 1989, the EPA established the Surface Water Treatment Rule, requiring filtration and disinfection for most drinking water systems that source their water from surface water or ground water sources under the direct influence of surface water. Following the Milwaukee *Cryptosporidium* outbreak, the EPA established the Interim Enhanced Surface Water Treatment Rule that strengthened existing provisions to reduce the risks of *Cryptosporidium* to consumers of large systems that serve more than 10,000 people. With the Long Term 1 Enhanced Surface Water Treatment Rule promulgated in 2002, the EPA expanded these protections to systems that served less than 10,000 people and formalized the risk trade-offs between microbial inactivation and disinfection byproducts. In 2006 the EPA finalized the Long Term 2 Enhanced Surface Water Treatment Rule, focusing on particular systems that were at higher risk for *Cryptosporidium* contamination or disinfection byproduct.<sup>1</sup>

The 70 ug/L of total trihalomethanes and 60 ug/L of haloacetic acids levels serve as the regulatory limits in our analysis for disinfectant byproducts.

### 1.3 *Lead and Copper Rule*

In 1991, the EPA promulgated a standard of 15 ug/L of lead or 1.3 mg/L of copper in no more than 10% of customer taps that are sampled. Since 1991, the EPA has promulgated two minor revisions, a set of short-term revisions to strengthen consumer education recommendations. The EPA is currently investigating the potential for long-term revisions to the Lead and Copper Rule that will strengthen the Rule. These revisions are not expected to decrease the maximum contaminant level for lead or copper, but to continue to refine the public education, sampling, lead service line replacement, and corrosion control requirements under the Rule.<sup>2</sup>

The 15 ug/L of lead or 1.3 mg/L of copper levels serves as the regulatory limit in our analysis.

### 1.4 *Hexavalent Chromium*

In 1991, the EPA promulgated a final total chromium drinking water rule of 0.1 mg/L of total Chromium (Cr (III) and Cr (VI)). A 2008 study conducted by the Department of Health and Human Services indicated that Cr (VI) is a potential carcinogen if ingested. The EPA is currently reassessing the health effects of Cr (VI) ingestion and will not reassess either a Cr (VI) or total Chromium drinking water standard until the health assessment is completed.<sup>3</sup>

The State of California established a separate standard for Cr (VI) of 0.01 mg/L in 2014. This 0.01 mg/L level serves as the regulatory limit in our analysis.<sup>4</sup>

### *1.5 Strontium*

Under the Safe Drinking Water Act, the EPA is required to publish a list, known as the Contaminant Candidate List (CCL) of potential candidates for a new drinking water regulation every five years. The EPA then must select at least five contaminants on the CCL and make a regulatory determination. Strontium was selected from the third contaminant candidate list (CCL3) for a regulatory determination. In 2014, the EPA issued a preliminarily favorable regulatory determination, i.e. to regulate Strontium. In January 2016, the EPA delayed the final regulatory determination of Strontium. The EPA did this in order to evaluate additional scientific evidence and to determine if there is a meaningful potential for risk reduction nationwide.<sup>5</sup>

The EPA currently has a health reference level of 1.5 mg/L. This level serves as the regulatory limit in our analysis.

### *1.6 Drinking Water Health Advisories for PFOA and PFOS*

In 2016, the Environmental Protection Agency finalized drinking water health advisories for two perfluoroalkyl substances (PFASs), perfluorooctanoic acid (PFOA) and perfluorooctanesulfonic acid (PFOS). The 2016 Drinking Water Health Advisory updated a provisional advisory set by the EPA in 2009. The drinking water health advisory is set at a combined PFOA and PFOS concentration of 70 ng/L. The 70 ng/L level was set to protect the most sensitive subpopulations of breastfed infants and fetuses.<sup>6</sup>

If a system measures more than a combined 70 ng/L of PFOA and PFOS in a sample, they should then quickly complete another round of sampling to confirm the measurements and assess the scope and source of the contamination. If additional sampling confirms PFOA PFOS levels above 70 ng/L, a drinking water system should notify their state primacy agency and their consumers. Communication to consumers should include the risks to fetuses, what actions the system is taking to address the high levels of PFOA and PFOS, and what actions consumers can take to protect themselves. Systems are recommended to either change their water source to avoid PFOA and PFOS or install activated carbon or reverse osmosis to reduce PFOA/PFOS concentration. Consumers can also install certain home treatment systems to reduce PFOA and PFOS concentrations.<sup>6</sup>

The EPA included PFOA and PFOS in the third Unregulated Contaminant Monitoring Rule list and has started efforts to update their risk assessment of PFASs. These are the first steps in starting the process for developing a new drinking water standard.

The current health advisory for PFOA and PFOS of 70 ng/L serves as the regulatory limit in our analysis.

## 2.0 Data Sources

### 2.1 *Drinking Water System Data*

For drinking water data, we use three different data sources: the Safe Drinking Water Information System (SDWIS), the Unregulated Contaminant Monitoring Rule (UCMR) and the Information Collecting Rule (ICR).

The Safe Drinking Water Information System is a dataset of all drinking water systems in the United States.<sup>7</sup> Data is typically self-reported by individual facilities available at the facility- or utility-level. From SDWIS, we take the state a facility is located in, the unit processes that are installed at each facility, the type of population served (i.e. community, transient non-community, non-transient non-community), and the population served by the system.

### 2.2 *Electricity Generation Emissions Data*

For electricity generation emissions data, we use two different data sources: marginal emission factors and average electricity emissions factors.

The marginal emission factors represent the emissions per kWh from the generator that is required to meet the last kWh of demand for a state.<sup>8</sup> We have marginal emission factors for NO<sub>x</sub>, SO<sub>2</sub>, and CO<sub>2</sub>. The marginal emission factors used for this paper are updated versions of the estimates developed in Siler-Evans et al.<sup>8</sup>

For PM<sub>2.5</sub> emissions we use average emission factors from EPA's Emission Inventories.<sup>9</sup> We calculate state-level average emission factors for PM<sub>2.5</sub> by taking the total emissions of PM<sub>2.5</sub> from electric generators in a state divided by the total electricity generation in that state.

### 2.3 *Chemical Manufacturing Emissions Data*

Data on chemical manufacturing emissions comes from four different sources.<sup>10-13</sup> The direct air emission and energy inputs are listed in Table S1.

*Table S1. Direct air emissions and energy inputs for chemicals consumed in water treatment.*

Chemical	Direct Air Emissions [kg <sup>-1</sup> ]	Energy Inputs [kg <sup>-1</sup> ]	Ref
Granular Activated Carbon		0.58 kWh Elec	10
		0.36 kg Bit Coal	
		0.126 m <sup>3</sup> Nat Gas	
Hypochlorite		0.017 kWh Elec	11
Generic Organic Chemical*	0.12 g NO <sub>x</sub>	5.4 kWh Elec	12
	0.098 g SO <sub>2</sub>	7.8x10 <sup>-4</sup> kg Bit Coal	
	0.0076 g PM <sub>2.5</sub>	2.3x10 <sup>-4</sup> L Pet	
	170g CO <sub>2</sub>	0.024 L RFO	
		0.12 m <sup>3</sup> Nat. Gas	
		9.3x10 <sup>-4</sup> L Diesel	
Generic Inorganic Chemical**	0.15 g SO <sub>2</sub>	0.068 kWh Elec	12
	0.056 g PM <sub>2.5</sub>	0.172 kg Bit Coal	
	770 g CO <sub>2</sub>	3.2x10 <sup>-5</sup> L Pet	
		0.021 m <sup>3</sup> Nat Gas	
		9.5x10 <sup>-4</sup> L Diesel	
Lime	96.5 g PM <sub>2.5</sub>	8.5 kWh Elec	13
	415 g CO <sub>2</sub>	0.108 kg Bit Coal	
		3.2x10 <sup>-5</sup> L Pet	
		0.021 m <sup>3</sup> Nat Gas	
		9.5x10 <sup>-4</sup> L Diesel	
Iron (III) Chloride		0.0019 kWh Elec	11

\* Includes Bimetallic Phosphate, Hexametaphosphate, Orthophosphate, Polyphosphate, Membrane Cleaning Chemicals, and Corrosion Inhibitors

\*\* Includes Alum, Iodine, Fluoride, Silicate, Permanganate, Sodium Bisulfate, Sodium Sulfite, and Sulfur Dioxide

Table S2 presents the air emissions for the five different fuel types used in manufacturing the chemicals used in drinking water treatment.

*Table S2. Air Emissions from Energy Sources<sup>13</sup>*

	CO <sub>2</sub> [g]	NO <sub>x</sub> [g]	SO <sub>2</sub> [g]	PM <sub>2.5</sub> [g]
Bituminous Coal [kg <sup>-1</sup> ]	2633	5.75	16.6	0
Petroleum [L <sup>-1</sup> ]	1721	2.6	0	0
Residual Fuel Oil [L <sup>-1</sup> ]	3263.2	7.03	5.12	0
Natural Gas [m <sup>-3</sup> ]	1960.9	1.6	0.0101	0
Diesel [L <sup>-1</sup> ]	2730	2.87	0.599	0

### 3.0 Drinking Water Treatment Unit Process Description and Inputs

Table S3 lists the unit processes for drinking water treatment included in this study. It includes the description of the process, the electrical inputs into the process, and the chemical inputs that are consumed in the process.

*Table S3. Unit processes modeled in this study for drinking water treatment.*

<i>Unit Process</i>	<i>Description</i>	<i>Electrical Input [kWh/m³]</i>	<i>Chemical Inputs [mg/L]</i>
<i>Suspended Solids Removal</i>			
Flocculation	Create floc through gentle mixing following coagulation.	0.008-0.022	80 (Alum)
Coagulation	Addition of a coagulant to the water to allow for the creation of floccs.	0.0005-0.0014	
Sedimentation	Remove settleable solids from in a quiescent basin.	0.0005-0.001	
<i>Filtration</i>			
Filtration, Generic	Filtration using a generic filter media	0.005-0.014	
Filtration, Cartridge	Filtration using a generic cartridge	0.005-0.014	
Filtration, Diatomaceous Earth	Filtration using diatomaceous earth as filter media	0.005-0.014	
Filtration, Greensand	Filtration using greensand as filter media.	0.005-0.014	
Filtration, Pressurized Sand	Filtration using sand media, with the influent water pressurized to overcome head loss in the filter.	0.005-0.014	
Filtration, Rapid Sand	Filtration using sand as the media, with removal that takes place throughout the media allowing for higher loading rates	0.005-0.014	
Filtration, Slow Sand	Filtration using sand as the media, with removal that takes place only at the top of the media	0.005-0.014	



Filtration, UF Membrane	Filtration using an ultrafiltration membrane	0.005-0.014	4.1 (Membrane Cleaning)
<i>Disinfection</i>			
Surface Water Hypochlorination	Addition of sodium hypochlorite to surface water sourced water for disinfection	0.00002-0.0005	1.9 (Hypochlorite)
Groundwater Hypochlorination	Addition of sodium hypochlorite to groundwater sourced water for disinfection	0.002	1.9 (Hypochlorite)
Iodine Addition	Addition of iodine for disinfection	0.008-0.022	1 (Iodine)
Ozonation	Addition for ozone for disinfection	0.23-0.35	
Ultraviolet Disinfection	Use of UV light for disinfection	0.01-0.5	
<i>Finished Water Quality Improvement</i>			
Fluoridation	Addition of fluorosillicic acid, sodium fluorosilicate, or other fluoride compound to promote dental health	0.008-0.022	1 (Fluoride)
Lime Soda Ash Softening	Addition of lime, quicklime, and/or soda ash in order to remove divalent ions	0.0085-0.023	7 (Soda Ash)
pH Adjustment	Addition of acid or base in order to adjust the pH of the finished water.	0.008-0.022	1 (Generic Inorganic)
Reducing Agent Addition	Addition of reducing agents to finished water	0.008-0.022	1 (Generic Inorganic)
<i>Corrosion Control</i>			
Bimetallic Phosphate Addition	Addition of bimetallic phosphate as a corrosion inhibitor	0.008-0.022	1 (Bimetallic Phosphate)
Hexametaphosphate Addition	Addition of hexametaphosphate as a corrosion inhibitor	0.008-0.022	1 (Hexametaphosphate)
Orthophosphate Addition	Addition of orthophosphate as a corrosion inhibitor	0.008-0.022	1 (Orthophosphate)
Polyphosphate Addition	Addition of polyphosphate as a corrosion inhibitor	0.008-0.022	1 (Polyphosphate)

Silicate Addition	Addition of silicate as a corrosion inhibitor	0.008-0.022	17 (Silicate)
Permanganate Addition	Addition of permanganate as a corrosion inhibitor	0.008-0.022	0.01 (Permanganate)
Sodium Bisulfate Addition	Addition of sodium bisulfate as a corrosion inhibitor	0.008-0.022	1 (Sodium Bisulfate)
Sodium Sulfite Addition	Addition of a sodium sulfite as a corrosion inhibitor	0.008-0.022	1 (Sodium Sulfite)
Sulfur Dioxide Addition	Addition of sulfur dioxide as a corrosion inhibitor	0.008-0.022	1 (Sulfur Dioxide)
<hr/> <i>Advanced Processes</i>			
Granular Activated Carbon	Use of granular activated carbon for pollution removal by adsorption.	0.029	76 (Activated Carbon)
Reverse Osmosis	Use of reverse osmosis for desalination or difficult to remove pollutants.	0.7989	4.1 (Membrane Cleaning)
<hr/>			

## 4.0 Chemical Manufacturing Sensitivity Analyses

In the main manuscript, we assume that the manufacturing of chemicals used for drinking water treatment follows the same distribution as the chemical manufacturing sector. To test the sensitivity of our results to this assumption, we compare it to five alternative scenarios. These five alternatives include: (1) no additional emissions from chemical manufacturing taking place in states that have non-attainment areas, (2) chemicals are manufactured evenly across the 48 contiguous states, (3) all chemicals are manufactured in the state with the highest marginal damages in scenario 2 (i.e. New Jersey), (4) all chemicals are manufactured in the state with the lowest marginal damages in scenario 2, (i.e. Nebraska) and (5) all chemicals are manufactured off-shore and so only climate damages occur to U.S. residents.

### 4.1 Accounting for Binding Air Emission Regulations on Chemical Manufacturing in Non-Attainment Areas

The first alternative scenario is that chemical manufacturing that takes place in states that have non-attainment areas do not emit additional chemicals, i.e. are subject to binding emission limitations. To model these binding emission limits on chemical manufacturing we assumed no additional emissions of NO<sub>x</sub>, SO<sub>2</sub>, and PM<sub>2.5</sub> in a state with one or more non-attainment areas for ozone (no additional emissions of NO<sub>x</sub>), SO<sub>2</sub>, and PM<sub>2.5</sub>. As shown in Table S4, this will reduce damages of those pollutants.

Table S4. Emissions and damages from chemical manufacturing with binding air emission regulations.

	Baseline Treatment Train		Regulated Treatment Train	
	Emissions [tons/yr]	Damages [\$M/yr]	Emissions [tons/yr]	Damages [\$M/yr]
NO <sub>x</sub>	1,900	12	6,300	38
SO <sub>2</sub>	2,400	71	3,200	91
PM <sub>2.5</sub>	2,000	94	2,100	101
CO <sub>2</sub>	2,100,000	93	5,000,000	215
<i>Total</i>		270		446

### 4.2 Chemicals are Manufactured Evenly Across 48 Contiguous US States

The second alternative scenario is that the chemicals that are manufactured evenly throughout the contiguous US states. For this analysis, we scale emissions in a state by 1/48. The modified version of Equation 3 in the manuscript is shown in Equation S1.

$$M_{h,j,l}^C = \left(\frac{1}{48}\right) * [\sum_f V_i Q_{i,f,j} (e_{cm,f,h}^C + \sum_d E_{d,f}^D e_{d,h}^D + E_f^W \sum_i e_{mf,l,h} \frac{V_i}{\sum_i V_i})] \quad (S1)$$

Table S5 shows the resulting emissions and damages from chemical manufacturing in the baseline and regulated treatment trains.

*Table S5. Emissions and damages from chemical manufacturing with chemical manufacturing evenly distributed across the contiguous states.*

	Baseline Treatment Train		Regulated Treatment Train	
	Emissions [tons/yr]	Damages [\$M/yr]	Emissions [tons/yr]	Damages [\$M/yr]
NO <sub>x</sub>	2,100	1.3	6,700	41
SO <sub>2</sub>	5,500	130	6,400	160
PM <sub>2.5</sub>	2,400	120	2,500	130
CO <sub>2</sub>	2,100,000	93	5,000,000	220
<i>Total</i>		363.4		541

#### *4.3 Chemicals are Manufactured in the State with Highest Damages*

A third alternative scenario is to assume that all chemicals are manufactured in New Jersey, the state with the highest marginal damages for chemical manufacturing. Table S6 shows the resulting emissions and damages from chemical manufacturing under this scenario.

*Table S6. Emissions and damages from chemical manufacturing with all chemicals manufactured in New Jersey.*

	Baseline Treatment Train		Regulated Treatment Train	
	Emissions [tons/yr]	Damages [\$M/yr]	Emissions [tons/yr]	Damages [\$M/yr]
NO <sub>x</sub>	2,100	28	6,900	96
SO <sub>2</sub>	5,100	380	5,200	380
PM <sub>2.5</sub>	2,400	660	3,000	820
CO <sub>2</sub>	2,100,000	91	5,000,000	216
<i>Total</i>		1,158		1,517

#### *4.4 Chemicals are Manufactured in the State with Lowest Damages*

A fourth alternative scenario is to assume that all chemicals are manufactured in Nebraska, the state with the highest marginal damages for chemical manufacturing. Table S7 shows the resulting emissions and damages from chemical manufacturing under this scenario.

*Table S7. Emissions and damages from chemical manufacturing with all chemicals manufactured in Nebraska.*

	Baseline Treatment Train		Regulated Treatment Train	
	Emissions [tons/yr]	Damages [\$M/yr]	Emissions [tons/yr]	Damages [\$M/yr]
NO <sub>x</sub>	2,300	12	7,500	41
SO <sub>2</sub>	6,100	43	8,300	58
PM <sub>2.5</sub>	2,300	32	2,700	38
CO <sub>2</sub>	2,300,000	98	5,500,000	240
<i>Total</i>		186		376

#### *4.5 Chemicals are Manufactured Off-Shore*

The last scenario modeled is one in which all chemicals are manufactured off-shore. In this scenario, there are no health or environmental damages in the United States but only climate damages from CO<sub>2</sub> emissions. For the baseline treatment train, there are 2.1 million short tons per year in emissions of CO<sub>2</sub> and \$93 million in damages (in \$2014). With the six studied regulations in place, there are 5.2 million short tons per year in emissions of CO<sub>2</sub> and \$230 million in damages (in \$2014).

## 5.0 Emissions and Damages from Drinking Water Treatment

### 5.1 Using AP2 for Valuing Air Emission Damages

Tables S8 and S9 report the total emissions and damages that result from the baseline treatment case and the regulatory compliance from the six standards case examined in this manuscript.

*Table S8. Emissions and damages resulting from the baseline treatment train.*

	Electricity Generation		Chemical Manufacturing	
	Emissions [tons/yr]	Damages [\$M/yr]	Emissions [tons/yr]	Damages [\$M/yr]
NO <sub>x</sub>	940	6.0	2,100	13
SO <sub>2</sub>	1,400	34	5,500	130
PM <sub>2.5</sub>	340	26	2,400	120
CO <sub>2</sub>	1,600,000	68	2,100,000	93
Total		133.8		363

*Table S9. Emissions and damages resulting from the baseline treatment train and installation of technologies to comply with the six drinking water standards studied here.*

	Electricity Generation		Chemical Manufacturing	
	Emissions [tons/yr]	Damages [\$M/yr]	Emissions [tons/yr]	Damages [\$M/yr]
NO <sub>x</sub>	1,300	7.9	7,200	44
SO <sub>2</sub>	2,000	50	6,500	160
PM <sub>2.5</sub>	440	34	2,900	150
CO <sub>2</sub>	2,000,000	88	5,200,000	230
Total		179.0		581

### 5.2 Using EASIUR for Valuing Air Emission Damages

As described in the main manuscript, we repeat the analysis using the EASIUR (Estimating Air pollution Social Impact Using Regression) model<sup>14, 15</sup> to price the damages associated with emissions of criteria air pollution. In general, EASIUR estimates the marginal damages from criteria air pollutants higher than AP2. This is borne out in our results as EASIUR estimates 2.2-2.3% higher damages resulting from electricity generation and 11-12% higher damages resulting from chemical manufacturing. Figure S1 shows the damages nationwide from electricity generation, chemical manufacturing, and total damages associated with drinking water treatment. Tables S10 and S11 compares the damages priced using AP2 and EASIUR models.

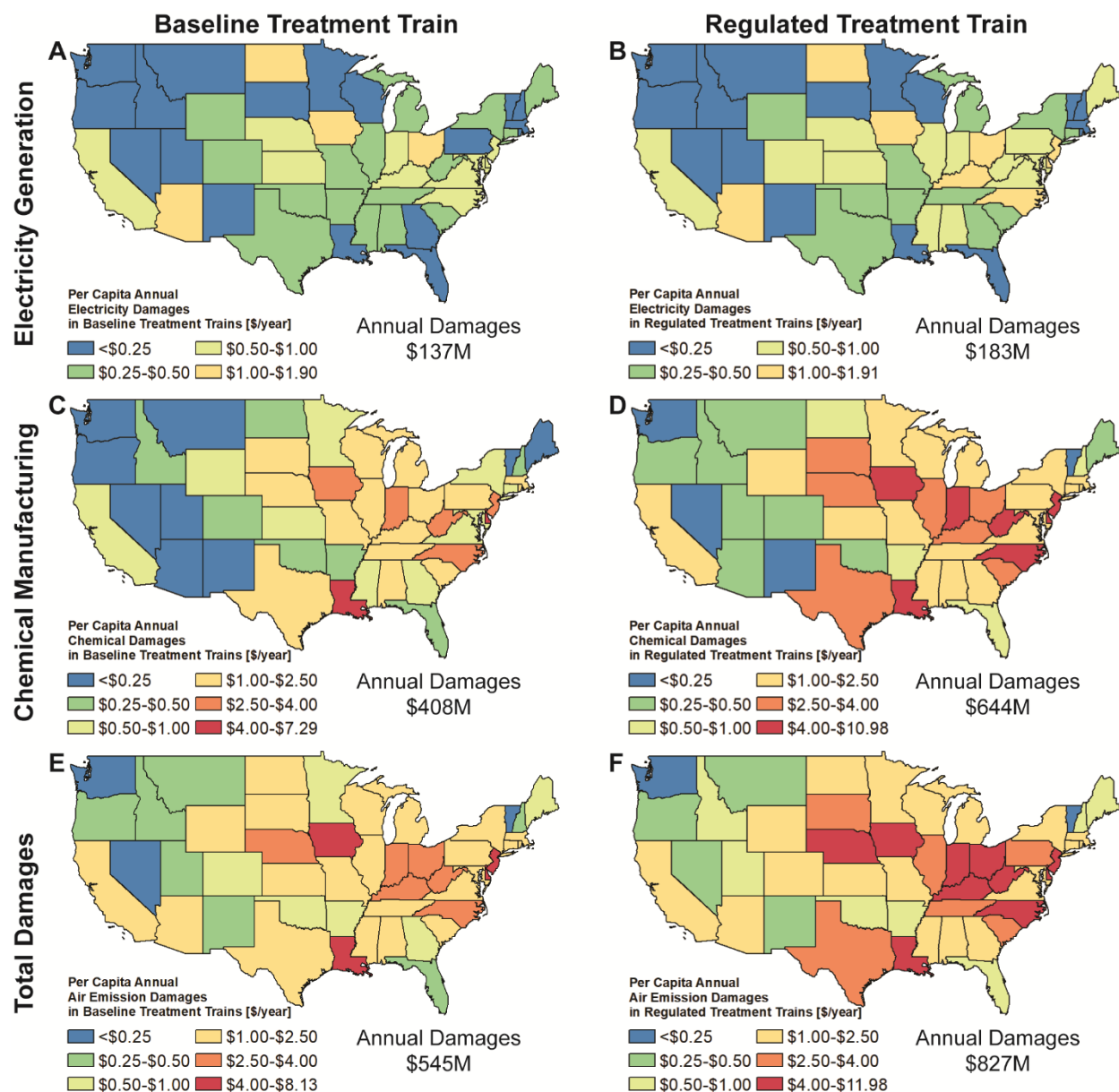


*Figure S1. Per capita air emission damages from emissions associated with drinking water treatment using the EASIUR model. Damages from electricity generation in each state in order to drive water treatment processes for (A) the baseline treatment train and (B) the regulated treatment train assuming compliance with all promulgated and proposed SDWA regulations. Damages from chemical manufacturing in each state to produce the chemicals for drinking water treatment in (C) the baseline treatment train and (D) the regulated treatment train. Total air emissions damages for (E) the baseline treatment train and (F) the regulated treatment train.*

Table S10. Emissions and damages resulting from the baseline treatment train.

	Electricity Generation Damages			Chemical Manufacturing Damages		
	EASIUR [\$M/yr]	AP2 [\$M/yr]	Percent Difference [%]	EASIUR [\$M/yr]	AP2 [\$M/yr]	Percent Difference [%]
NO <sub>x</sub>	7.6	6.0	27	15	13	15
SO <sub>2</sub>	32	34	-5.9	120	130	-7.7
PM <sub>2.5</sub>	30	26	15	180	120	53
CO <sub>2</sub>	68	68	0*	93	93	0*
Total	136.9	133.8	2.3	407	363	12

\*CO<sub>2</sub> damages are set at the social cost of carbon and do not vary between AP2 and EASIUR.

Table S11. Emissions and damages resulting from the baseline treatment train and installation of technologies to comply with the six drinking water standards studied here.

	Electricity Generation Damages			Chemical Manufacturing Damages		
	EASIUR [\$M/yr]	AP2 [\$M/yr]	Percent Difference [%]	EASIUR [\$M/yr]	AP2 [\$M/yr]	Percent Difference [%]
NO <sub>x</sub>	11	7.9	39	53	44	21
SO <sub>2</sub>	45	50	-10	140	160	-13
PM <sub>2.5</sub>	39	34	15	230	150	50
CO <sub>2</sub>	88	88	0*	230	230	0*
Total	183	179	2.2	644	581	11

\*CO<sub>2</sub> damages are set at the social cost of carbon and do not vary between AP2 and EASIUR.



## 6.0 Emissions and Damages from New Drinking Water Standards

### 6.1 Arsenic

Complying with the arsenic rule imposes air emission damages of \$952,000/year with \$949,000/year coming from electricity generation and \$3,500/year coming from chemical manufacturing. Figure S2 shows the distribution of these damages throughout the United States and Table S12 reports the total emissions and damages resulting from compliance.

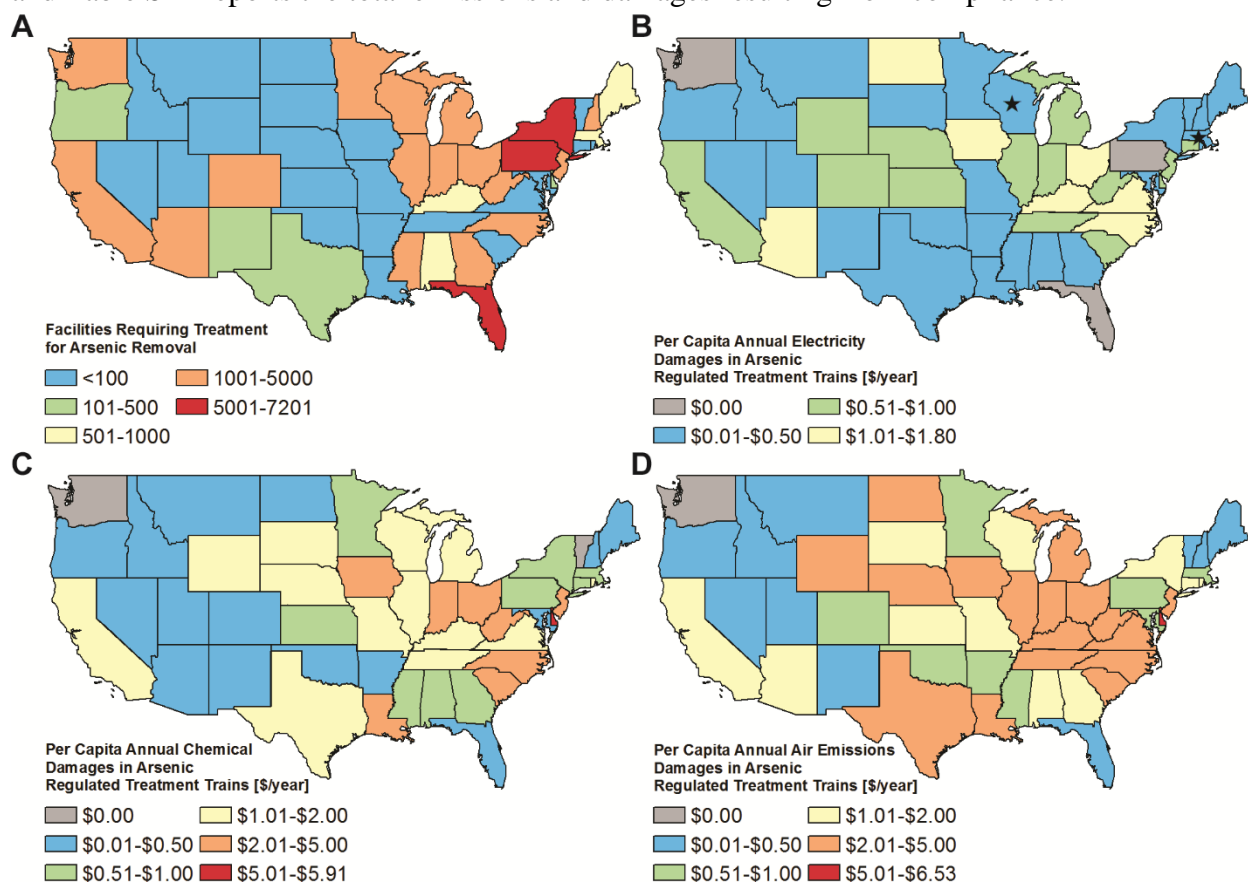


Figure S2. For arsenic (A) the number of facilities that require installation of arsenic removal technologies and the annualized per capita damages from (B) air emissions from electricity generation to drive arsenic removal, (C) air emissions from chemical manufacturing consumed during arsenic removal, and (D) total air emissions. A star indicates an increase in per capita damages in a state of more than 50% due to the arsenic standard.

Table S12. Emissions and damages from compliance with the arsenic standard.

	Electricity Generation		Chemical Manufacturing	
	Emissions [tons/yr]	Damages [\$K/yr]	Emissions [tons/yr]	Damages [\$K/yr]
NO <sub>x</sub>	8.6	45	0.03	190
SO <sub>2</sub>	6.7	190	0.05	1,200
PM <sub>2.5</sub>	1.9	180	0.01	390
CO <sub>2</sub>	12,000	540	38.31	1,700
Total		949		3,450

## 6.2 Hexavalent Chromium

Complying with the chromium (VI) rule imposes air emission damages of \$2,640,000/year with \$2,500,000/year coming from electricity generation and \$140,000/year coming from chemical manufacturing. Figure S3 shows the distribution of these damages throughout the United States and Table S13 reports the total compliance emissions and damages.

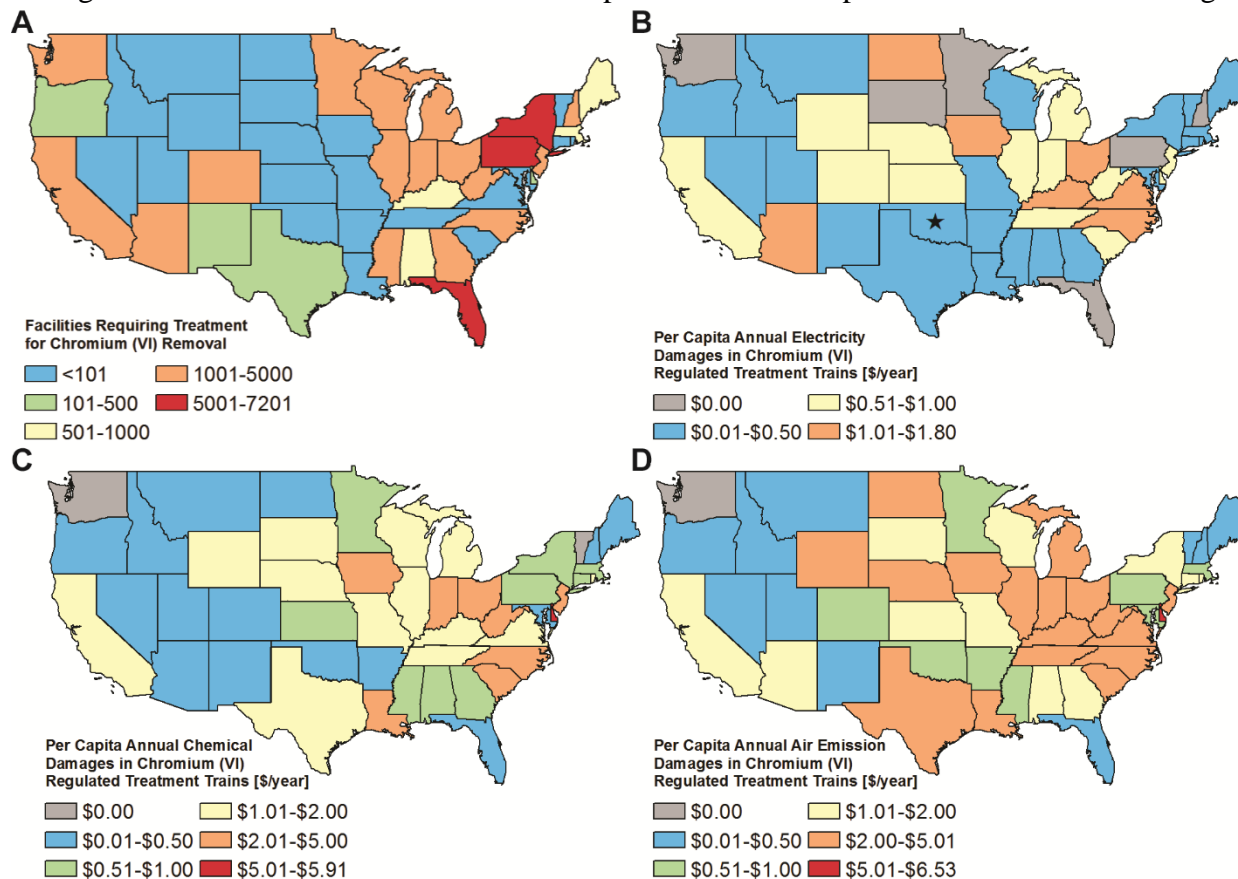


Figure S3. For hexavalent chromium (A) the number of facilities that require installation of hexavalent chromium removal technologies and the annualized per capita damages from (B) air emissions from electricity generation to drive hexavalent chromium removal, (C) air emissions from chemical manufacturing consumed during hexavalent chromium removal, and (D) total air emissions. A star indicates an increase in per capita damages in a state of more than 50% due to the proposed hexavalent chromium standard.

Table S13. Emissions and damages from compliance with the proposed Cr(VI) standard.

	Electricity Generation		Chemical Manufacturing	
	Emissions [tons/yr]	Damages [\$K/yr]	Emissions [tons/yr]	Damages [\$K/yr]
NO <sub>x</sub>	12	78	1.4	8.5
SO <sub>2</sub>	8	91	2.0	48
PM <sub>2.5</sub>	10	740	0.22	15
CO <sub>2</sub>	36,000	1,600	1,700	72
Total		2,493		143.9

### 6.3 Disinfectant Byproducts

Complying with the disinfectant byproduct rule imposes air emission damages of \$9.76M/year with \$1.26M/year coming from electricity generation and \$8.49M/year coming from chemical manufacturing. Figure S4 shows the distribution of these damages throughout the United States and Table S14 reports the total compliance emissions and damages.

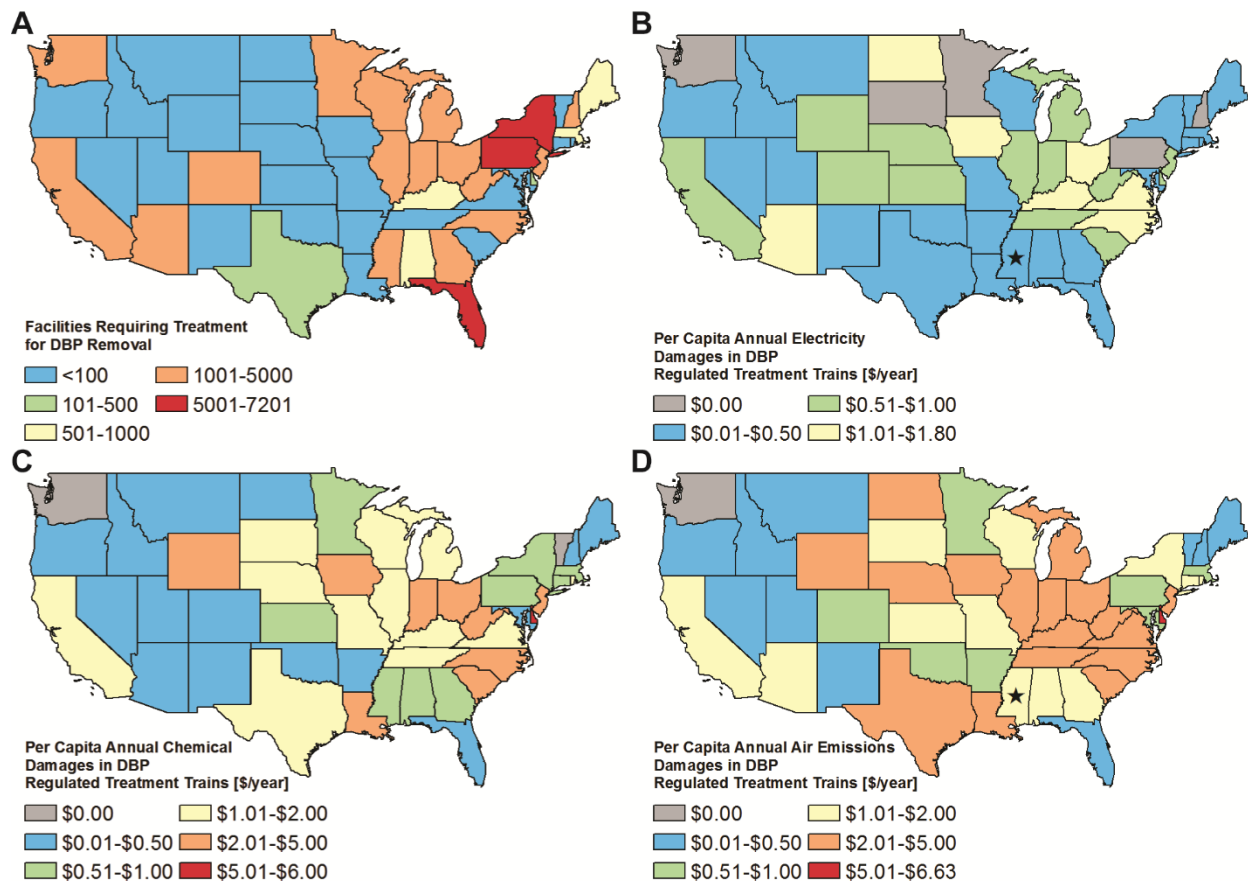


Figure S4. For DBPs (A) the number of facilities that require installation of DBPs removal technologies and the annualized per capita damages from (B) air emissions from electricity generation to drive DBP removal, (C) air emissions from chemical manufacturing consumed during DBP removal, and (D) total air emissions. A star indicates an increase in per capita damages in a state of more than 50% due to the DBP rule.

Table S14. Emissions and damages from compliance with the DBP standard.

	Electricity Generation		Chemical Manufacturing	
	Emissions [tons/yr]	Damages [\$K/yr]	Emissions [tons/yr]	Damages [\$K/yr]
NO <sub>x</sub>	9.9	50	220	1,400
SO <sub>2</sub>	33	640	42	980
PM <sub>2.5</sub>	2.1	80	4.7	320
CO <sub>2</sub>	11,000	490	130,000	5,800
Total		1,260		8,490

## 6.4 Lead and Copper

Complying with the lead and copper rule imposes air emission damages of \$787,000/year with \$549,000/year coming from electricity generation and \$237,000/year coming from chemical manufacturing. Figure S5 shows the distribution of these damages throughout the United States and Table S15 reports the total emissions and damages resulting from compliance.

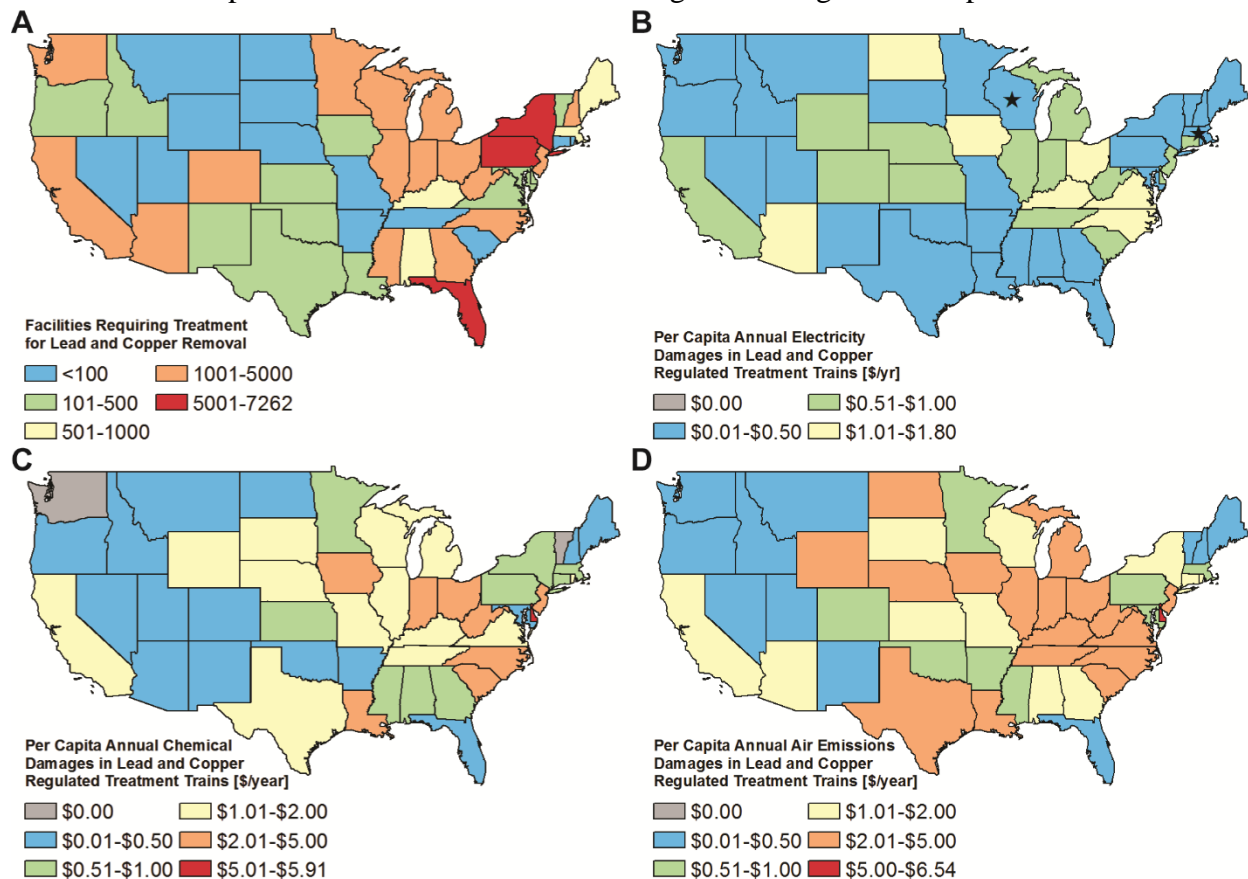


Figure S5. For lead and copper (A) the number of facilities that require installation of lead and copper removal technologies and the annualized per capita damages from (B) air emissions from electricity generation to drive lead and copper removal, (C) air emissions from chemical manufacturing consumed during lead and copper removal, and (D) total air emissions. A star indicates an increase in per capita damages in a state of more than 50% due to the lead and copper rule.

Table S15. Emissions and damages from compliance with the lead and copper standard.

	Electricity Generation		Chemical Manufacturing	
	Emissions [tons/yr]	Damages [\$K/yr]	Emissions [tons/yr]	Damages [\$K/yr]
NO <sub>x</sub>	5.0	31	2.3	14
SO <sub>2</sub>	7.0	160	3.3	79
PM <sub>2.5</sub>	1.1	65	0.37	25
CO <sub>2</sub>	6,700	290	2,700	120
Total		549		238

## 6.5 PFOA and PFOS

Complying with the PFOA/PFOS health advisory imposes air emission damages of \$225M/year with \$39.6M/year coming from electricity generation and \$185M/year coming from chemical manufacturing. Figure S6 shows the distribution of these damages throughout the United States and Table S16 reports the total emissions and damages resulting from compliance.

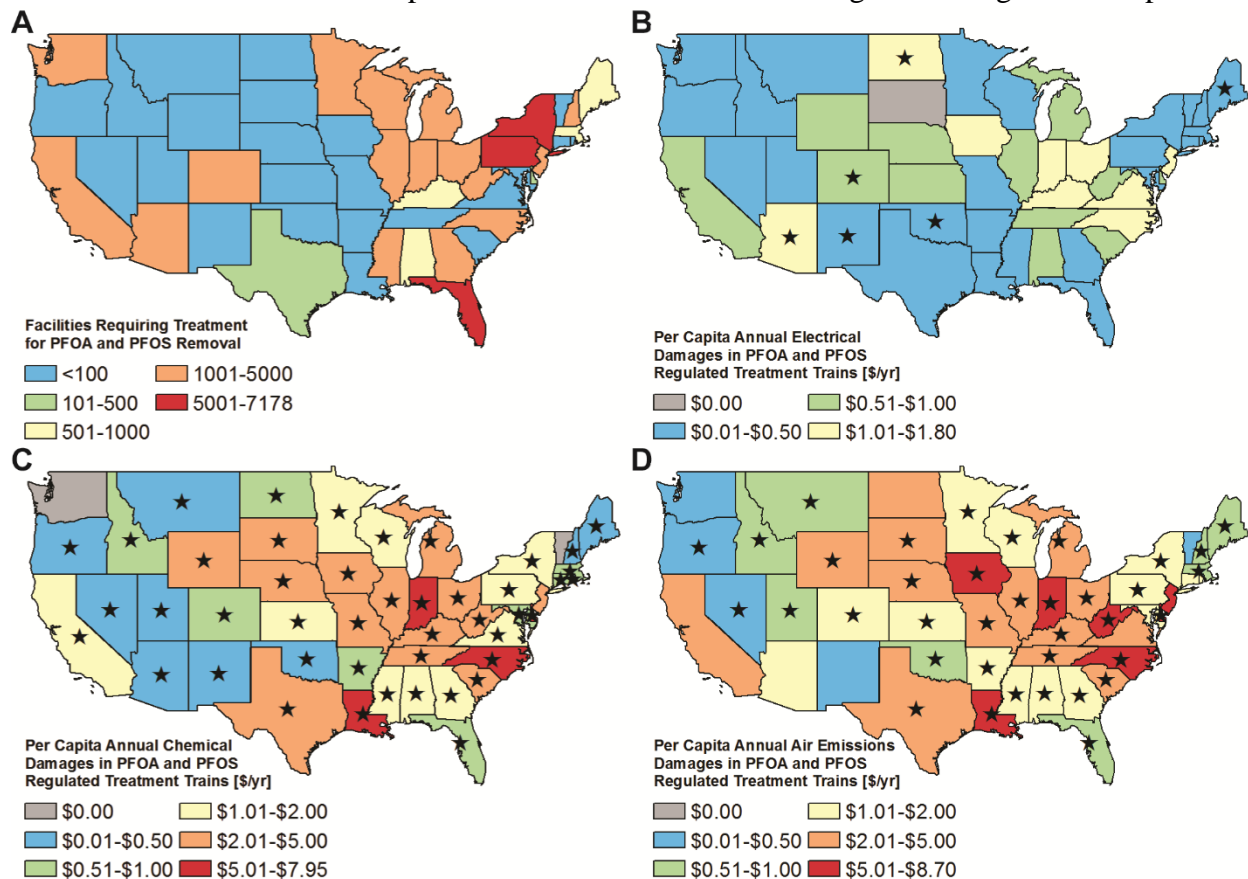


Figure S6. For PFOA and PFOS (A) the number of facilities that require installation of PFOA and PFOS removal technologies and the annualized per capita damages from (B) air emissions from electricity generation to drive PFOA and PFOS removal, (C) air emissions from chemical manufacturing consumed during PFOA and PFOS removal, and (D) total air emissions. A star indicates an increase in per capita damages in a state of more than 50% due to the PFOA and PFOS health advisory.

Table S16. Emissions and damages from compliance with the PFOA/PFOS health advisory.

	Electricity Generation		Chemical Manufacturing	
	Emissions [tons/yr]	Damages [\$M/yr]	Emissions [tons/yr]	Damages [\$M/yr]
NO <sub>x</sub>	270	1.6	4,800	30
SO <sub>2</sub>	490	15	910	21
PM <sub>2.5</sub>	83	6.5	100	7.0
CO <sub>2</sub>	390,000	17	2,900,000	130
Total		39.6		185

## 6.6 Strontium

Complying with the proposed strontium rule imposes air emission damages of \$24.2M/year with \$450,000/year coming from electricity generation and \$23.8M/year coming from chemical manufacturing. Figure S7 shows the distribution of these damages throughout the United States and Table S17 reports the total compliance emissions and damages.

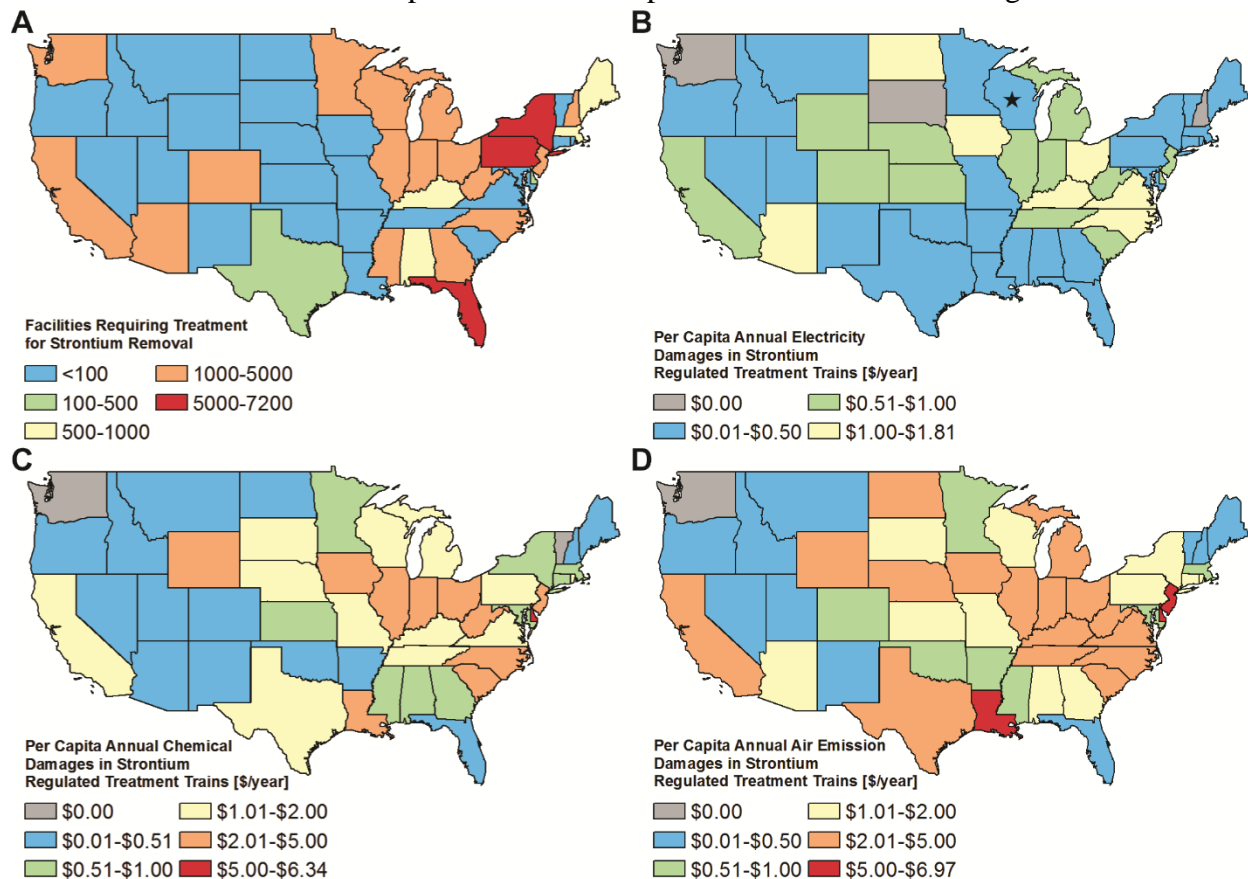


Figure S7. For strontium (A) the number of facilities that require installation of strontium removal technologies and the annualized per capita damages from (B) air emissions from electricity generation to drive strontium removal, (C) air emissions from chemical manufacturing consumed during strontium removal, and (D) total air emissions. A star indicates an increase in per capita damages in a state of more than 50% due to the proposed strontium standard.

Table S17. Emissions and damages from compliance with the proposed strontium standard.

	Electricity Generation		Chemical Manufacturing	
	Emissions [tons/yr]	Damages [\$K/yr]	Emissions [tons/yr]	Damages [\$K/yr]
NO <sub>x</sub>	3.6	23	21	130
SO <sub>2</sub>	5.3	120	38	900
PM <sub>2.5</sub>	0.96	75	420	22,000
CO <sub>2</sub>	5,200	230	26,000	1,100
Total		450		23,780

## 7.0 Nomenclature

### Symbols

$E$ : Energy consumption [kWh/m<sup>3</sup>], [kWh/g-chemical], or [MJ/g-chemical]

$e$ : Emissions factor per unit of energy [g/kWh] or [g/MJ]

$M$ : Annual mass of NO<sub>x</sub>, SO<sub>2</sub>, PM<sub>2.5</sub>, or CO<sub>2</sub> emissions [g/yr]

$Q$ : Chemical dosage [g-chemical/m<sup>3</sup>]

$\Psi$ : Annual water production [m<sup>3</sup>/yr]

### Subscripts

$cm$ : Chemical manufacturing

$d$ : Thermal fuel

$f$ : Chemical

$h$ : Treatment train (baseline or newly-regulated)

$i$ : Drinking water facility

$j$ : Air pollutant (NO<sub>x</sub>, SO<sub>2</sub>, PM<sub>2.5</sub>, or CO<sub>2</sub>)

$l$ : State

$\backslash mf$ : Marginal emissions factor

### Superscripts

$C$ : From chemical manufacturing

$D$ : From thermal fuel combustion

$W$ : Electricity consumption



## 8.0 References

1. U.S. Environmental Protection Agency Chemical Contaminant Rules. <https://www.epa.gov/dwreginfo/chemical-contaminant-rules> (March 25),
2. U.S. Environmental Protection Agency Lead and Copper Rule. <https://www.epa.gov/dwreginfo/lead-and-copper-rule> (March 25),
3. U.S. Environmental Protection Agency Chromium in Drinking Water. <https://www.epa.gov/dwstandardsregulations/chromium-drinking-water> (March 25, 2017),
4. Seidel, C.; Najm, I.; Blute, N.; Corwin, C.; Wu, X., National and California Treatment Costs to Comply with Potential Hexavalent Chromium. *Journal - American Water Works Association* **2013**, *105*, E320-E336.
5. U.S. Environmental Protection Agency Regulatory Determination 3. <https://www.epa.gov/ccl/regulatory-determination-3> (March 25, 2017),
6. U.S. Environmental Protection Agency Basic Information about Per- and Polyfluoroalkyl Substances (PFASs). <https://www.epa.gov/pfas/basic-information-about-and-polyfluoroalkyl-substances-pfass> (March 25, 2017),
7. U.S. Environmental Protection Agency Safe Drinking Water Information System (SDWIS). <https://www3.epa.gov/enviro/facts/sdwis/search.html> (March 25, 2017),
8. Siler-Evans, K.; Azevedo, I. L.; Morgan, M. G., Marginal emissions factors for the U.S. electricity system. *Environ Sci Technol* **2012**, *46*, (9), 4742-8.
9. U.S. Environmental Protection Agency Emissions Inventories. <http://www3.epa.gov/ttn/chief/eiinformation.html> (October 9, 2015),
10. Muñoz, I.; Milà-i-Canals, L.; Fernández-Alba, A. R., Life Cycle Assessment of Water Supply Plans in Mediterranean Spain. *Journal of Industrial Ecology* **2010**, *14*, (6), 902-918.
11. Althaus H-J, e. a., *Life Cycle Inventories of Chemicals No. 8, v. 2.0*. Dusseldorf, Switzerland, 2007.
12. Gingerich, D. B.; Sun, X. B., A. Patrick; Azevedo, I. M. L.; Mauter, M. S., Spatially resolved air-water emissions tradeoffs improve regulatory impact analyses for electricity generation. *Proceedings of the National Academy of Science* **2017**.
13. National Renewable Energy Laboratory National Renewable Energy Laboratory - Life-Cycle Inventory Database. . <https://www.lcacommons.gov/nrel/process/show/50158> (October 3, 2015),
14. Heo, J.; Adams, P. J.; Gao, H. O., Public Health Costs of Primary PM<sub>2.5</sub> and Inorganic PM<sub>2.5</sub> Precursor Emissions in the United States. *Environ Sci Technol* **2016**, *50*, (11), 6061-70.
15. Heo, J.; Adams, P. J.; Gao, H. O., Reduced-form modeling of public health impacts of inorganic PM<sub>2.5</sub> and precursor emissions. *Atmospheric Environment* **2016**, *137*, 80-89.



## **APPENDIX 2: SUPPORTING INFORMATION FOR CHAPTER 3 – AIR EMISSION BENEFITS OF BIOGAS ELECTRICITY GENERATION AT MUNICIPAL WASTEWATER TREATMENT PLANTS**

### **Supporting Information Summary:**

The supporting information contains descriptions of 1) wastewater treatment unit process descriptions and inputs; 2) data sources; 3) a summary of the method for estimating air emissions and damages associated with wastewater treatment; 4) tabulated emissions and damages from Figures 2 and 3; 5) uncertainty analyses for emissions and damages from wastewater treatment; 6) chemical manufacturing location sensitivity analyses; and 7) uncertainty analysis on biogas-fueled electricity generation.

This supporting information is 22 pages long and contains 1 figure (Figures S1) and 19 tables (Tables S1-S18).

## 1.0 Wastewater Treatment Unit Process Descriptions and Inputs

The Clean Watersheds Needs Survey identifies 252 unique technologies installed at 14,692 facilities in the United States. We model technologies that make up at least 1% of the technologies reported. Twenty-three technologies make up at least 1% of the technologies reported. These technologies are listed in Table S1. It includes the description of the process and the electrical and chemical inputs that are consumed in the process.

Table S1. Unit processes modeled in this study for wastewater treatment.

Unit Process	Description	Electrical Input <sup>1</sup> [kWh/m <sup>3</sup> ]	Chemical Inputs <sup>2</sup> [mg/L]
<i>Preliminary and Primary Treatment</i>			
Aerated Grit Removal	A type of grit removal chamber in which air is introduced to create a spiral flow pattern within the chamber.	0.01-0.02	
Comminution/Grinding	Processing of solids in order to reduce the size of large solids and returns the solids into the wastewater flow.		
Filtration	Removal of solids using a generic granular media in a filter.	0.005-0.014	
Grit Removal	A horizontal-flow grit chamber in which grit (e.g. sand, egg shells, broken glass, gravel) is allowed to settle from the wastewater.	0.01-0.02	
Screening	Removes large solids (e.g. debris and rags) before it enters the secondary treatment process.		
Sedimentation	Removal of solids by allowing solids to settle out of the waste stream.	0.008-0.01	
<i>Secondary Treatment</i>			
Activated Sludge	Biological treatment process that uses suspended microorganisms in order to reduce the BOD <sub>5</sub> and TSS concentration of wastewater.	0.33-0.60	
Aeration	Addition of air to activated sludge treatment processes in order to meet the oxygen needs of the microorganisms.	0.008-0.01	

Clarification	Circular tank with quiescent movement that follows a biological treatment process in order to allow sludge to settle and be returned to the biological treatment process or sent to the sludge treatment train.	0.01	
Lagoon	Engineered pond that uses microorganisms and macroorganisms in order to treat wastewater. Contains aerobic and anaerobic zones.	0.09-0.29	
Stabilization	Engineered pond that uses microorganisms and macroorganisms in order to treat wastewater. Contains only an aerobic zone.	0.008-0.01	
Trickling Filter	Biological treatment process that uses microorganisms that are attached to filter media (e.g. rocks, plastic media) in order to reduce the BOD <sub>5</sub> and TSS concentration of wastewater.	0.201-0.441	
<hr/> <i>Disinfection</i>			
Dechlorination	Addition of SO <sub>2</sub> to react with remaining free chlorine in the wastewater to remove chlorine before discharge into the environment.	0.03-0.15	1.11-22.1 (SO <sub>2</sub> )
Chlorine Disinfection	Addition of sodium hypochlorite to disinfect treated wastewater before discharge into the environment.	2x10 <sup>-5</sup> -5x10 <sup>-4</sup>	1.16-23.19 (NaOCl)
UV Disinfection	Use of ultraviolet light to disinfect treated wastewater before discharge into the environment.	0.015-0.066	
<hr/> <i>Tertiary Treatment</i>			
Denitrification/Nitrification	Use of biological treatment processes to convert nitrate in gaseous N <sub>2</sub> , removing it from the wastewater stream.	0.08-0.09	
Phosphorous Removal	Physiochemical treatment processes to crystallize phosphate into solid struvite.	0.06-0.14	
<hr/> <i>Sludge Treatment</i>			
Aerobic Digestion	Use of aerobic microorganisms to reduce the volume of sludge produced at a wastewater treatment facility.	0.05-0.30	

Anaerobic Digestion	Use of anaerobic microorganisms to reduce the volume of sludge produced at a wastewater treatment facility.	0.25-0.28	
Biogas Combustion	Collection and combustion of the biogas that results from anaerobic digestion, typically for electricity and thermal energy recovery.	***	
Gravity Thickening	Thickening of sludge to reduce water and equalize the sludge flow in a circular settling basin.		
Mechanical Biosolids Dewatering	Processing of biosolids following digestion using a mechanical process, typically a belt filter, to remove water and the volume of biosolids to be disposed of.	0.01-0.02	
Polymer Biosolids Dewatering	Use of polymers, typically polyelectrolytes, to condition biosolids and release absorbed water before ultimate disposal.	0.15	0.27-11.37 (Polyelectrolyte)

---

## 2.0 Data Sources

### 2.1 Wastewater Systems Data

The data on wastewater systems in the United States comes from the Clean Watersheds Needs Survey (CWNS) conducted by the U.S. EPA.<sup>3</sup> The CWNS takes place every four years and is required under Sections 205(a) and 516 of the Clean Water Act. The CWNS is undertaken in order to determine the capital investments needed to meet the Clean Water Act's expectations for the nation's water bodies.

From the CWNS, we use the following data on US wastewater treatment systems:

- Average daily flow for system
- Design daily flow for system
- County system is located in
- State system is located in
- Unit processes installed at a system.

We use the 2012 CWNS<sup>4</sup> for 49 states, Washington, D.C., and three U.S. territories. South Carolina did not participate in the 2012 CWNS and so we use the 2008 CWNS<sup>5</sup> for facilities located in the state of South Carolina. This dataset of municipal wastewater treatment facilities includes 14,692 unique systems, more than 99.6% of the total wastewater treatment facilities in the United States and its territories. We then remove Alaska, Hawaii, and the U.S. territories so that we are only modeling the contiguous United States.

### 2.2 Electricity Generation Emissions Data

There are two types of emissions factors from electricity generation and we use both types in this analysis. These different types are marginal emission factors and average emission factors.

A marginal emission factor represents the emissions associated with generating the last kWh of electricity in a region.<sup>6</sup> We use marginal emission factors for NO<sub>x</sub>, SO<sub>2</sub>, and CO<sub>2</sub> in an updated version of the estimates developed by Siler-Evans et al.<sup>6</sup>

An average emission factor represents the emissions associated with generating an average kWh of electricity in a region, i.e. it is the total emissions divided by total electricity generation. We calculate the average emission factors for PM<sub>2.5</sub> and VOCs using the EPA's National Emissions Inventories.<sup>7</sup> There are no marginal emission factors for these pollutants as the Continuous Emission Monitoring Systems does not collect data on these pollutants.

## 2.3 Chemical Manufacturing Emissions Data

Data on chemical manufacturing emissions comes from two different sources.<sup>8-9</sup> The energy inputs and direct emissions resulting from chemical manufacturing are listed in Table S2. The emissions associated with thermal fuel combustion are listed in Table S3. For emissions associated with electricity inputs we use state-level average emissions factors based on the National Emissions Inventories.<sup>7</sup>

*Table S2. Direct air emissions and energy inputs for chemicals consumed in water treatment.*

Chemical	Direct Air Emissions [kg <sup>-1</sup> ]	Energy Inputs [kg <sup>-1</sup> ]	Ref
Hypochlorite		0.017 kWh Elec	9
Generic Organic Chemical*	0.12 g NO <sub>x</sub>	5.4 kWh Elec	8
	0.098 g SO <sub>2</sub>	7.8x10 <sup>-4</sup> kg Bit Coal	
	0.0076 g PM <sub>2.5</sub>	2.3x10 <sup>-4</sup> L Pet	
	4.82 g VOCs	0.024 L RFO	
	170g CO <sub>2</sub>	0.12 m <sup>3</sup> Nat. Gas	
		9.3x10 <sup>-4</sup> L Diesel	
Generic Inorganic Chemical**	0.15 g SO <sub>2</sub>	0.068 kWh Elec	8
	0.056 g PM <sub>2.5</sub>	0.172 kg Bit Coal	
	770 g CO <sub>2</sub>	3.2x10 <sup>-5</sup> L Pet	
		0.021 m <sup>3</sup> Nat Gas	
		9.5x10 <sup>-4</sup> L Diesel	

\* Includes Bimetallic Phosphate, Hexametaphosphate, Orthophosphate, Polyphosphate, Membrane Cleaning Chemicals, and Corrosion Inhibitors

\*\* Includes Alum, Iodine, Fluoride, Silicate, Permanganate, Sodium Bisulfate, Sodium Sulfite, and Sulfur Dioxide

*Table S3. Air Emissions from Energy Sources<sup>10</sup>*

	CO <sub>2</sub> [g]	NO <sub>x</sub> [g]	SO <sub>2</sub> [g]	PM <sub>2.5</sub> [g]	VOCs [g]
Bituminous Coal [kg <sup>-1</sup> ]	2633	5.75	16.6	0	0.0563
Petroleum [L <sup>-1</sup> ]	1721	2.6	0	0	0.0455
Residual Fuel Oil [L <sup>-1</sup> ]	3263.2	7.03	5.12	0	0.0359
Natural Gas [m <sup>-3</sup> ]	1960.9	1.6	0.0101	0	0.0884
Diesel [L <sup>-1</sup> ]	2730	2.87	0.599	0	0.0241

## 2.4 Direct Emissions from Wastewater Treatment

In order to estimate direct emissions from wastewater treatment, we use literature-based emission factors of criteria air pollutants and greenhouse gasses from wastewater treatment. These emissions factors are listed in Table S4 and are scaled to cubic meter of wastewater treated.

Table S4. On-Site Air Emissions

	All Processes	Activated Sludge	Aerobic Digestion	Anaerobic Digestion (0% Combusted)	Anaerobic Digestion (100% Combusted)
NO <sub>x</sub>					
SO <sub>2</sub>					
VOCs	0.1017 g/m <sup>3</sup> <sup>11</sup>				
CO <sub>2</sub>		89-94 g/m <sup>3</sup> <sup>12</sup> 153-280 g/m <sup>3</sup> <sup>13</sup> 43.6	158 g/m <sup>3</sup> <sup>13</sup>	43.6 g/m <sup>3</sup> <sup>14</sup>	87.6 g/m <sup>3</sup> <sup>14</sup>
CH <sub>4</sub>		0 g/m <sup>3</sup> <sup>15</sup>	0 g/m <sup>3</sup> <sup>15</sup>	37.0 g/m <sup>3</sup> <sup>14</sup>	0.0054 g/m <sup>3</sup> <sup>14</sup>
N <sub>2</sub> O		3.2/7.0 g/PE·yr* <sup>16-18</sup>		0 g/m <sup>3</sup> <sup>14</sup>	0.0011 g/m <sup>3</sup> <sup>14</sup>

## 2.5 Biogas Electricity Factor Data

As described in the manuscript, the biogas electricity factors (BEFs) are taken from Stillwell et al.<sup>19</sup> and originally from an EPRI study.<sup>20</sup>

### 3.0 Method for Estimating Air Emission Damages from Wastewater Treatment

#### 3.1 Estimating Air Emissions from Wastewater Treatment

Air emissions associated with wastewater treatment stem from three sources: emissions directly from wastewater treatment, emissions from electricity generation, and emission from chemical manufacturing. The method for calculating emissions directly from wastewater treatment are detailed in the main manuscript. The method for calculating emissions from electricity generation and chemical manufacturing is detailed in our previous work.<sup>21</sup>

In brief, we calculate emissions from electricity generation,  $M_{i,j}^{Elec}$  [g/yr], using Equation S1 and emissions from chemical manufacturing,  $M_{i,j}^{Chem}$  [g/yr] using Equation S2.

$$M_{i,j}^{Elec} = \forall_i \sum_g \overline{W_g^{Elec}} e_{mf,j,l} \quad (S1)$$

As shown in Equation S1, emissions from electricity generation associated with facility  $i$  are the product of annual average water treatment demand,  $\forall_i$  [m<sup>3</sup>/yr], the sum of unit process average electricity consumptions for processes  $g$  installed at treatment facility  $i$ ,  $\overline{W_g^{Elec}}$  [kWh/m<sup>3</sup>], and the emissions factor for pollutant  $j$  in for electricity generated in state  $l$ ,  $e_{mf,j,l}$  [g/kWh]. Average electricity consumptions for the unit processes can be found in Table S1.

$$M_{i,j}^{Chem} = \sum_f \forall_i Q_{i,f} (e_{cm,f,j}^C + \sum_d E_{d,f}^D e_{d,j}^D + E_f^{Elec} \sum_l e_{mf,j,l} \frac{V_l}{\sum_l V_l}) \quad (S2)$$

Emissions from chemical manufacturing stem from three sources. These are:

- Direct emission from chemical manufacturing,  $e_{cm,f,j}^C$  [g-pollutant/kg-chemical]. These are listed in Table S2.
- Emissions from combustion of thermal fuel  $d$ , which is the product of thermal energy consumption,  $E_{d,f}^D$  [MJ/kg-chemical], and emission factors from thermal fuel combustion,  $e_{d,j}^D$  [g-pollutant/MJ]. Thermal energy consumption is listed in Table S2 and emissions factors from thermal fuel combustion are listed in Table S3.
- Emissions from electricity consumption, which is the product of electrical energy consumption,  $E_f^{Elec}$  [kWh/kg-chemical], and a weighted grid electricity emissions factor. The weighted grid electricity emission factors are state-level emissions factors,  $e_{mf,j,l}$  [g-pollutant/kWh] weighted by the share of chemical manufacturing that takes place in state  $l$  as defined by the value of the chemical manufacturing sector in the state,  $V_l$  [\$/yr].

These three sources are then multiplied by the annual average water treatment demand at plant  $i$ ,  $\forall_i$  [m<sup>3</sup>/yr], and the dosages of chemical  $f$ ,  $Q_{i,f}$  [kg-chemical/m<sup>3</sup>]. Dosages are listed in Table S1.

#### 3.2 Estimating Air Emission Damages from Wastewater Treatment

As described in the main manuscript we use AP2 and the social cost of carbon to price air emissions damages. We use Equations S3 and S4 and to calculate damages from electricity



generation at the facility-level,  $D_i^{elec}$  [\$/yr], and damages from chemical manufacturing at the state-level,  $D_l^{chem}$  [\$/yr].

$$D_i^{elec} = \sum_j d_{j,l} M_{i,j}^{Elec} \quad (S3)$$

Damages from electricity generation at the facility-level is the product of the total mass of pollutant  $j$ ,  $M_{i,j}^{Elec}$ , by the damages per marginal ton of pollutant  $j$  in the state  $l$  in which the facility is located,  $d_{j,l}$  [\$/g]. These damages are then summed up for all five pollutants.

$$D_l^{Chem} = \sum_j (d_{j,l} \frac{V_{l=L}}{\sum_l V_l} \sum_i M_{i,j}^{Chem}) \quad (S4)$$

Damages from chemical manufacturing are calculated at the state-level by summing up all emissions of pollutant  $j$  associated with chemical manufacturing that take place in the United States and assign those to state  $l$  based on its share of the US chemical manufacturing sector. The resulting emissions that take place in a state are then multiplied by the damages per marginal ton of pollutant  $j$  in the state  $l$ . These damages are then summed up for all five pollutants.

## 4.0 Emissions and Damages from Municipal Wastewater Treatment

### 4.1 Wastewater Treatment Emissions and Damages

Tables S5 and S6 report the total emissions and damages that result from treating wastewater in the United States. These are the results presented in Figure 2 of the manuscript.

*Table S5. Air emissions associated with municipal wastewater treatment in the United States.*

	Electricity Generation [tons/yr]	Chemical Manufacturing [tons/yr]	Direct [tons/yr]	Totals [tons/yr]
NO <sub>x</sub>	8000	133	113	8,250
SO <sub>2</sub>	14,700	293	0.71	15,000
PM <sub>2.5</sub>	1,690	14.4	0	1,700
VOCs	25.1	94.9	5040	5,160
CO <sub>2</sub>	10,600,000	162,000	13,800*	10,800,000
CH <sub>4</sub>			70,500	70,500
N <sub>2</sub> O			2460	2,460

\*Biogenic CO<sub>2</sub> adds an additional 9,840,000 tons of CO<sub>2</sub>.

*Table S6. Damages associated with emissions from municipal wastewater treatment in the United States.*

	Electricity Generation [\$M/yr]	Chemical Manufacturing [\$M/yr]	Direct [\$M/yr]	Totals [\$M/yr]
NO <sub>x</sub>	53.8	0.816	1.83	56.4
SO <sub>2</sub>	404	7.07	0.049	411
PM <sub>2.5</sub>	134	0.914	0	135
VOCs	0.151	0.468	83.8	84.4
CO <sub>2</sub>	459	7.04	6.01*	472
CH <sub>4</sub>			64.3	64.3
N <sub>2</sub> O			33.1	33.1
Totals	1,051	16.3	189	1256

\*Biogenic CO<sub>2</sub> would contribute an additional \$427 million in 2012\$.

### 4.2 Biogas Fueled Electricity Generation Emission Reductions and Benefits

Tables S7 and S8 reports the total emission changes, benefits and damages that result from biogas fueled electricity generation in the United States. These are the results presented in Figure 3 of the manuscript.

Table S7. Air emission changes associated with biogas-fueled electricity generation.

	Avoided Electricity [tons/yr]	Avoided Natural Gas Combustion [tons/yr]	Combusted Fugitive Methane [tons/yr]	Biogas Combustion [tons/yr]	Net Change [tons/yr]
NO <sub>x</sub>	-1,660	-112		25.5	-1,747
SO <sub>2</sub>	-2,910	-0.712		7.63	-2,903
PM <sub>2.5</sub>	-360	0		0	-360
VOCs	-7.55	-6.23		2.28	-11.5
CO <sub>2</sub>	-2,240,000	-13,820	0*	0*	-2,250,000
CH <sub>4</sub>		-2.54	-69,800		-69,800
N <sub>2</sub> O		0			0

\*Combusting previously released methane leads to an additional 155,000 tons of biogenic CO<sub>2</sub>.

Table S8. Air emission benefits and damages associated with biogas-fueled electricity generation.

	Avoided Electricity [\$M/yr]	Avoided Natural Gas Combustion [\$M/yr]	Combusted Fugitive Methane [\$M/yr]	Biogas Combustion [\$M/yr]	Net Change [\$M/yr]
NO <sub>x</sub>	-12.0	-1.83		0.161	-13.7
SO <sub>2</sub>	-88.4	-0.05		0.215	-88.2
PM <sub>2.5</sub>	-32.8	-0		0	-32.8
VOCs	-0.036	-0.11		0.014	-0.132
CO <sub>2</sub>	-108	-6.01	0*	0*	-114
CH <sub>4</sub>		-0.023	-63.7		-63.7
N <sub>2</sub> O		0			0
Totals	-241	-8.00	-63.7	0.39	-312

\*Combusting previously released methane leads to an additional \$6.75M in unpriced climate damages from biogenic CO<sub>2</sub>.

## 5.0 Uncertainty Analyses for Emissions and Damages from Municipal Wastewater Treatment

There are several variables that impact the emissions resulting from municipal wastewater treatment. These variables include: (1) electricity consumption in the unit processes, (2) chemical consumption in the unit processes, (3) the influent BOD<sub>5</sub> concentration, (4) and the influent flow rate for the wastewater.

### 5.1 Monte Carlo Analysis Input Parameters

As described in the main text, we perform Monte Carlo analysis in order to quantify the uncertainty in air emissions associated with wastewater treatment. Table S9 lists the distribution and parameters for the four variables we include in the analysis. These variables include the influent wastewater flow rate, the electricity consumption, and the chemical dosage.

Table S9. Input parameters for Monte Carlo Analysis

Variable	Distribution	Distribution Parameters	Notes
Influent Wastewater Flow Rate	Uniform	Min – $\bar{V}_{avg} - (\bar{V}_{design} - \bar{V}_{avg})$ Max – $\bar{V}_{design}$	Distribution is not allowed to go below 0 MGD.
Electricity Consumption	Triangular	Min – Minimum in Table S1 Peak – Average in Table S1 Max – Maximum in Table S1	
Chemical Dosage	Normal	<i>Polyelectrolyte</i> <sup>2</sup> Average – 2.84 mg/L SD – 2.45 mg/L <i>Hypochlorite</i> <sup>2</sup> Average – 6.87 mg/L SD – 7.59 mg/L <i>Sulfur Dioxide</i> <sup>2</sup> Average – 6.55 mg/L SD – 7.23 mg/L	Distribution is not allowed to go below 0 mg/L.

### 5.2 Electricity Consumption Uncertainty

Uncertainty surrounding the electricity consumption impacts the emissions and damages stemming from electricity generation. To perform uncertainty analysis, we modify our analysis by changing the  $W_g^{Elec}$  term in Equation S1. In the main analysis we used an average  $W_g^{Elec}$  and in the uncertainty analysis we used the extreme values listed in Table S1. We then recalculate the damages associated with emissions from electricity generation using Equation S3. The results of this analysis is shown in Table S10.

*Table S10. Sensitivity analysis for average electricity consumption, minimum electricity consumption, and maximum electricity consumption.*

	Baseline - Average		Minimum		Maximum	
	Emissions [tons/yr]	Damages [\$M/yr]	Emissions [tons/yr]	Damages [\$M/yr]	Emissions [tons/yr]	Damages [\$M/yr]
NO <sub>x</sub>	8000	53.8	5,420	36.5	10,600	71.1
SO <sub>2</sub>	14,700	404	9,870	272	19,400	536
PM <sub>2.5</sub>	1,690	134	1,140	91.2	2,240	177
VOCs	25.1	0.151	17.1	0.104	33.1	0.198
CO <sub>2</sub>	10,600,000	459	7,190,000	313	13,900,000	605
Totals		1,060		712		1,389

### 5.3 Chemical Dosage Uncertainty

Uncertainty surrounding the chemical dosage impacts the emissions and damages stemming from chemical manufacturing. To perform uncertainty analysis, we modify our analysis by changing the  $Q_{i,f}$  term in Equation S2. In the main analysis we used an average  $Q_{i,f}$  and in the uncertainty analysis we used the extreme values listed in Table S1. We then recalculate the damages associated with emissions from chemical manufacturing using Equation S4. The results of this analysis is shown in Table S11.

*Table S11. Sensitivity analysis for average chemical dosage, minimum chemical dosages, and maximum chemical dosages.*

	Baseline - Average		Minimum		Maximum	
	Emissions [tons/yr]	Damages [\$M/yr]	Emissions [tons/yr]	Damages [\$M/yr]	Emissions [tons/yr]	Damages [\$M/yr]
NO <sub>x</sub>	133	0.816	17.8	0.109	489	2.99
SO <sub>2</sub>	293	7.07	42.7	1.03	1,050	25.2
PM <sub>2.5</sub>	14.4	0.914	1.68	0.104	54.8	3.51
VOCs	94.9	0.468	9.07	0.045	379	1.87
CO <sub>2</sub>	162,000	7.04	21,800	0.946	594,000	25.8
Totals		16.3		2.24		59.4

### 5.4 Influent Flow Rate Uncertainty

Uncertainty surrounding the influent flow rate impacts emissions from all three sources. In the main analysis, we used the average daily flow reported in the CWNS. To perform this uncertainty analysis, we modify our analysis by changing the  $V_f$  term in Equations 1 and S1 and S2. We then recalculate the damages associated with emissions from biodegradation of wastewater using Equations 3 and S3-S5. The results of this analysis is shown in Table S12 and S13.

*Table S12. Air emissions associated with municipal wastewater treatment in the United States under the design flow rates for the municipal wastewater treatment plants.*

	Electricity Generation [tons/yr]	Chemical Manufacturing [tons/yr]	Direct [tons/yr]	Totals [tons/yr]
NO <sub>x</sub>	10,800	178	160	11,100
SO <sub>2</sub>	19,500	394	1.01	19,900
PM <sub>2.5</sub>	2,250	19.0	0	2,269
VOCs	34.2	124	7,110	7,270
CO <sub>2</sub>	14,400,000	217,000	196,000*	14,800,000
CH <sub>4</sub>			527,000	527,00
N <sub>2</sub> O			3430	3430

\*There is an additional 12.3 million tons of biogenic CO<sub>2</sub> produced.

*Table S13. Damages associated with emissions from municipal wastewater treatment in the United States under the design flow rates for the municipal wastewater treatment plants.*

	Electricity Generation [\$M/yr]	Chemical Manufacturing [\$M/yr]	Direct [\$M/yr]	Totals [\$M/yr]
NO <sub>x</sub>	71.3	1.09	2.6	75.0
SO <sub>2</sub>	520	9.52	0.693	530
PM <sub>2.5</sub>	171	1.21	0	172
VOCs	0.197	0.613	110	111
CO <sub>2</sub>	624	9.41	8.5*	642
CH <sub>4</sub>			481	481
N <sub>2</sub> O			46.2	46.2
Totals	1,390	21.8	650	2,060

\*There is an additional 12.3 million tons of biogenic CO<sub>2</sub> produced.

### 5.5 Biogas Flaring Uncertainty

There is uncertainty surrounding the amount of share of biogas produced at systems with anaerobic digestion but not reporting biogas usage that is flared. In the main manuscript, we assumed that 82% of biogas is flared and 18% is emitted to the environment, based on past research in this area.<sup>22</sup> We test the uncertainty by testing two additional cases, a 100% flared and 100% emitted to the environment. The results of this analysis are presented in Table S14. All emissions and damages from CO<sub>2</sub> are from biogenic CO<sub>2</sub>.

Table S14. Air emission and damages associated from biogas under different flaring scenarios.

	Baseline – 82% Flared		0% Flared		100% Flared	
	Emissions	Damages	Emissions	Damages	Emissions	Damages
	[ton/yr]	[\$M/yr]	[ton/yr]	[\$M/yr]	[ton/yr]	[\$M/yr]
<i>Baseline Scenario</i>						
CO <sub>2</sub> *	1,138,000	49.4	787,000	34.2	1,230,000	53.5
CH <sub>4</sub>	70,500	64.3	372,000	340	5,310	4.84
<i>Changes in Damages from Controlling Fugitive Emissions</i>						
CO <sub>2</sub> *	+155,000	+6.75	+903,000	+38.2	0	0
CH <sub>4</sub>	-61,000	-63.7	-368,000	-339	0	0

\*All CO<sub>2</sub> emissions and damages are biogenic CO<sub>2</sub>.

## 6.0 Chemical Manufacturing Location Sensitivity Analyses

In the main analysis, we assume that the distribution of the chemicals used in wastewater treatment follows the same distribution of the chemical manufacturing sector for all chemicals. We test the sensitivity of our results to this assumption, by comparing it to six different assumptions. These alternative assumptions are: (1) that chemicals are manufactured in the state they are used in, (2) that chemicals that are manufactured in states that have non-attainment areas have controls installed and do not emit pollutants that are limited, (3) that chemicals are manufactured evenly distributed across the 48 contiguous states, (4) that chemicals are manufactured in Nebraska, the state with the lowest marginal damages, (5) that chemicals are manufactured in New Jersey, the state with the highest marginal damages, and (6) that chemicals are manufactured off-shore.

For the baseline analysis, we assumed that wastewater treatment chemical manufacturing follows the geographical distribution of revenue in the chemical manufacturing sector.<sup>23</sup> Assuming that all chemical manufacturing occurs offshore reduces chemical manufacturing damages by 57%, while assuming that all chemical manufacturing occurs in the state with the highest marginal chemical manufacturing damages, New Jersey, increases damages by 96%. However, chemical manufacturing damages are the smallest part of total air damages and at most lead to a 1.6% difference in total damages under the six different chemical manufacturing scenarios listed in Table 1.

### 6.1 Chemicals are Manufactured in the State They Are Used In

The first alternative is that chemicals are manufactured in the state where they will be used. For this analysis, we modify Equation S2 as shown in Equation S5, by scaling it by the amount of wastewater in state  $l$  that is treated with chemical-requiring unit process  $g$ .

$$M_{l,g}^C = \sum_l \left[ \frac{V_{g,l}}{\sum_l V_{g,l}} (\sum_i V_i) \sum_j ((\sum_h Q_{j,h}) (e_{cm,j}^C + e_{fuel,j}^C + e_{mf,l}^E E_{elec,j}^C)) \right] \quad (S5)$$

Table S15 shows the resulting emissions and damages from chemical manufacturing under this scenario.

*Table S14. Sensitivity analysis for average electricity consumption, minimum electricity consumption, and maximum electricity consumption.*

	Baseline		In-State	
	Emissions [tons/yr]	Damages [\$M/yr]	Emissions [tons/yr]	Damages [\$M/yr]
NO <sub>x</sub>	133	0.816	124	0.872
SO <sub>2</sub>	293	7.07	281	8.30
PM <sub>2.5</sub>	14.4	0.914	16.8	1.52
VOCs	94.9	0.468	87.1	0.776
CO <sub>2</sub>	162,000	7.04	152,000	6.63
Totals		16.3		18.1



## 6.2 Emissions on Chemical Manufacturing Are Binding in States with Non-Attainment Areas

The second alternative is that chemical manufacturing in states with non-attainment areas are not allowed to emit additional pollutants that the state is not in standard for. To model these binding emission limits on chemical manufacturing zeroed out chemical manufacturing emissions of NO<sub>x</sub>, SO<sub>2</sub>, and PM<sub>2.5</sub> in a state with one or more non-attainment areas for ozone (no additional emissions of NO<sub>x</sub>), SO<sub>2</sub>, and PM<sub>2.5</sub>. Table S16 shows the resulting emissions and damages from chemical manufacturing under this scenario.

*Table S16. Sensitivity analysis for average electricity consumption, minimum electricity consumption, and maximum electricity consumption.*

	Baseline		Binding Regulations in Non-Attainment States	
	Emissions [tons/yr]	Damages [\$M/yr]	Emissions [tons/yr]	Damages [\$M/yr]
NO <sub>x</sub>	133	0.816	127	0.771
SO <sub>2</sub>	293	7.07	168	4.56
PM <sub>2.5</sub>	14.4	0.914	13.8	0.867
VOCs	94.9	0.468	94.9	0.468
CO <sub>2</sub>	162,000	7.04	162,000	7.04
Totals		16.3		13.7

## 6.3 Chemicals are Manufactured Evenly Throughout the 48 Contiguous States

The third alternative scenario is that chemicals are manufactured evenly throughout the lower 48 states in the US. For this analysis, we modify Equation S2 as shown in Equation S6.

$$M_{h,j,l}^C = \left(\frac{1}{48}\right) * \left[\sum_f V_i Q_{i,f,j} \left(e_{cm,f,h}^C + \sum_d E_{d,f}^D e_{d,h}^D + E_f^E \sum_i e_{mf,l,h} \frac{V_i}{\sum_i V_i}\right)\right] \quad (S6)$$

Table S17 shows the resulting emissions and damages from chemical manufacturing in the evenly distributed scenario.

*Table S17. Sensitivity analysis for average electricity consumption, minimum electricity consumption, and maximum electricity consumption.*

	Baseline		Evenly Distributed	
	Emissions [tons/yr]	Damages [\$M/yr]	Emissions [tons/yr]	Damages [\$M/yr]
NO <sub>x</sub>	133	0.816	142	0.771
SO <sub>2</sub>	293	7.07	292	6.21
PM <sub>2.5</sub>	14.4	0.914	16.2	0.800
VOCs	94.9	0.468	94.9	0.415
CO <sub>2</sub>	162,000	7.04	165,000	7.19
Totals		16.3		15.4

#### 6.4 Chemicals are Manufactured in the State with the Lowest Marginal Damages

The fourth alternative scenario is that chemicals are manufactured in Nebraska, the state with the lowest marginal damages for chemical manufacturing. Table S18 shows the emissions and damages from chemical manufacturing in this scenario.

*Table S18. Sensitivity analysis for average electricity consumption, minimum electricity consumption, and maximum electricity consumption.*

	Baseline		Nebraska	
	Emissions [tons/yr]	Damages [\$M/yr]	Emissions [tons/yr]	Damages [\$M/yr]
NO <sub>x</sub>	133	0.816	168	0.920
SO <sub>2</sub>	293	7.07	416	2.90
PM <sub>2.5</sub>	14.4	0.914	5.25	0.0734
VOCs	94.9	0.468	94.8	0.128
CO <sub>2</sub>	162,000	7.04	187,000	8.12
Totals		16.3		12.1

#### 6.5 Chemicals are Manufactured in the State with the Highest Marginal Damages

The fifth alternative scenario is that chemicals are manufactured in New Jersey, the state with the highest marginal damages for chemical manufacturing. Table S19 shows the emissions and damages from chemical manufacturing in this scenario.

*Table S19. Sensitivity analysis for average electricity consumption, minimum electricity consumption, and maximum electricity consumption.*

	Baseline		New Jersey	
	Emissions [tons/yr]	Damages [\$M/yr]	Emissions [tons/yr]	Damages [\$M/yr]
NO <sub>x</sub>	133	0.816	131	1.82
SO <sub>2</sub>	293	7.07	205	15.2
PM <sub>2.5</sub>	14.4	0.914	21.3	5.87
VOCs	94.9	0.468	94.8	2.47
CO <sub>2</sub>	162,000	7.04	152,000	6.62
Totals		16.3		32.0

#### 6.6 Chemicals are Manufactured Off-Shore

If chemical manufacturing takes place off-shore, then the only damages from chemical manufacturing to the US population is climate damages from greenhouse gas emissions. There are 162,000 tons of CO<sub>2</sub> emitted in this scenario for climate damages of \$7.04 million dollars in 2012 (in 2014\$).

## 7.0 Uncertainty Analyses on Biogas Fueled Electricity Generation

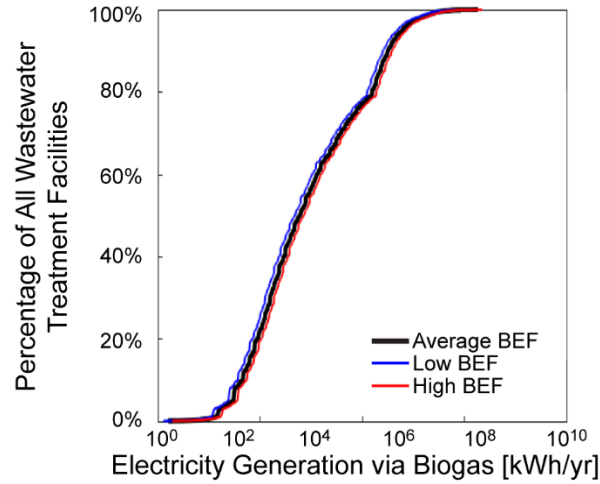


*Figure S1. Electricity generation via biogas at all municipal wastewater treatment plants with the design flow for wastewater treatment plants instead of the daily average flow. The different colors represent the three different biogas electricity factors (BEF).*

In Equation 5 in the main manuscript, the annual electricity generation is a product of two variables, the flow rate and the biogas electricity factor. In the main manuscript, we used the average daily flow rate and an average, low, and high biogas electricity factor. The remaining uncertainty is therefore around the flow rate. For the uncertainty analysis on the flow rate, we repeat the plant-level calculations in Equation 5 using the plant design flow as  $\dot{V}_l$ . The results of this analysis are shown in Figure S1.

## 8.0 Nomenclature

### Notation

- d: Marginal damages per short ton of air emissions [\$/g]  
D: Nationwide damages from air emissions [\$/yr]  
e: Unit emissions [g/kWh], [g/MJ], [g/g-chemical]  
E: Energy demand [kWh/yr], [MJ/yr]  
M: Mass of pollutants [g/yr]  
Q: Chemical dose [g/m<sup>3</sup>]  
V: Value of the chemical manufacturing sector [\$/yr]  
V̄: Volume of wastewater treated [m<sup>3</sup>/yr]  
W: Electricity consumed during wastewater treatment processes [kWh/m<sup>3</sup>]

### Superscripts

- C: Direct emissions from chemical manufacturing  
D: Emissions from thermal fuel combustion  
Chem: Emissions from chemical manufacturing  
Elec: Emissions from electricity generation

### Subscripts

- cm: Direct emissions from chemical manufacturing  
d: Thermal fuel  
f: Chemical  
g: Unit process  
i: POTW  
j: Air pollutant (i.e. NO<sub>x</sub>, SO<sub>2</sub>, PM<sub>2.5</sub>, VOC, CO<sub>2</sub>, CH<sub>4</sub>, N<sub>2</sub>O)  
l: State  
mf: Electricity emissions factor

## 9.0 References

1. Plappally, A. K.; Lienhard V, J. H., Energy requirements for water production, treatment, end use, reclamation, and disposal. *Renewable and Sustainable Energy Reviews* **2012**, *16* (7), 4818-4848.
2. Rodriguez-Garcia, G.; Molinos-Senante, M.; Hospido, A.; Hernandez-Sancho, F.; Moreira, M. T.; Feijoo, G., Environmental and economic profile of six typologies of wastewater treatment plants. *Water Res* **2011**, *45* (18), 5997-6010.
3. U.S. Environmental Protection Agency About the Clean Watersheds Needs Survey (CWNS). <https://www.epa.gov/cwns/about-clean-watersheds-needs-survey-cwns> (accessed June 10).
4. U.S. Environmental Protection Agency Clean Watersheds Needs Survey (CWNS) - 2012 Report and Data. <https://www.epa.gov/cwns/clean-watersheds-needs-survey-cwns-2012-report-and-data#access> (accessed June 10).
5. U.S. Environmental Protection Agency Clean Watersheds Needs Survey (CWNS) - 2008 Report and Data. <https://www.epa.gov/cwns/clean-watersheds-needs-survey-cwns-2008-report-and-data> (accessed June 10).
6. Siler-Evans, K.; Azevedo, I. L.; Morgan, M. G., Marginal emissions factors for the U.S. electricity system. *Environmental Science & Technology* **2012**, *46* (9), 4742-8.
7. U.S. Environmental Protection Agency Emissions Inventories. <http://www3.epa.gov/ttn/chief/eiinformation.html> (accessed October 9, 2015).
8. Gingerich, D. B.; Sun, X. B., A. Patrick; Azevedo, I. M. L.; Mauter, M. S., Spatially resolved air-water emissions tradeoffs improve regulatory impact analyses for electricity generation. *Proceedings of the National Academy of Science* **2017**, 1862–1867.
9. Althaus H-J, e. a., *Life Cycle Inventories of Chemicals No. 8*, v. 2.0. Dusseldorf, Switzerland, 2007.
10. National Renewable Energy Laboratory National Renewable Energy Laboratory - Life-Cycle Inventory Database. . <https://www.lcacommons.gov/nrel/process/show/50158> (accessed October 3, 2015).
11. Tata, P.; Witherspoon, J.; Lue-Hing, C., *VOC Emissions from Wastewater Treatment Plants: Characterization, Control and Compliance*. Lewis Publishers: Boca Raton, FL, 2016.
12. Hospido, A.; Moreira, M. T.; Fernandez-Couto, M.; Feijoo, G., Environmental Performance of a Municipal Wastewater Treatment Plant *International Journal of Life Cycle Assessment* **2004**, *9* (4), 261-271.
13. Monteith, H. D.; Sahely, H. R.; MacLean, H. L.; Bagley, D. M., A Rational Procedure for Estimation of Greenhouse-Gas Emissions from Municipal Wastewater Treatment Plants. *Water Environment Research* **2005**, *77* (4), 390-403.
14. Metcalf & Eddy, I.; Tchobanoglous, G. B., Franklin L.; Stensel, H. D., *Wastewater Engineering: Treatment and Reuse*. 4th ed.; McGraw Hill Higher Education: New York, NY, 2002.
15. Doorn, M. R. J.; Towprayoon, S.; Vieira, S. M. M.; Irving, W.; Palmer, C.; Pipatti, R.; Wang, C., Chapter 6: Wastewater Treatment and Discharge. In *2006 IPCC Guidelines for National Greenhouse Gas Inventories*, Change, I. P. o. C., Ed. Intergovernmental Panel on Climate Change: Geneva, Switzerland, 2006.

16. Czepiel, P.; Crill, P.; Harriss, R., Nitrous Oxide Emissions from Municipal Wastewater Treatment. *Environmental Science & Technology* **1995**, 29, 2352-2356.
17. California Air Resource Board; California Climate Action Registry; ICLEI - Local Governments for Sustainability; Registry, T. C. *Local Government Operations Protocol: For the quantification and reporting of greenhouse gas emissions inventories*; California Air Resources Board: Sacramento, CA, 2010.
18. U.S. Environmental Protection Agency *Inventory of U.S. Greenhouse Gas Emissions and Sinks 1990-2015*; U.S. Environmental Protection Agency: Washington, D.C., 2017.
19. Stillwell, A. S.; Hoppock, D. C.; Webber, M. E., Energy Recovery from Wastewater Treatment Plants in the United States: A Case Study of the Energy-Water Nexus. *Sustainability* **2010**, 2 (4), 945-962.
20. Burton, F. L. *Water and Wastewater Industries: Characteristics and Energy Management Opportunities*; Burton Environmental Engineering Electric Power Research Institute: Los Altos, CA, 1996.
21. Gingerich, D. B.; Mauter, M. S., Life-Cycle Air Emissions Damages of Municipal Drinking Water Treatment Under Current & Proposed Regulatory Standards. **under review**.
22. Shen, Y.; Linville, J. L.; Urgan-Demirtas, M.; Mintz, M. M.; Snyder, S. W., An overview of biogas production and utilization at full-scale wastewater treatment plants (WWTPs) in the United States: Challenges and opportunities towards energy-neutral WWTPs. *Renewable and Sustainable Energy Reviews* **2015**, 50, 346-362.
23. United States Census Bureau Annual Survey of Manufacturers 2013.  
<https://www.census.gov/manufacturing/asm/index.html> (accessed October 11, 2015).

## **APPENDIX 3: SUPPORTING INFORMATION FOR CHAPTER 4 - SPATIALLY RESOLVED AIR-WATER EMISSIONS TRADEOFFS IMPROVE REGULATORY IMPACT ANALYSES FOR ELECTRICITY GENERATION**

### **Supporting Information Description:**

This document contains a description of FGD systems and FGD wastewater treatment; the life cycle emissions inventory data; sensitivity analysis on the distribution of chemical manufacturing; details on the model for marginal emission damage estimates; sensitivity analysis on the price of carbon; a summary of the EPA's cost-benefit analysis of the final effluent limitation guidelines and our methodology for updating it; the emissions resulting from treating 1 m<sup>3</sup> of FGD wastewater; and the damages by pollutant using plant and marginal emission factors for auxiliary electricity demand.

This Supporting Information is available at:

<http://www.pnas.org/content/suppl/2017/02/01/1524396114.DCSupplemental/pnas.1524396114.sapp.pdf>

## **APPENDIX 4: SUPPORTING INFORMATION FOR CHAPTER 5 – QUANTITY, QUALITY, AND AVAILABILITY OF WASTE HEAT FROM UNITED STATES THERMAL POWER GENERATION**

### **Supporting Information Description:**

This document contains descriptions of 1) power plant cycles; 2) detailed analysis of exhaust gas composition and properties; 3) the list of the studies used to construct estimates of residual heat distribution; 4) sensitivity analysis results for the residual heat distribution; 5) description of the models for heat exchangers and transport distances; 6) description of the 21 scenarios used for residual heat forecasting; 7) the data set of residual heat generation at US power plants and instructions on how to access it; 8) electricity substitution calculations; 9) geospatial breakdowns of the residual heat locations and 10) sensitivity analysis for transport distances to natural gas prices.

This Supporting Information is available at:

<http://pubs.acs.org/doi/suppl/10.1021/es5060989>



## **APPENDIX 5: SUPPORTING INFORMATION FOR CHAPTER 6 – WATER TREATMENT CAPACITY OF FORWARD-OSMOSIS SYSTEMS UTILIZING POWER-PLANT WASTE HEAT**

### Supporting Information Description:

This document contains 1) the reactions in CO<sub>2</sub>-NH<sub>3</sub>-H<sub>2</sub>O systems; 2) detailed specifications for the ASPEN simulations; 3) the interfacial mass and heat transfer calculations in the rate-based model; 4) the activity coefficient calculations using the Electrolyte NRTL model; 5) the equilibrium constants and reaction rates for the models; 6) details on the parameter estimation methods in the mathematical model; 7) the parameters of the FO membrane model; 8) details on the membrane draw and feed solution modeling; 9) the finite element algorithm that we use for modeling the membrane; 10) the computational performance and accuracy of the chemistry, equilibrium stage, and rate-based models; 11) estimates of electrical duty in the system; and 12) the rates of mass transfer and reaction rate in the DSR column.

This Supporting Information is available at:

<http://pubs.acs.org/doi/suppl/10.1021/acs.iecr.5b00460>

## **APPENDIX 6: SUPPORTING INFORMATION FOR CHAPTER 7 - TECHNOECONOMIC ASSESSMENT OF WASTE HEAT DRIVEN FORWARD OSMOSIS SYSTEMS FOR ONSITE WASTEWATER TREATMENT**

Supporting Information Summary:

The supporting information contains descriptions of 1) the process meta-models; 2) the optimization problem formulation; and 3) the tabulated results presented in Figures 3 and 4 of the main manuscript.

This supporting information is 23 pages long and contains 3 figures (Figures S1-S3) and 13 tables (Tables S1-S13).

## 1.0 Process Meta-Models

### 1.1 Forward Osmosis Meta-Model

#### Discrete FO model

We modeled the FO process as a flat plate counter-current membrane with a discrete set of nodes ( $n$ ), as shown in Figure S1. Each node has an associated feed-side ( $f$ ) and draw-side ( $d$ ). The key variables for each node are the flowrate ( $Qf, Qd$ ), concentration ( $Cf, Cd$ ), water flux ( $Jw$ ), and salt flux ( $Js$ ). In our model, we consider three components ( $j$ ): sodium chloride ( $j1$ ), ammonium bicarbonate ( $j2$ ), and water ( $j3$ ). The model iteratively solves the implicit mass balance equations and water and salt flux equations.

#### Mass balance

Since the feed-side and draw-side flows are counter-current, the index of the inlets and outlet of the nodes are different and is reflected in Figure S1 and in the mass balance Equations S1-S4.

For the mass balance, we fix the density to  $1000 \left( \frac{kg}{m^3} \right)$ .

The output flowrate and concentration of feed nodes is calculated with Equations S1 and S2.

$$Qf_n = Qf_{n-1} - \left( Jw_n + \frac{1}{\rho} \sum_j Js_{j,n} \right) Area_n \quad \forall n \quad (S1)$$

$$Cf_{j,n} = Qf_{n-1} Cf_{j,n-1} - Js_{j,n} Area_n \quad \forall n, j1, j2 \quad (S2)$$

Where  $Qf_n$  and  $Qf_{n-1}$  are the feed flowrate  $\left( \frac{m^3}{s} \right)$  out of and into node  $n$ , respectively,  $Jw_n$  is the water flux  $\left( \frac{m^3}{m^2s} \right)$  for node  $n$ , and  $Js_{c,n}$  is the salt flux  $\left( \frac{kg}{m^2s} \right)$  for salt  $j$  ( $j1$  or  $j2$ ) and node  $n$ ,  $\rho$  is the fixed density  $\left( \frac{kg}{m^3} \right)$ ,  $Area_n$  is the membrane area ( $m^2$ ) for node  $n$ ,  $Cf_{j,n}$  and  $Cf_{j,n-1}$  is the concentration  $\left( \frac{kg}{m^3} \right)$  for salt  $j$  and out of and into node  $n$ , respectively.

The output flowrate and concentration of draw nodes is calculated with equations S3 and S4.

$$Qd_n = Qd_{n+1} + \left( Jw_n + \frac{1}{\rho} \sum_c Js_{j,n} \right) Area_n \quad \forall n \quad (S3)$$

$$Cd_{j,n} = Qd_{n+1} Cf_{j,n+1} - Js_{j,n} Area_n \quad \forall n, j1, j2 \quad (S4)$$

Where the notation is the similar to the feed-side except that the variables are draw-side (noted by  $d$ ) and index  $n + 1$  is the inlet to node  $n$ .

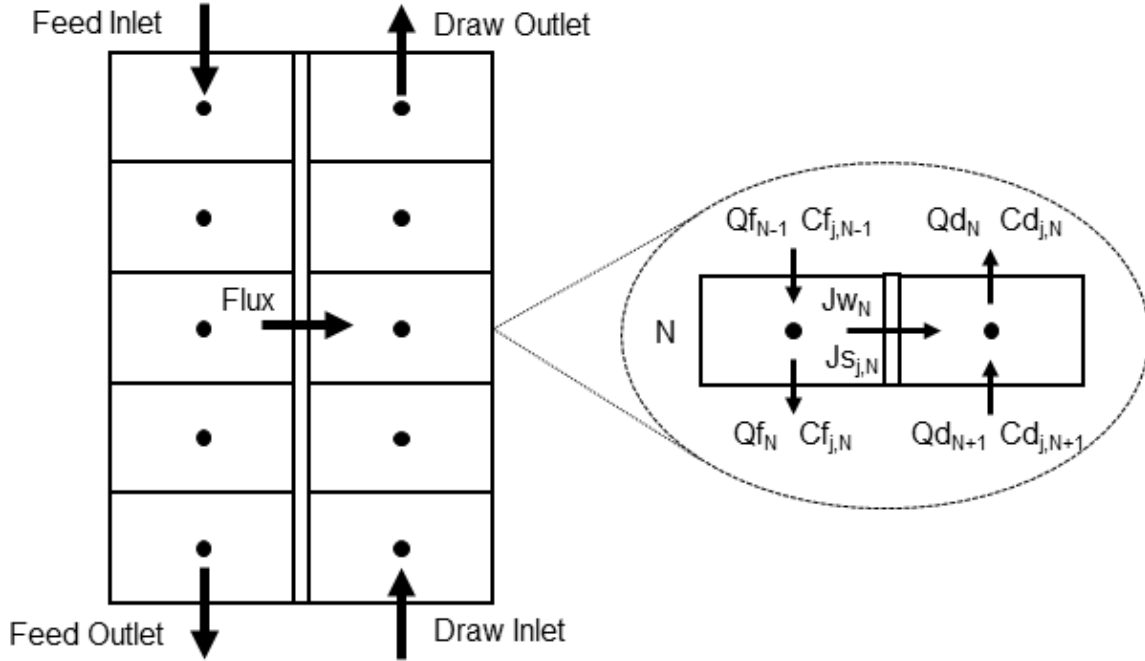


Figure S1. Discrete nodes, flow directions, and variables for the flat plate counter-current FO module. The dots represent the center of each node and the surrounding box is the boundary. A subsection of node N is provided with the relevant flowrates (Q), concentrations (C), water flux (Jw), and salt flux (Js) labeled.

#### Water and salt flux

The water flux for each node is calculated in equation S5.

$$Jw_n = A \left[ \left( \pi f_n \exp \left( \frac{Jw_n}{k} \right) - \pi d_n \exp(-Jw_n K) \right) \right] \quad (S5)$$

Where  $J_w$  is the water flux  $\left( \frac{m^3}{m^2 s} \right)$  from the feed to the draw,  $A$  is the pure water permeability coefficient  $\left( \frac{m}{Pa s} \right)$ ,  $\pi f_n$  and  $\pi d_n$  is the bulk feed and draw osmotic pressure (Pa),  $k$  is the feed mass transfer coefficient  $\left( \frac{m}{s} \right)$ , and  $K$  is the solute resistivity for diffusion in the sweep side porous support  $\left( \frac{s}{m} \right)$ ; refer to McCutcheon and Elimelech on how to determine  $k$  and  $K$  parameters.<sup>1</sup>

The salt flux for each node is calculated in equation S6.

$$Js_{j,n} = B_j [Cf_{j,n} - Cd_{j,n}] \quad (S6)$$

Where  $Js_{j,n}$  is the salt flux  $\left( \frac{kg}{m^2 s} \right)$  for salt  $j$  ( $j1$  or  $j2$ ) from the feed to the draw,  $B_j$  is the salt permeability coefficient  $\left( \frac{m}{s} \right)$ , and  $Cf_{j,n}$  and  $Cd_{j,n}$  are the concentration of the feed and draw, respectively.

### Fixed parameters and intermediate variables

In our model, there are various fixed parameters and intermediate variables. The fixed parameters include solution, membrane, membrane module parameters, and operating conditions. The solution parameters are: the density at 1000  $\left(\frac{kg}{m^3}\right)$ , viscosity at  $8.95 \times 10^{-4}$  (Pa s), solute diffusivity at  $1.5 \times 10^{-9}$   $\left(\frac{m^2}{s}\right)$ , and Reynolds number at 1000. The membrane parameters are: structural parameter at  $500 \times 10^{-6}$  (m), pure water permeability coefficient at  $10^{-12}$   $\left(\frac{m}{Pa\ s}\right)$ , sodium chloride salt permeability coefficient at  $6.5 \times 10^{-8}$   $\left(\frac{m}{s}\right)$ , and ammonium bicarbonate salt permeability coefficient at  $10.5 \times 10^{-8}$   $\left(\frac{m}{s}\right)$ . The membrane module parameters are: height at 0.001 (m) and the width is adjusted such that the inlet feed flowrate has a Reynolds number of 1000. Note that the membrane module length is an input variable to adjust membrane area. The operating conditions are: draw concentration is 3M ammonium bicarbonate and the inlet draw flowrate is half the inlet feed flowrate.

The intermediate variables include the osmotic pressure in the feed and draw. In our model, we assume the bulk osmotic pressure is the sum of the osmotic pressure from sodium chloride and ammonium bicarbonate as shown in Equation S7.

$$\pi_b = \pi_{j1} + \pi_{j2} \quad (S7)$$

Where  $\pi_b$  is the bulk osmotic pressure (Pa) and  $\pi_{j1}$  and  $\pi_{j2}$  are the osmotic pressure (Pa) of sodium chloride and ammonium bicarbonate, respectively. We estimate the osmotic pressure of sodium chloride and ammonium bicarbonate as a function of concentration as shown in Equations S8 and S9.

$$\pi_{j1} = 4260 C_{j1} + 0.7 C_{j1}^2 \quad (S8)$$

$$\pi_{j2} = 4410 C_{j2} - 0.32 C_{j2}^2 \quad (S9)$$

Where  $C_{j1}$  and  $C_{j2}$  are the concentrations  $\left(\frac{mmol}{L}\right)$  of sodium chloride (j1) and ammonium bicarbonate (j2).

### Solution method

The model is solved with an iterative method. Initially, the model guesses a water and salt flux. Then three iterative steps are repeated until an error tolerance is reached. Given a guessed water and salt flux, step 1 calculates the concentration and flowrates given a guessed water and salt flux. Given the concentration determined in step 1, step 2 calculates the water and salt flux. Given the calculated water and salt flux determined in step 2, step 3 updates the guessed water and salt flux. This process is repeated until the water and salt flux between iterations has a relative error less than 0.1%.

### Forward Osmosis Meta-Model

We use the forward osmosis model presented above to develop regression models for water and salt recovery as a function of membrane area. We simulate the forward osmosis model for a range of membrane areas (dependent on flowrate of case study) and fit the equations for recoveries greater than 20%. The form of the regression model for water recovery is shown in Equation S10.

$$R_j = \beta_{0,j} + \beta_{1,j}Area_{mem} + \beta_{2,j}Area_{mem}^2 + \epsilon \quad \forall j \text{ (S10)}$$

Where  $R_j$  is the recovery for component  $j$  (sodium chloride  $j1$ , ammonium bicarbonate  $j2$ , water  $j3$ ),  $\beta$  are the regression coefficients, and  $Area_{mem}$  is the membrane area. The regression coefficients for the case studies are presented in Tables S1-3 and all  $R^2$  values were greater than 0.99. Additionally, we present the simulation and fit for the base PC w/CC case in Figure S2.

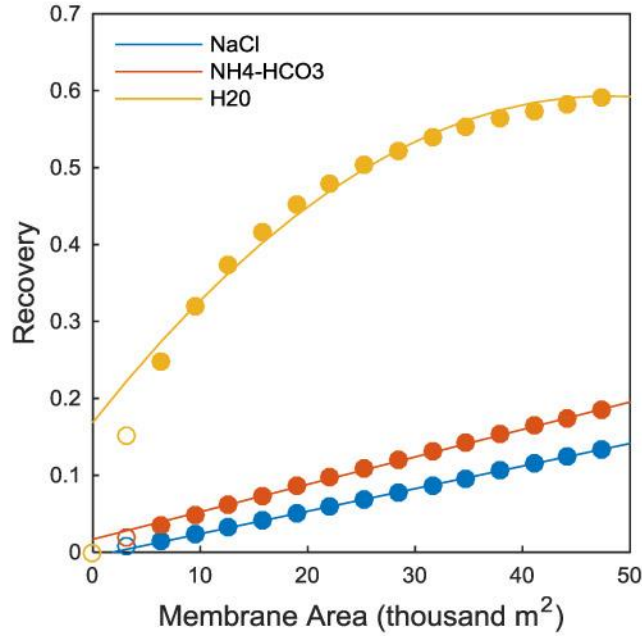


Figure S2. Forward osmosis simulation and regression for the base PC w/CC case. The circles are simulations, filled circles are used for the regression, and the dotted line is the fitted polynomial.

Table S1. Forward osmosis meta-model coefficients.

	$\beta_0$	$\beta_1$	$\beta_2$
PC w/o CC			
Sodium Chloride	-5.43E-03	2.92E-06	
Ammonium Bicarbonate	1.45E-02	3.72E-06	
Water	1.52E-01	2.05E-05	-2.59E-10
PC w/CC			
Sodium Chloride	-5.07E-03	2.42E-06	
Ammonium Bicarbonate	1.38E-02	3.10E-06	
Water	1.39E-01	1.78E-05	-1.89E-10
IGCC			
Sodium Chloride	-3.08E-02	6.70E-04	
Ammonium Bicarbonate	8.34E-03	2.98E-04	
Water	4.88E-02	7.37E-03	-1.57E-05
Plant Bowen			
Sodium Chloride	-4.15E-03	1.19E-06	
Ammonium Bicarbonate	1.12E-02	1.61E-06	
Water	1.06E-01	1.06E-05	-6.64E-11

Table S2. Forward osmosis meta-model coefficients for the draw solution concentration sensitivity analysis.

	$\beta_0$	$\beta_1$	$\beta_2$
2 M			
Sodium Chloride	-1.59E-03	2.45E-06	
Ammonium Bicarbonate	1.24E-02	4.04E-06	
Water	8.08E-02	1.74E-05	-2.32E-10
3 M*			
Sodium Chloride	-5.43E-03	2.92E-06	
Ammonium Bicarbonate	1.45E-02	3.72E-06	
Water	1.52E-01	2.05E-05	-2.59E-10
4 M			
Sodium Chloride	-8.01E-03	3.30E-06	
Ammonium Bicarbonate	1.16E-02	3.74E-06	
Water	1.51E-01	2.72E-05	-3.84E-10
5 M			
Sodium Chloride	-1.10E-02	3.67E-06	
Ammonium Bicarbonate	1.02E-02	3.77E-06	
Water	1.67E-01	3.02E-05	-4.44E-10

Table S3. Forward osmosis meta-model coefficients for the feed solution concentration sensitivity analysis.

	$\beta_0$	$\beta_1$	$\beta_2$
0.4 M			
Sodium Chloride	-1.30E-02	3.77E-06	
Ammonium Bicarbonate	1.29E-02	3.49E-06	
Water	1.68E-01	2.76E-05	
0.6 M*			
Sodium Chloride	-5.43E-03	2.92E-06	
Ammonium Bicarbonate	1.45E-02	3.72E-06	
Water	1.52E-01	2.05E-05	
0.8 M			
Sodium Chloride	-1.62E-03	2.50E-06	
Ammonium Bicarbonate	1.71E-02	3.83E-06	
Water	1.37E-01	1.38E-05	

## 1.2 Distillation Column Meta-Model

We use an the ASPEN model described in our past work<sup>2</sup> in order to build a dataset on the performance of the distillation column under the of inputs listed in Table S4. We use this model to record the outputs listed in Table S4.

Table S4. Inputs, Input Ranges, and Outputs from the ASPEN Distillation Column Model

Variables	Range
<i>Inputs</i>	
Number of Trays	[10-30]
NH <sub>4</sub> HCO <sub>3</sub> Feed Concentration	[0.75M-2.0 M]
NH <sub>3</sub> Concentration in Treated Water	[100-1000 ppb]
Volumetric Flow Rate In	[4-30 m <sup>3</sup> /hr]
Tray Diameter	[0.5-3.0 m]
<i>Outputs</i>	
Heat Duty Requirement	
Mass Based Flow Rate In	
Mass Based Flow Rate of Treated Water	
Volumetric Flow Rate of Treated Water	

We use this ASPEN model to build two different sets of regression models, one for a low flow distillation column (flow rate <100 m<sup>3</sup>/hr) and one for a high flow distillation column (flow rate >100 m<sup>3</sup>/hr). These regression models model the number of trays ( $N_{\text{trays}}$ ) in the distillation column and the required heat duty ( $Q_{\text{required}}$ ) in the reboiler for the distillation column as a function of the water recovery (WR) observed in the distillation column. Tables S5 and S6 present the coefficients for the high flow and low flow distillation column that are used in Equations S11 and S12.



$$N_{tray} = \exp(\beta_0) R_{dis}^{\beta_1} + \epsilon \quad (S11)$$

$$Q_{requird} = \beta_0 + \beta_1 + \beta_2 * WR^2 + \epsilon \quad (S12)$$

*Table S5. Number of Trays Meta-Model Coefficients*

	$\beta_0$	$\beta_1$	$R^2$
High-Flow Column	1.75	-0.547	0.9934
Low-Flow Column	1.69	-0.574	0.9896

*Table S6. Reboiler Heat Duty Meta-Model*

	$\beta_0$	$\beta_1$	$\beta_2$	Adjusted $R^2$
High-Flow Column	365	1060	8980	0.9973
Low-Flow Column	357	1010	8890	0.9967

### 1.3 Brine Treatment Train Meta-Model

We build a model of a flash distillation column in ASPEN. The flash distillation column operates at a temperature of 91°C and a pressure of 1 atm. A feed stream at a concentration of approximately 1.2M (twice the feed flow rate) and enters at a temperature of 50°C at a pressure of 1.01 atm to account for pressure losses within the system. Based on this ASPEN model, we calculate an energy consumption of 317.6 MJ/m<sup>3</sup>, an ammonia recovery of 90% and a 30% recovery of water.

## 2.0 Optimization Problem Formulation

We formulate the forward osmosis and crystallization process using a nonlinear programming (NLP) problem. Our objective is to minimize the costs of treating the wastewater to achieve zero liquid discharge. The NLP problem encompasses the 5 main process units: 1) forward osmosis module, 2) heat exchangers, 3) distillation column, 4) ammonia recovery unit, 5) crystallizer unit.

In this problem, there are 14 streams, noted by subscript  $i$  and labeled in Figure S3. Each stream  $i$  has an associated mass flow,  $M_{i,j}$ , where  $j$  is the component of the stream. There are three components of the stream:  $j1$ ) sodium chloride,  $j2$ ) ammonium bicarbonate,  $j3$ ) water. Additionally, each stream has an associated temperature,  $T_i$ . These state variables are related by mass and energy balances and process performance equations presented in the following sections.

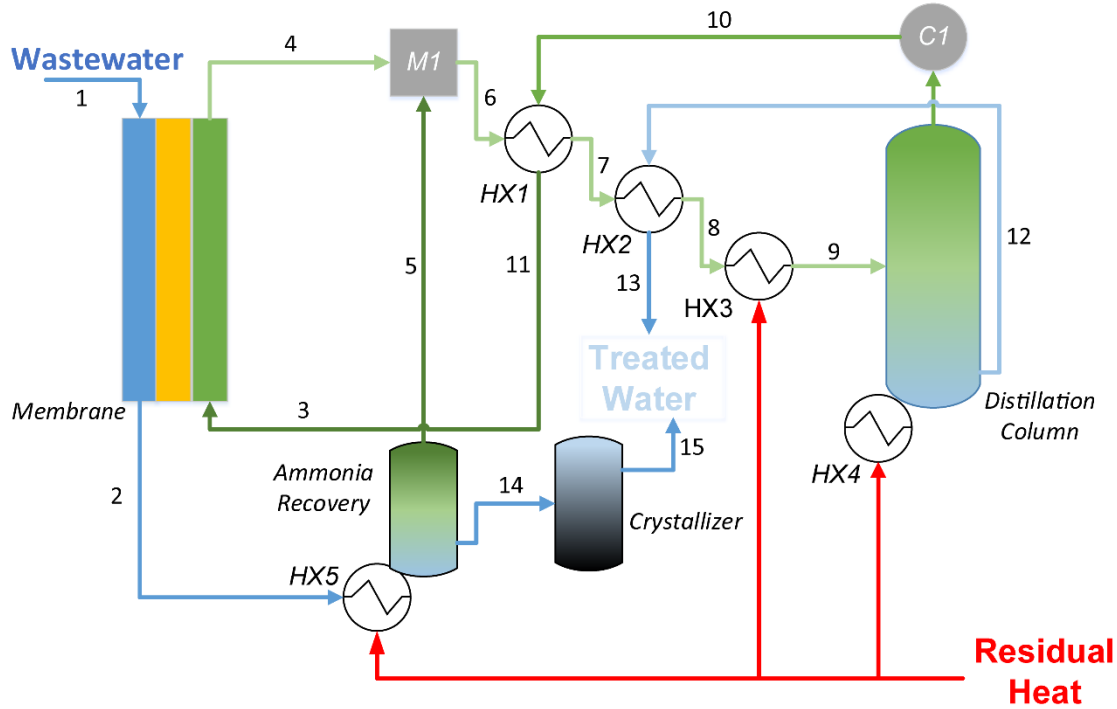


Figure S3. Streams in the optimization model.

### 2.1 FO module

The mass balance for each component in the FO module is represented by the constraint shown in Equation S13.

$$M_{i1,j} + M_{i3,j} = M_{i2,j} + M_{i4,j} \quad \forall j \quad (\text{S13})$$

Where  $M_{i,j}$  is the mass flow [kg/s] associated with stream  $i$  and component  $j$ . Stream  $i1$  and  $i3$  are the FO module inlets, while stream  $i2$  and  $i4$  are the FO module outlets.

The mass of each component that crosses the membrane is based on the recovery,  $R_{mem,j}$ , as shown in Equation S14.

$$R_{mem,j} = \beta_{0,j} + \beta_{1,j}Area_{mem} + \beta_{2,j}Area_{mem}^2 \quad \forall j \quad (S14)$$

Where  $\beta_{0,j}$ ,  $\beta_{1,j}$ ,  $\beta_{2,j}$  are the parameters estimated in the meta-model described in Section S1.1, and  $A_{mem}$  is the membrane area. The recovery is used to relate the inlet mass flow rate to the outlet mass flow rate as enforced in the constraints shown in Equations S15-S17.

$$M_{i1,j1}R_{mem,j1} + M_{i3,j1} = M_{i4,j1} \quad (S15)$$

$$M_{i3,j2}R_{mem,j2} + M_{i1,j2} = M_{i2,j2} \quad (S16)$$

$$M_{i1,j3}R_{mem,j3} + M_{i3,j3} = M_{i4,j3} \quad (S17)$$

Note that equations (S15) and (S17) have the same form with different stream components  $j$ , while constraint (S16) has a different form. This difference arises because component  $j2$ , which is ammonium bicarbonate, backpermeates from the draw to the feed solution, while  $j1$  and  $j3$ , which are sodium chloride and water, permeates from the feed to the draw solution.

## 2.2 Mixer

The mixer combines the diluted draw and the recovered ammonia bicarbonate stream before preheating and eventual distillation. The mixing is represented in Equation S18.

$$M_{i6,j} = M_{i4,j} + M_{i5,j} \quad \forall j \quad (S18)$$

## 2.3 Heat Exchangers

There are five heat exchangers in the proposed process. Three of the heat exchangers are used to preheat the dilute draw solution to 100 °C before being fed into the distillation column. Two of these preheaters (heat exchanger 1 and 2) exchange heat between two liquid streams, while the other preheater (heat exchanger 3) exchanges heat between a liquid stream and the flue gas. The final two heat exchangers (heat exchanger 4 and 5) boil water in the distillation and ammonia recovery unit by providing heat from the flue gas.

Heat exchangers have a cold and hot stream, indicated by the subscripts  $C$  and  $H$ , respectively. There is no change in mass flow rate for the cold and hot stream as represented by the constraint shown in Equation S19.

$$M_{i,j} = M_{i',j} \quad \forall ii' \in HE_{ii'} \quad (S19)$$

Where  $i$  is the inlet and  $i'$  is the outlet for a cold or hot stream, which is represented by set  $HE_{ii'}$ . Table S7 shows the cold and hot stream pairs for each heat exchanger. For heat exchanger 4 and 5 the cold stream is the boiling water in the distillation or ammonia recovery unit, and therefore

the mass flow rate is not relevant or assigned to a stream  $i$ . For heat exchanger 3, 4, and 5 the hot stream is flue gas and the mass flow rate is also not relevant to the optimization model.

*Table S7. Cold and hot stream pairs for the heat exchanger.*

Heat exchanger	Inlet cold stream	Outlet cold stream	Inlet hot stream	Outlet hot stream
1	$i6$	$i7$	$i10$	$i11$
2	$i7$	$i8$	$i12$	$i13$
3	$i8$	$i9$		
4				
5				

The heat duty of the heat exchanger,  $Q_{ex}$  (kW), is determined by Equation S20.

$$Q_{ex} = U Area_{ex} \Delta T_{chen} \quad (S20)$$

Where  $U$  is the overall heat transfer coefficient (kW/m<sup>2</sup> °C),  $A_{ex}$  is the heat exchanger area (m<sup>2</sup>), and  $\Delta T_{chen}$  is Chen's temperature difference (°C). The Chen's temperature difference is determined using Equation S21.

$$\Delta T_{chen} = \left( (T_{H,out} - T_{C,in})(T_{H,in} - T_{C,out}) \right)^{\frac{1}{3}} * \left( \frac{1}{2} (T_{H,out} - T_{C,in})(T_{H,in} - T_{C,out}) \right)^{\frac{1}{3}} \quad (S21)$$

Where  $T_{C,in}$  and  $T_{C,out}$  are the temperatures of the inlet and outlet cold stream, respectively, and  $T_{H,in}$   $T_{H,out}$  are the temperatures of the inlet and outlet hot stream, respectively. Table S8. shows whether these temperatures are a variable or a parameter. The temperature is a variable if noted with  $T_i$  and is a parameter otherwise. TFG stands for temperature of the flue gas.

*Table S8. The temperature of the inlet and outlet of the cold and hot stream for each heat exchanger.*

Heat exchanger	$T_{C,in}$	$T_{C,out}$	$T_{H,in}$	$T_{H,out}$
1	$T_{i6}$	$T_{i7}$	$T_{i10}$	$T_{i11}$
2	$T_{i7}$	$T_{i8}$	$T_{i12}$	$T_{i13}$
3	$T_{i8}$	$T_{i9}$	TFG	TFG-10
4	100 °C	100 °C	TFG	TFG-10
5	100 °C	100 °C	TFG	TFG-10

When the temperature is a variable, (cold stream for heat exchanger 1, 2, and 3, and hot stream for heat exchanger 1 and 2) the heat duty relates the temperature of the inlet and outlet cold and hot stream through the simple heating constraints shown in Equations S22 and S23.

$$Q_{ex} = (\sum_j M_{C,in,j}) Cp (T_{C,out} - T_{C,in}) \quad (S22)$$

$$Q_{ex} = (\sum_j M_{H,in,j}) Cp (T_{H,in} - T_{H,out}) \quad (S23)$$

Where the summation of  $M_{*,in,j}$  is the total mass flow rate in the hot and cold stream, and  $Cp$  is the specific heat capacity of water (assumed to be 4.186 kJ/kg °C).

We assume that the minimum approach temperature is 5 °C, as represented in the constraints shown in Equation S24 and S25.

$$T_{C,in} + 5 \leq T_{H,out} \quad (S24)$$

$$T_{C,out} + 5 \leq T_{H,in} \quad (S25)$$

## 2.4 Distillation Column

The component mass balance in the heat exchanger is represented in the constraint represented by Equation S26.

$$M_{i9,j} = M_{i10,j} + M_{i12,j} \quad \forall j \quad (S6)$$

Where stream  $i9$  is the feed, stream  $i10$  is the distillate, and stream  $i12$  is the bottoms of the distillation column.

We assume that no sodium chloride will be present in the distillate, as represented by the constraint in the following Equation S27.

$$M_{i10,j1} = 0 \quad (S27)$$

We also assume that the concentration of ammonium bicarbonate in the bottoms is equal to 1 ppm, which shown in Equation S28.

$$M_{i12,j2} * 1E6 = \sum_j M_{i12,j} \quad (S28)$$

Water separation is dictated by the water recovery in the distillation column,  $R_{dis}$ , and is determined by Equation S29.

$$M_{i10,j3} = M_{i9,j3} R_{dis} \quad (S29)$$

We estimate the required heat duty and number of trays for the distillation column to obtain the water recovery in the distillation column through a meta-model described in SI section 1.2. The required heat duty and number of trays is determined by the constraints established in Equations S30 and S31.

$$Q_{ex4} = (\beta_0 + \beta_1 R_{dis} + \beta_2 R_{dis}^2) \sum_j M_{i12,j} \quad (S30)$$

$$N_{tray} = \exp(\beta_0) R_{dis}^{\beta_1} \quad (S31)$$

## 2.5 Ammonia Recovery Unit

The component mass balance in the ammonia recovery unit is represented by Equation S32.

$$M_{i2,j} = M_{i4,j} + M_{i5,j} \quad \forall j \quad (S32)$$

The ammonia-bicarbonate recovery is fixed to 90% and is enforced by the constraint shown in Equation S33.

$$M_{i5,j2} = 0.9 M_{i2,j2} \quad (S33)$$

The water recovery in the ammonia recovery unit is fixed to 30% and is enforced by Equation S34.

$$M_{i5,j3} = 0.3 M_{i2,j3} \quad (S34)$$

The required heat duty of the ammonia recovery unit is determined by the constraint shown in Equation S35.

$$Q_{ex5} = M_{i5,j3} \hat{Q}_{AR} \quad (S35)$$

Where  $Q_{ex5}$  is the heat duty of the ammonia recovery unit,  $\hat{Q}_{AR}$  is the specific thermal energy demand (kJ per kg of water distillate).

## 2.6 Chemical Addition

Ammonia bicarbonate must be added to replenish the ammonium bicarbonate is lost in the product water from the distillation column. We add the ammonia bicarbonate just before the draw solution enters the FO module as represented in the constraint shown in Equation S36.

$$M_{i3,j2} = M_{i11,j2} + M_{add,j2} \quad (S36)$$

Where  $M_{add,j2}$  is the mass of ammonia bicarbonate added.

## 2.7 Condenser

The cooling duty of the condenser is determined using Equation S37.

$$Q_{Cond} = H_{vap} M_{i10,j3} \quad (S37)$$

Where  $Q_{Cond}$  is the cooling duty of the condenser,  $H_{vap}$  is the heat of vaporization of water, and  $M_{i10,j3}$  is the water mass flowrate in the distillate.

The cooling duty of the chiller is determined by Equation S38.

$$Q_{chiller} = (\sum_j M_{i11,j}) C_p (T_{i11} - 50) \quad (S38)$$

The total cooling duty is the sum of the cooling duty of the condenser and chiller, as shown in Equation S39.

$$Q_C = Q_{cond} + Q_{chiller} \quad (S39)$$

## 2.8 Objective Function

The objective of the model is to minimize the cost of the system. We base the cost model parameters on the NETL ICARUS model<sup>3</sup> and standard engineering references.<sup>4</sup> The total cost is the summation of 7 components as shown in Equation S40.

$$obj = Cost_{mem} + Cost_{dis} + Cost_{crys} + Cost_{ex} + Cost_{chem} + Cost_{ar} + Cost_{cond} \quad (S40)$$

Where the subscripts: *mem* is membrane module, *dis* is distillation column, *crys* is the crystallizer, *ex* is the heat exchangers, *chem* is the chemicals, *ar* is the ammonia recovery, *cond* is the condenser and chiller.

The membrane cost is calculated using Equation S41.

$$Cost_{mem} = CV_{mem} * Area_{mem} \quad (S41)$$

Where  $CV_{mem}$  is the variable cost of the membrane.

The distillation cost is calculated by Equation S42.

$$Cost_{dis} = CF \left( 17400 + 75 \left( HTU * N_{tray} * \pi * D_{dis} * 0.05 * 7740 \right)^{0.85} + \frac{\pi}{4} * D_{dis}^2 * HTU * N_{tray} * 7600 + 13705 + 180 * Area_{ex4} \right) \quad (S42)$$

Where  $CF$  is the capital recovery factor,  $HTU$  is the height of the transfer unit,  $D_{dis}$  is the diameter of the distillation column,  $A_{ex4}$  is the area of the heat exchanger for the reboiler. The cost of the crystallizer is calculated with Equation S43.

$$Cost_{crys} = CV_{crys} \sum_j M_{i4,j} \quad (S43)$$

Where  $CV_{crys}$  is the variable cost of the crystallizer.

The cost of the preheating heat exchangers is calculated by Equation S44.

$$Cost_{ex} = CF \left( 3 * 13705 + 180 * (Area_{ex,1} + Area_{ex,2} + Area_{ex,3}) \right) \quad (S44)$$

The cost of the chemicals is calculated with Equation S45.

$$Cost_{chem} = CV_{chem} M_{add,j2} \quad (S45)$$

Where  $CV_{chem}$  is the variable cost of the ammonia-bicarbonate.

The cost of the ammonia recovery unit is calculated using Equation S46.

$$Cost_{ar} = CV_{ar} \sum_j M_{i5,j} + CF(13705 + 180 * Area_{ex,5}) \quad (S46)$$

Where  $CV_{ar}$  is the variable cost of the ammonia recovery unit.

The cost of the of the condenser and chiller is calculated by Equation S47.

$$Cost_{cond} = CV_{cond} Q_c \quad (S47)$$

Where  $CV_{cond}$  is the variable cost of the condenser.



### 3.0 Tabulated Results

#### 3.1 Base Case Results

Table S9 shows the tabulated results that are presented in Figure 3 of the manuscript. Table S10 shows the design characteristics of the optimized systems.

*Table S9. Tabulated optimization results.*

	PC w/o CC	PC w/CC	IGCC	Plant Bowen
Costs [\$K/yr]				
Chemical	174	213	1.3	403
Condenser	64	77	0.7	153
Crystalizer	1259	1502	2.5	3062
Distillation	33	36	10.2	105
Exchangers	36	42	5.2	121
Membrane	326	400	2.9	743
Ammonia Recovery	108	128	1.9	260
Total Cost	1999	2399	25	4847
Cost per Cubic Meter [\$ /m <sup>3</sup> ]	2.04	2.04	2.36	2.06
Hourly Energy Use [MJ/hr]	2281	2276	1554	2293

Table S10. Optimized system designs.

	PC w/o CC	PC w/CC	IGCC	Plant Bowen
Key flow rates [m <sup>3</sup> /hr]				
Feed into FO module	111.6	134.3	1.2	268.6
Draw into FO module	55.8	67.3	0.6	134.3
Concentrated wastewater out of FO module	59.9	71.5	0.1	145.6
Diluted draw solution out of FO module	107.5	130.1	1.7	257.2
Wastewater into ammonia recovery system*	59.9	71.5	0.1	145.6
Wastewater into crystallizer	42.2	50.4	0.1	102.7
Key concentrations [M]				
Feed into FO module (NaCl)	0.60	0.60	0.08	0.60
Draw into FO module (NH <sub>4</sub> -HCO <sub>3</sub> )	3.0	3.0	3.0	3.0
Concentrated wastewater out of FO module (NaCl)	1.0	1.1	0.6	1.0
Concentrated wastewater out of FO module (NH <sub>4</sub> -HCO <sub>3</sub> )	0.3	0.3	1.0	0.3
Diluted draw solution out of FO module (NaCl)	0.039	0.040	0.006	0.037
Diluted draw solution out of FO module (NH <sub>4</sub> -HCO <sub>3</sub> )	1.4	1.4	1.0	1.4
Wastewater into ammonia recovery system	0.0	0.0	0.0	0.0
Wastewater into crystalizer (NaCl)	1.5	1.5	0.9	1.5
Wastewater into crystalizer (NH <sub>4</sub> -HCO <sub>3</sub> )	0.040	0.041	0.149	0.038
Key recoveries [-]				
Water recovery in FO module	49%	49%	90%	48%
NaCl rejection in FO module	94%	94%	89%	94%
Ammonium bicarbonate rejection in FO module	90%	90%	93%	90%
Water recovery in the Distillation column	62%	62%	71%	62%
Heat duty [kW]				
Distillation column	40.0	48.3	0.446	96.3
Thermal ammonia recovery	1.45	1.73	0.003	3.54
Size				
Membrane area [m <sup>2</sup> ]	23330	28620	210	53190
Number of trays [-]	10	10	11	10
Height of distillation column [m]	2.9	2.9	3.4	2.9
Heat exchanger 1 [m <sup>2</sup> ]	186.3	224.7	1.88	480.5
Heat exchanger 2 [m <sup>2</sup> ]	215.6	260.9	3.72	534.1
Heat exchanger 3 [m <sup>2</sup> ]	1053	1272	13.9	4473
Heat exchanger 4 [m <sup>2</sup> ]	837.4	1011	9.32	4255
Heat exchanger 5 [m <sup>2</sup> ]	30.4	36.2	0.063	156.3

### 3.2 Sensitivity Analysis Results

Table S11-13 present the tabulated results of the sensitivity analyses shown in Figure 4.

*Table S11. Tabulated results for the concentration draw solution sensitivity analysis.*

	Concentration of Draw Solution [M]			
	2	3*	4	5
Costs [\$K/yr]				
Chemical	112	175	228	275
Condenser	71	65	58	52
Crystalizer	1589	1257	1066	963
Distillation	33	33	32	31
Exchangers	9	9	9	9
Membrane	293	327	325	313
Ammonia Recovery	133	107	93	86
Total Cost	2240	1973	1811	1728
Cost per Cubic Meter [\$ /m <sup>3</sup> ]	2.29	2.02	1.85	1.77
Hourly Energy Use [MJ/hr]	3025	2415	2046	1790

\*Indicates value used in base case analysis.

*Table S12. Tabulated results for the draw solution flow rate sensitivity analysis.*

	Flow Rate of Draw Solution [M]				
	50%	100%*	150%	200%	250%
Costs [\$K/yr]					
Chemical	123	175	205	215	218
Condenser	32	65	98	130	163
Crystalizer	1503	1257	1158	1128	1115
Distillation	27	33	39	45	50
Exchangers	7	9	10	11	13
Membrane	285	327	348	345	336
Ammonia Recovery	126	107	100	98	97
Total Cost	2104	1973	1958	1972	1993
Cost per Cubic Meter [\$ /m <sup>3</sup> ]	2.15	2.02	2.00	2.02	2.04
Hourly Energy Use [MJ/hr]	1584	2415	3199	3914	4543

\*Indicates value used in base case analysis.

*Table S13. Tabulated results for the feed solution concentration sensitivity analysis.*

	Concentration of Feed Solution [M]		
	0.4	<b>0.6*</b>	0.8
Costs [\$K/yr]			
Chemical	191	175	145
Condenser	65	65	65
Crystalizer	826	1257	1634
Distillation	34	33	32
Exchangers	9	9	9
Membrane	392	327	244
Ammonia Recovery	74	107	135
Total Cost	1590	1973	2119
Cost per Cubic Meter [\$ / m <sup>3</sup> ]	1.63	2.02	2.32
Hourly Energy Use [MJ/hr]	2042	2415	2879

\*Indicates value used in base case analysis.

## 4.0 Nomenclature

### Symbols

A:	Pure water permeability coefficient [m/Pa·s]
Area:	Area [m <sup>2</sup> ]
B:	Salt permeability coefficient [m/s]
$\beta$ :	Regression coefficient [-]
C:	Concentration [kg/m <sup>3</sup> ]
CF:	Capital factor [-]
Cost:	Cost [\$]
$c_p$ :	Specific heat capacity [kJ/kg·°C]
CV:	Variable Cost [\$/unit]
D:	Diameter
Qd:	Draw side
$\epsilon$ :	Error [-]
Qf:	Feed side
HTU:	Heat of transfer unit in distillation column [m]
$H_{\text{vap}}$ :	Heat of vaporization [kJ/kg]
J:	Flux [m <sup>3</sup> /m <sup>2</sup> ·s]
K:	Solute resistivity for diffusion in sweep side porous support [s/m]
$\kappa$ :	Feed mass transfer coefficient [m/s]
M:	Mass flow rate [kg/s]
N:	Number [-]
$\pi$ :	Osmotic pressure [Pa]

Q: Heat Duty [kW]  
 $\hat{Q}$ : Specific Thermal Energy [kJ/kg of distillate]  
Q<sub>c</sub>: Total Cooling Duty [kW]  
R: Recovery [%]  
T: Temperature [°C]  
U: Overall heat transfer coefficient [kW/m<sup>2</sup>·°C]  
ρ: Density [kg/m<sup>3</sup>]

### **Subscripts**

ar: Ammonia recovery  
C: Cold  
chem: Chemical  
chen: Chen's Approximate Temperature Difference [°C]  
cond: Condenser  
crys: Crystallizer  
dis: Distillation column  
ex: Heat exchanger  
FG: Flue gas  
H: Hot  
i: Stream  
j: Component  
mem: Membrane  
n: Node  
s: Salt

tray: Trays in the distillation column

w: Water

## 5.0 References

1. McCutcheon, J. R.; Elimelech, M., Influence of concentrative and dilutive internal concentration polarization on flux behavior in forward osmosis. *Journal of Membrane Science* **2006**, 284 (1–2), 237-247.
2. Zhou, X.; Gingerich, D. B.; Mauter, M. S., Water Treatment Capacity of Forward-Osmosis Systems Utilizing Power-Plant Waste Heat. *Industrial & Engineering Chemistry Research* **2015**, 54 (24), 6378-6389.
3. Loh, H. P.; Lyons, J.; White III, C. W. *Process Equipment Cost Estimation Final Report*; National Energy Technology Laboratory: Morgantown, WV, 2002, 2002.
4. Towler, G.; Sinnott, R., *Chemical Engineering Design: Principles, Practice, and Economics of Plant and Process Design*. 2nd Edition ed.; Elsevier, Ltd.: Oxford, UK, 2013.



## **APPENDIX 7: SUPPORTING INFORMATION FOR CHAPTER 8 - REDESIGNING THE REGULATED POWER PLANT: OPTIMIZING ENERGY ALLOCATION TO ELECTRICITY GENERATION, WATER TREATMENT AND CARBON CAPTURE PROCESSES AT COAL-FIRED GENERATING FACILITIES**

Supporting Information Summary:

The supporting information contains descriptions of 1) energy consumption of carbon capture and the trade-offs of using different technologies, 2) energy consumption of water treatment and the trade-offs of using different technologies, 3) maximum revenue strategies for the six different regulatory scenarios included in the analysis, and 4) the parasitic losses for carbon capture and water treatment.

This supporting information is 13 pages long and contains 9 figures (Figures S1-S9) and 2 tables (Tables S1 and S2).

## 1.0 Carbon Capture Models

### 1.1 Carbon Capture Process Overviews

In this study we look at three different types of carbon capture processes: solvents, sorbents, and membranes.

#### Solvents – Amine Processes

In amine processes, the CO<sub>2</sub>-containing exhaust gas is fed into the bottom of an absorber unit. An aqueous amine solution is added to the top of the absorber. The CO<sub>2</sub> reacts with the amine solution and is absorbed into the liquids. The CO<sub>2</sub> rich solvent is then fed into a regeneration unit.<sup>8</sup> In the regeneration unit, steam is added to strip the CO<sub>2</sub> from the solvent.<sup>2</sup> The solvent is returned to the absorber and the concentrated CO<sub>2</sub> gas is pressurized and sent to storage.

#### Sorbents – Zero Valent Iron

In a zero valent iron sorbent process, the CO<sub>2</sub>-containing exhaust gas is fed into the bottom of an absorber unit. The absorption unit is packed with zero valent iron pellets. The CO<sub>2</sub> absorbs on to the zero valent iron. The column is then heated and CO<sub>2</sub> is released as a concentrated stream where it is pressurized and sent to storage.<sup>3</sup>

#### Membranes

In membrane processes, the CO<sub>2</sub>-containing exhaust gas is pressurized before entering the membrane unit. Once the pressurized exhaust gas enters the membrane unit, CO<sub>2</sub> selectively permeates through the membrane. The membrane is designed to selectively allow transport of CO<sub>2</sub> across the membrane, but not N<sub>2</sub> or other gasses. The CO<sub>2</sub> permeate is then pressurized and sent to storage. In many designs of a membrane system a second pass of the flue gas will be required to achieve a 90% CO<sub>2</sub> recovery.<sup>6,12</sup>

### 1.2 Energy Consumption for Carbon Capture

Table S1 shows the energy consumption from 11 different studies of thermally-driven carbon capture using amine solvents and electrically-driven carbon capture using membranes. Each process includes a description of the plant and carbon capture process. We also report if the energy consumption is from a simulation or is the reported thermodynamic minimum.

The processes have their energy consumption reported on either a MJ/kgCO<sub>2</sub> or a kWh/kgCO<sub>2</sub> basis. To compare the energy consumption between thermally-driven processes and electrically-driven processes we determine the equivalent electrical or thermal energy, i.e. the amount of electricity that the steam could have generated or the amount of steam it took to generate the electricity, respectively. For the thermal energy processes, we assume that the steam used in the process is taken from before the LP turbines and so the equivalent electrical energy only considers the efficiency of the LP turbine. For the electrical energy processes, we

assume that the electricity used in the process was generated using steam from all of the turbines and use an overall efficiency of the plant.

$$E_E = Q \cdot R_{LP} \cdot \eta_{IS} \cdot \frac{1000 \text{ kJ}}{1 \text{ MJ}} \cdot \frac{1 \text{ kWh}}{3600 \text{ kJ}} \quad (1)$$

We use equation (1) to convert the thermal energy consumption of thermal processes,  $Q$  in [MJ/kgCO<sub>2</sub>], into the equivalent electrical energy,  $E_E$  in [kWh/kgCO<sub>2</sub>]. To do so, we multiply the thermal energy consumption by the percent of enthalpy that enters the LP turbine and is lost during steam expansion,  $R_{LP}$  in [%], and the isentropic efficiency of the turbine and generator,  $\eta_{IS}$  in [%]. For the NETL plant used in the main manuscript  $R_{LP}$  is 26.51%. As described in the manuscript, the isentropic efficiency of the turbine and generator is assumed to be 90%.

$$Q_E = \frac{E}{R_{Turbines} \cdot \eta} \cdot \frac{3600 \text{ kJ}}{1 \text{ kWh}} \cdot \frac{1 \text{ MJ}}{1000 \text{ kJ}} \quad (2)$$

We use equation (2) to convert the electrical energy of membrane processes and two studies of a thermal amine process,  $E$  in [kWh/kgCO<sub>2</sub>], into the equivalent thermal energy  $Q_E$  in [MJ/kgCO<sub>2</sub>]. To do so, we divide the electrical energy consumption by the percent of enthalpy that enters the turbines and is converted into the mechanical work of spinning the turbine blades in all three turbines,  $R_{Turbines}$  in [%], and the isentropic efficiency of the turbine and generator,  $\eta_{IS}$  in [%]. For the NETL plant used in the main manuscript  $R_{Turbines}$  is 50.12%. As described in the manuscript, the isentropic efficiency of the turbine and generator is assumed to be 90%.

For the analysis in the manuscript we focus on three different thermal energy consumption studies that use different amine solutions and one membrane process that is for a plant similar to the NETL plant. We use thermal energy estimates of 3.54 MJ/kgCO<sub>2</sub> for an Econamine MEA system,<sup>1,2</sup> an estimate of 2.85 MJ/kgCO<sub>2</sub> for a Zeolite 13X Temperature Swing Adsorption system,<sup>3</sup> an estimate of 2.48 MJ/kgCO<sub>2</sub> for the Cansolv tertiary amine,<sup>4</sup> and an idealized estimate of 1.9 MJ/kgCO<sub>2</sub> for the thermodynamic minimum of a MEA system.<sup>5</sup> For an electricity driven process we use an estimate of 0.19 kWh/kgCO<sub>2</sub> because the system modeled has a similar capacity to the NETL model plant.<sup>6</sup>

Table S1. Carbon Capture Energy Consumption Studies

Thermal – Amine Processes 90% CO <sub>2</sub> recovery	Thermodynamic, Real-World, or Simulation Value	Reported Thermal Energy Consumption [MJ/kgCO <sub>2</sub> ]	Electrical Energy Equivalent Consumption [kWh/kgCO <sub>2</sub> ]	Citation
<i>Econamine FG Plus System</i> Estimate is from the 2007 NETL Baseline Report used in IECM and kept for 2013 NETL Baseline Report. The (Zhai and Rubin 2013) paper is for a 589 gross MW supercritical plant	Simulation	3.52-3.56	0.23-0.24	1,2
<i>Econamine FG Plus System</i> 550MW net subcritical plant detailed 2013 NETL Baseline report. *Estimate is given in kWh/kgCO <sub>2</sub> and thermal energy equivalent is calculated.	Simulation	2.48*	0.31	7
<i>IECM Model - Amine Process</i> *Estimate is given in kWh/kgCO <sub>2</sub> and thermal energy equivalent is calculated.	Simulation	2.00*	0.25	
<i>Amine Process</i> Simulation of 800 MW supercritical PC plant. Description of process refers to 2007 NETL report	Simulation	3.56-3.60	0.24	8
Simulation of a 300 MW subcritical PC plant	Simulation	3.12	0.21	9
<i>Zeolite 13X TSA Process</i> Zeolite 13X in a temperature swing adsorption process for heating just the zeolite	Real-World	2.85	0.19	3
<i>Cansolv Process</i> NETL does not make a distinction between the heat duty from the subcritical and supercritical processes	Simulation	2.5	0.17	4
<i>MEA Process</i> The authors assume that 5% of the water in the MEA solvent solution is also evaporated in the reaction, which increases the energy consumption. Recovery is 99%, and scaled down to 90%.	Thermodynamic	2.0  (2.2 for 99% recovery)	0.13  (0.15 for 99% recovery)	10
<i>Solid Sorbents (Fiber Sorbent or in Packed Beds)</i> Recovery is 99% and scaled down to 90%.	Thermodynamic	0.52-1.45 (0.57-1.59 for 99% recovery)	0.03-0.09 (0.04-0.10 for 99% recovery)	10
<i>MEA Process</i>	Thermodynamic	1.9	0.13	5

Table S1 (Continued)

Electrical – Membrane Process 90% CO <sub>2</sub> recovery	Thermodynamic or Simulation Value	Reported Electrical Energy Consumption [kWh/kgCO <sub>2</sub> ]	Thermal Energy Equivalent [MJ/kgCO <sub>2</sub> ]	Citation
<i>IECM Model</i> Includes Compression	Simulation	0.45	3.6	
<i>Polyactive Membrane Process</i> 1210 MW with a net electric of 555 MW with a two- step Polyactive membrane process. Includes compression at a temperature of 25, 30, and 50°C. Uses both compression and vacuum to drive the separation.	Simulation	0.31-0.48	2.5-3.8	11
<i>Two-Step Membrane Separation</i> 550 MW plant citing 2010 NETL Cost and Performance Baseline Report. Modeled using COMSOL to solve series of PDEs. Uses both compression and vacuum to drive the separation.	Simulation	0.19	1.5	6
<i>Two-Step Membrane Separation</i> 900 gross MW ultra-supercritical plant with a gross efficiency of 49.1% using vacuum	Simulation	0.133	1.1	12

### 1.3 Carbon Capture Trade-offs

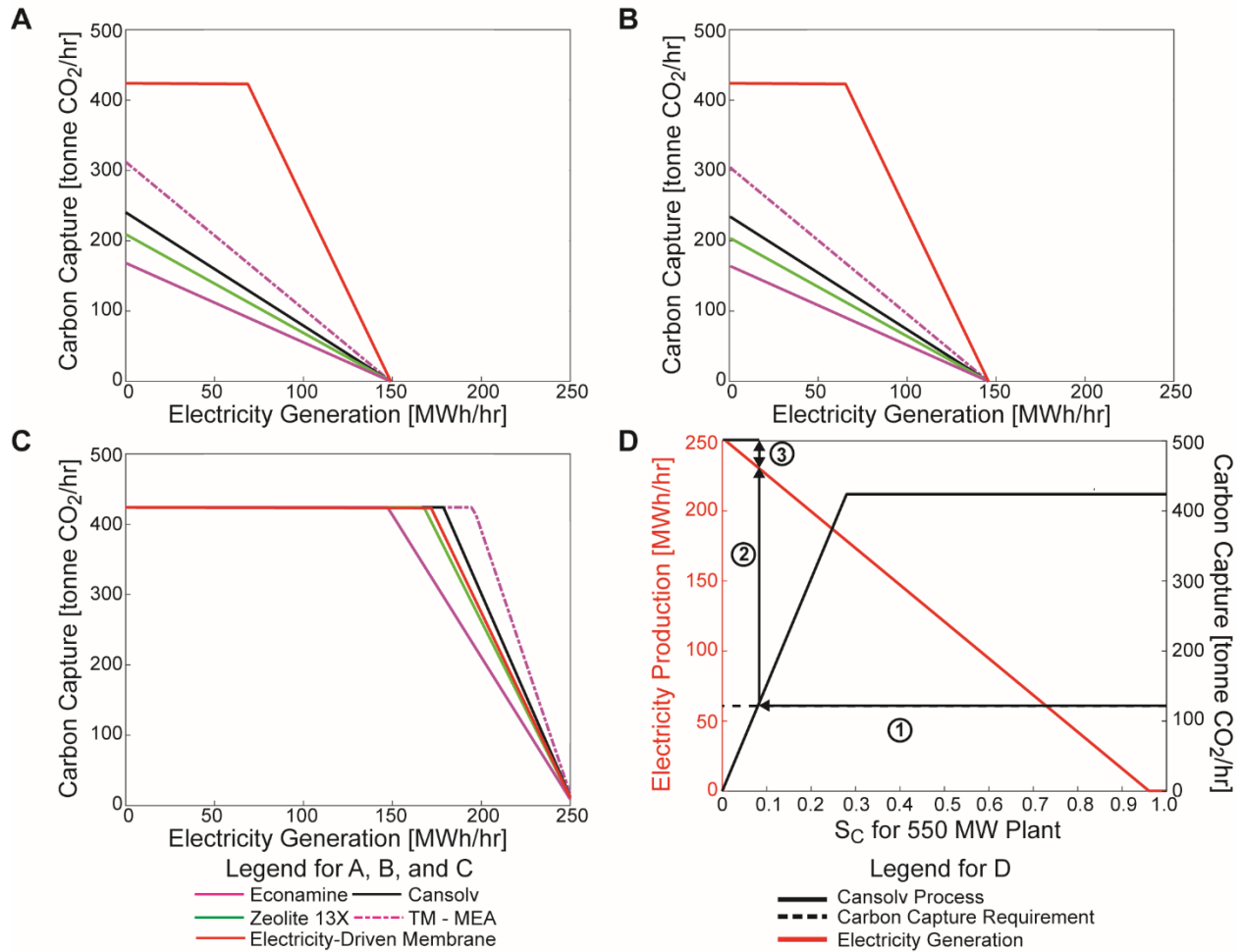
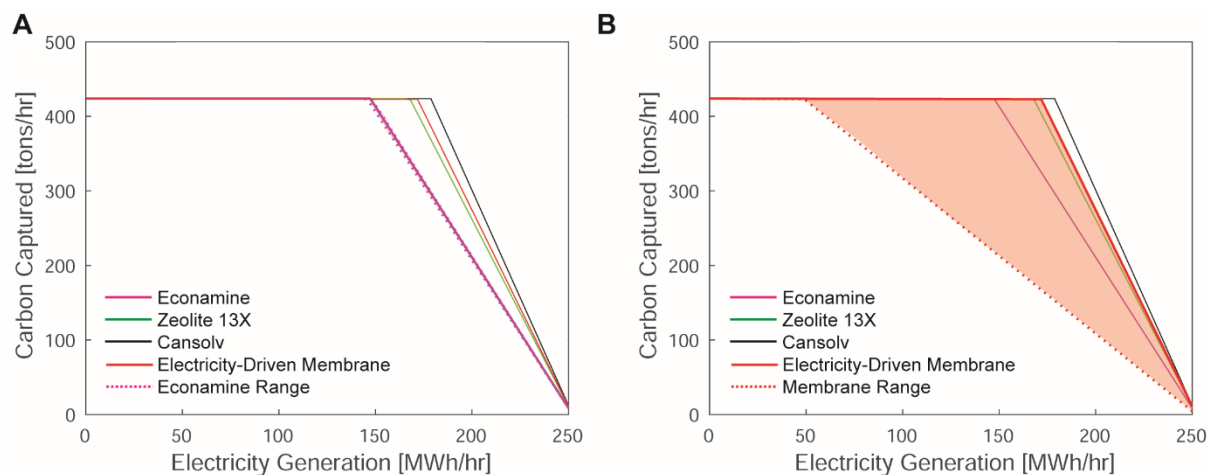


Figure S1. Trade-offs between steam allocation for carbon capture and electricity generation for adsorption processes (Econamine (MEA), Cansolv, Zeolite 13X, thermodynamic limit for MEA) and an electricity-driven membrane separation process for the (A) HP turbine, (B) IP turbine, and (C) LP turbine. Panel (D) shows the electricity production-carbon capture trade-off curve for the Cansolv process in the LP turbine. The dashed line represents the minimum amount of carbon that needs to be captured under the Clean Power Plan. Plot D shows how to calculate the parasitic losses for carbon capture and water treatment by (1) reading across the carbon capture requirement line over to the black carbon capture line and then (2) reading up to the corresponding electricity generation line in red. This difference (3) between the maximum electricity generation and the electricity generation at the carbon capture requirement is the parasitic loss.

The trade-offs between steam allocation for carbon capture using four different carbon capture technologies and electricity generation are presented in Figure S1. As is shown in Figure S1A and S1B, the membrane processes are the most efficient processes with the lowest parasitic loss for HP and IP steam. Figure S1C shows that for LP steam, Cansolv is the most efficient process. Figure S1D shows the parasitic loss for a LP steam driven Cansolv process.

## 1.4 Carbon Capture Energy Consumption Sensitivity Analyses



*Figure S2. The carbon capture-electricity generation relationship using LP steam given the range of (A) thermal energy consumption for Econamine MEA processes and (B) electrical energy consumption for membrane separation processes. In each panel the dashed lines represent the ranges of carbon capture possible.*

In the main manuscript we used an average Econamine  $H_{C,j}$  of 3.54 GJ/tonne CO<sub>2</sub> in Equation 2 and an average electricity consumption  $a_j$  of 0.19 MWh/tonne CO<sub>2</sub> for the membrane process in Equation 4. But as reported in Table S1, there is variability in the energy consumption for the Econamine process and the membrane processes. To understand the impact of this variability, we re-run Equations 2 and 4 using the highest and lowest Econamine  $H_{C,j}$ 's and membrane process  $a_j$ 's reported in Table S1. In Figure S2, the dashed lines show the resulting range of parasitic losses for the low pressure turbine. As can be seen from Figure S2, the Cansolv process still imposes the lowest parasitic loss over the range of observed energy consumptions. Therefore, our conclusion that the Cansolv process imposes the lowest parasitic loss is robust.

## 2.0 Water Treatment Models

### 2.1 FGD Wastewater Treatment Process Overview

In this study we look at six different wastewater treatment processes: multiple effect distillation, multi-stage flash distillation, thermal vapor recompression, forward osmosis, chemical precipitation and biological treatment, and mechanical vapor recompression.

#### Multiple Effect Distillation

In multiple effect distillation, the FGD wastewater to be treated is sprayed onto a series of steam-containing tubes. This causes the steam in the tubes to condense and a portion of the wastewater to evaporate. This condensation in the tubes is the treated water that can be reused within the plant. The vapor is collected and used as the steam in the next effect to heat the remaining brine. The next effect is at a lower pressure, allowing further recovery of water from the FGD wastewater.

#### Multi-stage Flash Distillation

In multi-stage flash distillation, the FGD wastewater to be treated is heated using steam and flash boiled. The vapor is then condenses on tubes containing the FGD wastewater and can be reused within the plant. The latent heat released in the condensation process is used to preheat the FGD wastewater. The brine that remains then moves into the next stage where a lower pressure allows for further recovery of water from the FGD wastewater.

#### Thermal Vapor Recompression

In thermal vapor recompression, steam is used to compress a vapor stream. The increase in the vapor pressure leads to an increase in the condensation temperature. The higher condensation temperature of the vapor allows the vapor to serve as a heating medium in an evaporation process to treat the flue gas desulfurization wastewater. This produces a concentrated brine of the FGD wastewater and a vapor/steam stream that can be recycled within the plant

#### Forward Osmosis

In forward osmosis, the FGD wastewater to be treated is fed into a membrane unit with a more concentrated draw solution of  $\text{NH}_3\text{HCO}_3$ . Water from the FGD wastewater is passively pulled across the semi-permeable membrane, diluting the draw solution. The diluted draw solution is then fed into a distillation column. In the distillation column, the ammonia and carbonate species are stripped away, producing from the bottom a treated water stream that can be recycled within the plant. The top is then sent back to the membrane unit and the process repeats.

#### Chemical Precipitation and Biological Treatment



In chemical precipitation, hydroxide, iron, and organosulfides are added to the FGD wastewater. The addition of these chemicals leads to the precipitation of many trace elements from the FGD wastewater, including arsenic, lead, and mercury. Following chemical precipitation the FGD wastewater is then introduced into aerobic and anaerobic bioreactors. The aerobic bioreactor reduces the biochemical oxygen demand of the wastewater. In the anaerobic bioreactor nitrogen is removed and a proprietary microbial community reduces the selenium.

Chemical precipitation and biological treatment is the best available technology established by the Environmental Protection Agency for compliance with the effluent limitation guidelines. It does not produce water that can be reused within the plant and does not meet the standards for zero liquid discharge.

### Mechanical Vapor Recompression

In mechanical vapor recompression, a compressor is used to compress a vapor stream. Increasing the pressure of the vapor increases the condensation temperature. The increase in the condensation temperature allows the vapor to serve as a heating medium to drive evaporation in the flue gas desulfurization wastewater. This produces a vapor/steam stream that can be recycled within the plant and a concentrated brine that can be fed into a crystallizer.

Mechanical vapor recompression followed by crystallization is the best available technology established by the Environmental Protection Agency for achieving zero liquid discharge of flue gas desulfurization.

## 2.2 *Energy Consumption for Water Treatment*

Table S2 shows reported thermal and electrical energy consumption for four thermal technologies (multiple effect distillation, multi-stage flash distillation, thermal vapor recompression, forward osmosis) and the two regulatory best available technologies under the Effluent Limitation Guidelines for flue gas desulfurization wastewater treatment (chemical precipitation and biological treatment and mechanical vapor recompression). We also report if the value is from a simulation of the process, a real-world installation of the system, or the thermodynamic minimum.

These processes are reported in either MJ/m<sup>3</sup> or kWh/m<sup>3</sup> depending if the energy source is thermal or electrical energy. In order to compare between the two, we calculate the equivalent electrical energy or equivalent thermal energy of the processes. We do this using the procedure described above in SI Section 1.0.

For the analysis in the main manuscript, we select more conservative values reported in the literature. These values are 1,710 MJ/m<sup>3</sup> for membrane distillation, 477 MJ/m<sup>3</sup> for multiple effect distillation, 1,080 MJ/m<sup>3</sup> for multi-stage flash distillation, 333 MJ/m<sup>3</sup> for thermal vapor recompression,<sup>13</sup> 409 MJ/m<sup>3</sup> for forward osmosis,<sup>14</sup> 5 kWh/m<sup>3</sup> for reverse osmosis,<sup>15</sup> 0.71 kWh/m<sup>3</sup> for chemical precipitation and biological treatment, and 37.4 kWh/m<sup>3</sup> for chemical precipitation and evaporation.<sup>16</sup>

Table S2. Water Treatment Consumption Studies

Thermal	Thermodynamic, Real-World, or Simulation Value	Reported Thermal Energy Consumption [MJ/m <sup>3</sup> ]	Electrical Energy Equivalent Consumption [kWh/ m <sup>3</sup> ]	Electrical Energy Consumption [kWh/m <sup>3</sup> ]	Citation
<i>Multiple Effect Distillation</i> Feed Salinity of 30,000 ppm, Feed Temperature of 56°C, and 65% Recovery	Simulation	476	32		13
<i>Multiple Effect Distillation</i>	Real-World	145-230	9.6-15	2.25	15
<i>Multi-Stage Flash Distillation</i> Feed Salinity of 30,000 ppm, Feed Temperature of 56°C, and 65% Recovery	Simulation	1,071	71		13
<i>Multi-Stage Flash Distillation</i>	Real-World	190-282	13-19	3.75	15
<i>Thermal Vapor Recompression</i> Feed Salinity of 30,000 ppm, Feed Temperature of 56°C, and 65% Recovery	Simulation	313	21		13
<i>Thermal Vapor Recompression</i>	Real-World	227	15	1.7	15
<i>Forward Osmosis</i> Feed Salinity of 30,000 ppm, Feed Temperature of 56°C, and 65% Recovery	Simulation	409	27	0.02	14
Electrical	Thermodynamic, Real-World, or Simulation Value	Reported Electrical Energy Consumption [kWh/ m <sup>3</sup> ]	Thermal Energy Equivalent Consumption [MJ/ m <sup>3</sup> ]		Citation
<i>Chemical Precipitation &amp; Biological Treatment</i>	Real-World	0.71	5.7		16
<i>Mechanical Vapor Recompression</i> 65% Recovery	Real-World	37.4	168		16

### 2.3 Water Treatment Trade-offs

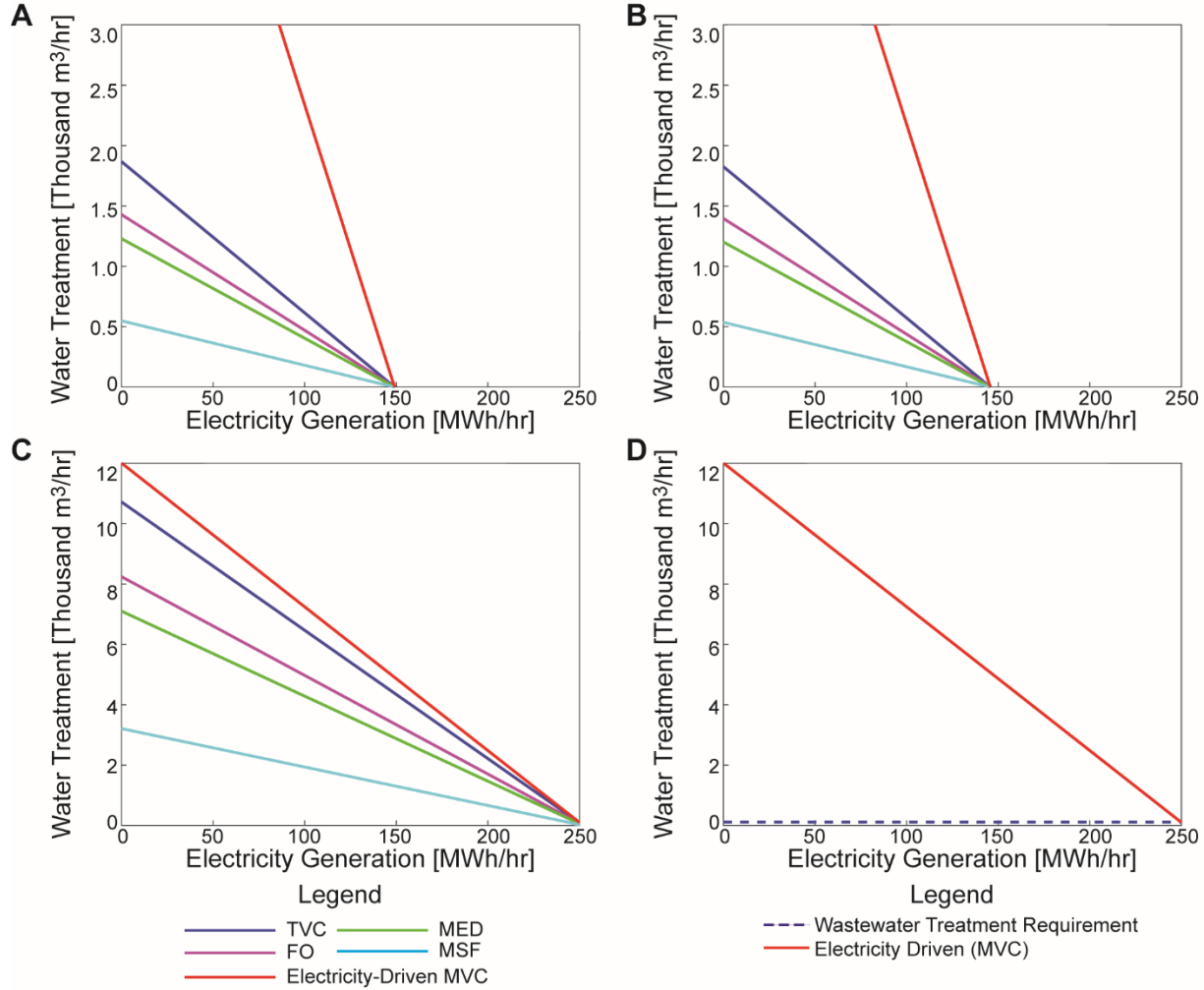


*Figure S3. Trade-offs between steam allocation for electricity and water deionization processes. Panels A, B, and C show the water production and electricity generation trade-offs for the HP turbine, IP turbine, and LP turbines, respectively. As seen in these panels, MVC is the most efficient water production technology as it can produce the most water with the same amount of energy. Panel D show the trade-offs between electricity generation and water production using MVC using electricity generated in the LP turbine. The dashed line represents the wastewater treatment need of the plant, shows that all turbines can meet the water need while imposing a parasitic loss of 2.6 MWh for LP steam use.*

The trade-offs between steam allocation for water treatment using five different water treatment technologies and electricity generation are presented in Figure S2. As is shown in Figure S2A-C, the electricity driven mechanical vapor recompression processes is the most efficient process with the lowest parasitic loss. Figure S2D shows the parasitic loss for using mechanical vapor recompression.

### 3.0 Revenue Maximizing Energy Allocations

Figures S2-S5 present the optimal revenue and allocation of low pressure steam, electricity, and residual heat for five of the six different regulatory scenarios analyzed in the main manuscript. For each regulatory scenario we look at the allocation for five different combinations of potential energy sources: only electricity (E); only steam (S); steam and electricity (S+E); steam and residual heat (S+RH); and steam, electricity, and residual heat (S+E+RH).

#### *3.1 Revenue Maximal Steam Allocation Under No Carbon Capture and CPBT Wastewater Treatment Regulatory Option*

When the power plant does not capture carbon and treats FGD wastewater to a chemical precipitation and biological treatment standard, the only energy source that is used is electricity. The plant consumes 80 kWh/hr for FGD wastewater treatment under this scenario.

### 3.2 Revenue Maximal Steam Allocation Under No Carbon Capture and ZLD Wastewater Treatment Regulatory Option

Figure S4 shows the steam allocation that maximizes the revenue of the power plant when treating FGD wastewater to a ZLD standard and not capturing carbon.

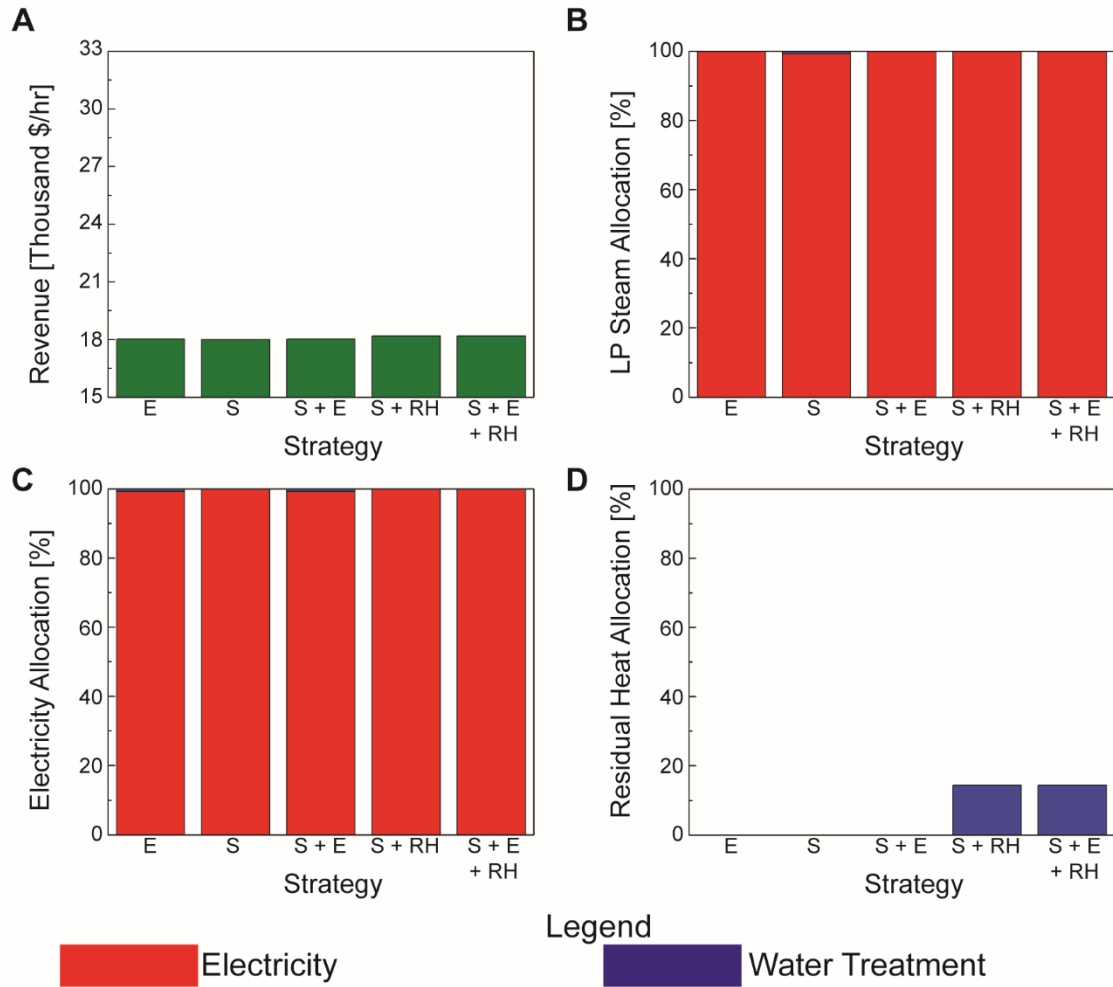


Figure S4. The (A) maximum revenue and the (B) allocation of low pressure steam to electricity or water treatment, (C) allocation of electricity to sell or to treat wastewater, and (D) allocation of residual heat to treat wastewater for the ZLD standard for FGD wastewater treatment. The five different strategies are: only electricity (E); only steam (S); steam and electricity (S+E); steam and residual heat (S+RH); and steam, electricity, and residual heat (S+E+RH). N.B. That steam is not used for water treatment under the CPBT standard and that water treatment requires 0.9% of electricity generated to be performed.

### 3.3 Revenue Maximal Steam Allocation Under Carbon Capture with No Market for Carbon Credits and CPBT Wastewater Treatment Regulatory Option

Figure S5 shows the steam allocation that maximizes the revenue of the power plant when treating FGD wastewater using electricity to a CPBT standard and capturing carbon with a carbon market price of \$0/tonne.

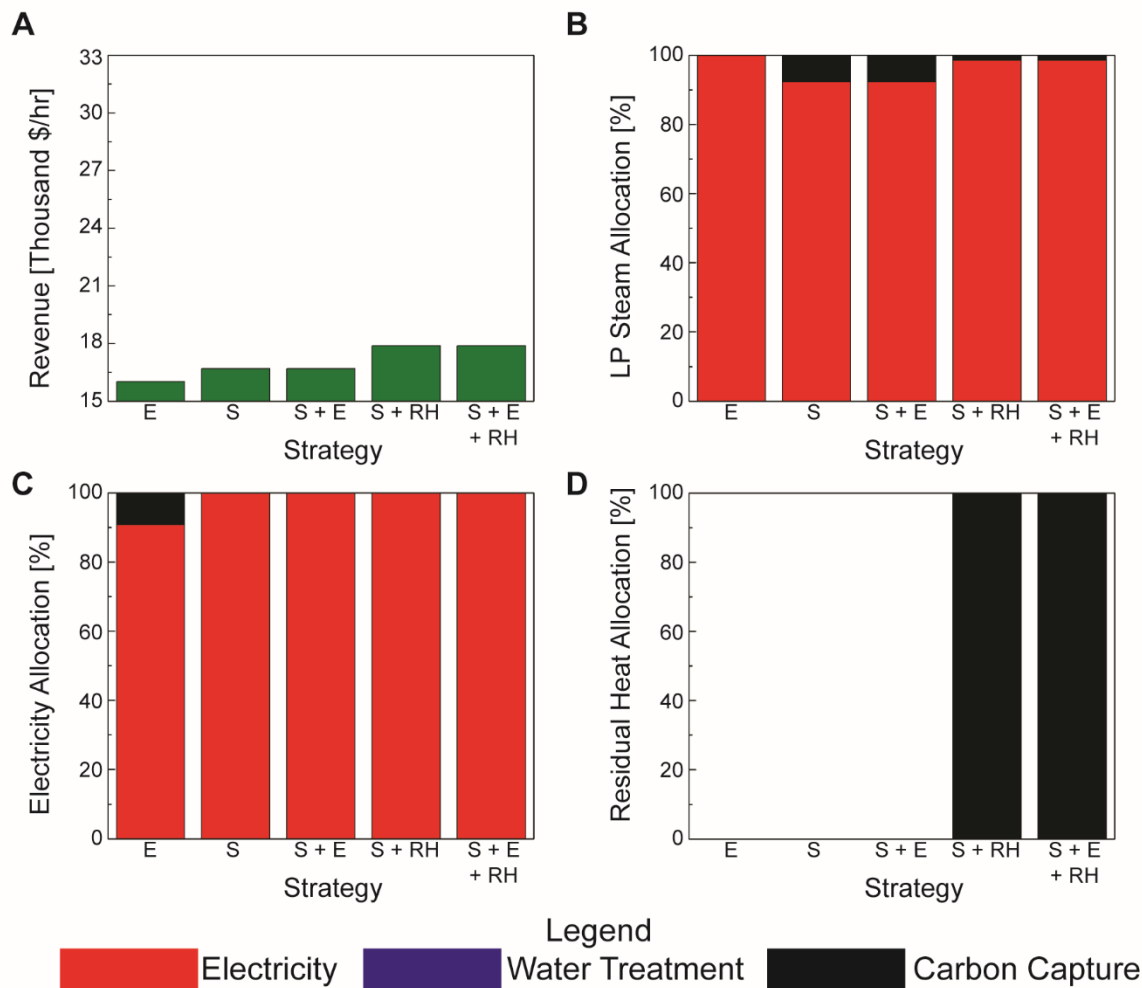


Figure S5. The (A) maximum revenue and the (B) allocation of low pressure steam to electricity or carbon capture; (C) allocation of electricity to sell, for carbon capture, or to treat wastewater; and (D) allocation of residual heat to capture carbon. The five different strategies are: only electricity (E); only steam (S); steam and electricity (S+E); steam and residual heat (S+RH); and steam, electricity, and residual heat (S+E+RH). N.B. That a small amount of electricity (<0.03% of LP turbine generation) is used for FGD wastewater treatment.

### 3.4 Revenue Maximal Steam Allocation Under Carbon Capture with No Market for Carbon Credits and ZLD Wastewater Treatment Regulatory Option

Figure S6 shows the steam allocation that maximizes the revenue of the power plant when treating FGD wastewater to a ZLD standard and capturing carbon with a carbon market price of \$0/tonne.

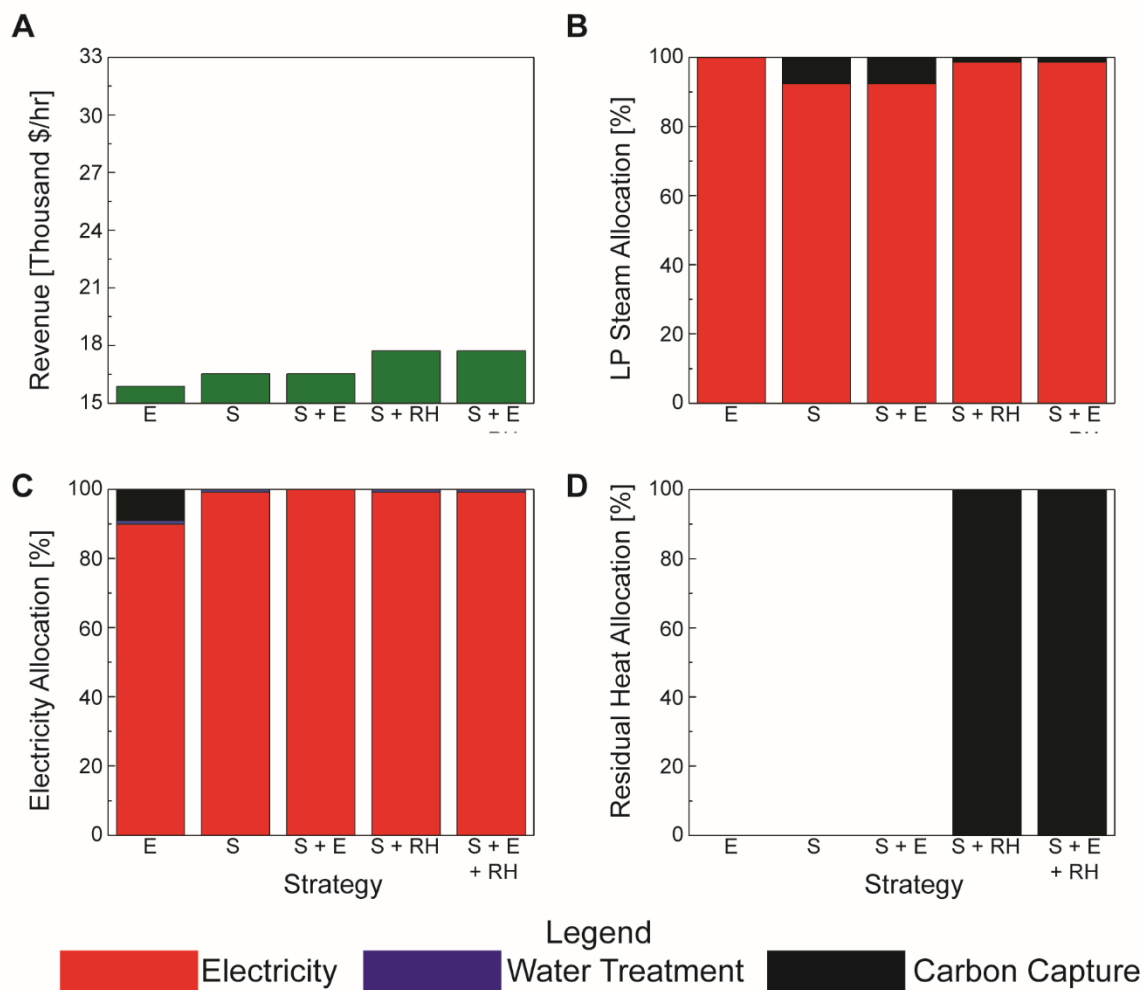


Figure S6. The (A) maximum revenue and the (B) allocation of low pressure steam to electricity, wastewater treatment, or carbon capture; (C) allocation of electricity to sell, for wastewater treatment, or to carbon capture; and (D) allocation of residual heat to wastewater treatment or capture carbon for the evaporation standard for FGD wastewater treatment no cost of carbon. The five different strategies are: only electricity (E); only steam (S); steam and electricity (S+E); steam and residual heat (S+RH); and steam, electricity, and residual heat (S+E+RH).

### 3.5 Revenue Maximal Steam Allocation Under Carbon Capture with a Market for Carbon Credits at the Social Cost of Carbon and CPBT Wastewater Treatment Regulatory Option

Figure S7 shows the steam allocation that maximizes the revenue of the power plant when treating FGD wastewater using electricity to a CPBT standard and capturing carbon with a carbon market price equivalent to the social cost of carbon of \$59.44/tonne.

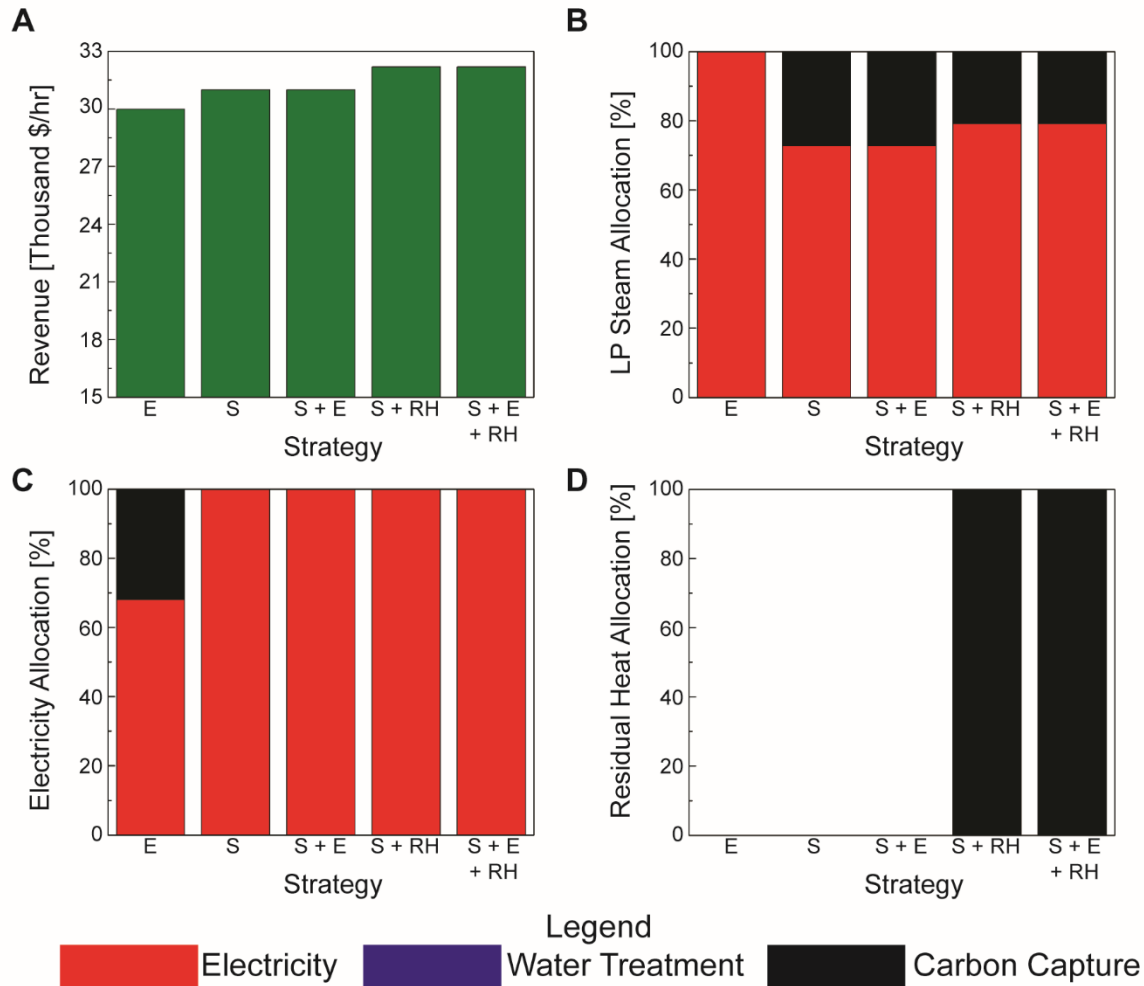


Figure S7. The (A) maximum revenue and the (B) allocation of low pressure steam to electricity or carbon capture; (C) allocation of electricity to sell, for wastewater treatment, or to carbon capture; and (D) allocation of residual heat to capture carbon for the CPBT standard for FGD wastewater treatment and a market value for carbon at the social cost of carbon. The five different strategies are: only electricity (E); only steam (S); steam and electricity (S+E); steam and residual heat (S+RH); and steam, electricity, and residual heat (S+E+RH). N.B. That a small amount of electricity (<0.04% of LP turbine generation) is used for FGD wastewater treatment.



### 3.6 Revenue Maximal Steam Allocation Under Carbon Capture with a Market for Carbon Credits at the Social Cost of Carbon and ZLD Wastewater Treatment Regulatory Option

Figure S8 shows the steam allocation that maximizes the revenue of the power plant when treating FGD wastewater using electricity to a ZLD standard and capturing carbon with a carbon market price equivalent to the social cost of carbon of \$59.44/tonne.

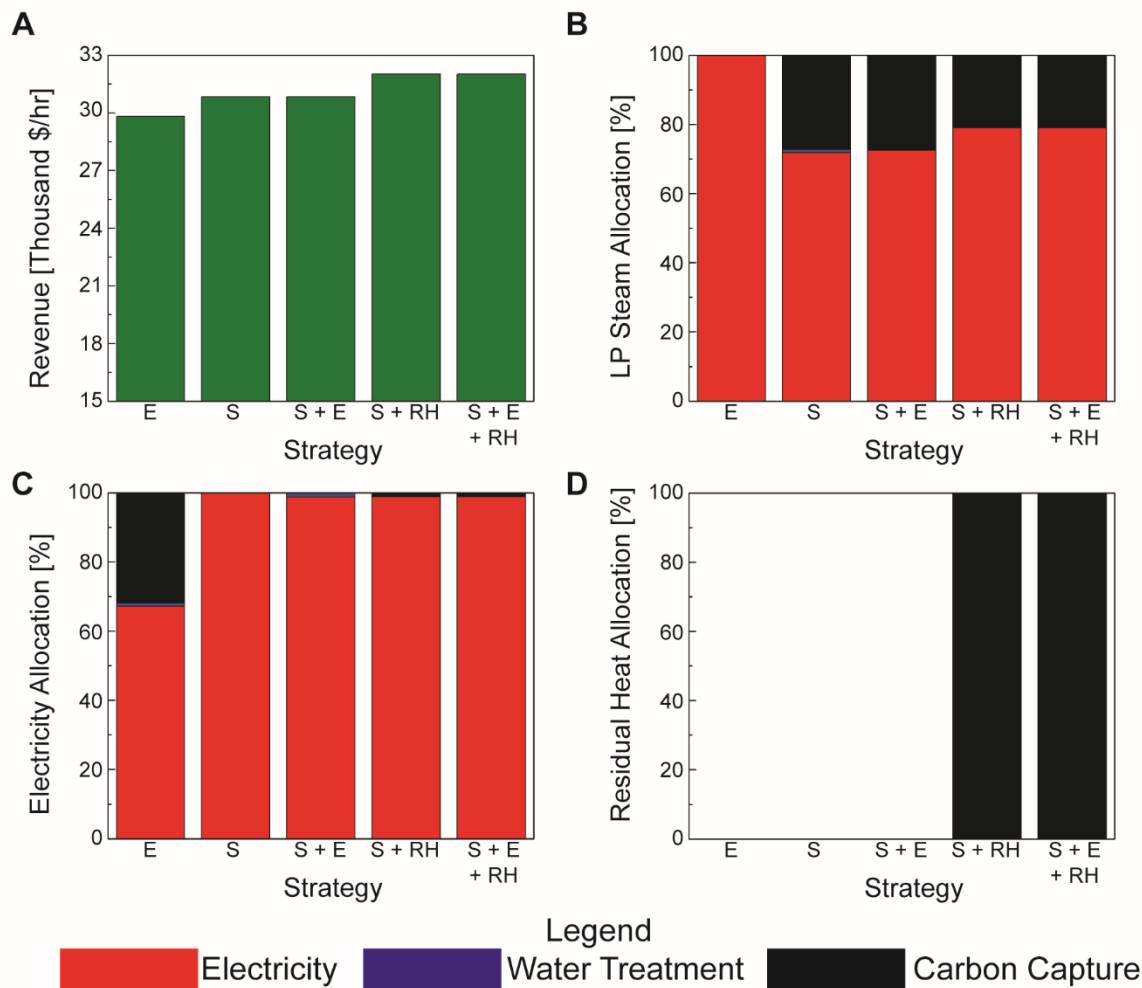
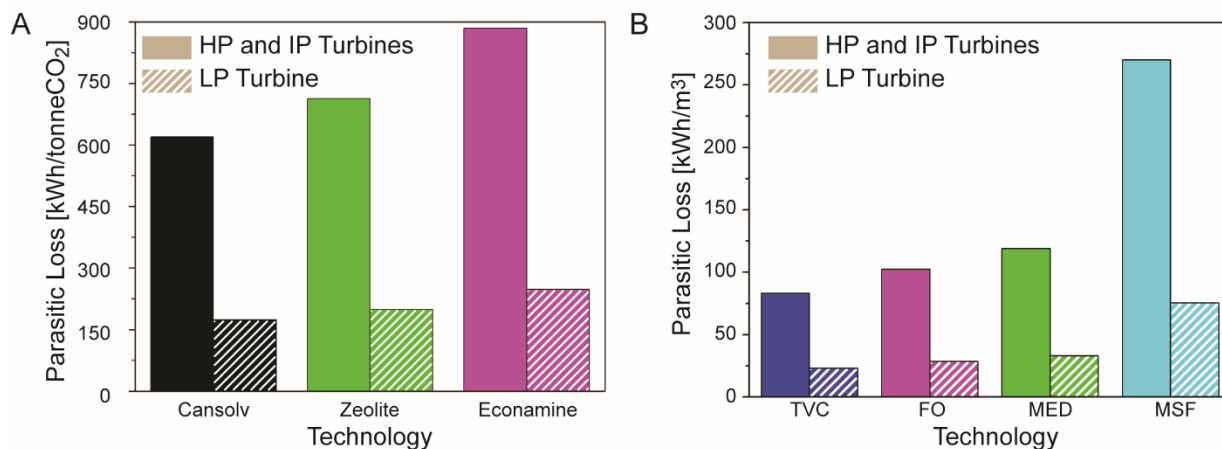


Figure S8. The (A) maximum revenue and the (B) allocation of low pressure steam to electricity, water treatment, or carbon capture; (C) allocation of electricity to sell, for wastewater treatment, or to carbon capture; and (D) allocation of residual heat to wastewater treatment or capture carbon for the ZLD standard for FGD wastewater treatment and a market value for carbon at the social cost of carbon, \$59.44/tonne. The five different strategies are: only electricity (E); only steam (S); steam and electricity (S+E); steam and residual heat (S+RH); and steam, electricity, and residual heat (S+E+RH).

## 4.0 Parasitic Loss Analysis



*Figure S9. Parasitic losses of (A) the three thermal options for carbon capture and (B) the four thermal options for wastewater treatment.*

Figure S9 shows the parasitic losses associated with carbon capture and water treatment. The low pressure turbine steam has a lower parasitic loss because the environmental control technologies can recover a greater share of the enthalpy in the steam than is converted into electricity in the turbine.

For carbon capture, Cansolv has the lowest parasitic losses at 620 kWh/tonne using HP or IP steam and 173 kWh/tonne using LP steam. Zeolite 13X has the second lowest parasitic loss at 712 kWh/tonne using HP or IP steam and 199 kWh/tonne using LP steam. Econamine is the least efficient option with a parasitic loss of 885 kWh/tonne using HP or IP steam and 247 kWh/tonne using LP steam.

For wastewater treatment, TVC has the lowest parasitic losses of 80 kWh/m<sup>3</sup> using HP or IP steam and 24 kWh/m<sup>3</sup> from LP steam. FO has a parasitic loss of 104 kWh/m<sup>3</sup> using HP or IP steam and 31 kWh/m<sup>3</sup> using LP steam. MED has a parasitic loss of 121 kWh/m<sup>3</sup> using HP or IP steam and 36 kWh/m<sup>3</sup> using LP steam. MSF has the highest parasitic loss of the technologies considered at 272 kWh/m<sup>3</sup> for HP and IP steam and 79 kWh/m<sup>3</sup> for LP steam.

## 5.0 References

1. Zhai, H.; Ou, Y.; Rubin, E. S. Opportunities for Decarbonizing Existing U.S. Coal-Fired Power Plants via CO<sub>2</sub> Capture, Utilization and Storage. *Environ. Sci. Technol.* **2015**, *49* (13), 7571–7579.
2. Zhai, H.; Rubin, E. S. Comparative Performance and Cost Assessments of Coal- and Natural-Gas-Fired Power Plants under a CO<sub>2</sub> Emission Performance Standard Regulation. *Energy & Fuels* **2013**, *27* (8), 4290–4301.
3. Marx, D.; Joss, L.; Hefti, M.; Mazzotti, M. Temperature Swing Adsorption for Postcombustion CO<sub>2</sub> Capture: Single- and Multicolumn Experiments and Simulations. *Ind. Eng. Chem. Res.* **2016**, *55* (5), 1401–1412.
4. National Energy Technology Laboratory. *Cost and Performance Baseline for Fossil Energy Plants Volume 1a: Bituminous Coal (PC) and Natural Gas to Electricity*; Morgantown, WV, 2015; Vol. 1a.
5. Le Moulec, Y. Assessment of carbon capture thermodynamic limitation on coal-fired power plant efficiency. *Int. J. Greenh. Gas Control* **2012**, *7*, 192–201.
6. Ramasubramanian, K.; Verweij, H.; Winston Ho, W. S. Membrane processes for carbon capture from coal-fired power plant flue gas: A modeling and cost study. *J. Memb. Sci.* **2012**, *421–422*, 299–310.
7. National Energy Technology Laboratory. *Cost and Performance Baseline for Fossil Energy Plants Volume 1 : Bituminous Coal and Natural Gas to Electricity*; 2013; Vol. 1.
8. Sanpasertparnich, T.; Idem, R.; Bolea, I.; deMontigny, D.; Tontiwachwuthikul, P. Integration of post-combustion capture and storage into a pulverized coal-fired power plant. *Int. J. Greenh. Gas Control* **2010**, *4* (3), 499–510.
9. Khalilpour, R.; Abbas, A. HEN optimization for efficient retrofitting of coal-fired power plants with post-combustion carbon capture. *Int. J. Greenh. Gas Control* **2011**, *5* (2), 189–199.
10. Lively, R. P.; Chance, R. R.; Koros, W. J. Enabling Low-Cost CO<sub>2</sub> Capture via Heat Integration. *Ind. Eng. Chem. Res.* **2010**, *49* (16), 7550–7562.
11. Maas, P.; Nauels, N.; Zhao, L.; Markewitz, P.; Scherer, V.; Modigell, M.; Stolten, D.; Hake, J.-F. Energetic and economic evaluation of membrane-based carbon capture routes for power plant processes. *Int. J. Greenh. Gas Control* **2016**, *44*, 124–139.
12. Skorek-Osikowska, A.; Kotowicz, J.; Janusz-Szymańska, K. Comparison of the energy intensity of the selected CO<sub>2</sub> capture methods applied in the ultra-supercritical coal power plants. *Energy & Fuels* **2012**, *26* (11), 120118122117008.
13. Bohra, M.; Mauter, M. S. Water Production Capacity of Power Plant Waste Heat Driven Thermal Desalination Processes.
14. Zhou, X.; Gingerich, D. B.; Mauter, M. S. Water Treatment Capacity of Forward-Osmosis Systems Utilizing Power-Plant Waste Heat. *Ind. Eng. Chem. Res.* **2015**, *54* (24), 6378–6389.
15. Al-Karaghoul, A.; Kazmerski, L. L. Energy consumption and water production cost of conventional and renewable-energy-powered desalination processes. *Renew. Sustain. Energy Rev.* **2013**, *24*, 343–356.
16. Gingerich, D. B.; Sun, X.; Behrer, A. P.; Azevedo, I. M. L.; Mauter, M. S. Air Emission Implications of Expanded Wastewater Treatment at Coal-Fired Generators. *Proc. Natl. Acad. Sci.*
17. Hausmann, A.; Sanciolo, P.; Vasiljevic, T.; Weeks, M.; Duke, M. Integration of

membrane distillation into heat paths of industrial processes. *Chem. Eng. J.* **2012**, 211-212, 378–387.